Stillwater Complex, Montana: Rock Succession, Metamorphism, and Structure of the Complex and Adjacent Rocks

GEOLOGICAL SURVEY PROFESSIONAL PAPER 999

Stillwater Complex, Montana: Rock Succession, Metamorphism and Structure of the Complex and Adjacent Rocks

By NORMAN J PAGE

GEOLOGICAL SURVEY PROFESSIONAL PAPER 999

UNITED STATES GOVERNMENT PRINTING OFFICE, WASHINGTON : 1977

UNITED STATES DEPARTMENT OF THE INTERIOR

JAMES G. WATT, *Secretary*

GEOLOGICAL SURVEY

Dallas L. Peck, ***Director***

First printing 1977
Second printing 1982

For sale by the Distribution Branch, U.S. Geological Survey,
604 South Pickett Street, Alexandria, VA 22304

CONTENTS

ILLUSTRATIONS

TABLES

STILLWATER COMPLEX, MONTANA: ROCK SUCCESSION, METAMORPHISM, AND STRUCTURE OF THE COMPLEX AND ADJACENT ROCKS

By NORMAN J PAGE

ABSTRACT

Along the northern border of the Beartooth Mountains in Stillwater, Sweetgrass, and Park Counties, Mont., a terrane of Precambrian rocks overlain by Paleozoic, Mesozoic, and Cenozoic sedimentary rocks contains the differentiated stratiform ultramafic and mafic Stillwater Complex. In addition to the complex, several groups of Precambrian rocks are distinguished by mineralogic, petrologic, chemical, structural, and age criteria as follows: (1) regionally metamorphosed rocks consisting of granitic gneisses, migmatites, biotite schists, and amphibolitic gneisses, (2) hornfelsed metasedimentary rocks that form the contact aureole of the Stillwater Complex, and (3) a sequence of quartz monzonites distinguished by grain size, mineralogy, and mutual intrusive relations. Rocks of the contact aureole of the complex are comparatively rich in MgO, total iron, Cr, and Ni and are depleted in K_2O and Na_2O; they range in grade from pyroxene hornfels near the complex to albite-epidote hornfels away from it. They consist of (1) a finely layered sequence of metasedimentary rocks displaying relict small-scale crossbedding, cut-and-fill structures, and graded bedding that suggest a high-energy environment, (2) a diamictite unit of questionable glacial origin, (3) blue metaquartzites, possibly cherts, (4) an iron-formation that may have formed by chemical precipitation, (5) massive fine-grained metasedimentary rocks, and (6) layered rocks with no relict sedimentary features.

The Precambrian geologic record in the vicinity of the Stillwater Complex shows a lengthy and complicated history of multiple deformation, contact and regional metamorphism, erosion, sedimentation, and several episodes of igneous intrusion. Interpretation of these events is hindered by effects of the Late Cretaceous to Eocene Laramide orogeny. In early Precambrian time, prior to about 3,140 m.y. (million years), erosion of a terrane consisting of rocks with ultramafic, mafic, and intermediate compositions provided clastic and chemical components to the sediments that accumulated in nearby basins. These MgO- and total iron-enriched sedimentary rocks were folded at least twice and were possibly involved in a low-grade regional metamorphism. Between 2,750 and 3,140 m.y., the Stillwater magma was intruded and fractionated, forming magmatic sediments, and was the heat source for the development of the contact aureole. During this time this terrane must have been a stable area. Later within the same time span, the block containing the Stillwater Complex and hornfelsed metasedimentary rocks was juxtaposed next to the early Precambrian regionally metamorphosed rocks, probably by wrench faults, one of which may be the Mill Creek-Stillwater fault zone. Along the eastern part of this zone at 2,750 m.y., a sequence of quartz monzonites was intruded and contact metamorphosed some of the older rocks. By the time of these intrusions the regionally metamorphosed rocks were probably already complexly folded and past the peak of the regional metamorphic event that formed the gneisses and migmatites. Between 1,600 and 1,800 m.y. mafic dikes were intruded, a penetrative deformation developed, and a low-grade regional metamorphic event affected the Stillwater Complex and adjacent rocks. Before the Cambrian, the terrane was faulted, rotated and tilted, uplifted, and eroded to form the ancestral Beartooth Mountains. By Middle Cambrian time the ancestral mountains had subsided and become the site for deposition of 8,000–10,000 ft (2,438–3,048 m) of marine and continental sedimentary rocks until the Late Cretaceous. Volcanism began in Late Cretaceous time, and the Laramide deformation began and continued through the early Eocene. Since then, the area has undergone uplift, erosion, glaciation, and faulting.

INTRODUCTION

The Stillwater Complex, a differentiated, stratiform mafic and ultramafic intrusive body of Precambrian age, crops out in Stillwater, Sweetgrass, and Park Counties, Mont., for about 48 km along the northern margin of the Beartooth Mountains. The report area includes most of the Mt. Wood and Mt. Douglas quadrangles and parts of the Mt. Rae, Mt. Cowen, and McLeod Basin quadrangles (fig. 1). This report concentrates on the smaller area adjacent to the southern margin of the complex in which the most significant geologic relations are exposed (fig. 2).

The Stillwater Complex is only partly exposed, and its original size and shape are unknown. Original intrusive contacts with folded metasedimentary rocks are visible in the western third of the exposures and only locally in the eastern third. Elsewhere in the eastern part, the complex is itself intruded by quartz monzonite plutons. Original contacts in the central part are obscured by the upper plate of a thrust fault that moved metasedimentary rocks northward over the lower part of the complex. Intrusive contacts are found only on the south side of the complex. To the north, the complex is overlain unconformably by Paleozoic and Mesozoic sedimentary rocks that were folded and faulted during the Laramide orogeny.

Knowledge of the geology of the Stillwater Complex and the adjacent rocks is necessary to appraise

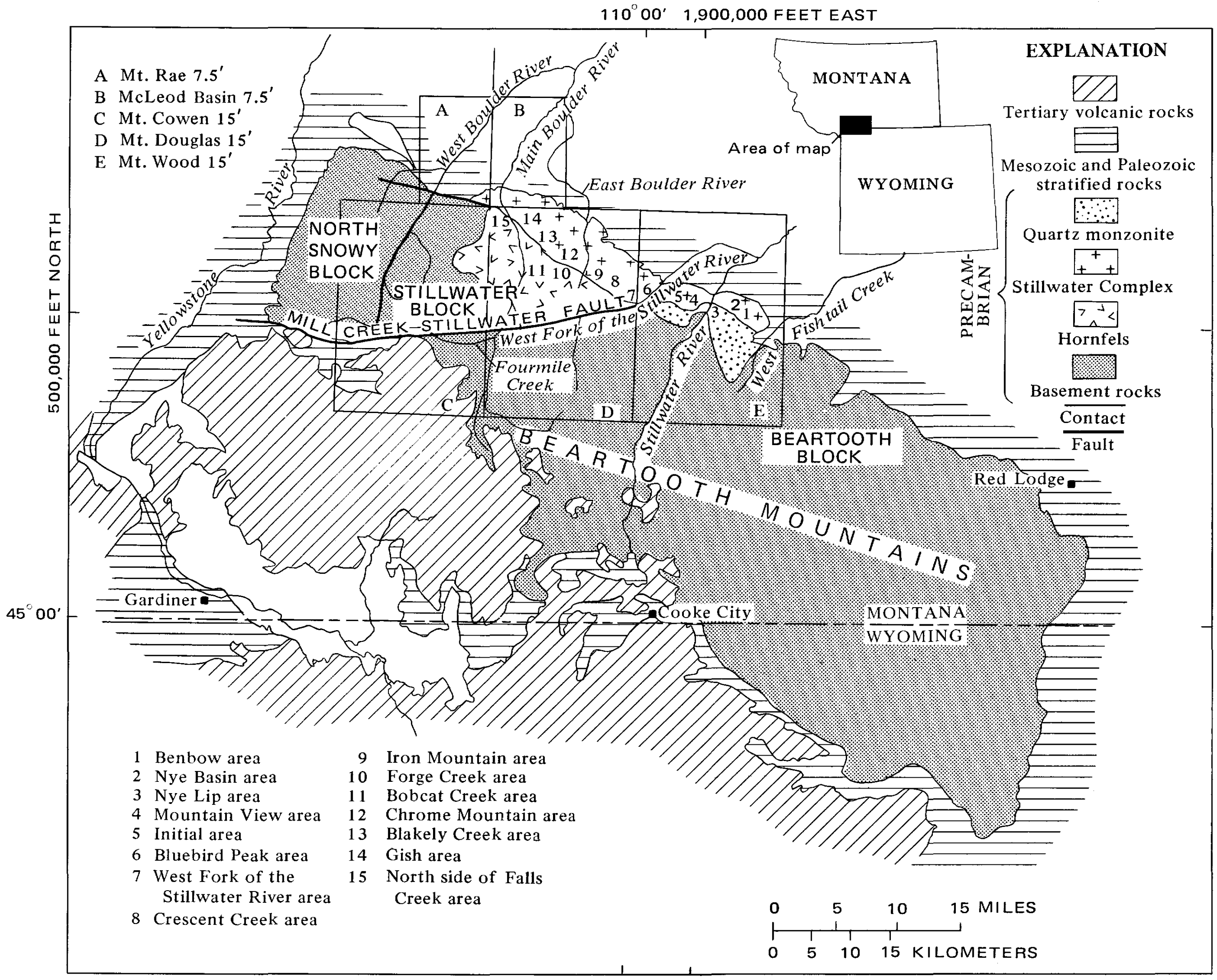

FIGURE 1.—Generalized geologic map of the Beartooth Mountains, showing location of quadrangles (A–E) and areas discussed in text (1–15). Boundary between North Snowy block and Stillwater block is fault along West Boulder River; between Stillwater block and Beartooth block, the Mill Creek–Stillwater fault.

the mineral resource potential (Page and Dohrenwend, 1973) of the area. Known potential resources of chromium (Jackson, 1968), copper (Dayton, 1971), nickel (Cornwall, 1966), platinum-group metals (Page and others, 1973), iron, coal (Calvert, 1916), and aluminum are associated with either rocks of the complex or the adjacent rocks. Understanding of the petrology, mineralogy, and tectonic development of this region is an important factor in unravelling the metallogenic processes responsible for the mineralization associated with the complex. Therefore, this study was undertaken to supply the basic geologic background information needed to evaluate the potential resources of the area.

This region has been studied since 1920 as part of several overlapping, comprehensive investigations of structure, stratigraphy, geochemistry, and petrology of the complex. Jones, Peoples, and Howland (1960) summarized the igneous and tectonic structures of the Stillwater Complex, but they lacked information on the Basal zone of the complex and wallrocks immediately adjacent to the complex. Therefore their study concentrated on Paleozoic and younger structural development of the area. Their work and the present study have drawn on the excellent mapping done as part of investigations of the chromite deposits and their geologic environment (Westgate, 1921; Peoples, 1932, 1933, 1936; Howland, 1933; Vhay, 1934; Wilson, 1936; Peoples and Howland, 1940; Wimmler, 1948; Howland and others, 1949; Richards, 1952; Peoples and others, 1954; Jackson and others, 1954; Howland, 1955; Vail, 1955; Richards, 1958; U.S. Geological Survey, 1971).

Other reports have concentrated on the petrology, mineralogy, and geochemistry of parts of the complex. Hess (1938a, b; 1939, 1940, 1941, 1960) and Hess and Phillips (1938, 1940) discussed the Banded and Upper gabbro zones, whereas Jackson (1960, 1961, 1963, 1967, 1968, 1969, 1970, 1971) and Page, Shimek, and Huffman (1972) studied the Ultramafic zone. Howland (1933), Howland, Peoples, and Sampson (1936), Page (1971a, b; 1972), Page and Jackson (1967), Leonard, Desborough, and Page (1969), and Page, Riley, and Haffty (1969, 1971, 1972) were concerned with the Basal zone and the distribution and origin of sulfide minerals and platinum metals within the Stillwater Complex. Page and Nokleberg (1972) discussed the quartz monzonite that intrudes the eastern third of the complex. Finally, the most recent textbook-type summary is contained in Wager and Brown (1967).

The details of rock succession, metamorphism, and structure of the Stillwater Complex and adjacent rocks discussed in this report form part of a body of knowledge intimately related to and based on previously published results of earlier studies. In order to obtain a unified series of detailed maps at one scale, the present study required considerable new mapping, field examination, and compilation that resulted in maps at a scale of 1:12,000 (Page and Nokleberg, 1974) for the complex and at 1:62,500 (Page and others, 1973a, b) for the Mt. Wood and Mt. Douglas quadrangles. This report is based on these maps and serves as an extended explanation, analysis, and synthesis of the information on them. The report is tightly tied to Page and Nokleberg's (1974) map; locations given here are referred to Montana South coordinates, topographic, and place names shown on their map.

Published reports stemming from the present study included (1) Page and Nokleberg's (1972) discussion of the quartz monzonites intrusive into the eastern third of the complex; (2) Page and Koski's (1973) description of the diamictite; (3) Page, Riley, and Haftty's (1969, 1971, 1972), Page and Jackson's (1967), and Page's (1971a, b; 1972) studies of sulfides and platinum mineral distribution in the complex; (4) Page, Shimek, and Huffman's (1972) study of a cyclic unit; and (5) Page and Dohrenwend's (1973) summary of mineral resources for the area.

ACKNOWLEDGMENTS

E. D. Jackson and A. L. Howland encouraged the start of this study in 1967 and since then contributed samples, unpublished mapping, and scientific discussion to the project. W. J. Nokleberg was assigned to the project for slightly over a year in 1969 and 1970, and R. A. Koski was my field assistant in 1971; both participated in the 1:12,000-scale mapping, and we three spent about 20 man-months in the field. John Stuckless, Richard Shimek, and John Dohrenwend participated in the laboratory work. Various mining companies and their personnel facilitated this project, especially AMAX Exploration Inc., Anaconda Co., Cyprus Mines Corp., Johns-Manville, W. G. Mouat, and Grant Smith. AMAX Exploration Inc. and Anaconda Co. made drill cores available for examination, logging, and sampling.

PETROLOGY AND ROCK SUCCESSION OF THE STILLWATER COMPLEX AND ADJACENT ROCKS

Diverse rock-forming processes in sedimentary, igneous, and metamorphic environments that span time from early Precambrian through the Paleozoic, Mesozoic, and Cenozoic Eras are represented within the Stillwater Complex area. All three environments are represented in the Precambrian, whereas sedimentary processes have dominated since then. This section details the rock succession of the Precambrian rock units.

The rocks are treated in eight major groups (fig. 2): (1) regionally metamorphosed rocks consisting of granitic gneisses and associated metasedimentary rocks of Precambrian age, (2) hornfelsed metasedimentary rocks of Precambrian age in the contact aureole of the Stillwater Complex, (3) the Stillwater Complex of Precambrian age, (4) an intrusive quartz monzonite sequence of Precambrian age, (5) mafic dikes and sills of Precambrian age, (6) sedimentary rocks of Paleozoic and Mesozoic age with representatives of every period except the Silurian, (7) intermediate and siliceous intrusive rocks of Tertiary age, and (8) semiconsolidated to unconsolidated glacial and alluvial sediments of Quaternary age. All of the rock groups except for the eighth have been involved in different degrees, types, and periods of deformation, and a discussion of their geologic and age relations is therefore important to a study of structures they exhibit and for dating the relative ages of the deformations. Isotopic dating by Nunes and Tilton (1971) provides the source of maximum and minimum absolute ages assigned to the Precambrian units. Assignment to periods and description of the Paleozoic and Mesozoic sedimentary rocks are based on the work of Vhay (1934).

Plate 1 gives the terminology used in this report and shows stratigraphic relations of bedded rocks within the area bounded by the edges of the Mt. Wood and Mt. Douglas 15-minute quadrangles, which in-

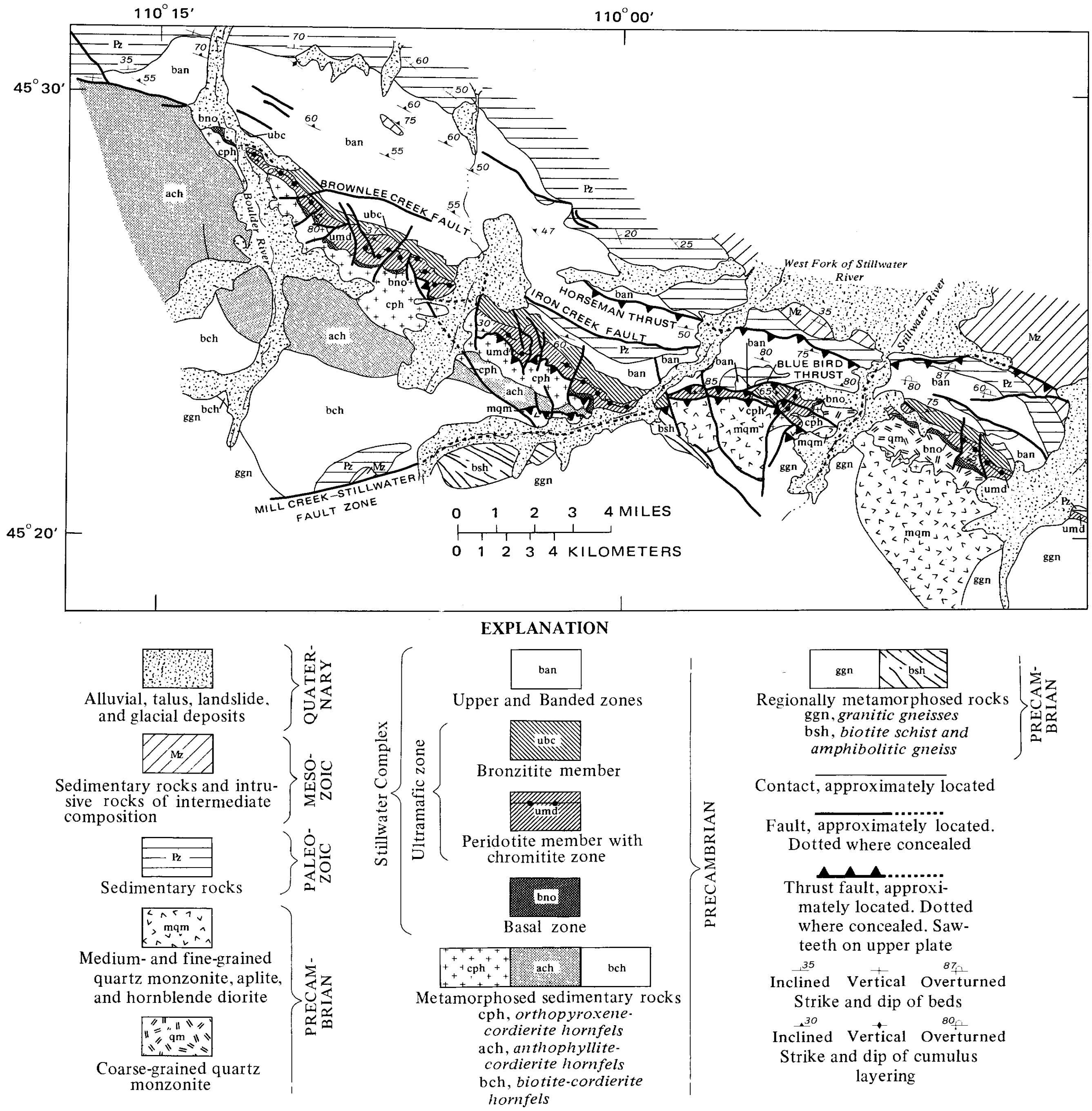

FIGURE 2.—Generalized geologic map of the Stillwater Complex and adjacent rocks. Modified from Page, Simons, and Dohrenwend (1973a, b) and Page and Nokleberg (1974).

cludes the area of the detailed mapping. The generalized columnar section is based on mapping by Page and Nokleberg (1974) and Page, Simons, and Dohrenwend (1973a, b).

REGIONALLY METAMORPHOSED ROCKS

Regionally metamorphosed rocks underlie most of the area of the Beartooth Mountains in southwestern Montana and northwestern Wyoming and comprise granitic gneiss and associated metasedimentary rocks of Precambrian age (Foose and others, 1961). Over half of the Mt. Wood and Mt. Douglas quadrangles contains exposures of these rocks, but their occurrence on the 1:12,000-scale map (Page and Nokleberg, 1974) is limited to the southern parts of the Stillwater River and the West Fork of the Stillwater

River areas (figs. 1, 2). Rocks south of the Stillwater Complex have been described by Page and Nokleberg (1970a, b; 1972), Butler (1966, 1969), and Jones, Peoples, and Howland (1960). Studies of similar rocks elsewhere in the Beartooth Mountains include Bentley (1966), Casella (1964, 1969), Eckelmann and Poldervaart (1957), Foose, Wise, and Garbarini (1961), Harris (1959), James (1946), Larsen, Poldervaart, and Kirchmayer (1966), Poldervaart and Bentley (1958), Prinz (1964), Rowan (1969), Rowan and Larsen (1970), Skinner (1969), and Skinner, Bowes, and Khoury (1969). Within the area of detailed mapping, Page and Nokleberg (1970a, 1972, 1974) divided the regionally metamorphosed rocks into granitic gneiss, biotite gneiss, plagioclase gneiss, amphibolitic gneiss, and biotite schist.

CONTACT AND AGE RELATIONS

The contact of the regionally metamorphosed rocks with other rocks within the detailed map area (fig. 2) is everywhere a fault except in the Bluebird Peak area (coordinates: 502,700 N.; 1,879,000 E.) where fine-grained quartz monzonite intrudes biotite schist. Relative age relations are shown by dikes of fine-grained quartz monzonite in the biotite schist and inclusions of biotite schist in the quartz monzonite. Within the metamorphic rocks, contacts between individual units are generally sharp and distinct. Contacts between granitic gneiss, biotite schist, and amphibolitic gneiss are usually parallel to subparallel with the foliation in the granitic gneiss and banding in the other units. Locally the contacts are gradational, according to Butler (1966), but within the area of the 1:12,000-scale map observed contacts are sharp.

The biotite gneiss has three modes of occurrence: (1) as inclusions in the intrusive quartz monzonite, (2) as selvages or screens between the intrusive quartz monzonite and hornfels pendants and between different intrusive quartz monzonites, and (3) as an isolated fault block where it is associated with a lens of amphibolitic gneiss (coordinates: 500,270 N.; 1,893,200 E.). Where the biotite gneiss occurs as inclusions and selvages, it is locally cut by dikes of quartz monzonite (coordinates: 499,050 N.; 1,903,820 E.), but it more typically has a gradational contact within about a 1.5-3-m interval. The biotite gneiss isolated in the fault block is highly sheared and partly recrystallized and resembles a flaser gneiss. Within this area it is typically highly altered and contains abundant secondary sericite and epidote. The spatial relations and intrusive nature of the quartz monzonite into the biotite gneiss inclusions and selvages indicate that the biotite gneiss is older than the quartz monzonite. A reasonable conclusion is that the biotite gneiss forms inclusions and pendants of regionally metamorphosed rocks in the quartz monzonite.

Catanzaro and Kulp (1964) dated zircons in the granitic gneiss along the Stillwater River, which were described (Butler, 1966, p. 61) as detrital zircons with abundant overgrowths. They interpreted their U-Pb data as 2,700-m.y. (million year)-old zircon overgrowths on cores with a minimum age of 3,120 m.y. Gast, Kulp, and Long (1958), using K-Ar and Rb-Sr methods to study micas and microclines, obtained a 2,750±150-m.y. age for the gneiss and considered this the age of granitization or gneiss formation. Nunes and Tilton (1971) dated two samples of granitic gneiss by U-Pb zircon methods and obtained zircon ages of 2,850 and 3,815 m.y. They also dated zircons from three samples of biotite schist that occur in the regionally metamorphosed rocks. Using an episodic lead-loss model, the minimum age of the schist zircons is 3,140 m.y., and using a continuous diffusion model, it is 3,300 m.y. These zircons are primarily round with small outgrowths—but lack overgrowths—indicating that they are detrital (Nunes and Tilton, 1971, p. 2237) and that the ages derived for the schists are minimum ages. Thus the regionally metamorphosed rocks were formed during a metamorphic event between 3,750 and 2,850 m.y. ago from parent materials, including pelitic sedimentary rocks, that are at least 3,120 m.y. old.

LITHOLOGY, MINERALOGY, AND CHEMISTRY

The regionally metamorphosed rocks are divided into different units on the basis of mineralogy and texture. An attempt was made to use definitions of the terms that parallel those applied by other studies in the Beartooth Mountains. The lithologies are defined as follows: (1) granitic gneiss containing less than 10 volume percent mafic minerals, (2) biotite gneiss greater than 10 volume percent, (3) plagioclase gneiss containing less than 5 volume percent of potassium feldspar, (4) amphibolitic gneiss containing amphibole as the dominant mafic mineral, and (5) biotite schist in which biotite-rich rocks have a schistose texture.

Granitic gneiss, the dominant rock type, is a foliated rock with alternating bands of felsic and mafic minerals. Not all the rocks are discernibly banded when observed in the field, but cut, etched, and stained slabs generally show a foliation (fig. 3). The foliation is defined by parallel, elongated feldspar porphyroblasts and parallel muscovite and biotite flakes or by the more readily observed felsic and mafic mineral banding.

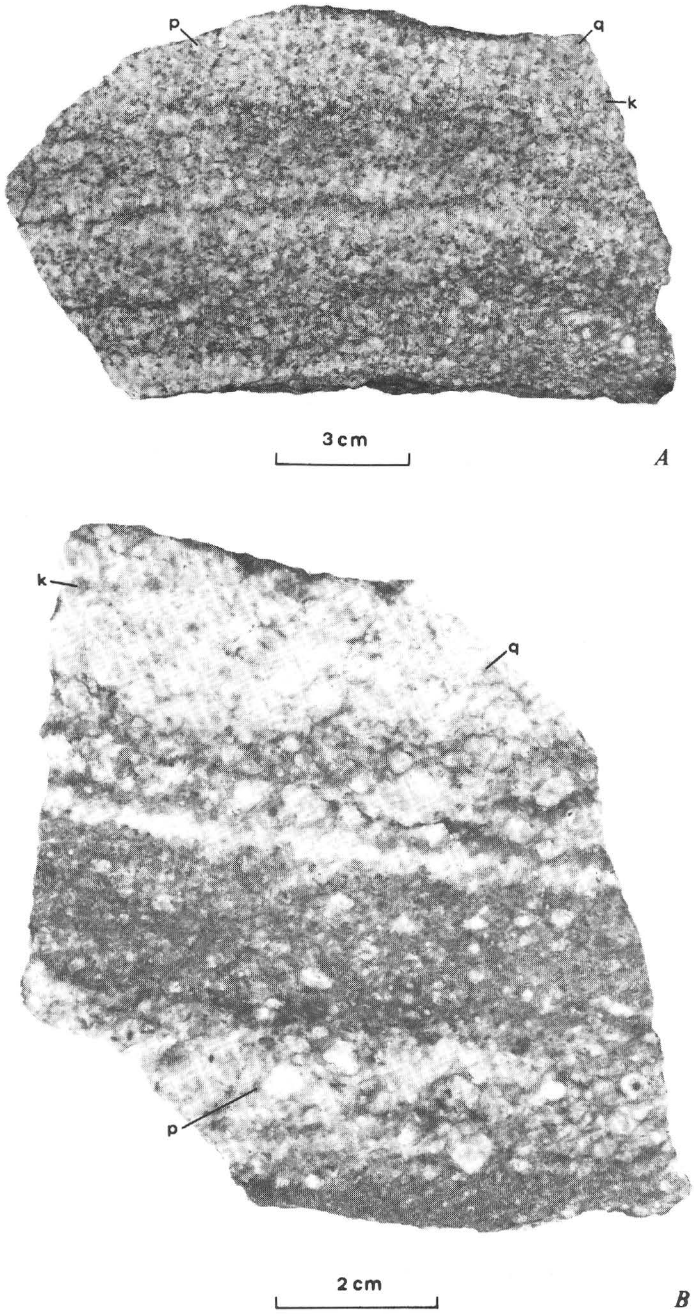

FIGURE 3.—Stained slabs of granitic gneiss showing foliation and banding. Dark mineral is biotite. Light minerals are plagioclase (p), potassium feldspar (k), and quartz (q). *A*, Typical granitic gneiss. *B*, Interlayered granitic gneiss (light bands) and biotite gneiss (dark bands).

Common minerals of the granitic gneiss are plagioclase ($An_{0.7}$-$An_{16.2}$)[1], microcline ($Or_{93.0}$-$Or_{97.9}$)[1], quartz, muscovite, biotite, epidote, and local red garnet. Minor minerals are magnetite, pyrite, zircon, apatite, and the secondary alteration minerals, chlorite and sericite. Table 1 gives modes of typical granitic gneisses; these and additional modes from the study area are plotted in figure 4 and are compared with modes of gneisses from other regions of the regionally metamorphosed rocks. Zoned plagioclase porphyroblasts with cores slightly more calcic than rims, locally with patchy zoning, are typical of this coarse- to medium-grained seriate inequigranular gneiss. Microcline, commonly perthitic, and strained sutured quartz form a finer grained matrix for the porphyroblasts. Microcline, commonly with myrmekite on its margins, has partly replaced plagioclase. The relative abundance of muscovite over biotite appears typical of the granitic gneisses studied.

The modal and chemical data (table 1 and fig. 4) show that the granitic gneiss ranges in composition from quartz monzonite to quartz diorite. Most modes fall within the compositional range of granodiorite and quartz diorite.

Plagioclase gneiss is a medium-grained quartzofeldspathic rock (table 1) that contains similar minerals as the granitic gneiss but has less than 5 volume percent potassium feldspar. Neither muscovite nor red garnet has been observed in the mappable extent of the gneiss in the fault block east of the Stillwater River. Page and Nokleberg (1972) report one analysis of the plagioclase, which generally occurs as porphyroblasts in a matrix of quartz and biotite, as $Or_{0.6}Ab_{98.6}An_{0.7}$.

Biotite gneiss is a foliated rock containing more than 15 volume percent mafic minerals, dominantly biotite, typically surrounding feldspar augen with a sheaflike texture. Common major constituents are plagioclase, quartz, microcline, biotite, and epidote. Hornblende has been reported by Butler (1966) to be a constituent. Apatite is the major accessory mineral, but zircon, sphene, magnetite and secondary alteration products, chlorite, and sericite are present. Table 1 shows modes and analyses of two typical biotite gneisses.

Amphibolitic gneiss is a well-foliated, locally lineated (Butler, 1966) rock containing, by volume, 19–70 percent olive to brown-green hornblende, 10–40 percent plagioclase (An_{35-55}), 4–18 percent brown biotite, and 9–30 percent unstrained quartz, garnet, and locally staurolite. Analyses and modes are given for selected samples in table 1. In outcrop, the amphibolitic gneisses are poorly foliated (appearing homogeneous) to well foliated. The segregation of the more felsic and mafic minerals into bands (varying in thickness from several millimeters to several centimeters) defines the foliation. Some previous workers (for example, Eckelmann and Poldervaart, 1957) have interpreted the amphibolitic gneisses as having

[1]Electron microprobe analyses reported in Page and Nokleberg (1972).

TABLE 1.—*Chemical, spectrographic, and modal analyses of metamorphic rocks in the Beartooth Mountains*

[Chemical analyses by P. L. D. Elmore, James Kelsey, Gillison Chloe, Hezekiah Smith, J. H. Glenn, and Lowell Artis under the supervision of Leonard Shapiro by rapid-rock methods; spectrographic analyses by Chris Heropoulos; modal analyses based on at least 1,000 points counted on a 4×2.5 cm thin section; N=not detected at limit of detection; n.d.=not determined or not looked for; Tr.=trace; L=less than. Montana South coordinates given for locations]

	Granitic gneiss					Biotite gneiss		Plagioclase gneiss	Amphibolitic gneiss		Biotite schist				
	S2269	4BB69	54BR69	3BB70	2FT71	54BB69	19VC69	1FC69	3BB69	13VC69A	2BB69	1BB70	2BB70	56WF70	
Chemical analyses (weight percent)															
SiO_2	73.5	73.1	73.9	74.3	73.9	70.0	57.9	73.5	50.6	47.4	59.7	68.9	69.6	73.8	57.29
Al_2O_3	14.5	14.9	15.4	14.6	15.2	15.7	15.6	14.3	15.8	14.6	16.2	13.6	13.6	11.6	18.50
Fe_2O_3	.08	.48	.80	.37	.68	.90	4.0	.52	2.1	2.7	1.8	1.3	1.0	1.2	3.47
FeO	.84	.44	.28	.28	.48	2.4	3.9	1.8	7.8	10.9	10.9	4.9	4.5	4.0	7.99
MgO	.23	.17	.32	.17	.44	1.3	4.2	.55	7.5	7.9	3.9	3.0	2.8	2.4	5.81
CaO	1.2	.94	1.2	.85	1.1	2.7	6.3	2.0	10.7	10.4	1.5	1.2	2.3	1.5	.34
Na_2O	4.5	3.7	4.1	3.8	3.9	3.6	2.8	4.4	2.6	2.0	1.6	1.5	2.5	1.8	.91
K_2O	3.9	4.1	3.2	4.9	3.4	2.2	1.9	1.4	.44	.61	2.3	2.3	1.6	1.6	2.83
H_2O^+	.32	.87	.79	.65	.89	1.1	1.5	1.0	.85	1.4	1.3	2.1	1.2	1.1	1.97
H_2O^-	.13	.01	.10	.00	.06	.04	.08	.06	.14	.01	.12	.11	.15	.18	.12
TiO_2	.10	.02	.06	.02	.10	.33	.68	.23	.72	1.0	.51	.50	.49	.48	.77
P_2O_5	.09	.02	.02	.03	.02	.07	.46	.05	.10	.06	.11	.01	.08	.05	.05
MnO	.00	.04	.00	.00	.00	.05	.11	.02	.14	.22	.12	.07	.06	.04	.07
CO_2	<.05	.02	.02	.02	.02	.02	.02	<.05	<.05	.02	<.05	.02	<.05	<.05	.00
Total (rounded)	99	99	100	100	100	100	99	100	99	99	100	100	100	100	100.05
Semiquantitative, six-step spectrographic analyses (parts per million)															
B	N	N	N	N	N	N	N	N	N	N	15	N	7	10	n.d.
Ba	1,000	500	1,000	300	70	700	700	700	50	70	300	500	500	300	500
Be	N	1.5	1	N	1	N	1.5	N	N	N	N	N	N	N	1
Co	N	N	N	N	N	7	20	5	30	50	15	20	15	20	35
Cr	10	N	1.5	N	3	20	100	7	300	300	300	200	300	300	720
Cu	2	.7	L.7	.7	L.7	15	30	5	5	30	100	50	50	100	110
La	N	N	N	N	N	N	50	30	N	N	N	N	N	N	30
Ni	7	N	N	N	1.5	10	50	2	150	150	100	150	100	70	250
Pb	30	50	30	100	30	30	15	30	N	N	15	20	30	20	n.d.
Sc	N	3	N	N	N	7	20	N	30	50	20	15	10	10	30
Sr	500	70	200	70	200	300	500	300	100	100	150	100	200	100	40
V	5	N	N	N	7	50	150	30	200	300	100	100	70	70	280
Y	N	15	N	N	N	10	15	N	15	20	15	15	20	10	15
Zr	30	30	50	20	70	100	50	150	20	50	50	150	100	100	120
Ce	N	N	N	N	N	N	N	N	N	N	N	N	N	N	n.d.
Ga	20	15	20	30	20	20	20	20	10	15	15	15	10	15	n.d.
Yb	N	1.5	1	N	N	1	1.5	N	2	3	2	1.5	2	1.5	n.d.
Modal analyses (volume percent)															
Quartz	[1]24.8	36.0	28.3	36.0		37.0		[1]34.2	0.5		28.8	55.2	56.6	57.0	23.0
Potassium feldspar	21.5	14.8	13.1	14.8		7.4		3.3							
Plagioclase	42.1	33.0	33.6	41.0		38.3		48.4	31.6		6.7	2.0	11.1	9.1	3.9
Hornblende									66.5		[2]0.3				
Anthophyllite													6.2		2.5
Cordierite												4.2			1.5
Garnet		1.8									17.5	Tr.	.4	.7	
Staurolite											4.4	6.4		2.1	22.6
Biotite		2.4	1.2	3.3		12.9					41.7	30.3	24.7	30.1	42.1
Muscovite		11.0	18.9	4.2											
Epidote			4.4			1.8									2.3
Zircon		Tr.		Tr.		.1					.4	.2	Tr.	.2	
Apatite				Tr.		.5							Tr.	Tr.	
Sphene						.1									
Opaque minerals		.2	.5	.7		.5			.2		.8	.3	1.0	.8	.1
Mafic minerals	11.9							14.4							2.0
Alteration						1.4									
Unknown									1.2						

[1]Count on etched and stained rock slabs.
[2]Colorless amphibole, probably tremolite.

S2269: 497,800 N., 1,899,060 E.
4BB69: 500,420 N., 1,877,050 E.
54BR69 500,300 N., 1,816,250 E.
3BB70: 502,000 N., 1,874,740 E.
2FT71: 488,540 N., 1,935,580 E.
54BB69: 501,040 N., 1,881,430 E.
19VC69: 501,220 N., 1,895,740 E.
1FC69: 495,840 N., 1,900,070 E.
3BB69: 500,680 N., 1,877,140 E.
13VC69A: 501,340 N., 1,893,080 E.
2BB69: 501,790 N., 1,877,100 E.
1BB70: 503,610 N., 1,877,830 E.
2BB70: 501,490 N., 1,875,740 E.
56WF70: 499,480 N., 1,868,960 E.

a metasedimentary origin, but others (for example, vandeKamp, 1969) have used trends of chemical variations to interpret certain amphibolitic gneisses in the Beartooth Mountains as having a meta-igneous origin. A recent discriminant function analysis of chemical analyses of amphibolites by LaFountain (1971), who attempted to separate sedimentary and igneous sources, emphasized the difficulties of using presently accepted chemical plots to distinguish between origins. Without textural, structural, or other geologic evidence, it appears almost impossible to decide on a sedimentary or igneous origin of

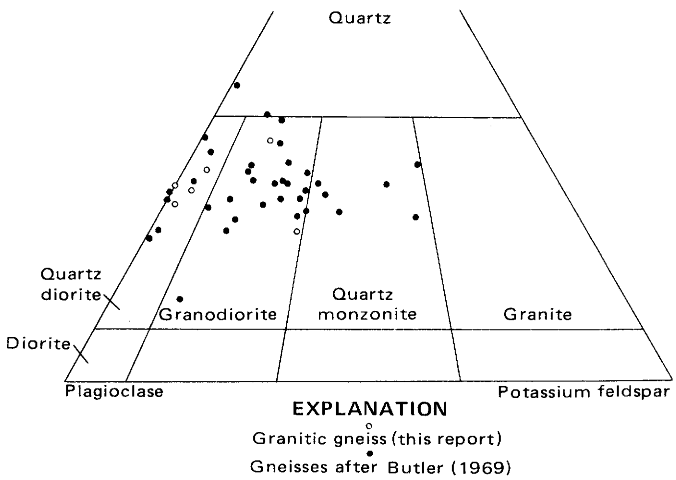

FIGURE 4.—Triangular diagram showing modal data for regionally metamorphosed rocks in the Beartooth Mountains. Compositional names and subdivisions after Bateman, Clark, Huber, and Rinehart (1963).

high grade amphibolites. Because of conflicting intions, the amphibolitic gneiss is not assigned to either a metasedimentary or metaigneous origin at this time.

Biotite schist is a medium- to fine-grained rock with a well-developed foliation defined by biotite flakes that parallel the rare compositional layering. Common minerals are quartz, biotite, plagioclase, garnet, staurolite, cummingtonite, anthophyllite, and cordierite (table 1). Minor minerals are zircon, apatite, magnetite, and chlorite. Some olive-brown biotite-hornblende-quartz-plagioclase schists were mapped with the biotite schists. Elongate lenses of strained quartz, elongate feldspar grains, and biotite grains alined parallel to subparallel form a lepidoblastic to nematoblastic texture in most biotite schists. Plagioclase occurs as grains that are locally zoned. Garnet porphyroblasts, generally filled with inclusions, are locally concentrated into layers, but elsewhere they appear to be scattered in the rock with no indication of a relict compositional layering. Staurolite occurs as fine-grained anhedral branching grains between grain boundaries or as stubby subhedral crystals less than 0.2 mm long. Cordierite is generally partly altered to chlorite and serpentine. Cummingtonite and anthophyllite occur as sheaflike bundles. Observed assemblages in the biotite schist are (1) quartz-biotite-plagioclase, (2) quartz-biotite-plagioclase-garnet, (3) quartz-plagioclase-staurolite, (4) quartz-biotite-plagioclase-garnet-staurolite, (5) quartz-biotite-plagioclase-garnet-cummingtonite, (6) quartz-biotite-plagioclase-garnet-staurolite-cordierite, and (7) quartz-biotite-plagioclase-staurolite-cordierite-anthophyllite. On the basis of the modes and the chemical analyses in table 1, the biotite schist probably is a metamorphosed pelitic sediment.

HORNFELSED METASEDIMENTARY ROCKS IN THE CONTACT AUREOLE OF THE STILLWATER COMPLEX

AREAL EXTENT AND PREVIOUS WORK

Dark metasedimentary rocks lying within the contact aureole of the Stillwater Complex extend southward from the base of the complex in a triangular wedge to the Mill Creek–Stillwater fault (figs. 1, 2). Similar rocks occur below the base of the complex in the Mountain View area, sporadically in the Mt. Wood quadrangle, and in the northeastern part of the Mt. Cowen quadrangle.

Most of the metasedimentary rocks are predominantly massive, fine grained, and structureless, but several other lithologies are present: (1) a finely layered hornfels containing relict sedimentary structures, (2) diamictite, (3) blue metaquartzite, (4) iron-formation, and (5) compositionally layered rocks without observable sedimentary structures. The finely layered hornfels containing sedimentary structures occurs only at the headwaters of Bobcat Creek, whereas other compositionally layered rocks have been found locally along the entire strike length of the aureole. Diamictite (Page and Koski, 1973) has been observed from the Mountain View area westward to the Boulder River. The iron-formation and blue metaquartzite occur only west of the Bluebird Peak area except for rare, isolated inclusions in the quartz monzonite.

Map relations suggest that the above order of lithologies is in stratigraphic order from bottom to top, but the section is complexly deformed. An overall thickness cannot be given for the sequence, but on the East Boulder Plateau, the area between the main Boulder and the East Boulder Rivers, the maximum width of outcrops of the hornfels is about 10 km. Figure 5 shows reconstructed diagrammatic columnar sections for the hornfels at five different localities that are shown in figure 1; reconstructions took into account repetition due to folding and faulting where known, but in the upper part of the Chrome Mountain–Bobcat Creek section the upper massive hornfels may be thickened by folding. There is very little difference in the chemical compositions of various types of layered and massive hornfels (see following parts of this report), and therefore they probably represent a single type of metasedimentary rock. The only distinctive units, the iron-formation, blue metaquartzite, and diamictite, are tentatively correlated as shown in figure 5.

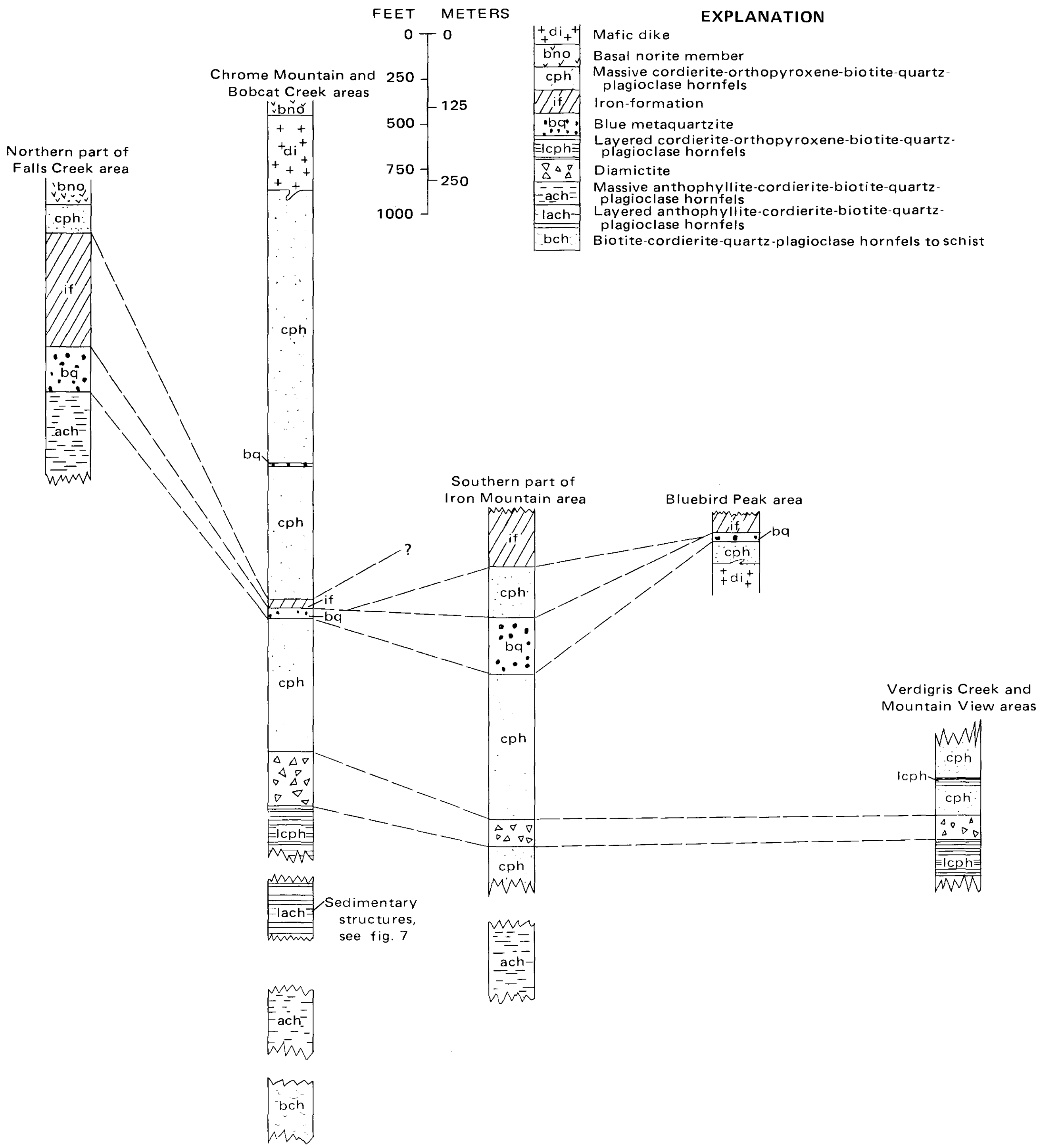

FIGURE 5.—Diagrammatic columnar sections of hornfels. Thicknesses approximate. Dashed lines represent tentative correlations. See figure 1 for location of areas.

Howland (1933, 1954) was one of the first to study these rocks, and he concentrated on exposures in the Mountain View area and the Boulder River valley. Butler (1966) gave a brief description of the hornfels and the aureole, but since then, little new descriptive material has been published.

LITHOLOGY AND PETROGRAPHY

LAYERED HORNFELS

The only known exposures of layered hornfels are in cliffs on the south side of the headwaters of Bobcat Creek (Coordinates: 518,150 N.; 1,834,640 E.) between elevations of 9,250 and 9,750 ft at about 1.6 km south of the base of the Stillwater Complex. These rocks may be correlative with other hornfels without relict sedimentary structures (fig. 5). Figure 6 shows the observed geology and the traverse route for the columnar section (pl. 1) of the layered hornfels in upper Bobcat Creek. The layering along the traverse strikes about east-west and dips between 25° and 40° S., steepening toward the south end of the traverse. The attitudes of layering in the nearby outcrops and the south-facing sedimentary top directions suggest that the traverse is located on the southern limb of an anticline, now broken by faults (see Page and Nokleberg, 1974). The bottom of the section is covered by talus, and the top intruded by a mafic dike that has been sheared and probably faulted. Only between elevations of 9,250 and 9,500 ft were details of the stratigraphy discernible because the upper part of the exposure is highly weathered and covered by lichen. To the west, along strike, only small segments of the stratigraphy detailed in the columnar section are observable because of the sheared and weathered nature of the outcrops.

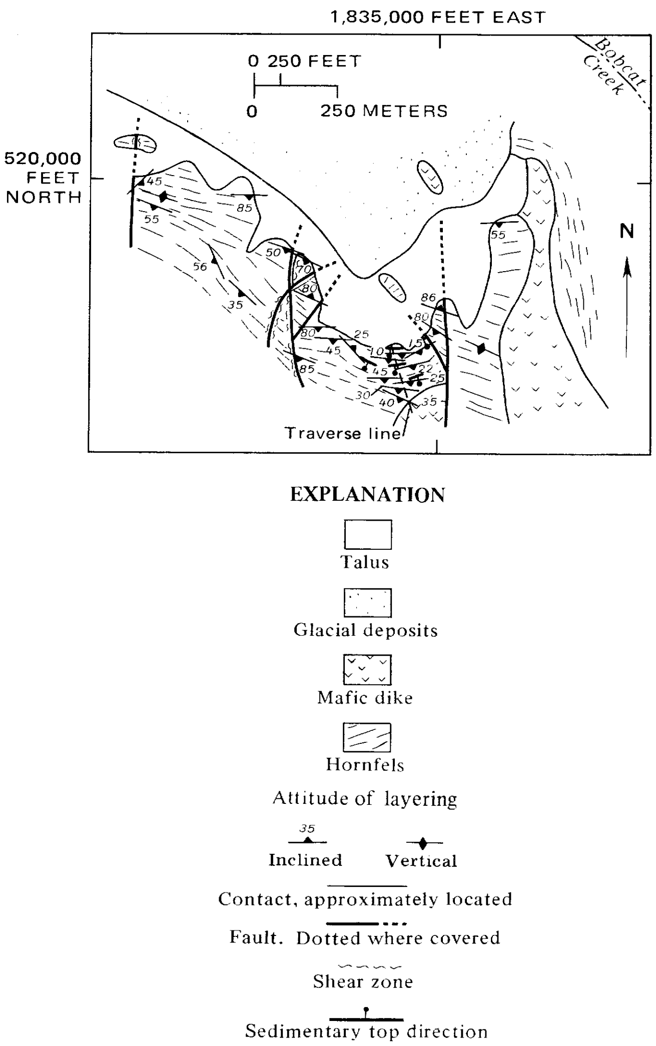

FIGURE 6.—Geologic sketch map of upper Bobcat Creek showing the traverse route of the columnar section (pl. 1). From Page and Nokleberg (1974).

The measured section (pl. 1) consists of 88.4 m of hornfelsed rocks that exhibit well-preserved layering, grain-size changes—mainly of quartz—, and other sedimentary structures. The details of the sedimentary features are well preserved even though the metamorphic grade as indicated by the assemblages of anthophyllite, cummingtonite, cordierite, biotite, plagioclase, and quartz is relatively high. Layering ranges in thickness from less than 3.2 mm to over a meter. Layering less than about 1.27 cm thick is called lamination, 1.27–7.2 cm very thinly layered, 7.62–60.96 cm thinly layered, 60.96–121.92 cm thickly layered, and over 121.92 cm massive. Layering as used in reference to the Bobcat Creek locality refers to relict bedding defined either by the alternating quartz-rich layers with thin biotite layers—analogous to shaly partings—or by layers bounded by discontinuous changes in grain size. Preserved crossbeds marked by biotite and amphibole-rich partings, ripple marks, cut-and-fill channellike structures, and graded layering indicate that the layering is relict sedimentary bedding.

The rocks change upward from laminated and thinly layered fine-grained hornfels to more massive and thickly layered coarse-grained hornfels, suggesting a change in original rocks from shales and mudstones to sandstones. The bladed hornfels in the lower part of the section consists of large anthophyllite or cummingtonite blades or both, up to 7.6 cm long, randomly oriented in a matrix of quartz and cordierite. The unusual texture suggests an original lithology different from the sandstones, shales, and mudstones. The bladed rock may have been silicified carbonate rock that was thermally metamorphosed.

Other dominant characteristics of the metasedimentary rocks portrayed in the columnar section (pl. 1) are fine-scale sedimentary structures such as graded beds and crossbedding and the abundance of thinly bedded rocks—beds are rarely thicker than 0.61 m. Graded bedding, marked by changes in quartz grain size, was observed in several places, especially lower in the section. Both normal and one example of reverse grading were observed (pl. 1). Crossbeds occur near 12.5 m and 19.2 m in the section; the lower occurrence is about 1.2 m thick and consists of individual crossbeds up to 7.6 cm across and generally about 3.8 cm wide (pl. 1). Cut-and-fill structures (fig. 7*A*, *B*) are more common. One structure observed resembled ripple marks; three structures appeared to be slumps. The preservation of these sedimentary structures suggests that most of the hornfelses are metasedimentary rocks that were deposited in water. The fineness of these structures suggests that they formed in a high-energy environment similar to a turbidity current or a surf zone.

Most of the hornfels in the Bobcat Creek section have a coarse to fine granoblastic or hornfelsic texture and contain anthophyllite, cummingtonite, plagioclase, quartz, cordierite, and biotite as major constituents. Accessory minerals are zircon and opaque minerals, generally magnetite. Chlorite and sericite occur as secondary minerals and are abundant in fractures and joints as well as in the more weathered rocks. They replace the ferromagnesium minerals, especially cordierite. Table 3 gives some modes of these rocks; chemical analyses are given by Beltrame (1972). Observed metamorphic mineral assemblages are (1) quartz-biotite-cordierite, (2) quartz-biotite-cordierite-anthophyllite, (3) quartz-biotite-cordierite-plagioclase-anthophyllite, (4) quartz-biotite-cordierite-anthophyllite-unknown mineral, and (5) quartz-biotite-cordierite-plagioclase-anthophyllite-cummingtonite.

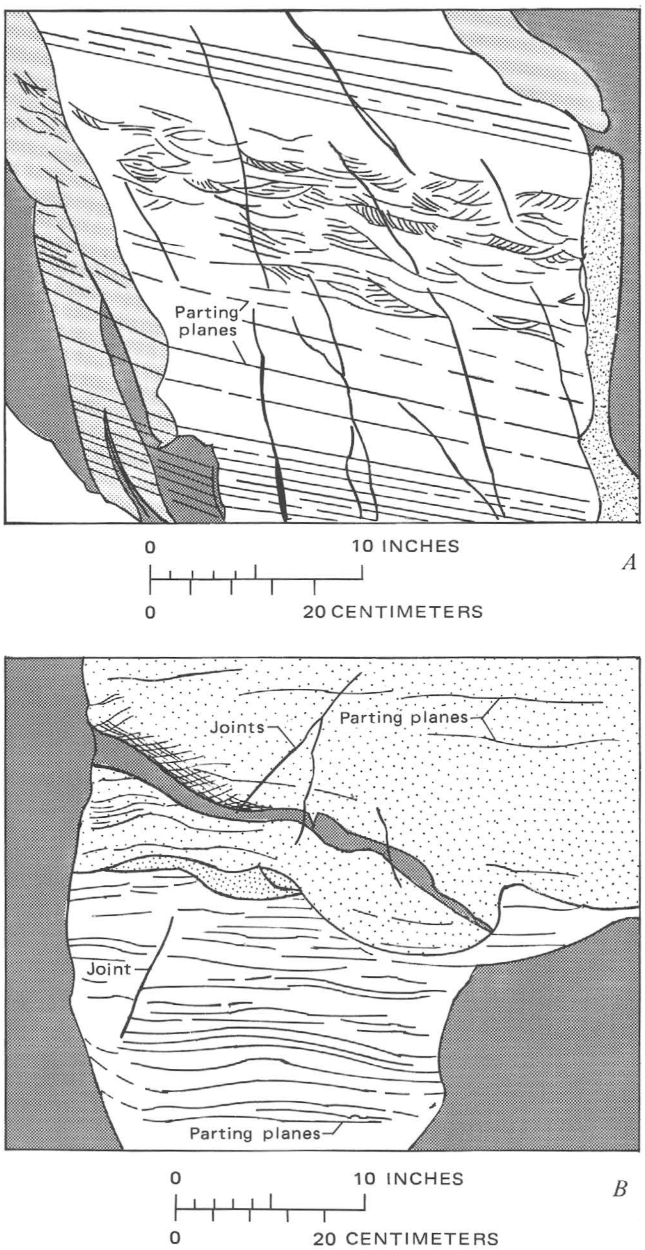

FIGURE 7.—Relict sedimentary structures. *A*, Crossbedding. *B*, Cut-and-fill structures. In *B*, closely spaced dots, fine-grained hornfels; widely spaced dots, medium-grained hornfels. Traced from polaroid photographs.

Each of the minerals contributes its own characteristics to the granoblastic texture of the hornfels. The quartz grains are angular to subangular and range in diameter from a few millimeters to a centimeter. These grains most likely represent relict clastic grains that may have partly recrystallized during metamorphism. Quartz may show sutured contacts or form a mosaic with approximately 120° corners where three grains join depending on the abundance of quartz or quartz-to-quartz contacts in the rocks. Biotite typically occurs in single, subhedral to anhedral books up to 2 or 3 mm long or in clusters of grains with opaque oxides on the margins of the biotite; rarely does the biotite show a preferred orientation, but it is most concentrated in the mafic partings. The dark laminae in the crossbedded rocks consist of biotite. Cordierite forms porphyroblasts 2–5 mm in diameter that enclose inclusions of quartz and biotite, but it also forms interlocking mosaics of finer grains that make up a groundmass for the subangular to angular quartz grains. Cyclic twins are rare; polysynthetic, penetration, and simple twins, common. Either plagioclase, anthophyllite, cummingtonite, two of these minerals, or all three may also be major constituents. Plagioclase is commonly zoned and appears to have relict clastic grain shapes. Anthophyllite and cummingtonite form porphyroblasts that enclose quartz, biotite, and locally cordierite; cummingtonite also occurs as lamellae in and intergrown with anthophyllite. The darker colored partings and laminae recognized in the field consist of anthophyllite, cummingtonite, and biotite with lesser amounts of quartz, cordierite, and plagioclase, whereas the adjacent rocks have more abundant quartz, cordierite, and plagioclase.

METAMORPHOSED DIAMICTITE

Metamorphosed diamictite is found in exposures scattered along a northwest-trending belt for 22 or 24 km (Page and Koski, 1973). Some occurrences are adjacent to the Basal zone of the Stillwater Complex, whereas others are almost 1.6 km from the Basal zone. Owing to the complexity of the geology and the sparsity of outcrops, continuity of the diamictite over the trend distance cannot be proved, but within areas of continuous outcrops and simple structure, units of diamictite 30.5–61 m thick can be traced in the hornfelsed rocks. Interfingering relations between the different rock types and the diamictite were not observed.

The diamictite consists of a quartz-cordierite-biotite-plagioclase-orthopyroxene matrix enclosing on the average 10–15 percent poorly sorted rock megaclasts with diverse shapes, sizes, angularity, lithologic types, and textures. Megaclasts consist of fragments with layered massive blue-gray metaquartzitic, gneissic, schistose, granitoid, and volcanic textures and lithologies. They range in size from microscopic, single grains of quartz to room-sized boulders, but the median size is between 15 and 18 cm. Most of the megaclasts are rectangular or elliptical in shape but also show two-dimensional shapes of triangles, pears, cigars, squares, trapezoids, pentagons, and parallelograms. The megaclasts are dominantly subround to subangular. Major minerals in the megaclast material are the same as in the matrix material. Further details on the megaclasts are given by Page and Koski (1973).

Crude layering is present in the matrix material but is rarely observed in the field. Slabbed and etched surfaces show crude layering, and a few dropstones (megaclasts that have disturbed the underlying layers and were later covered by material) are observed.

The diamictite matrix consists by volume, of 20–40 percent quartz, 30–40 percent cordierite, 15–20 percent orthopyroxene, 5–10 percent plagioclase, 0.5–3 percent biotite, less than 3 percent sulfide and oxide minerals, and minor amounts of zircon, garnet, secondary chlorite, and sericite. The subrounded to subangular quartz grains average less than a millimeter in diameter (0.2–3.5 mm) and locally are composed of more than one quartz crystal. Some quartz grains are enclosed by sieve-textured orthopyroxene and anhedral masses of twinned and untwinned cordierite. The orthopyroxene and cordierite could be metamorphic equivalents of various combinations of chlorite and clay minerals that may have composed the parent diamictite matrix.

BLUE METAQUARTZITE

Blue metaquartzite occurs as thin layers in the metasedimentary hornfels but forms a very distinctive rock, resistant to weathering and fairly easy to trace by its float. Occurrences are limited to the hornfels found west of Bluebird Peak and within 1.6 km from the base of the Stillwater Complex, except for thin (a few centimeters to a couple of meters thick) blue metaquartzite layers in the Mountain View area and isolated outcrops in Nye Basin. Outcrop widths and thickness of the metaquartzite unit, where measurable, are on the order of 15.2–30.5 m but range from less than 3.0 m to over 305 m. Rarely can a layer or lens of blue metaquartzite be traced or extended for more than about 762 m along strike.

South of Iron Mountain and Chrome Mountain where the mapping was done by tracing float, the connection of isolated lenses or layers of blue metaquartzite is difficult. The series of lenses or layers could be interpreted as a single horizon that has been folded to give the repetitions found in outcrop or as several different horizons interlayered in the metasedimentary hornfels. Between the Chrome Mountain area and the Boulder River the blue metaquartzite layers seem to define a moderately continuous single horizon that is complexly faulted and folded. This suggests that the similar repetition between Iron Mountain and Chrome Mountain may also result from folding and faulting.

The blue metaquartzite is in contact with massive hornfels on both sides or with massive hornfels and iron-formation. Contacts are generally obscured, but where observed, the blue metaquartzite appears to have sharp contacts with the massive hornfels and a gradational contact over a few inches or a foot with the iron-formation. A chlorite-quartz schist occurs locally as interlayers in the blue metaquartzite (for example, at coordinates: 523,980 N., 1,833,500 E.). The chlorite-quartz schist appears to be a highly sheared and altered variety of hornfels. The schist interlayers apparently acted as gliding planes on which the quartzite folded and in so doing were highly sheared and possibly hydrothermally altered.

Over 98 percent by volume of the metaquartzite is quartz that has strong undulatory extinction and sutured contacts. Quartz grains average about 7 or 8 mm in diameter but attain a maximum diameter of 1.5 cm. Locally (about coordinates: 524,000 N.; 1,833,000 E.) in weathered outcrops the quartz appears to form rounded pebbles, but in thin section, the quartz grains show sutured contacts. The rock may be a metamorphosed quartz pebble conglomerate. Chlorite, limonite, zircon, and opaque minerals form the other 2 percent of the metaquartzite. The major minerals in the schistose interlayers are chlorite, quartz, epidote, tremolite, and opaque minerals. Generally the metaquartzite is highly fractured, and the fractures are coated by iron oxides and chlorite.

IRON-FORMATION

Metasedimentary rocks composed of layers enriched in magnetite and interlayered with quartz and ferromagnesium mineral-enriched layers were mapped as iron-formation. The boundaries of the unit were chosen and defined by the appearance of a strongly magnetic layer in either the hornfels or metaquartzite. The iron-formation is in many places near and locally in contact with blue metaquartzite, such as in the area between Chrome Mountain and the Boulder River. Layers and lenses of iron-formation crop out from west of the Bluebird Peak to a point west of the Boulder River within 1.6 km of the base of the Stillwater Complex. The best exposures occur above the Great Falls Creek trail (coordinates: 539,370 N.; 1,816,940 E.) west of the Boulder River where the alternating layers of silicate and magnetite-rich material can be seen in the cliffs. On the ridge north of Bobcat Creek (coordinates: 526,680 N.; 1,828,650 E.) well-exposed layers are isoclinally folded. Elsewhere the exposures are generally poor. Iron-formation was found in only two localities east of the Bluebird Peak. On north side of the ridge between Flume and Nye Creeks (coordinates: 502,340 N.; 1,909,370 E.) iron-formation is in contact with hornfels and occurs as an inclusion in the medium-grained quartz monzonite. In Nye Basin a small isolated outcrop of iron-formation (coordinates: 501,100 N.; 1,913,800 E.) was observed near the basal contact of the Stillwater Complex.

Outcrop widths range from a few meters to over 305 m but usually are about 60 m wide. Enough data were found in about 14 localities to reconstruct crudely the thickness of the iron-formation. Figure 8 shows the variation in thickness along the extent of the unit. The outcrop widths of iron-formation probably are not true stratigraphic thickness but may represent repetition by folding and faulting; for example, the width of iron-formation shown in section 14 (fig. 8) west of the Boulder River probably represents units repeated by folding. No stratigraphic top or bottom is inferred by the orientation of the sections, but in all sections the Stillwater Complex lies stratigraphically above the rocks shown in the columns. One of the few places below the complex where a large volume of continuous iron-formation might be present is from south of Blakely Creek to a point west of the Boulder River. If the iron-formation is nearly continuous in this area, its area would be about 4.8 km long by about 122 m wide.

Figure 9 shows a typical section of iron-formation as intersected in a drill hole near Crescent Creek. No stratigraphic top nor bottom and no true thickness are implied by the section. The section illustrates the interlayered nature of the quartz-biotite-cordierite-orthopyroxene hornfels with the iron-formation and the nature of the contact of the iron-formation with the blue metaquartzite. The contact with the metaquartzite is sharp only if the thin quartz-rich layers in the iron-formation are disregarded. The section also illustrates the variation between massive and thinly layered lithologies in the unit. Layers are generally 1.6 mm–7.6–10.2 cm thick; most magnetite layers are between 1.6 mm and 1.9 cm thick. Figure 10 shows thinly layered iron-formation in thin section. The layers of quartz and magnetite are graded in composition; the parts that are richer in magnetite appear to show grading caused by proportions of magnetite and quartz.

Surface outcrops of the iron-formation tend to be deeply weathered, and so the lithologic description of the unit is based on drill core from the Iron Mountain and Crescent Creek areas supplemented by outcrop samples. Core samples of the iron-formation are also altered; the mafic minerals are replaced partly by chlorite and amphibole. Major minerals are magnetite, quartz, orthopyroxene, cordierite, clinopyroxene, and garnet in the iron-formation that was metamorphosed to pyroxene hornfels grade and quartz, magnetite, cordierite, anthophyllite, and cummingtonite in the iron-formation of the hornblende-hornfels facies. Locally sulfide minerals are present as minor and accessory constituents. Peoples (1932) and Howland (1933) both reported the presence of fayalite, but none has been identified in the present study.

Secondary minerals include chlorite, talc, and amphiboles as alteration products after mafic silicate minerals. Carbonate and sulfide minerals occur in veins and fractures. Quartz occurs as subrounded to subangular grains, locally with sutured contacts, and locally contains a large number of inclusions of pyroxene and amphibole in the centers of the grains. The pyroxenes, amphiboles, and garnet form poikiloblastic crystals, with orthopyroxene locally attaining 2 cm in diameter. Both pyroxenes have exsolution lamellae.

For chemical analysis, six samples of iron-formation from surface exposures were selected on the basis of two criteria: (1) small amounts of alteration products relative to talc, amphiboles, and other minerals and (2) a subjective appraisal of how well

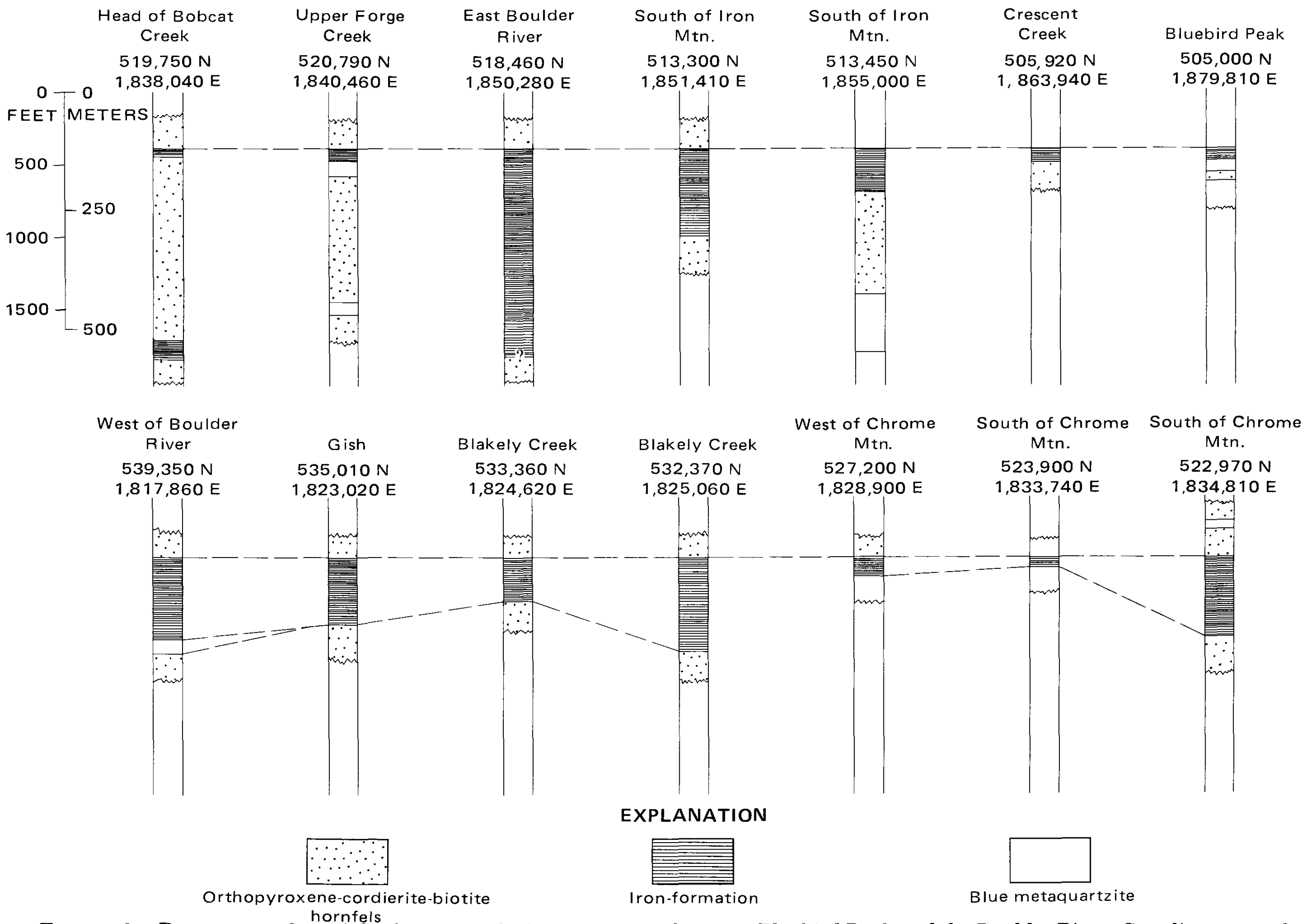

FIGURE 8.—Reconstructed partial columns for the iron-formation between Bluebird Peak and the Boulder River. Coordinates are from near the contact of the iron-formation with other units. All sections constructed perpendicular to strike of units.

the sample represented typical rocks from the unit. Table 2 lists rapid-rock chemical, semiquantitative spectrographic, and gold, sulfur, and rubidium quantitative analyses. For completeness, the analysis of a fayalite rock collected by Peoples (1932) is also included. The relatively low content of Al_2O, CaO, Na_2O, and K_2O and the significant content of MgO and SiO_2 reflect chemically the quantities of quartz, pyroxenes, and amphiboles present in the samples. The chemistry of the major elements in the iron-formation appears to be very similar to other magnetite-rich iron-formations of Precambrian age as summarized by James (1966, p. W21); the content of minor elements falls within the range of minimum and maximum concentrations given by James (1966, p. W45).

COMPOSITIONALLY LAYERED HORNFELS AND MASSIVE HORNFELS

Most of the exposed hornfels below the base of the Stillwater Complex consists of fine- to medium-grained apparently unlayered or massively layered rocks that are called massive hornfels in this report. Locally, compositionally layered hornfels are present, but no relict sedimentary features have been observed in these rocks. Although they are similar in mineralogy, petrology, and chemistry to the layered hornfels with sedimentary structures in the Bobcat Creek section, they are not correlated because of lack of mappable stratigraphic units upon which to base a correlation. During the 1:12,000-scale mapping, massive and compositionally layered hornfels without sedimentary structure were not separated as individual units. In many places, the lichen covering and the weathering of the outcrops of hornfels obscure and preclude the recognition of layering, and thus my estimate of the volume of massive hornfels in the area may be excessive. Indeed, the words "massive hornfels" may be a misnomer and may only indicate the obscurity of layering. Areas in

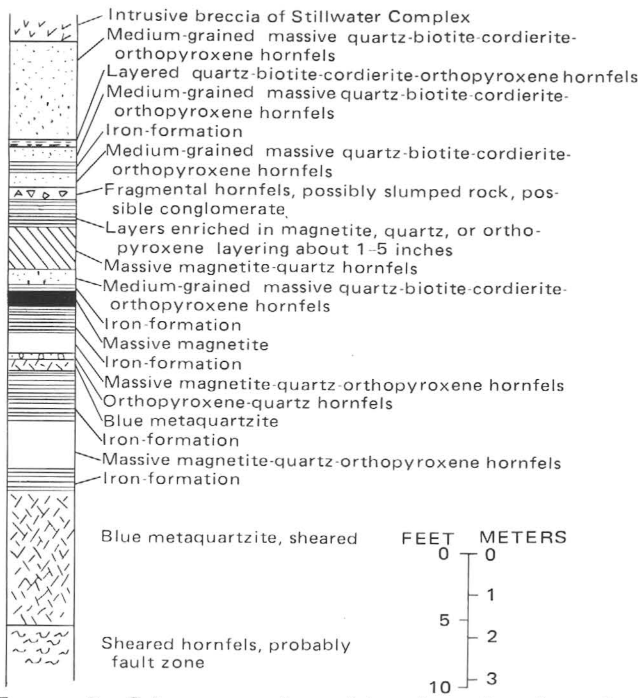

FIGURE 9.—Columnar section of iron-formation from the Crescent Creek area. Thicknesses are drilling widths.

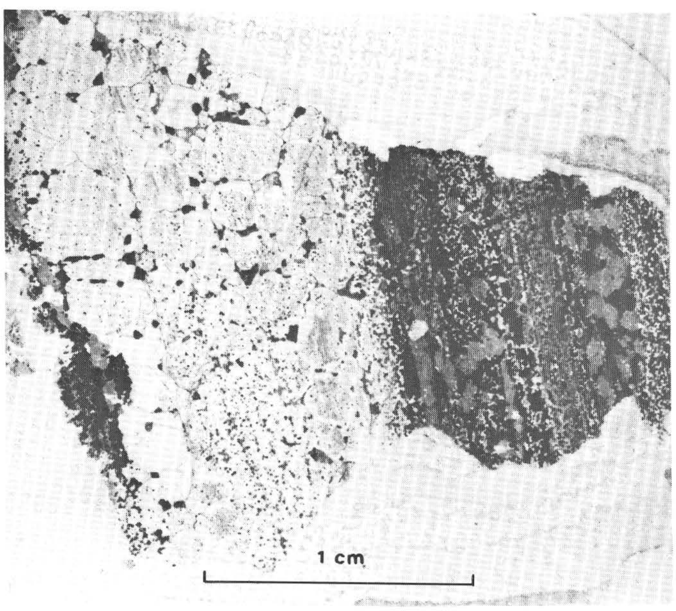

FIGURE 10.—Thin section showing graded bedding. Black mineral, magnetite; light mineral, quartz. Sample CC-1/458.

which compositional layering is well developed include (1) the Mountain View area, both north and south of Verdigris Creek (coordinates: 502,100 N.; 1,899,900 E.), (2) the area south and west from Iron Mountain, exposed mainly as blocks in float (coordinates: 518,240 N.; 1,852,880 E.), and (3) west of the Boulder River, south of Great Falls Creek (coordinates: 527,070 N.; 1,819,500 E.).

TABLE 2.—*Chemical and spectrographic analyses of iron-formation*

[Rapid-rock analyses by Hezekiah Smith; spectrographic analyses by R. E. Mays]

	55IM69A	55IM69B	51BR69A	26BR71	27BR71	29BR71	Peoples
Chemical analyses (weight percent)							
SiO_2	42.1	38.6	76.4	45.6	46.3	37.2	31.02
Al_2O_3	2.2	2.3	1.6	1.7	19.7	2.2	.72
Fe_2O_3	23.6	28.4	4.1	8.8	2.7	28.1	5.75
FeO	26.8	25.4	12.7	30.6	17.1	27.4	58.97
MgO	3.0	2.6	.81	11.3	10.8	3.2	1.44
CaO	.52	1.1	3.5	.31	.40	1.1	1.04
Na_2O	.01	.00	.05	.00	.56	.01	....
K_2O	.05	.00	.25	.07	.44	.04	....
H_2O^+	1.1	1.2	.83	1.4	1.6	.80	.83
H_2O^-	.22	.25	.03	.05	.05	.04	....
TiO_2	.00	.04	.00	.04	1.2	.06	....
P_2O_5	.01	.02	.01	.00	.00	.00	....
MnO	.02	.05	.11	.23	.14	.08	....
CO_2	.03	.02	.06	.04	.02	.02	....
Sum	100	100	100	100	101	100	99.77
S[1]	.005	.01	.04	.03	.09	.02	....
Semiquantitative spectrographic analyses (parts per million)							
Mn	200	500	1500	1500	1000	700	....
Ba	7	15	20	[2]N	10	3	....
Co	N	N	N	15	70	N	....
Cr	10	20	5	300	1000	15	....
Cu	30	30	7	20	150	3	....
Ni	7	7	5	70	500	5	....
Sc	N	N	N	30	30	N	....
V	10	10	N	100	300	10	....
Zr	N	N	N	N	20	20	....
Au[3]	.0129	.0069	.0114	.0173	.0226	.0084	....
Rb[4]	<20	<20	<20	<20	<20	<20	....

[1]Total S and S determined by X-ray fluorescence; analyst, B. P. Fabbi.
[2]N, not detected at limit of detection.
[3]Au analyzed radiochemically; analyst, L. J. Schwarz.
[4]Rb determined by X-ray fluorescence; analyst, B. P. Fabbi.

Sample	*Description and location*
55IM69A	Iron-formation; quartz, magnetite, orthopyroxene, talc, amphiboles as alteration. Montana South coordinates: 517,490 N.; 1,855,540 E.
55IM69B	Iron-formation; quartz, magnetite, orthopyroxene, clinopyroxene, blue-green amphibole. Montana South coordinates: 517,490 N.; 1,855,540 E.
51BR69A	Iron-formation; quartz, magnetite, orthopyroxene, amphiboles as alteration. Montana South coordinates: 536,380 N.; 1,820,970 E.
26BR71	Iron-formation; magnetite, orthopyroxene, amphiboles, moderately altered. Montana South coordinates: 539,380 N.; 1,816,960 E.
27BR71	Iron-formation; quartz, magnetite, orthopyroxene, cordierite, amphiboles; Montana South coordinates: 539,380 N.; 1,816,850 E.
29BR71	Iron-formation; quartz, magnetite, clinoamphibole, anthophyllite; Montana South coordinates: 539,260 N.; 1,816,690 E.
Peoples	Fayalite rock, Blakely Creek, Mont., analyst A. H. Phillips (Peoples, 1932, p. 31).

Layers range in thickness from less than ≈1 cm to more than ≈61 cm; most of the layering is less than ≈15 cm thick. Layers are composed of varying proportions of the three light-colored minerals, quartz, cordierite, and plagioclase, and the dark-colored minerals, orthopyroxene without exsolution lamellae, biotite, anthophyllite, and cummingtonite. Figure 11 shows examples of the compositional layering in sawed slabs.

Massive and compositionally layered hornfels occurs in both the pyroxene hornfels and hornblende

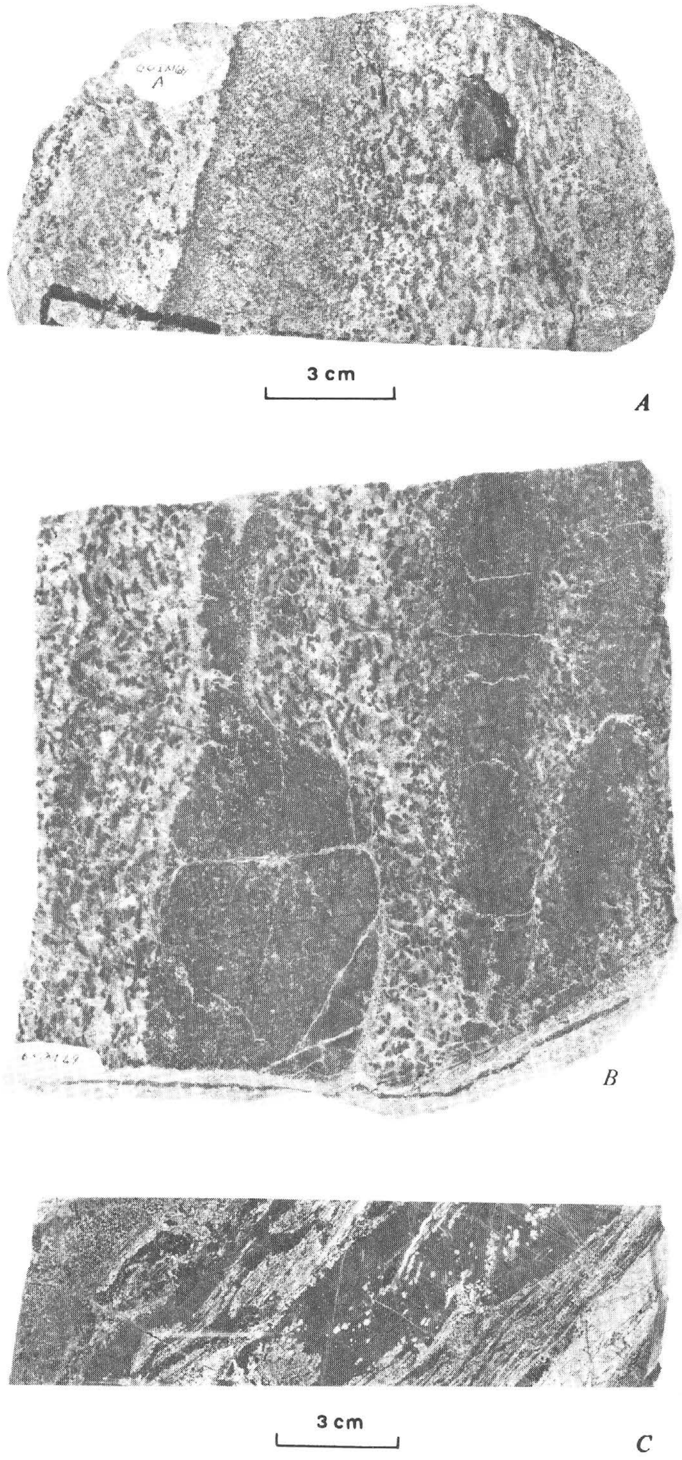

FIGURE 11.—Examples of compositional layering in metasedimentary rocks. *A*, Weathered surface. Dark minerals are orthopyroxene and minor biotite. Light minerals are quartz, cordierite, and minor plagioclase. *B*, Sawed slab. Black mineral is orthopyroxene; dark-gray mineral is cordierite; light-gray to white minerals are plagioclase and quartz. Slab is 18 cm wide. *C*, Hydrofluoric acid etched slab. Dark minerals are orthopyroxene and cordierite; light minerals are plagioclase and quartz.

hornfels facies parts of the Stillwater aureole. Mineral assemblages of both hornfels types in the hornblende hornfels facies are similar and typified by the mineral assemblages in the Bobcat Creek section, and the description of hornblende hornfels facies rocks need not be repeated here. The mineralogy of massive and compositionally layered rocks found within the pyroxene hornfels facies is discussed subsequently.

By far the most common mineral assemblage within the area mapped as rocks of the pyroxene hornfels facies (Page and Nokleberg, 1974; Page and others, 1973a, b) is the quartz-cordierite-plagioclase-orthopyroxene-opaque mineral assemblage with or without biotite. Most of the layered and massive hornfels is composed of various proportions of these minerals. Table 3 lists the observed mineral assemblages and the number of thin sections in which a particular assemblage was found. Most of the assemblages, such as those with and without quartz or biotite, can be found interlayered and interlensed on the scale of a thin section. Modes are given in table 4. Other modes are combined with these data and shown in figure 12. Most rocks consist of more than 40 percent by volume of cordierite, orthopyroxene, and biotite and rarely more than 15–20 percent of plagioclase (fig. 12*A*). Cordierite is far more abundant than orthopyroxene or biotite (fig. 12*B*).

The fine- to medium-grained layered and massive hornfels has equigranular to inequigranular hornfelsic or granoblastic texture and weathers to a brown surface. Subangular to subrounded quartz grains and subhedral to anhedral plagioclase grains up to 4 or 5 mm in diameter are generally enclosed in a matrix of cordierite, orthopyroxene, and biotite. Locally quartz forms large poikiloblastic grains that appear as matrix material for subhedral to euhedral cordierite crystals, and plagioclase forms close-packed anhedral masses and layers with a mosaic texture. Orthopyroxene occurs as porphyroblasts with subhedral crystal margins poikiloblastically

TABLE 3.—*Metamorphic mineral assemblages and number of occurrences in thin sections of rocks of the pyroxene hornfels facies associated with the Stillwater Complex*

[Cord, cordierite; Plagio, plagioclase; Opx, orthopyroxene]

Biotite present		Biotite absent	
Quartz and iron ores present			
Cord+Plagio+Opx	54	Cord+Plagio+Opx	3
Cord+Plagio	10	Cord+Plagio	1
Cord+Opx	12	Cord+Opx	4
Plagio+Opx	1	Plagio+Opx	1
Cord	3		
Total	80	Total	9
Quartz absent; iron ores present			
Cord+Plagio+Opx	25	Cord+Plagio+Opx	1
Cord+Plagio	4	Cord+Opx	4
Cord+Opx	22		
Cord	3		
Total	54	Total	5

enclosing biotite, cordierite, ore minerals, plagioclase, and quartz. Locally, orthopyroxene forms anhedral branching grains in the interstices between quartz, plagioclase, and cordierite. In finer grained rocks, orthopyroxene occurs as subhedral to anhedral granular grains, generally less than a millimeter in diameter. There are no obvious correlations between mineral assemblage, rock composition, or distance from the Basal zone of the Stillwater Complex with the textures exhibited by orthopyroxene. Cordierite occurs in five different ways. About a kilometer from the contact between hornfels and the complex, cordierite is found as cyclic twinned porphyroblasts full of inclusions of quartz, biotite, and opaque minerals. Nearer the Basal zone it occurs as euhedral to subhedral crystals enclosed in a matrix of quartz, but more frequently cordierite occurs as close-packed anhedra with approximately hexagonal-shaped cross sections that form a mosaic of grains in which three grains make about 120° corners between edges. The mosaic of cordierite grains forms the matrix for quartz and plagioclase. Locally such a cordierite matrix contains scattered grains or lenses of more euhedral to subhedral grains. Cordierite also forms clots of grains that in polarized light look like fan-shaped aggregates with groups of crystals fanning out in two directions. Biotite occurs in at least three distinctive ways: (1) as subhedral flakes randomly oriented, (2) as poikiloblastic grains with subhedral margins enclosing quartz and cordierite, and (3) as coatings or along margins of iron-oxide minerals (mainly magnetite). The last occurrence is common in rocks very rich in cordierite where magnetite with biotite coatings forms fine inclusions in the centers of the cordierite crystals. Opaque minerals occur as inclusions in all minerals, as discrete grains along mineral boundaries, and in the corners where three grains meet. The quartz and plagioclase probably are relict clastic grains, whereas the matrix may be recrystallized clastic or diagenetic components such as clay and chlorite. The matrix more likely represents a chemically precipitated component or material of both clastic and chemical origin.

Plagioclase compositions range from $Ab_{40}An_{60}$ to $Ab_{70}An_{30}$ in most hornfels as determined optically. Orthopyroxene compositions average 62.1 (36 determinations) and range from about En_{50} to En_{74} using Himmelberg and Jackson's (1967) X-ray method. These determinations probably can be considered to be only crude estimates, since Jackson's technique was developed primarily for orthopyroxenes in the Stillwater Complex and the orthopyroxene in the hornfels appears to be slightly different because it rarely has any type of exsolution lamellae. Biotite is generally dark brown, but no estimates of its composition have been made yet. The composition of cordierite is difficult to estimate (see Deer and others, 1962 for summary).

Iiyama in 1956 suggested that the $(Fe^{+2}+Mn)/(Fe^{+2}+Mn+Mg)$ ratio could be estimated from the 2θ diffraction angle of the (004) with $CuK\alpha$ radiation. Miyashiro, Iiyama, Yamasaki, and Miyashiro (1955) and Miyashiro (1957) found that cordierite forms a continuous series of orthorhombic pseudohexagonal structures by the distortion of the hexagonal structure. Miyashiro defined a distortion index that has been found to be independent of MgO-FeO and Al_2O_3-SiO_2 substitution (Harwood and Larson, 1969). Therefore, Iiyama's (1956) technique appeared to be applicable, and early in the study of the Stillwater hornfels, Iiyama's (1956) study of the optical properties and unit cell dimensions of cordierite was reviewed and his X-ray data used to refine unit cells by a least-squares computer program (Evans and others, 1963). In most specimens close agreement between the refined cells and those calculated by Iiyama was found. In testing his method, material was obtained from Reinhardt who published 15 cordierite mineral analyses, but without calculated mineral formulae and X-ray data (Reinhardt, 1968, table III, p. 461). In order to check the purity of Reinhardt's (1968) samples, mineral formulae of the general type $Al_3(Mg, Fe^{+2})_2\ Si_5AlO_{18}$ were calculated from his analyses using the hydrogen equivalent method of Jackson, Stevens, and Bowen (1967), and X-ray work was done on splits of samples donated by Reinhardt (samples W-53, D-34, and R-124). Least-squares refined unit cells were calculated from diffraction data that were measured using quartz as an internal standard. Table 5 lists the calculated formulae and unit cell data for these specimens. The right-hand column gives a refined unit cell for one Stillwater cordierite specimen that was separated for analytical work. This was never completed because of the difficulty in removing fine magnetite and biotite inclusions.

A combination of Iiyama's (1956) and Reinhardt's (1968) data, especially the $CuK\alpha$, 2θ for d(004) of cordierite, and the$(Fe^{+2}+Mn/Mg+Fe^{+2}+Mn)$ ratio, allows a determinative curve to be drawn. Iiyama (1956, p. 390) claimed an error of ±10 percent, but I consider the ratios for Stillwater cordierite obtained by this curve as nominal values that show relative differences and will eventually be refined by electron microprobe studies. Figure 13 gives the 2θ of d(004) versus $(Fe^{+2}+Mn/Mg+Fe^{+2}+Mn)$ X 100 working curve and composition ranges of some cordierite specimens from rocks of the pyroxene hornfels facies. The ratios of $(Fe^{+2}+Mn/Mg+Fe^{+2}+Mn)$ X 100 in Stillwater cordierite range from about 50 to 10, but most are between 20 and 30.

Other metamorphic mineral assemblages (table 6) than those shown in table 2 are found locally in some

TABLE 4.—*Modal analyses, in volume percent, of*

[Modes based on at least 1,000 points on a 4 x 2.5-cm thin section; locations

	53FC69A	MV-KB	MV-KC	MV-KD	[1]SR-5	[1]SR-8	[1]SR-10	[1]SR-12	[1]SR-17	52NB69	60IM69C	58IM69
Quartz	10.8	0.4	41.8	38.1	2.0	10.8	23.8	23.6	9.8	...	2.4	...
Potassium feldspar	...	16.5	...	...	...	...	...	...	...	...	...	...
Plagioclase	6.6	1.8	8.5	5.8	n.d.	2.2	5.8	5.2	73.0	4.3	3.1	...
Orthopyroxene	13.6	11.5	8.4	6.6	25.4	17.2	11.2	7.8	12.2	41.3	16.6	39.0
Anthophyllite	...	...	...	...	...	...	...	...	...	...	...	...
Cordierite	34.4	49.1	36.1	45.6	58.2	47.5	47.8	44.0	n.d.	49.8	67.8	55.8
Biotite	14.0	17.4	3.4	1.8	12.0	20.0	10.2	17.8	5.0	1.6	8.6	...
Chlorite	...	...	...	...	...	...	...	...	...	...	...	...
Zircon	...	...	...	...	...	...	...	...	...	...	...	...
Sphene	...	...	...	...	...	...	...	...	...	...	...	...
Zoisite	...	...	...	...	...	...	...	...	...	...	...	...
Opaque minerals	4.0	3.3	1.8	3.3	2.4	2.3	1.2	1.6	n.d.	3.0	1.5	5.2
Calcite	...	...	...	...	...	...	...	...	...	...	...	...
Alteration products	16.6	...	...	...	...	...	...	...	...	...	...	...
Unidentified	...	...	...	...	...	...	...	...	...	...	...	...

[1]500 counts, Beltrame (1972, p. 17).
[2]500 counts, Beltrame (1972, p. 30).
[3]Leucoxene.

samples of pyroxene hornfels from the exposures south of the east half of the complex. Most of the samples containing these assemblages were found within 30 meters, and many within a meter, of intrusive quartz monzonite or aplite, except for rare occurrences of spinel in inclusions in the Basal zone of the complex. The assemblage quartz+biotite+cordierite+orthopyroxene+plagioclase+microcline+opaque minerals is by far the most common assemblage in this environment. The assemblages in table 6 are those common to all the pyroxene hornfels with addition of microcline, spinel, garnet, or both microcline and spinel. Quartz, plagioclase, cordierite, orthopyroxene, biotite, and opaque minerals show the same textures as they do elsewhere in the pyroxene hornfels.

Microcline, with patchy tartan twinning, locally perthitic, forms porphyroblasts that poikiloblastically enclose the other minerals. The zones of microcline development are 9.1-15.2 m wide and appear to die out away from the siliceous intrusive rocks. In thin section, microcline poikiloblasts are limited to lenses and bands usually less than half a centimeter wide. In one sample from within 61 cm of a contact of hornfels with an aplite, brown hornblende is developed at the contact of microcline and orthopyroxene; the more common phenomenon is a sharp microcline-orthopyroxene contact. Grain shapes and the occurrence of the microcline suggest that locally it has pseudomorphosed cordierite.

The green to olive-green spinel is probably a hercynite and has two modes of occurrence. The less common occurrence (observed once) consists of euhedral to subhedral crystals of spinel, less than half a millimeter long, at the corner joints of three cordierite grains. This was found in the assemblage biotite+cordierite+orthopyroxene+plagioclase+spinel+opaque minerals, which occurs in a hornfels inclusion in the Basal norite member (fig. 14*A*). The more common occurrence consists of fine-grained euhedral to subhedral clots of spinel crystals forming a wormy texture with cordierite (fig. 14*B*). The clots are less than 2 mm in size on the average and contain spinel crystals a few tenths of a millimeter in diameter. Since rocks containing this texture occur in contact with either aplite dikes or quartz monzonites, the spinel probably resulted from contact metamorphism by the quartz monzonites and not from the thermal aureole of the Stillwater Complex. Poikiloblasts of garnet were found in very few hornfels samples (table 6) and only in quartz-biotite-cordierite-plagioclase hornfels that occurs near aplite dike contacts. Their development is probably also related to the later intrusive event.

The spatial relation of these assemblages with the intrusive quartz monzonite sequence is strengthened by the occurrence of inclusions in the aplite dikes of cordierite-spinel clots, cordierite-garnet inclusions, xenocrysts of cordierite and garnet, and an inclusion containing the assemblage cordierite-spinel-sillimanite. The only known occurrence of aluminosilicates is in hornfels inclusions in the aplites.

CHEMICAL CHARACTERISTICS OF THE METASEDIMENTARY ROCKS

The hornfelses have chemical compositions similar to clastic rocks, but with important differences, as is shown by the chemical analyses (table 7). Analyses by Beltrame (1972) from the Mountain View and Chrome Mountain areas are included in table 7 for comparison with the other analyses. His analyses for the Bobcat Creek area are also used in the follow-

chemically analyzed sample of metasedimentary rocks

and chemistry given in table 6. Tr., trace amount; n.d., not determined]

53IM69	6IM70	4IM70	54CM69	50CM69	2CM70	[2]CM14	[2]CM6	[2]CM7	[2]CM8	[2]CM11	1BR71	26VC69	3VC69
28.6	14.6	28.0	1.3	19.4	2.0	...	...	...	...	21.4	27.3	22.1	4.1
...	...	...	...	...	...	...	...	...	...	...	...	...	...
3.3	1.9	.2	...	...	...	...	.2	.4	.8	...	1.8	9.2	1.6
...	14.3	...	24.9	...	24.6	43.0	31.4	6.4	18.0	...	...	...	...
...	...	...	...	4.8	...	...	...	...	...	...	2.3	...	...
33.6	47.1	29.9	52.8	26.7	44.6	53.0	53.4	37.8	49.4	...	32.0	51.5	59.7
33.4	18.5	38.6	17.4	45.4	24.1	.5	10.2	25.2	10.6	...	32.0	14.0	26.4
...	...	...	...	...	...	...	...	...	...	42.8	...	...	...
...	Tr.	Tr.	...	...	...	...	...	...	...	...	Tr.	...	...
...	...	...	...	...	...	...	...	...	...	...	...	.5	...
...	...	...	...	...	...	...	...	...	...	24.3	...	...	...
1.1	3.6	...	3.6	3.7	4.7	3.5	.2	.2	1.0	1.6	4.5	2.7	1.5
...	...	...	...	...	...	...	...	...	...	7.7	...	...	...
...	...	...	...	...	...	...	...	...	...	...	...	...	...
...	...	...	...	...	...	...	...	...	...	[3]1.9	...	...	6.6

ing discussion. Although the definition of the chemical parameters of Precambrian sedimentary and metasedimentary rocks has been the object of several recent studies (for example, Condie and others, 1970; Naqvi and Hussain, 1972), there are relatively few chemical descriptions of older Precambrian metasedimentary rocks. And as this type of information forms the basis for the development of models of sedimentation in geologic history such as those reviewed and discussed by Veizer (1973), the geochemistry of the hornfelses is documented and compared with other terranes in some detail.

Hornfelses show a wide range of composition, but they are relatively enriched in FeO and MgO and depleted in K_2O and Na_2O. Compositions are similar to lithic sandstone and graywacke (Pettijohn, 1963). A comparison (table 8) of the average composition of the 32 hornfelses with averages of lithic sandstones (Pettijohn, 1963; Nanz, 1953), graywackes (Condie and others, 1970; Pettijohn, 1963), shales (Clarke and Washington, 1924), and andesites (Taylor, 1969) shows that the hornfelses contain higher amounts of total iron and MgO and slightly higher Al_2O_3 than the other average rock types in table 8 and are depleted in K_2O and Na_2O. Ratios of Na_2O to K_2O are similar to those of the other graywackes, but the amounts of K_2O and Na_2O that are below 1.5 percent in the hornfels are anomalous for graywackes and other sediments (Pettijohn, 1963, figs. 2 and 3). A plot of the absolute amounts of K_2O and Na_2O in the hornfels (fig. 15) shows that the contents are, in general, lower then the most Precambrian graywackes considered by Condie (1967), although some of the amounts in the hornfelses are similar to the Sheba Formation in the Fig Tree Group, Republic of South Africa.

Semiquantitative minor- and trace-elements data are given in table 7 and in Beltrame (1972) for hornfelses from the Stillwater Complex area. The hornfels are enriched in chromium and nickel compared with average granites, andesites, tholeiites, and graywackes. To evaluate the possible enrichment of the hornfels in other elements, the average minor-element content is compared with Vinogradov's (1962) and Mason's (1958) average contents for earth's crust in table 9. Both the minor-element data in table 7 and in Beltrame (1972) were used to derive average values for the hornfels. The enrichment factors (average value in hornfels divided by Vinogradov's average value for the crust) show that chromium and nickel are strongly enriched in the hornfels; cobalt, scandium, copper, yterbium, and vanadium are weakly enriched; and all other elements considered are either diluted or are in about the same concentrations as Vinogradov's estimate of concentrations for the earth's crust.

The enrichment in chromium and nickel may indicate something about the characteristics of the source area of the metasedimentary rocks. Using strontium, an element depleted in amount as compared with the earth's crust, as an ordinate, and chromium and nickel concentrations as abscissas, the hornfels are compared with various other rock types in figure 16*A* and *B*. Both chromium and nickel show enrichment with respect to graywacke, tholeiite, shale, and granite. Condie, Macke, and Reimer (1970) showed that graywacke in both the Sheba and Belvue Road Formations in the Fig Tree Group, South Africa, of Precambrian age are enriched in nickel. A comparison of their nickel analyses of the Fig Tree Group with the Stillwater hornfels shows the close similarities of both sets of rocks (fig. 16*A*). Fig Tree shale (Danchin, 1967) has a similar chromium enrichment as the hornfels (fig. 16*B*).

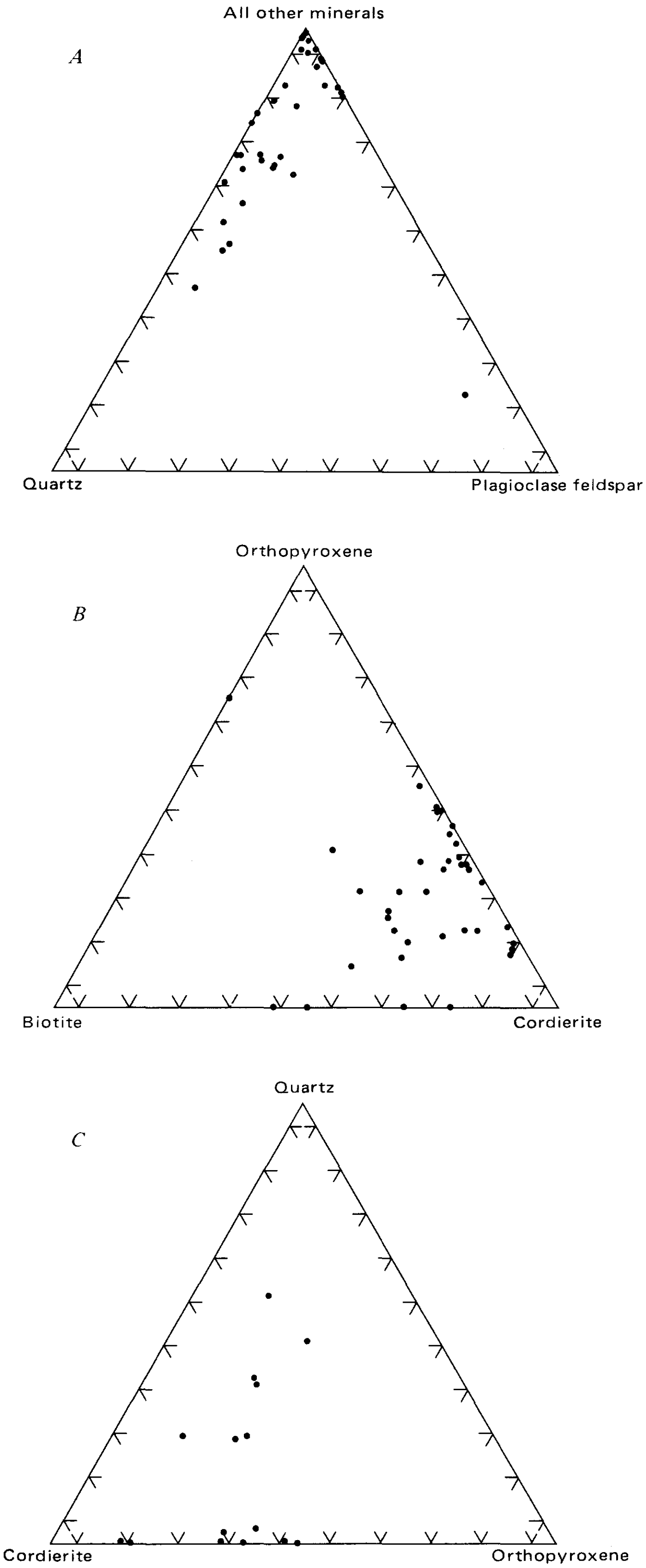

FIGURE 12.—Triangular diagrams showing modes of minerals, in volume percent, in hornfels associated with the Stillwater Complex. *A*, Quartz, plagioclase, and all other minerals (mainly cordierite, orthopyroxene, and biotite). *B*, Orthopyroxene, biotite, and cordierite. *C*, Quartz, cordierite, and orthopyroxene.

TABLE 5.—*Calculated formulae and unit cell parameters for Reinhardt's (1968) samples and unit cell parameters for one specimen of the Stillwater Complex*

	W53		D34		R124		M14/725
Mineral formulae calculated by hydrogen equivalent method (Jackson and others, 1967)							
Si^{+4}	4.975		5.035		5.031		----------
		6.000		6.000		6.000	----------
Al^{+3}	1.024		.965		.969		----------
Al^{+3}	2.971		2.999		2.919		----------
Fe^{+3}	.015	2.987	.046	3.048	.108	3.028	----------
Ti^{+4}	.001		.003		.001		----------
Mg^{+2}	1.624		1.423		1.359		----------
Fe^{+2}	.371	2.013	.321	1.756	.479	1.842	----------
Mn^{+2}	.018		.012		.004		----------
Na^{+1}	.017		.040		.039		----------
K^{+1}	.015	.32	.256	.296	.126	.179	----------
Ca^{+2}					.014		----------
$(Mn+Fe^{+2})/(Mg+Mn+Fe^{+2}) \times 100$	.194		.190		.262		----------
Refined least-square unit cell parameters							
a	17.056±0.01		17.068±0.005		16.91		17.109±0.004
b	9.700±0.008		9.698±0.004		9.72		9.714±0.004
c	9.347±0.005		9.358±0.006		9.48		9.356±0.008
V, A^3	1546.5 ±1.3		1549.1 ±1.0		1557.0		1554.9 ±1.1
$2\theta(004)$	38.512		38.521		38.587		38.638

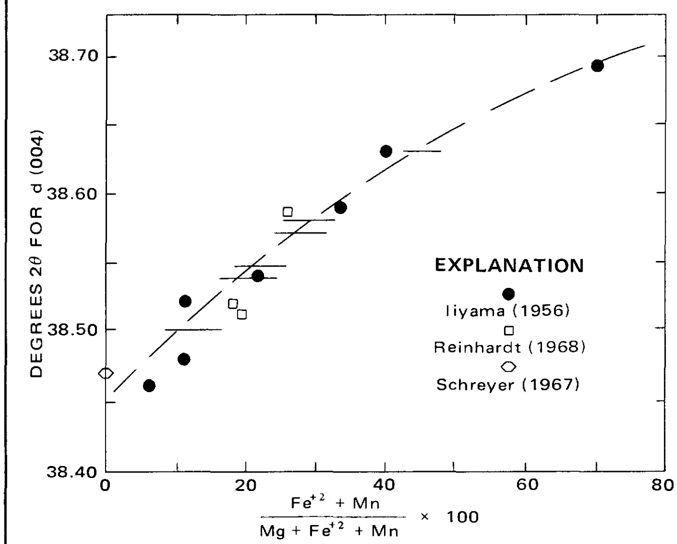

FIGURE 13.—X-ray determinative curve for $(Fe^{+2}+Mn/Mg+Fe^{+2}+Mn) \times 100$ ratio of cordierite. Horizontal lines indicate possible ratios for individual specimens of cordierite from the Stillwater Complex.

TABLE 6.—*Mineral assemblages in pyroxene hornfels rocks associated with aplite and quartz monzonite intrusive rocks*

[Qz, quartz; Bio, biotite; Cord, cordierite; Plagio, plagioclase; Ksp, potassium feldspar; Spn, spinel; Garn, garnet; Opx, orthopyroxene]

Qz+Bio+ores+Cord+Opx+Plagio+Ksp+
Qz+Bio+ores+Cord+Opx+Plagio+Ksp+Spn
Bio+ores+Cord+Opx+Plagio+Spn
Qz+Bio+ores+Cord+Opx+Plagio+Spn
Qz+Bio+Cord+Plagio+Garn

The chemical data place restrictions on hypotheses of provenance or source of the material that formed the metasedimentary rocks if an isochemical model is assumed for metamorphism. Although Bel-

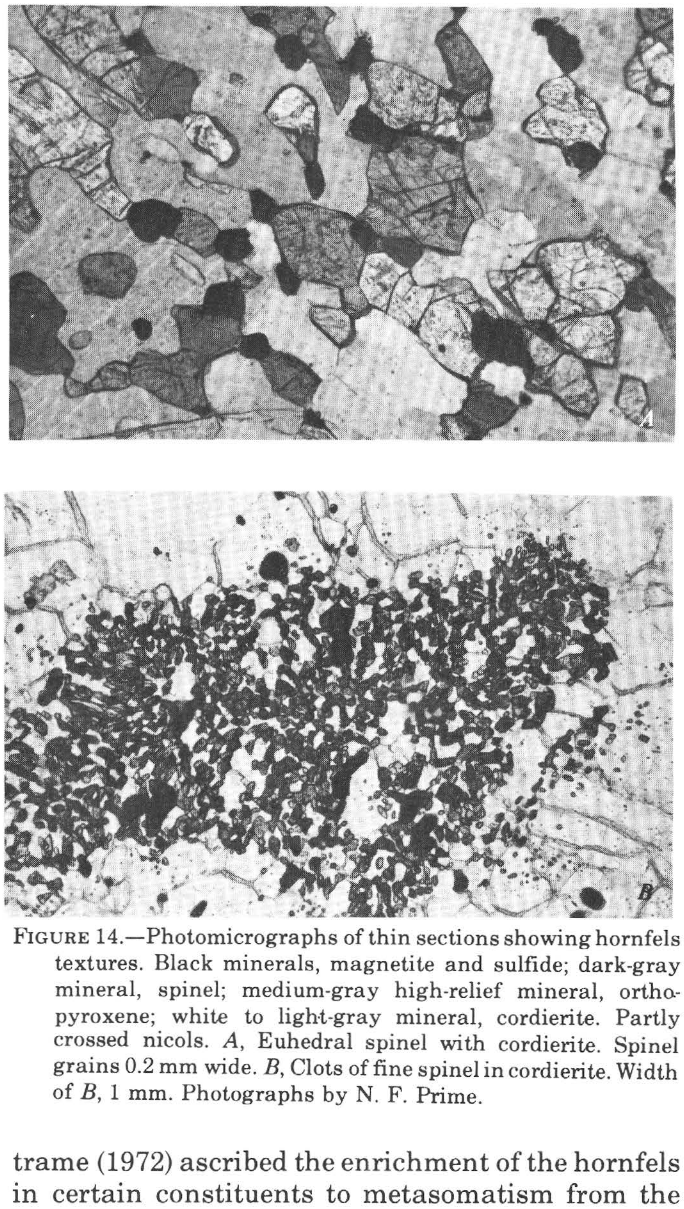

FIGURE 14.—Photomicrographs of thin sections showing hornfels textures. Black minerals, magnetite and sulfide; dark-gray mineral, spinel; medium-gray high-relief mineral, orthopyroxene; white to light-gray mineral, cordierite. Partly crossed nicols. *A*, Euhedral spinel with cordierite. Spinel grains 0.2 mm wide. *B*, Clots of fine spinel in cordierite. Width of *B*, 1 mm. Photographs by N. F. Prime.

trame (1972) ascribed the enrichment of the hornfels in certain constituents to metasomatism from the Stillwater Complex, the distance (9 to 10 km) over which this metasomatism must have been effective makes an isochemical model more attractive, except perhaps for the rocks either included in the complex or very near the Basal zone of the complex. In addition, the close chemical similarities of the metasedimentary rocks with the Fig Tree Group of Precambrian age in South Africa, whose chemistry was not controlled by metasomatism by a stratiform mafic and ultramafic intrusion, support an isochemical model. One way to account for the enrichment of nickel, chromium, cobalt, copper, and vanadium is to hypothesize that a large amount of ultramafic material in the source area was weakly attacked by weathering, rapidly eroded, and then incorporated in the metasediments. Another way is to postulate that there was a large amount of mafic volcanic rocks in the source area that were chemically weathered and contributed to the increase in these elements in the metasedimentary rocks. An ultramafic or mafic source area such as postulated could also account for the total iron and MgO enrichment in the hornfels.

Ratios of Al_2O_3 to Na_2O were suggested by Pettijohn (1957, p. 509) as indices of maturity for sandstones because Al_2O_3 is one of the least mobile oxides and Na_2O is the oxide readily lost during weathering and not added to sandstones during sedimentation. Values of the Al_2O_3 to Na_2O ratio for average arkoses, graywackes, and lithic sandstones are 5.7, 4.8, and 4.5 respectively (Pettijohn, 1957, p. 509), and for orthoquartzite, 20.4. The index increases with increasing maturity. Ratios of Al_2O_3 to Na_2O for the hornfels samples range from 5 to 142, most of them closer in value to the average for orthoquartzite. Considering the present mineralogy and the possible precursors, these values are absurd because they indicate extremely mature sediments and are in direct conflict with the previous hypothesis of rapidly weathered mafic or ultramafic source. The high maturity indices may indicate a mixed mechanical and chemical origin for the metasediments, but they certainly do not indicate a mature sediment.

If the Al_2O_3 to Na_2O ratios indicate a mixed mechanical (clastic) and chemical precipitate origin for the metasedimentary rocks below the Stillwater Complex, these rocks should be compared with rocks known to have such an origin. The Iron River-Crystal Falls district of Michigan contains formations in the Precambrian Paint River Group that include siltstone, slate, and graywacke of such an origin (James and others, 1968). Table 10 compares the average hornfels adjacent to the Stillwater Complex (see table 7 for individual analyses) with four rocks from the Paint River Group. The slate-siltstone unit of the Dunn Creek Slate contains 6–12 percent iron (James and others, 1968) as chlorite in the siltstone and as carbonate and sulfide minerals in the slate. The Hiawatha Graywacke has 12–22 percent iron, most of which is in the matrix chlorite and siderite (James and others, 1968, p. 60). The Paint River Group also has extremely high Al_2O_3–Na_2O ratios (5–141) that are not applicable as maturity indices but are similar to those for the hornfels from the Stillwater area. The comparatively high TiO_2 content of the hornfels parallels the high TiO_2 contents in the Paint River Group. These strong chemical similarities suggest that the metasedimentary rocks below the Stillwater Complex originated from mixed chemical and mechanical processes, as did the Paint River Group. The association of the hornfels with iron-formation and blue meta-quartzites also supports this comparison. Linear variations in FeO content perpendicular to the trend of the layering in the hornfels, as recorded by Beltrame (1972) in the Stillwater River area, may reflect gradual changes in

TABLE 7.—*Chemical analyses, semiquantitative spectrographic analyses, and*

[Chemical analyses by P. L. D. Elmore, James Kelsey, Gillison Chloe, Hezekiah Smith, and James Glen under Leonard Shapiro by rapid-rock

	54BE69	53FC69A	MV-KB	MV-KC	MV-KD-1	MV-KD-2	[1]SR-5	[1]SR-8	[1]SR-10	[1]SR-12	[1]SR-17	52NB69	60IM69C	58IM69
Chemical analysis (weight percent)														
SiO_2	47.8	60.1	53.9	69.5	66.6	66.0	51.8	58.5	61.7	63.1	60.2	49.4	58.5	47.2
Al_2O_3	25.7	17.0	20.8	14.8	14.8	16.3	21.35	18.72	16.11	15.76	18.78	21.3	18.2	20.6
Fe_2O_3	.80	.69	.80	.90	.90	.90	n.d.	n.d.	n.d.	n.d.	n.d.	1.3	.49	1.2
FeO	12.0	10.1	11.4	5.5	6.4	6.4	13.87	10.74	9.39	8.80	5.88	4.8	10.1	17.1
MgO	9.8	5.4	7.7	4.3	4.9	4.9	7.80	6.42	5.40	5.43	3.81	5.3	5.6	10.4
CaO	.10	1.1	.30	1.2	.60	.63	.00	.70	1.19	.44	6.27	13.9	1.7	.28
Na_2O	.18	.81	.57	1.3	.90	.90	.00	1.08	1.29	.99	3.52	2.4	1.9	.17
K_2O	.15	1.5	2.4	.69	1.5	1.4	1.43	1.62	1.13	2.19	.95	.30	.98	.16
H_2O^+	1.7	2.0	1.1	1.2	1.8	1.8	n.d.	n.d.	n.d.	n.d.	n.d.	.47	1.1	.85
H_2O^-	.26	.23	.10	.07	.14	.07	n.d.	n.d.	n.d.	n.d.	n.d.	.17	.21	.15
TiO_2	.90	.89	1.2	.73	.77	.81	1.36	1.45	0.97	1.11	.52	.54	.89	1.1
P_2O_5	.06	.06	.02	.01	.02	.02	n.d.	n.d.	n.d.	n.d.	n.d.	0.6	.08	.08
MnO	.09	.06	.07	.05	.02	.05	.11	.09	.09	.08	.07	.07	.11	.12
CO_2	<.05	<.05	.02	.04	.04	.06	n.d:	n.d.	n.d.	n.d.	n.d.	<.05	<.05	<.05
Sum	100	100	100	100	99	100	97.72	99.32	97.27	97.90	100	100	100	99
Semiquantitative, six-step spectrographic analyses (parts per million)														
B	N	N	N	N	N	N	n.d.	n.d.	n.d.	n.d.	n.d.	N	N	N
Ba	507	500	500	200	700	700	270	470	510	260	560	170	200	5
Ce	N	N	N	N	N	N	70	0	90	30	330	N	N	N
Co	110	50	50	30	30	30	66	79	80	78	80	<30	50	100
Cr	1,000	700	700	500	500	500	750	580	620	740	30	700	500	1,000
Cu	20	100	70	100	150	100	190	76	110	148	30	500	30	150
La	N	N	N	N	N	N	150	0	80	30	290	N	N	N
Nb	N	N	7	7	7	7	19	...	9	13	9	N	N	N
Ni	1,000	300	500	200	300	300	0	260	210	220	33	500	300	700
Pb	N	7	10	10	10	10	N	n.d.	n.d.	n.d.	n.d.	N	10	N
Sc	30	20	50	20	20	20	N	n.d.	n.d.	n.d.	n.d.	30	20	30
Sr	N	70	50	100	100	100	30	120	200	85	500	200	100	N
V	300	150	200	150	150	150	N	n.d.	n.d.	n.d.	n.d.	150	150	300
Y	N	10	10.	10	N	N	N	n.d.	n.d.	n.d.	n.d.	15	20	N
Zn	N	N	N	N	N	N	130	136	106	109	59	N	N	N
Zr	10	70	100	150	150	150	120	175	160	155	165	20	150	7
Ga	15	15	30	20	15	20	25	...	22	23	19	15	15	15
Yb	N	1.5	2	1.5	1	1	n.d.	n.d.	n.d.	n.d.	n.d.	1	2	N
Rb	n.d.	n.d.	n.d.	n.d.	n.d.	n.d.	80	95	55	110	40	n.d.	n.d.	n.d.
Rb	...	...	129	22	45	48	...	...	...	...	...	...	...	...
Bulk density (g/cm^3)														
Density	2.745	2.84	2.81	2.725	...	2.902	...	...	...	...	...	...	2.775	2.924

Sample	*Description and location*
54BE69	Cordierite-orthopyroxene-quartz-plagioclase-biotite hornfels; Montana South coordinates: 496,220 N., 1,919,040 E.
53FC69A	Cordierite-biotite-orthopyroxene-quartz-plagioclase hornfels; Montana South coordinates: 495,560 N., 1,912,380 E.
MV-KB	Cordierite-potassium feldspar-biotite-orthopyroxene-plagioclase hornfels; Montana South coordinates: 502,100 N.; 1,900,760 E.
MV-KC	Quartz-cordierite-plagioclase-orthopyroxene-biotite hornfels; Montana South coordinates: 502,070 N.; 1,900,760 E.
MV-KD-1,	Cordierite-quartz-orthopyroxene-plagioclase-biotite hornfels; Montana South coordinates: 502,050 N.; 1,900,760 E.; the -1 and -2 are two different splits of the same sample.
SR-5	Cordierite-orthopyroxene-biotite-quartz hornfels; Montana South coordinates: 502,120 N.; 1,900,900 E.
SR-8	Cordierite-biotite-orthopyroxene-quartz-plagioclase hornfels; Montana South coordinates: 502,100 N.; 1,900,930 E.
SR-10	Cordierite-quartz-orthopyroxene-biotite-plagioclase hornfels; Montana South coordinates; 502,020 N.; 1,900,890 E.
SR-12	Cordierite-quartz-biotite-orthopyroxene-plagioclase hornfels; Montana South coordinates: 502,000 N.; 1,900,950 E.
SR-17	Plagioclase-orthopyroxene-quartz-biotite hornfels; Montana South coordinates: 501,980 N.; 1,901,030 E.
52NB69	Cordierite-orthopyroxene-plagioclase-biotite hornfels; Montana South coordinates: 499,160 N.; 1,916,400 E.
601M69C	Cordierite-orthopyroxene-biotite-plagioclase-quartz hornfels; Montana South coordinates: 511,020 N.; 1,849,880 E.
52NB69	Cordierite-orthopyroxene-plagioclase-biotite hornfels; Montana South coordinates: 499,160 N.; 1,916,400 E.
60IM69C	Cordierite-orthopyroxene-biotite-plagioclase-quartz hornfels; Montana South coordinates: 511,020 N.; 1,849,880 E.
58IM69	Cordierite-orthopyroxene-opaque minerals hornfels; Montana South coordinates: 513,660 N.; 1,852,300 E.
53IM69	Cordierite-biotite-quartz-plagioclase hornfels; Montana South coordinates: 506,280 N.; 1,852,020 E.
4IM70	Biotite-cordierite-quartz-plagioclase hornfels; Montana South coordinates: 506,870 N.; 1,849,850 E.

[1]Chemical and spectrographic analyses by Beltrame (1972, p. 17, 30).

the depositional environment of the sediments or in the source of the sediments and not the metasomatic changes.

STILLWATER COMPLEX

AREAL EXTENT AND PREVIOUS WORK

The stratiform mass of mafic and ultramafic rocks that form the Stillwater Complex strikes northwest across the northern margin of the Beartooth Mountains (figs. 1, 2). Parts of the complex are exposed for about 48 km along strike in the Mt. Wood (Page and others, 1973a), Mt. Douglas (Page and others, 1973b), and Mt. Cowen 15-minute quadrangles and in the Mt. Rae (Richards, 1952, 1958), McLeod Basin, and Emerald Lake 7½-minute quadrangles, Montana. Because the complex is tilted on edge, north-south traverses give the apparent thickness of the complex, which is a maximum of 5.5 km. Exposures of the complex are fairly extensive.

bulk densities of metasedimentary rocks adjacent to the Stillwater Complex

methods; spectrographic analyses by Chris Heropoulos. N, not detected at limit of determinations; n.d., not determined or not looked for]

[1]58IM69	4IM70	6IM70	54CM69	52CM69	3CM70	50CM69	2CM70	[1]CM14	[1]CM6	[1]CM7	[1]CM8	[1]CM11	19BR68	1BR71	26VC69	3VC69
Chemical analyses (weight percent)																
66.1	56.9	52.8	53.3	54.3	47.4	53.5	49.5	48.5	50.8	51.0	50.4	53.6	67.6	63.9	56.1	44.8
14.0	19.0	19.7	20.6	19.8	19.0	20.5	21.4	21.6	22.2	22.2	22.2	16.8	14.2	14.6	17.9	23.2
1.1	1.0	.47	.66	.46	.44	.47	.14	......	......	......	......	......	1.6	1.1	1.4	1.3
6.1	9.7	13.3	13.4	10.4	13.6	11.3	14.6	18.33	16.03	14.98	14.44	10.62	4.6	7.8	8.9	10.5
3.7	5.1	7.4	7.9	5.6	8.1	6.3	8.4	11.10	9.51	8.37	8.25	7.92	3.0	5.7	4.3	6.5
.98	.51	.40	.30	.32	.53	.20	.30	.02	.04	.15	.17	4.56	1.4	.54	1.7	.58
2.8	.84	.60	.19	.91	1.5	1.0	.45	.13	.14	.26	.23	1.09	3.1	.84	2.0	1.3
1.0	3.2	1.8	.81	2.7	.84	2.5	1.6	.09	.48	.69	.91	.23	.80	1.0	3.0	4.6
3.2	2.6	1.7	1.1	3.5	6.6	2.4	1.4	......	......	......	......	......	2.8	2.9	3.3	4.7
.30	.28	.20	.22	.23	.30	.16	.17	......	......	......	......	......	.28	.14	.30	.32
.58	.78	1.1	1.1	.77	1.1	1.0	1.1	.78	1.14	1.11	1.07	.53	.54	.64	.90	1.1
.06	.07	.08	.08	.07	.08	.08	.08	......	......	......	......	......	.06	.04	.07	.08
.04	.03	.08	.06	.06	.09	.06	.06	.13	.12	.11	.07	.03	.02	.04	.03	.08
< .05	< .05	< .05	< .05	< .05	< .05	< .05	< .05	......	......	......	......	......	< .05	.04	< .05	< .05
100	100	100	100	99	100	99	99	100.68	100.46	98.87	97.74	95.38	100	101	100	99
Semiquantitative, six-step spectrographic analyses (parts per million)																
N	10	N	N	N	N	N	N	N	......	N	N	N	N	N	N	N
150	500	500	200	500	200	300	300	< 20	......	< 20	320	170	100	100	500	700
N	N	N	N	N	N	N	N	0	......	20	0	100	N	N	N	N
20	30	50	70	70	50	50	50	67	......	54	66	62	15	30	20	50
300	300	500	1,000	700	700	500	700	1,400	......	900	1,000	360	700	500	700	50
10	70	70	100	20	50	50	70	158	......	126	134	48	70	150	2	70
N	N	N	N	N	N	N	N	40	......	20	10	0	N	N	N	30
N	N	N	10	N	N	N	N	6	......	10	22	......	N	N	N	N
200	500	700	700	500	500	500	700	550	......	310	390	133	100	300	300	500
N	10	7	N	7	N	N	N	n.d.	......	n.d.	n.d.	n.d.	15	10	7	N
15	20	30	30	20	20	20	30	n.d.	......	n.d.	n.d.	n.d.	10	20	20	30
70	50	30	10	50	30	20	15	0	......	40	30	80	70	30	200	100
100	150	200	200	200	150	150	200	n.d.	......	n.d.	n.d.	n.d.	100	150	150	200
10	15	N	10	15	N	15	N	n.d.	......	n.d.	n.d.	n.d.	10	15	10	15
N	N	N	N	N	N	N	N	146	......	104	133	112	N	N	N	N
100	100	100	70	70	70	50	70	< 10	......	40	50	55	70	100	100	100
10	20	20	15	15	15	20	20	4	......	12	20	......	10	15	20	20
N	1.5	N	1	1.5	N	1.5	N	n.d.	......	n.d.	n.d.	n.d.	1	2	1.5	1.5
n.d.	n.d.	n.d.	n.d.	n.d.	n.d.	n.d.	n.d.	0	......	25	50	10	n.d.	n.d.	n.d.	n.d.
......	......	......	......	......	......	......	......	......	......	......	......	......	......	......	5	......
Bulk density (g/cm^3)																
......	2.83	2.87	2.835	2.785	2.795	2.81	2.835	......	......	......	......	......	2.72	2.78	2.767	2.88

Sample	*Description and location*
6IM70	Cordierite-biotite-quartz-orthopyroxene-plagioclase hornfels; Montana South coordinates: 509,580 N.; 1,847,430 E.
54CM69	Cordierite-orthopyroxene-biotite-quartz hornfels; Montana South coordinates: 519,400 N.; 1,838,000 E.
52CM69	Cordierite-quartz-biotite hornfels; Montana South coordinates: 515,480, N.; 1,836,450 E.
3CM70	Quartz-cordierite-biotite hornfels; Montana South coordinates: 518,530 N.; 1,836,820 E.
50CM69	Biotite-cordierite-quartz-anthophyllite hornfels; Montana South coordinates: 512,600 N.; 1,836,600 E.
2CM70	Cordierite-orthopyroxene-biotite-quartz hornfels; Montana South coordinates: 517,200 N.; 1,841,510 E.
CM14	Cordierite-orthopyroxene-biotite hornfels; Montana South coordinates: 525,910 N.; 1,831,200 E.
CM6	Cordierite-orthopyroxene-biotite-plagioclase hornfels; Montana South coordinates: 524,100 N.; 1,833,080 E.
CM7	Cordierite-biotite-orthopyroxene-plagioclase hornfels; Montana South coordinates: 524,110 N.; 1,833,030 E.
CM8	Cordierite-orthopyroxene-biotite-plagioclase hornfels; Montana South coordinates: 524,160 N.; 1,832,980 E.
CM11	Quartz-chlorite-zoisite schist; Montana South coordinates: 524,210 N.; 1,832,880 E.
19BR68	Quartz-chlorite-muscovite-staurolite-plagioclase schist; Montana South coordinates: 525,340 N.; 1,823,350 E.
1BR71	Cordierite-biotite-quartz-anthophyllite-plagioclase hornfels; Montana South coordinates: 537,740 N.; 1,802,860 E.
26VC69	Cordierite-quartz-biotite-plagioclase hornfels; Montana South coordinates: 502,010 N.; 1,877,100 E.
3VC69	Cordierite-biotite-quartz-plagioclase hornfels; Montana South coordinates: 502,940 N.; 1,893,740 E.

An informal stratigraphic nomenclature used to describe the internally conformable layers of the complex that range from dunitic to noritic to anorthositic compositions has developed from the early work of Peoples (1936, p. 358) through that of Jones, Peoples, and Howland (1960), Hess (1960), and Jackson (1961) to this report. In addition, an extensive terminology was developed by Jackson (1967) to describe rocks such as these formed by crystal accumulation and to describe the primary internal features of these magmatic sediments. Although other variants of this terminology are available (Hess, 1960; Wager and others, 1960), Jackson's (1967) terminology is used here.

STRATIGRAPHY AND LITHOLOGY

Figure 17 gives idealized composite columnar sections for the Stillwater Complex and shows the

TABLE 8.—*Comparison of average chemical analyses (weight percent) of hornfels adjacent to the Stillwater Complex with other average rock types*

[Tr. = trace]

	1	2	3	4	5	6	7	8
SiO_2	56.5	56.80	56.30	66.2	59.8	64.4	58.11	59.5
Al_2O_3	18.8	8.48	17.24	10.2	12.9	15.5	15.40	17.2
Fe_2O_3	.88	1.67	3.83	7.01	6.56	6.54	4.02'	
FeO	10.5		5.09				2.45	6.10
MgO	6.4	1.24	2.54	4.50	4.44	3.12	2.44	3.42
CaO	1.3	15.25	1.0	1.97	3.18	2.22	3.10	7.03
Na_2O	1.1	1.31	1.23	1.80	2.83	3.74	1.30	3.68
K_2O	1.4	1.46	3.79	1.58	2.23	2.44	3.24	1.60
H_2O^+	1.5	.50					4.99	
H_2O^-	.20							
TiO_2	.89	.10	.77	.52	.55	.62	.65	.70
P_2O_5	.06	Tr.					.17	
MnO	.07		.10				Tr.	
CO_2	<.05	12.95					2.63	

1. Average of 31 hornfels analyses reported in table 7.
2. Calcareous subgraywacke (Molasse) (Pettijohn, 1963, p. 86, table 4, anal. C).
3. Precambrian lutite (Nanz, 1953, p. 57).
4. Average Precambrian graywacke, Sheba Formation of the Fig Tree Group, Republic of South Africa (Condie and others, 1970, p. 2766, table 2, no. 1, total Fe as Fe_2O_3).
5. Average Precambrian graywacke, Belvue Road Formation of the Fig Tree Group, Republic of South Africa (Condie and others, 1970, p. 2766, table 2, no. 2, total Fe as Fe_2O_3).
6. Average Precambrian graywacke, Wyoming (Condie, 1967).
7. Average shale (Clarke and Washington, 1924, p. 32).
8. Andesite, average data for major elements compiled from analyses of circum-Pacific calc-alkaline andesite (Taylor, 1969, p. 60).

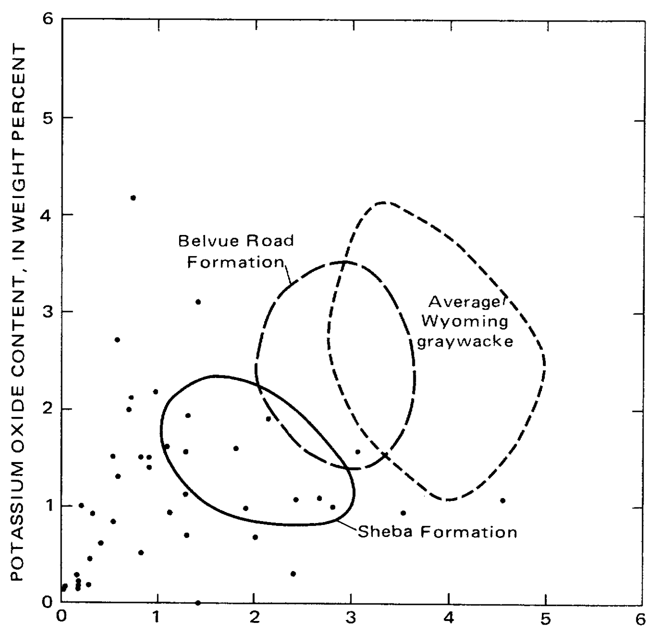

FIGURE 15.—Potassium oxide and sodium oxide content for hornfels adjacent to the Stillwater Complex compared with other Precambrian graywackes. Fields of the average Wyoming graywacke and the Belvue Road and Sheba Formations of the Fig Tree Group of South Africa from Condie, Macke, and Reimer (1970).

TABLE 9.—*Comparison of the average minor- and trace-element content of the hornfels with estimates of contents for the earth's crust*

Element	Average hornfels	Number of samples	Earth's crust: Vinogradov (1962)	Earth's crust: Mason (1958)	Enrichment factor[1]
	Values in parts per million				
Ba	329	37	650	400	0.5
Ce	59	14	70	46	.8
Co	52	37	18	23	2.9
Cr	646	37	83	200	7.8
Cu	87	37	47	45	1.9
La	60	16	29	18	2.1
Nb	9	18	20	24	.5
Ni	362	37	58	80	6.2
Pb	10	13	16	15	.6
Sc	23	22	10	5	2.3
Sr	81	37	340	450	.2
V	169	22	90	110	1.9
Y	13	15	29	40	.5
Zn	107	15	83	65	1.3
Zr	94	37	170	160	.6
Ga	16	37	19	15	.8
Yb	1.4	16	.33	3	4.2
Rb	73	19	150	120	.5

[1]Enrichment factor = content in average hornfels divided by Vinogradov's value for the earth crust.

names assigned for mappable units by various authors. The right-hand columnar section gives the terminology used in this report. The Basal zone, Ultramafic zone, Banded zone, and Upper zone correspond to the subdivisions used by Jones, Peoples, and Howland (1960) and Jackson (1961). In this report and on Page and Nokleberg's map (1974) the Basal zone is divided into two parts, a Basal norite member and an overlying Basal bronzite cumulate member. The division of the Ultramafic zone into a Peridotite member and an overlying Bronzitite member follows the usage of Jackson (1961, p. 2–4). Although Hess (1960) mineralogically divided the upper part of the complex into his Norite, Lower Gabbro, Anorthosite, Upper Gabbro, and Hidden Zones, and three anorthosite subzones, none of these units were mapped in the field, and inasmuch as the 1:12,000-scale maps were prepared without separating gabbroic and anorthositic units, the terminology of Jones, Peoples, and Howland (1960), and Jackson (1961) is retained.

The Basal zone (fig. 17) includes those rocks that occur stratigraphically below the lowest cyclic unit beginning with an olivine cumulate or olivine-bronzite cumulate and ending with a bronzite cumulate. It is composed of magmatic sediments or cumulates of orthopyroxene, clinopyroxene, plagioclase, olivine, or combinations thereof and of rocks of noritic and gabbroic composition that exhibit ophitic igneous textures. This zone is found along the southern part of the complex. Except for the section from the West Fork of the Stillwater River to Chrome Mountain where it lies beneath a south-dipping thrust, it is exposed discontinuously along the entire strike length of the complex. Maximum known thicknesses are about 366 m, but the average is abut 152 m.

Intrusive relations of the Basal norite member into

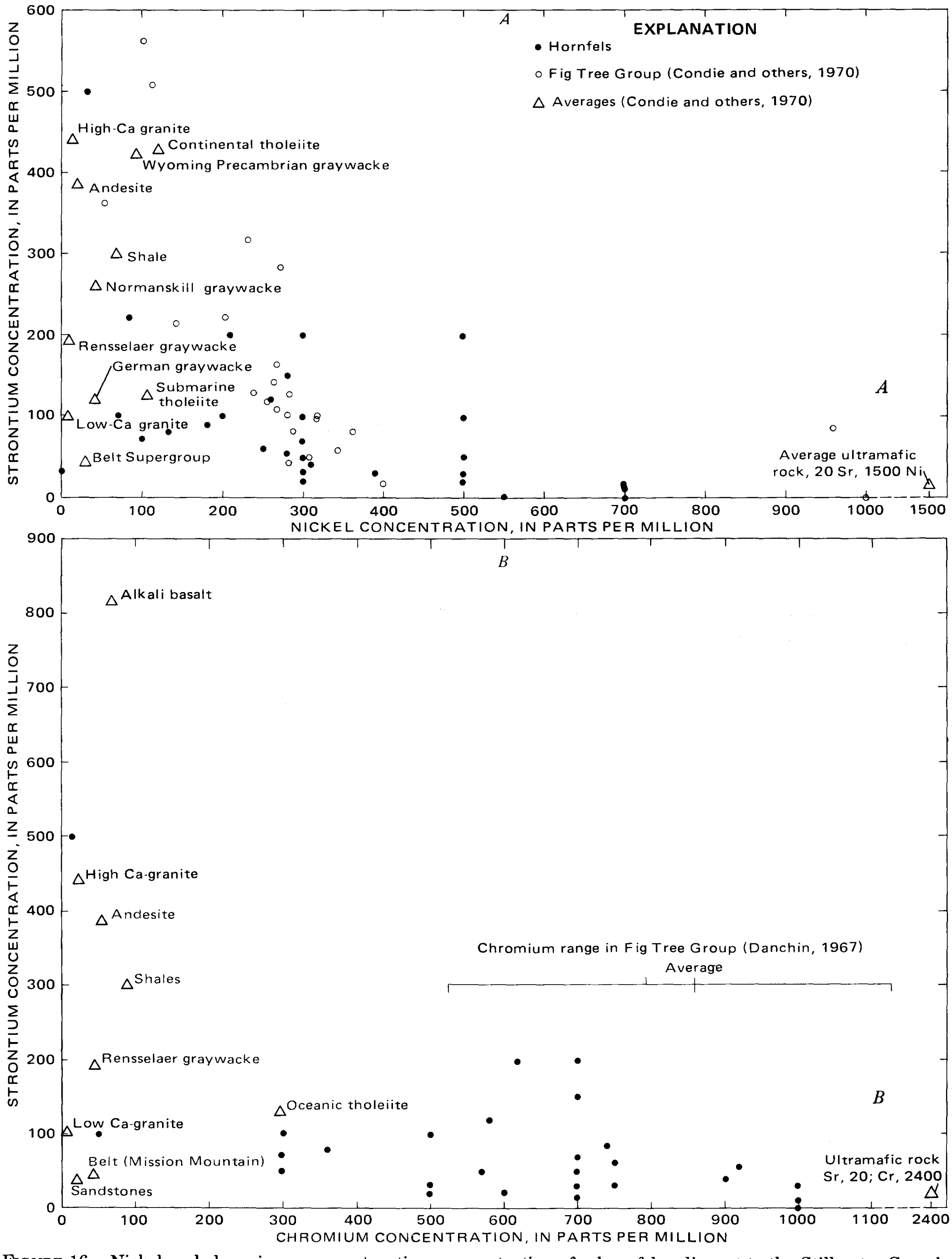

FIGURE 16.—Nickel and chromium versus strontium concentrations for hornfels adjacent to the Stillwater Complex compared with other rock types. *A*, Nickel. *B*, Chromium.

the hornfels can be observed in Verdigris Creek in the Mountain View area (coordinates: 503,450 N.; 1,898,250 E.) and from Chrome Mountain westward, specifically in the unnamed creek between Blakely

TABLE 10.—*Comparison of the average composition (in weight percent) of hornfels adjacent to the Stillwater Complex with the composition of rocks in the Paint River Group*

	1	2	3	4	5
SiO_2	56.52	59.19	49.85	62.75	51.18
Al_2O_3	18.77	14.61	13.88	7.05	11.95
Fe_2O_3	.88	1.51	3.75	1.94	8.09
FeO	10.47	11.28	14.10	16.36	12.15
MgO	6.46	2.94	3.32	2.95	2.42
CaO	1.33	.09	.20	.38	1.12
Na_2O	1.10	.12	.10	.05	2.12
K_2O	1.40	2.38	2.74		1.86
H_2O^+	1.54	4.69	4.90	3.14	1.42
H_2O^-	.20	.07	.14	.23	.03
TiO_2	.89	1.45	1.45	.40	.51
P_2O_5	.06	.01	.09	.10	.34
MnO	.07	.10	.24	1.17	2.71
CO_2		1.25	4.09	3.83	3.70
C		.25	.69		
S		.08	1.51		
Sum		100.02	101.05		
Less O for S		.04	.76		
Total		99.98	100.29		99.80

1. Average hornfels adjacent to the Stillwater Complex, 32 analyses (table 7, this report).
2. Siltstone from the gray sericitic slate and siltstone unit of the Dunn Creek Slate (James and others, 1968, p. 41, table 4).
3. Slate from the gray sericitic slate and siltstone unit of the Dunn Creek Slate (James and others, 1968, p. 41, table 4).
4. Hiawatha Graywacke, James and others (1968, p. 60, table 12).
5. Stambaugh Formation, laminated facies (James and others, 1968, p. 67, table 13).

and Bobcat Creeks (coordinates: 529,540 N.; 1,898,160 E.). In the section from the Benbow area to the Initial area, inclusions of hornfels are found in the Basal zone. Figure 18 shows small inclusions of cordierite-pyroxene hornfels in the Basal norite member. In drill core, hornfels inclusions are found up into the lower part of the Peridotite member.

The lower part of the Basal zone, here informally termed the Basal norite member, is composed of alternating lensoid masses or layers in which olivine, orthopyroxene, clinopyroxene, plagioclase, hornblende, biotite, quartz, oxide, and sulfide minerals form a variety of crystallization sequences and orders. Rocks with one crystallization sequence or order can be persistent over large volumes (tens of feet thick by thousands of feet long and unknown amounts down dip), but also several different orders of crystallization can be found within one hand specimen and even within one thin section. In addition to the highly irregular distribution of rocks with different orders of crystallization, grain size varies from coarse to fine in an irregular manner (fig. 19). Rocks with all gradations of textures from magmatic sediments with cumulate textures, including both apposition and current-formed textures, to ophitic, diabasic, and gabbroic textures are observed within small areas. The most distinctive texture is one in which the pyroxenes show ragged, sutured, subhedral margins against plagioclase. Rocks from the Basal norite member are characterized by extreme variability of orders of mineral crystallization, grain size, and texture over short distances. Nowhere has a continuous fine-grained ophitic chill-zone diabase been found between the Basal norite and adjacent country rocks, as has been inferred to exist (Hess, 1960; Wager and Brown, 1967). Indeed, fine-grained ophitic gabbros occur throughout the sequence with an apparent irregular distribution. The Basal norite member locally contains an abundance of hornfels inclusions that range in size from microscopic to greater than 305X61 m in outcrop size (coordinates: 497,000 N.; 1,917,570 E.). Some of the hornfels inclusions were incorporated into the Basal norite; others apparently reacted and contaminated the magma. Massive sulfide layers, pods, and disseminated grains of dominantly pyrrhotite, pentlandite, and chalcopyrite are also present. The lower contact of the Basal norite member is an intrusive contact. Locally at the contact, an intrusive breccia of norite, hornfels, and massive sulfide minerals is formed and is intruded by the quartz monzonite. Basal norite locally forms dikes and pods in the hornfels (coordinates: 503,450 N.; 1,898,550 E.).

The upper part of the Basal zone, here informally called the Basal bronzite cumulate member, is composed of layers of coarse- to fine-grained hypidiomorphic granular orthopyroxene cumulates. The lower contact is gradational over a few tens of feet with the underlying Basal norite member but is marked by a sharp increase in the amount of plagioclase, by the appearance of ophitic-, diabasic-, and gabbroic-textured rocks, and by the presence locally of current-formed magmatic sediments. The upper contact is marked either by the disappearance of orthopyroxene as a cumulus crystal and the appearance of olivine as cumulus crystal or by orthopyroxene joined by olivine as cumulus crystals. The horizon is sharp and, where observed, about one crystal thick.

Conformably overlying the Basal zone is the Ultramafic zone, which consists of repetitions of olivine, chromite, olivine-chromite, olivine-bronzite, and bronzite cumulates that are termed cyclic units. The Ultramafic zone may locally show onlapping relations to the Basal zone. The upper contact of the Ultramafic zone is marked by the appearance of cumulus plagioclase. The contact seems to be conformable and marked by a one-crystal-thick horizon, as exposed in the Mountain View area (coordinates: 507,810 N.; 1,896,940 E.), but on the East Boulder Plateau north of Lost Mountain (coordinates: 528,440 N.; 1,840,540 E.), cobble- and boulder-sized subrounded to subangular fragments (lenses?) of bronzite cumulate are found above the Ultramafic zone in the

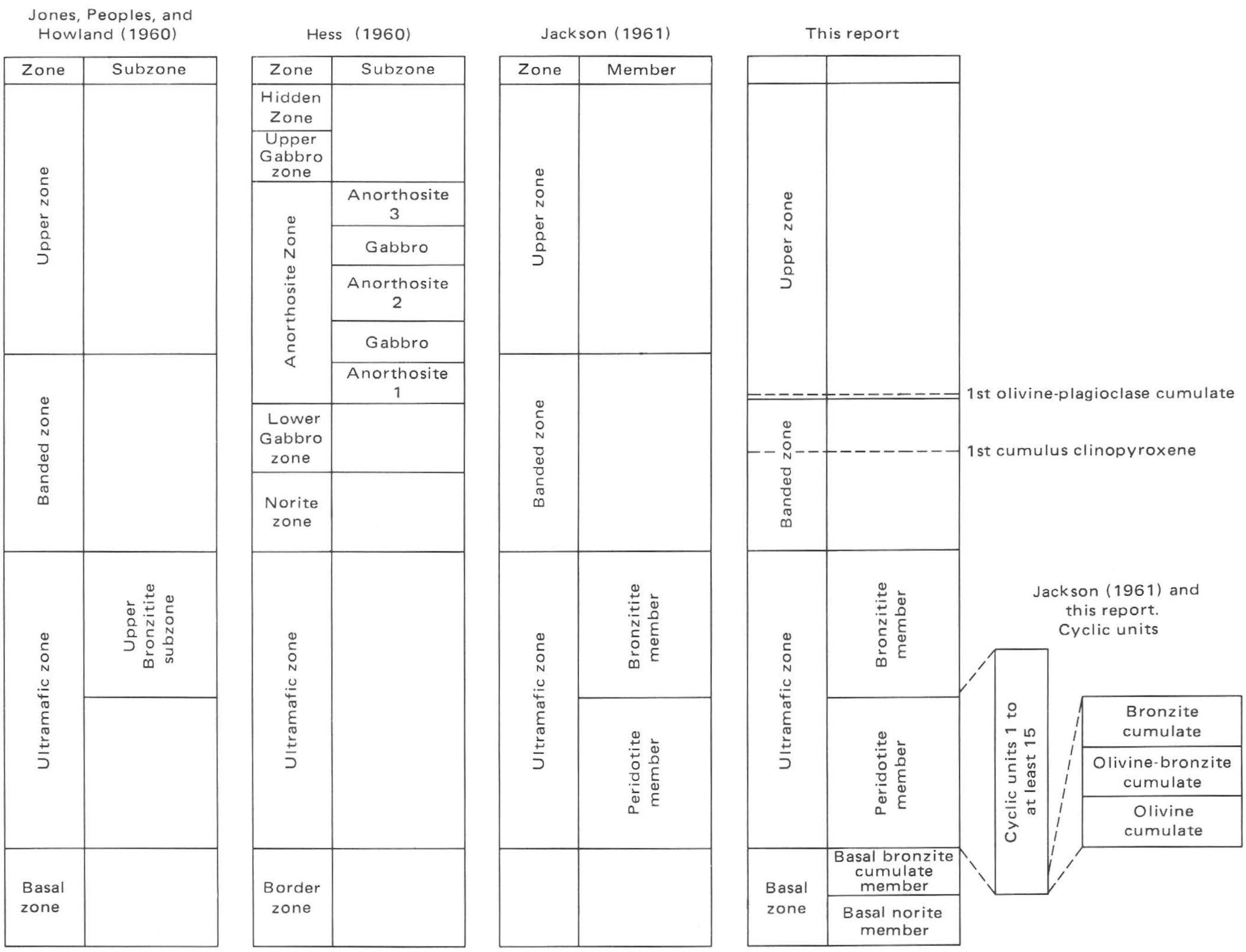

FIGURE 17.—Idealized columnar sections showing subdivisions of the Stillwater Complex used by various authors.

plagioclase-bronzite cumulate. These fragments may have been derived from the Ultramafic zone, which suggests that the intervening contact may be locally an erosional surface. The Ultramafic zone averages about 1,070 m thick and is thicker in the basin structures (Jackson, 1963).

The Peridotite member, the lower of two members in the Ultramafic zone, consists of cyclic units (Jackson, 1961, 1963, 1967, 1968, 1969, 1970, 1971), which are repetitions of cumulate patterns; at least 15 cyclic units are recognized in the Peridotite member. Cyclic units are of two types: (1) normal, complete units that invariably contain the same sequence of cumulus phases: olivine, olivine+bronzite, and bronzite, and (2) beheaded units (Jackson, 1970, p. 390–401) that lack an olivine+bronzite or a bronzite layer, or both. Cyclic units range in thickness from about 381 m (Mountain View area, unit 2 of Jackson, 1968, p. 1506) to less than 3.05 m (Iron Mountain area; coordinates: 514,660 N.; 1,859,600 E). In the Benbow, Nye Basin, and Mountain View areas where Jackson (1961, 1963, 1968, 1969) and Page, Shimek, and Huffman (1972) were able to distinguish and correlate them, the cyclic units have been numbered in sequence upward from 1 to 15. Cumulus chromite and chromite+olivine occur in at least 13 of cyclic units near the base or in the lower part of the olivine cumulates (Jackson, 1963, 1967). The chromite cumulates are designated by letters A to K sequentially from the lowest zone to the highest zone. Cyclic units were not mapped in the field because of the difficulty in characterizing each unit without supporting chemical and petrologic work for rock sequences. Instead, the rock types olivine, chromite, olivine+bronzite, and bronzite cumulates were distinguished for mapping purposes (Page and Nokleberg 1974). In areas where the chromite zones had been identified and correlated by chemical analyses and detailed

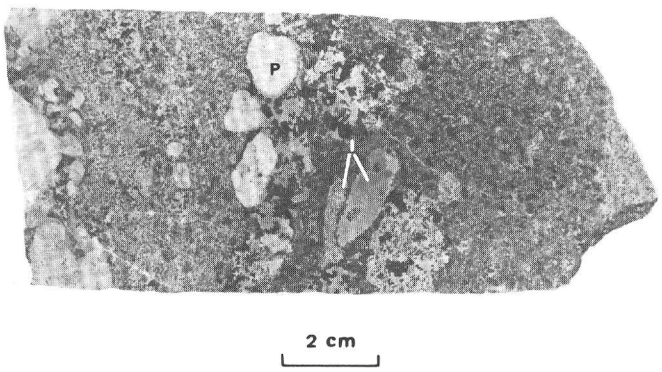

FIGURE 18.—Hydrofluoric acid etched slab of the Basal norite member containing cordierite-pyroxene hornfels inclusions (I) and plagioclase phenocrysts (P).

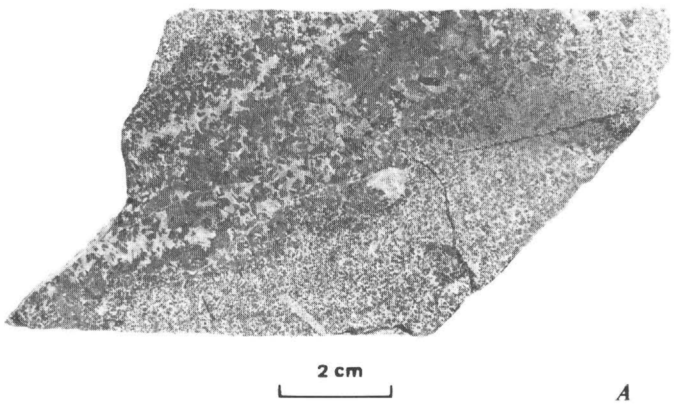

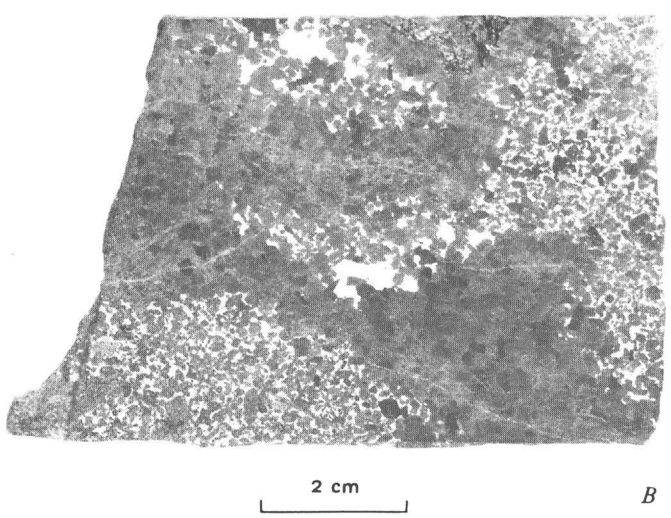

FIGURE 19.—Slabs of the Basal zone norite showing rapid variation in grain size. *A*, Banded norite. *B*, Patchy norite.

stratigraphy and where they are in reasonable stratigraphic position, they were identified by a letter symbol by Page and Nokleberg (1974). Jones, Peoples, and Howland (1960, p. 290) correlated some chromitite zones from the Benbow to West Fork of the Stillwater River area and from there westward tentatively identified the G chromite zone. Jackson (1963) gave a correlation diagram of the zones for the entire strike length of the complex on the basis of detailed chromitite stratigraphy and analytical data, but the extension of chromitite stratigraphy beyond the West Fork of the Stillwater River area is doubtful on Page and Nokleberg's map because part of the Peridotite member is covered by a thrust plate of hornfels. For this reason, other westward correlations are suspect because individual chromitite zones cannot be physically traced.

The Bronzitite member, the upper member in the Ultramafic zone, consists of a single thick layer of cumulus bronzite that attains a maximum thickness of 1,070 m and averages about 366 m in thickness. The cumulates are fine to coarse grained. Units in which grain size changes from coarse to fine upward appear to form repeated cycles throughout the sequence. From 3-6 m below the top of the Bronzitite member in the Benbow area (coordinates: 500,320 N.; 1,921,080 E.), a concentration of cumulus chromite can be traced for several meters along strike. Elsewhere the unit has not been studied in enough detail for possible extensions of the chromitite zone to be traced.

Another unit in the Ultramafic zone is called intrusive dunite because it shows intrusive relations, diking, and stoping with other rocks. The wallrocks in contact with the dunite show no effects of metamorphism, which indicates that the intrusive dunite and the wallrocks were at about the same temperature at the time of emplacement. Hess (1938a, 1960) and Jackson, Howland, Peoples, and Jones (1954) have previously called attention to its occurrence. Intrusive dunite is exposed in the Mountain View area (Jackson and others, 1954), in the Iron Mountain area (coordinates: 515,520 N.; 1,859,240 E.), in the upper Forge Creek area (coordinates: 522,360 N.; 1,842,500 E.), in the Chrome Mountain area (coordinates 525,350 N.; 1,835,620 E.), and in the Boulder River area (Howland and others, 1949). The largest mass is in the upper Forge Creek area where its intrusive relations are well exposed. The intrusive dunite generally occurs in the lower part of the Peridotite member; the occurrence at Iron Mountain is anomalous in that intrusive dunite occurs more than 91 m above the base of the member. The dunite is characterized by (1) lack of poikilitic or oikocrystic orthopyroxene or clinopyroxene, (2) closely packed olivine grains with similar compositions to the adjoining olivine and olivine-bronzitite cumulates, (3) wispy, irregular, discontinuous thin (one to several crystals wide) chromitite seams, (4) highly irregular contacts, and (5) blocks and fragments of other cumulates as inclusions.

The Banded and Upper zones, which are stratigraphically above the Ultramafic zone, were not mapped separately. They have an aggregate maximum thickness of about 4,267 m. The acceptance of Hess' (1960) subdivisions above the Ultramafic zone, as was done by Wager and Brown (1967), should be viewed with caution since not enough mapping exists to develop useful and mappable stratigraphy. The following remarks record some local observations and indicate some of the complexities involved in finding a useful stratigraphic classification. The zones under consideration consist of alternating layers of orthopyroxene+plagioclase, orthopyroxene +clinopyroxene+plagioclase, olivine+plagioclase, and plagioclase cumulates. Jones, Peoples, and Howland (1960, p. 280, 290) suggested that the boundary between the Banded and Upper zones should be at the base of the lowest tractolite (olivine+plagioclase cumulate) in the sequence. In sections in the Benbow, Mountain View, and Nye Basin areas, in the area on the east side of the West Fork of the Stillwater River, in the area from Iron Mountain to Picket Pin, and in the area west of the East Boulder River, the use of this horizon would define the Banded zone as consisting of a thick orthopyroxene+plagioclase cumulate in the stratigraphically lower part of the unit and repetitions of orthopyroxene+plagioclase and orthopyroxene+clinopyroxene+plagioclase cumulates in the upper part. This subdivision probably corresponds to Hess' (1960) Norite Zone and Lower Gabbro Zone. Two, and possibly more, thin (3-6-m-wide) plagioclase cumulates occur in the middle of the Banded zone (coordinates: 508,270 N.; 1,899,870 E., for example). The repetitious nature of one- and two-pyroxene+plagioclase cumulates suggests that the upper part may contain cyclic units analogous to those in the Ultramafic zone. All of the Banded zone contains well-developed mineral-graded and size-graded layers ranging in thickness from less than a centimeter to a few meters.

In the eastern sections of gabbroic rocks one and possibly two olivine+plagioclase cumulates are known. The base of the lowermost marks the base of the Upper zone. The contact between the Banded zone and the overlying olivine+plagioclase cumulate is irregular (coordinates: 509,750 N.; 1,900,980 E.) and may represent a break equivalent to an erosional interval in the sequence. In the central part of the complex from Picket Pin to Iron Mountain, at least five distinctive and possibly nine occurrences of olivine+plagioclase cumulate layers are recognized. Farther to the west, Hess (1960, p. 82) identified six olivine+plagioclase cumulates in the East Boulder Plateau section. In the Mountain View area the sequence is olivine+plagioclase, plagioclase, plagioclase+orthopyroxene, plagioclase+clinopyroxene+orthopyroxene cumulates; the same sequence is also found in the Picket Pin sequence where it is repeated at least five times. These repetitious sequences of cumulates in the lower part of the Upper zone correspond to Hess's (1960) Anorthosite Zone which he reported as 1,890 m thick.

In the eastern part of the Banded and Upper zones (Page and Nokleberg, 1974) several faults have trends parallel to the strike of the cumulate layering. Some of the faults were found only as a result of detailed mapping of petrologic units (E. D. Jackson, oral commun., 1968) of a part of the complex. Many other faults are suspected to exist, and they cause major problems in interpreting the stratigraphic section.

Exposures of the stratigraphically higher parts of the Upper zone were not examined for this report, but Hess (1960) described this part of the zone. His report implied that the upper part of his Upper Gabbro Zone contains plagioclase and orthopyroxene cumulates (Hess, 1960, p. 88-95). Cyclic layering is probably present. Above the highest exposed 244 m of the Upper Gabbro Zone of Hess (1960), which is identified by containing hypersthene (inverted pigeonite), Hess (1960, p. 101-108) postulated the existence of a Hidden Zone by analogy to the Skaergaard and Bushveld Complexes.

AGE

The Stillwater Complex has been the object of many recent geochronologic studies, many of which have conflicting interpretations as to the absolute age of the complex. On a relative scale the complex is younger than metasedimentary rocks that it intruded and hornfelsed and older than the coarse-grained quartz monzonite that forms dikes and intrudes and stopes the Basal zone.

The hornfels is considered to have a minimum age of about 3,140 m.y. on the basis of studies by Nunes and Tilton (1971). The quartz monzonite was studied by Nunes and Tilton (1971) by U-Pb method on zircons. They dated zircons that they considered to be primary igneous phases from the coarse-grained quartz monzonite (samples J14-4, J24-5, table 2, p. 2237) and from the aplite (sample J7-5 and A29-2, table 2, p. 2237). They assigned an age of about 2,750 m.y. to the intrusive event of the coarse-grained quartz monzonite and suggested that the aplite is about 60 m.y. younger.

The age of the complex is bracketed therefore between 3,140 and 2,750 m.y. (p. 5). More precise definition of the age of the complex on the basis of the present isotopic information is debatable. Kistler, Obradovich, and Jackson (1969) tested K-Ar and Rb-Sr ages of plagioclase, pyroxene, mica, and whole rocks from the Stillwater Complex and interpreted their data as meaning that (1) the complex was emplaced at 2,600 m.y. or (2) there was a metamorphic event at 2,600 m.y. that was superimposed on the complex, which could be as old as 3,800±400 m.y. A K-Ar whole-rock age of a specimen from the Basal zone was given as 3,200+200 m.y. (Kistler and others, 1969). Almost all the samples of Kistler, Obradovich, and Jackson (1969) came from the eastern section of the complex which was intruded at 2,700 m.y. by quartz monzonite and indeed underwent a thermal event as they suggested. Schwartzman (1970), Schwartzman and Giletti (1968), Fenton and Faure (1969), and Powell, Skinner, and Walker (1969) made various attempts to date either the complex or its thermal aureole with no definitive success because of the complicated geologic history of the complex after intrusion. Nunes and Tilton (1971) collected a sample of the Basal norite member from Nye Basin (sample A29-3) that contains abundant granitic dikes and hornfels inclusions and as yet is the only sample from the Basal zone that contains zircon. They argued strongly that the zircons are either comagmatic with the complex or were reset by the Stillwater magma, but they also described zircons from the blue metaquartzite that are very similar to those from the Basal zone and stated that they were metasomatically formed. An alternative interpretation that I prefer is that the zircons in the one sample of the Basal norite member were derived from inclusions of blue metaquartzite. The possibility of two contrary interpretations and the uniqueness of the occurrence cast some doubt on assigning an age of 2,750 m.y. to the complex on the basis of the U-Pb study of this sample of zircon from the complex. P. A. Mueller (written commun., 1973) obtained three different Rb-Sr isochrons for the hornfels: one for a suite in the Stillwater River valley, another for a suite collected south of Chrome Mountain, and the third suite along the Boulder River. In the Stillwater River valley suite he found an isochron of 2,719±76 m.y., whereas in the Chrome Mountain suite he obtained an isochron of 2,822+23 m.y., and in the Boulder River area an isochron of 2,573+29 m.y. The 2,719-m.y. age can be interpreted as the age of resetting by intrusion of the quartz monzonite, and the 2,822-m.y. age might be interpreted as the age of the Stillwater Complex thermal aureole. Thus, the Stillwater Complex is at least 2,750 m.y. old and may be more than 3,140 m.y. old. I prefer to regard its age as being closer to 3,140 m.y.

PETROLOGY, MINERALOGY, AND LITHOLOGY

Many detailed petrologic and mineralogic studies have been done on the Stillwater Complex, and that information is not repeated here. The major concentration of studies has been on the Ultramafic zone, especially the Peridotite member and the chromite horizons; exceptions are Hess' (1938a, b, 1939, 1941, 1949, and 1960) and Hess and Phillips' (1938, 1940) studies on the Banded and Upper zones and Howland's (1933, 1954) studies on the Basal zone. Studies on the Peridotite member and the Ultramafic zone include Wimmler (1948), Howland (1955), Howland, Garrels, and Jones (1949), Peoples and Howland (1940), Jones, Peoples, and Howland (1960), Jackson (1960, 1961, 1963, 1967, 1968, 1969, 1970, 1971), Page and Jackson (1967), Page (1971a, b), and Page, Shimek, and Huffman (1972). Wager and Brown (1967) presented a mineralogic and petrologic summary of most of these data.

INTRUSIVE QUARTZ MONZONITE SEQUENCE

AREAL EXTENT AND PREVIOUS WORK

Granitic intrusive rocks, a suite of quartz monzonite, aplite, and hornblende quartz diorite, crop out between the Stillwater Complex and the metamorphic rocks (see Page and others, 1973a, b). They extend from West Fishtail Creek to a point slightly west of the West Fork of the Stillwater River, a distance of about 24 km along the east third to half of the Stillwater Complex. Recorded occurrences of intrusive granitic rocks in the eastern Beartooth Mountains are meager (Skinner and others, 1969; Casella, 1969), but McMannis, Palmquist, and Reid (1971a, b, c) recorded two periods of development of felsic magmas in the area northwest of the Stillwater Complex area in the North Snowy block of the Beartooth Mountains (for location see fig. 1).

Jones, Peoples, and Howland (1960), Butler (1966), and Jackson (1967) were first to recognize the intrusive nature of the quartz monzonite, which was locally called the Mouat quartz monzonite pluton by Butler (1966, p. 54-55) on the west side of the Stillwater River immediately south of the Stillwater Complex. Page and Nokleberg (1970a, b; 1972) presented petrologic and structural evidence for the intrusive nature of a sequence of granitic rocks. They identified the following mappable units listed here from oldest to youngest: coarse-grained quartz monzonite (equivalent to the Mouat quartz monzonite pluton), medium-grained quartz monzonite, hornblende quartz diorite, fine-grained quartz monzonite, and numerous aplite dikes.

CONTACT AND AGE RELATIONS

The contact between the coarse-grained quartz monzonite and the Basal zone is poorly exposed, but the coarse-grained quartz monzonite definitely forms dikes and is intrusive into the Basal zone as seen in exposures on new mining roads and in drill core. Between Benbow and Mountain View, diking relations can be observed at several specific localities. On the east side of Golf Course Point, Benbow area, in a roadcut at about 8,900-ft elevation (coordinates 495,700 N.; 1,919,570 E.), the coarse-grained quartz monzonite forms an intrusive breccia zone about one-third of a meter wide that encloses fragments of the Basal norite member. Within Nye Basin (coordinates: 500,570 N.; 1,914,700 E.) dikes of granitic rocks cut the Basal norite member, which is a fine-grained diabasic rock. Jackson, Howland, Peoples, and Jones (1954) recorded an example of intrusive relations in their mapping of the Nye Lip area (surrounding coordinates: 502,940 N.; 1,909,500 E.), a small part of which is shown in figure 20. Most of this exposure has been destroyed by trenching. In the Mountain View area along the north side of Verdigris Creek (coordinates: 503,270 N.; 1,899,100 E.), the granitic rocks form dikes in the hornfels, which contains pods, dikes, and sills of the Basal norite member.

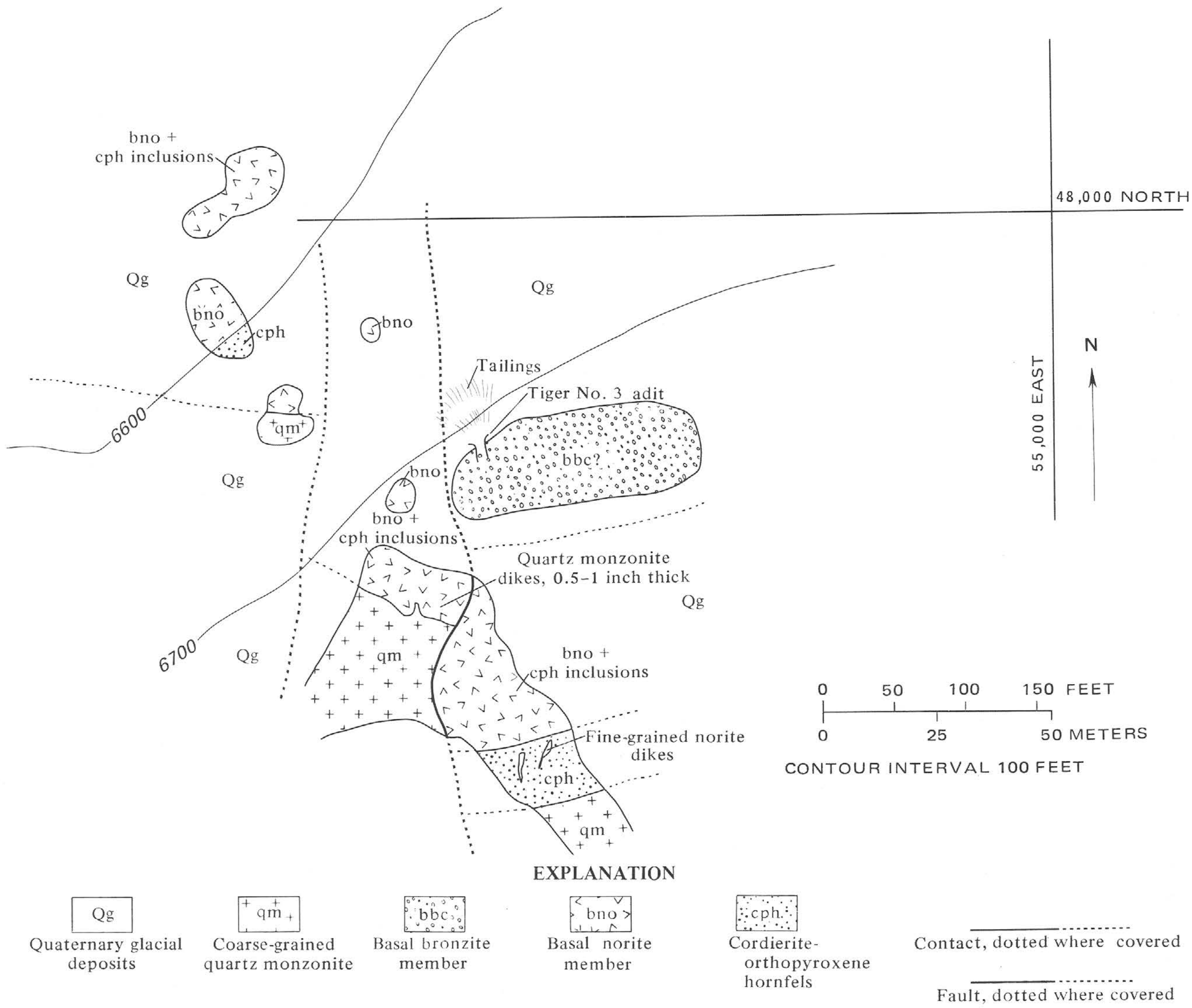

FIGURE 20.—Geologic sketch map of part of the Nye Lip area showing intrusive relations of the coarse-grained quartz monzonite. (Modified from Jackson and others, 1954; coordinates are those used by Jackson and others, 1954, in the Nye Lip area.)

The coarse-grained quartz monzonite contains inclusions of the Basal norite member and hornfels (fig 21) ranging in size from single-grain xenocrysts of orthopyroxene and cordierite to those large enough to map (see Page and Nokleberg, 1972). On the west margins of the coarse-grained quartz monzonite on the ridge north of Verdigris Creek, there are abundant inclusions and stoped pieces of hornfels, Basal norite, and massive sulfide. Along the southwest margin the coarse-grained quartz monzonite contains abundant orthopyroxene xenocrysts. Mineralized Basal norite member and hornfels form a large inclusion on Granite Ridge (coordinates: 503,260 N.; 1,901,970 E.), a zone about a meter wide of contaminated coarse-grained quartz monzonite rich in sulfides and mafic minerals. Elsewhere the quartz monzonite is homogeneous and apparently uncontaminated. Excellent exposures of Basal norite inclusions in the coarse-grained quartz monzonite occur east of the Stillwater River on the cliffs that form the ridge between Nye and Flume Creeks (coordinates: 501,780 N.; 1,906,350 E. and 502,340 N.; 1,909,370 E.). The northernmost inclusion dominantly contains mineralized Basal norite but has a small amount of iron-formation, and layered metaquartzite is in contact with the norite. This is one of the few occurrences of iron-formation and metaquartzite east of Bluebird Ridge. On the north side of the ridge between Nye and Flume Creeks (coordinates: 499,440 N.; 1,910,210 E.) an area about 18.3 by 15.2 m of coarse-grained quartz monzonite contains abundant angular inclusions of hornfels and norite that range in diameter from 12.7 cm to about 3.0 m.

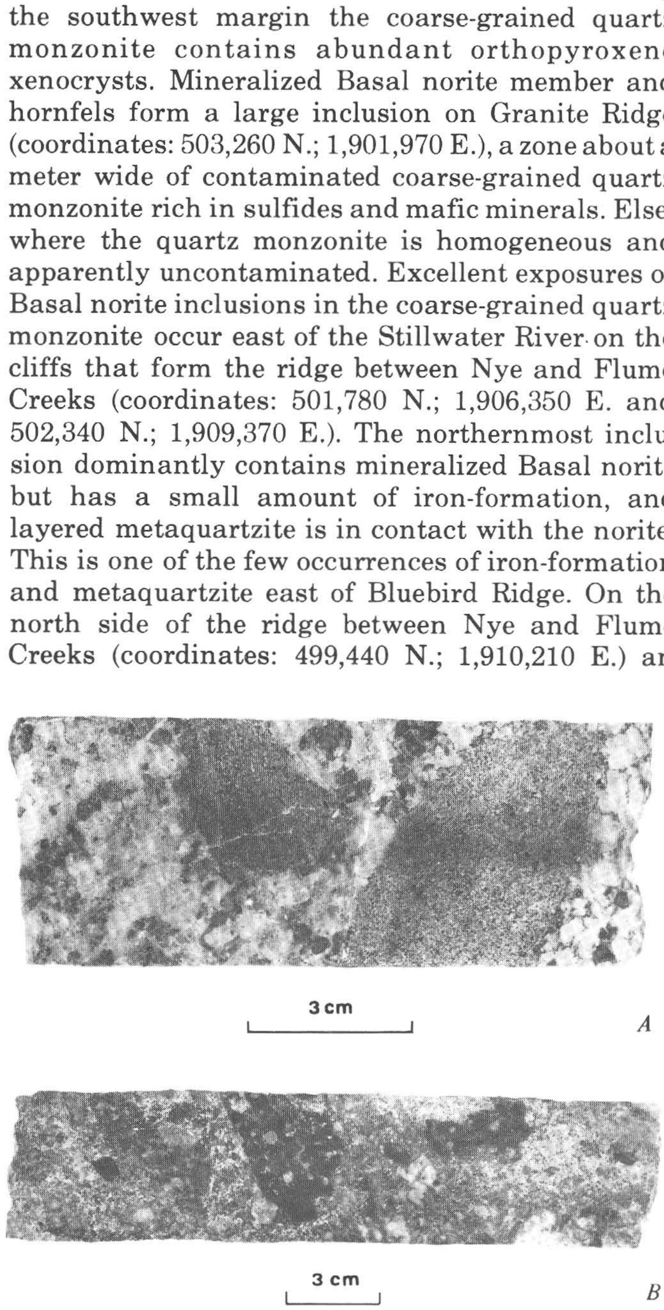

FIGURE 21.—Hydrofluoric-acid-etched slabs of coarse-grained quartz monzonite from drill core containing inclusions of Basal zone norite and hornfels. *A*, Finer grained hornfels inclusions. *B*, Dark-colored altered inclusions of Basal zone norite.

Drilling in Nye Basin indicates that the contact between the Basal zone and the quartz monzonite is partly faulted. Figure 22, based on examination of core from drill holes in the Mountain View and Nye Basin areas, shows the complexities that occur at the contact. The sequence of events illustrated is as follows: (1) the Basal norite member intruded, brecciated, and hornfelsed the metasedimentary rocks, (2) the coarse-grained quartz monzonite invaded this breccia and intrusive zone, intruding and brecciating both hornfels and the Basal norite member, (3) the contact was later faulted, sheared, and brecciated, and (4) either during events (2) and (3) or after, the mafic minerals in all rocks were chloritized and serpentinized, and the feldspar altered. All diking and stoping relations and inclusions in the quartz monzonite are the result of this sequence of events.

Most of the relations discussed above refer to the north margin of the coarse-grained quartz monzonite. Along the south margin, a series of hornfels pendants extend from northeast of the headwaters of Flume Creek westward along the south side of the ridge between Flume and Nye Creeks to the Stillwater River (Page and Nokleberg, 1972, 1974). The block of hornfels south of the Bluebird fault in the Mountain View area is also thought to be a pendant, and the small piece of hornfels on the south side of Granite Ridge (coordinates: 502,130 N.; 1,901,120 E.) may also be a pendant. The coarse-grained quartz monzonite near the contacts appears to be contaminated by the hornfels and is enriched in mafic material. On the ridge (coordinates: 495,160 N.; 1,915,820 E. and 499,060 N.; 1,906,280 E.) dikes of coarse-grained quartz monzonite can be observed to intrude the pendants; similar relations are found on the south side of Granite Ridge (coordinates: 502,250 N.; 1,901,060 E.). The northern limits of all the individual hornfels pendants follow a fairly linear west-northwesterly strike with few irregularities. The pendants east of the Stillwater River are also alined in this direction. This alinement may indicate the existence of a preintrusion fault that controlled emplacement of the coarse-grained quartz monzonite.

The medium-grained quartz monzonite is intrusive into the coarse-grained quartz monzonite. Along the ridge line north of Flume Creek, the medium-grained quartz monzonite forms dikes and apophyses in the coarse-grained rock. The dikes range in size from 1

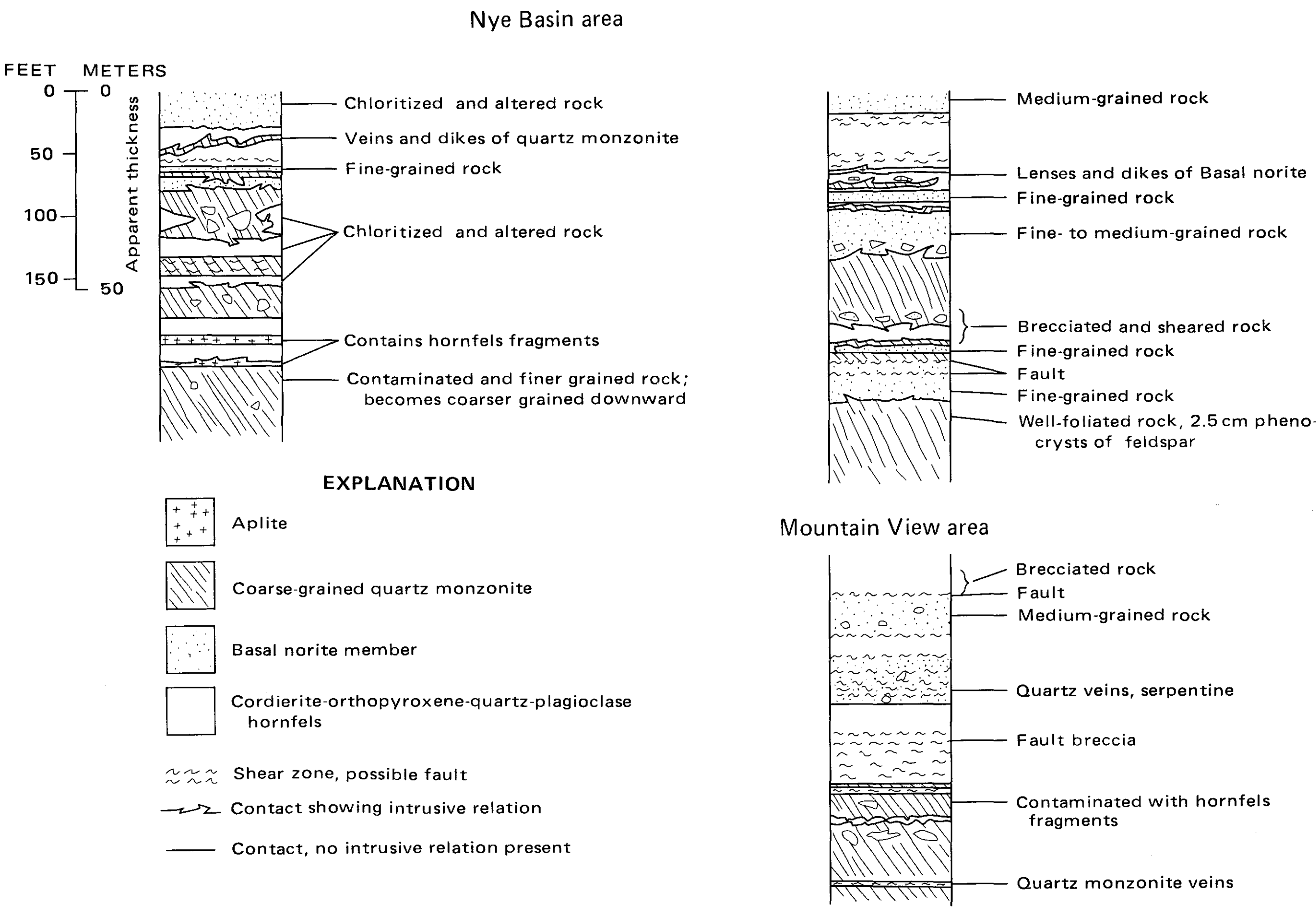

FIGURE 22.—Schematic diagrams of drill core showing contact relations between the coarse-grained quartz monzonite and the Basal norite member.

cm to 90 m across (examples are at coordinates: 497,800 N.; 1,909,480 E. and 496,990 N.; 1,911,350 E.). In addition the medium-grained quartz monzonite intrudes the hornfels pendants along the south side of the ridge. The age relations are well defined (coordinates 497,510 N.; 1,908,770 E. and 498,570 N.; 1,907,140 E.) and demonstrate that the medium-grained quartz monzonite is younger than the pendants. The southern contact of the pendants with the medium-grained rock is highly irregular in comparison with the northern contact and suggests much more stoping activity. On the west side of the Stillwater River (coordinates: 501,300 N.; 1,892,630 E.) intrusive contacts of the medium-grained quartz monzonite are well exposed.

The hornblende quartz diorite forms dikes in and contains inclusions of the medium-grained quartz monzonite on the south side of Flume Creek (coordinates: 493,760 N.; 1,911,990 E.). At the other occurrence south of the Initial Creek area (coordinates: 501,620 N.; 1,887,840 E.), no relative age relations are exposed.

South of Flume Creek (coordinates: 494,360 N.; 1,910,100 E.), the fine-grained quartz monzonite forms dikes in the hornblende quartz diorite and in the area south of Initial Creek near the headwaters of Cathedral Creek (near coordinates: 502,000 N.; 1,882,500 E.) is intrusive into the medium-grained quartz monzonite. Intrusive relations (coordinates: 502,530 N.; 1,890,780 E. and 500,580 N.; 1,887,960 E., for example) show that the fine-grained rock is younger than medium-grained quartz monzonite.

Aplite dikes occur throughout the mass of granitic intrusive rocks and also are found in hornfels and the Basal norite member of the complex. Their best development and exposure are in the Mountain View area (coordinates: 502,150 N.; 1,898,260 E.) where they form a dike swarm of contaminated and uncontaminated aplites in the hornfels and cut across both the coarse- and medium-grained quartz monzonites. In many other localities the relative age relations of the aplites to other granitic rocks can be determined (coordinates: 494,990 N.; 1,916,100 E.; 503,340 N.; 1,899,700 E. and 501,250 N.; 1,899,130 E.).

In summary, the diking and stoping relations indicate the following sequence of intrusion: (1) Basal norite into hornfels, (2) coarse-grained quartz monzonite, (3) medium-grained quartz monzonite, (4) hornblende quartz diorite, (5) fine-grained quartz monzonite, and (6) numerous aplites. Wherever intrusive relations are exposed in the area mapped, the sequence of events is the same.

Nunes and Tilton (1971) determined U-Pb ages of zircons from the coarse-grained quartz monzonite and from the aplite. The zircons from the coarse-grained rock were euhedral and large, and those from the aplite samples finer grained; both were considered to be primary igneous zircon by Nunes and Tilton (1971). They gave $^{207}Pb/^{206}Pb$ ages between 2,700 and 2,750 m.y. for the granitic rocks (Nunes and Tilton, 1971, p. 2237) and interpreted that quartz monzonites were emplaced about 2,750 m.y. by an intrusive event that may have lasted 60 m.y.

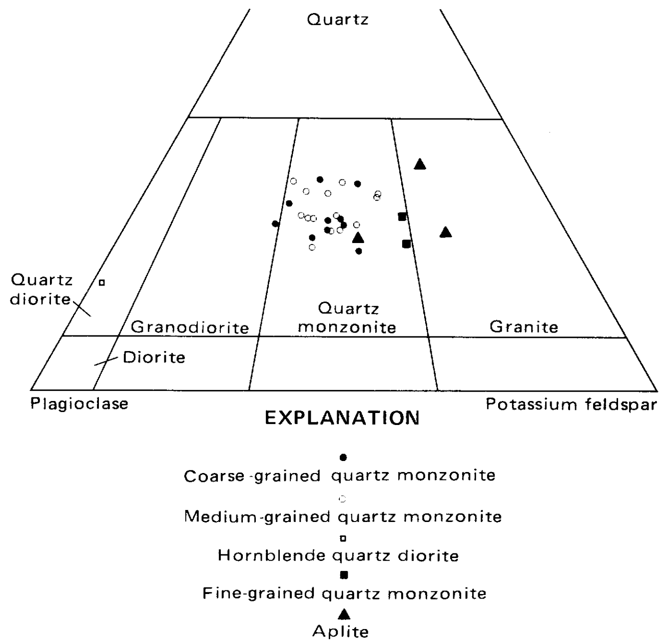

FIGURE 23.—Triangular diagram of modal quartz, plagioclase, and potassium feldspar in granitic intrusive rocks. Compositional names and subdivisions after Bateman, Clark, Huber, Moore, and Rinehart (1963).

LITHOLOGY AND PETROGRAPHY

The quartz monzonite exhibits relict xenomorphic to hypidiomorphic-granular, equigranular, and porphyritic textures. Overprinted on the igneous texture is one of metamorphic origin that consists of seriate grain boundaries in which muscovite, biotite, chlorite, quartz, and feldspar are recrystallized along feldspar-quartz grain contacts. This texture is a result of recrystallization during and after the development of a postemplacement penetrative mineral foliation. The granitic rocks are distinguished by relict textures, major differences in grain size, and mutual intrusive relations; composition and mineralogy are minor aids for identification. A modal mineralogic classification proposed by Bateman, Clark, Huber, Moore, and Rinehart (1963) is used for naming the rocks (fig. 23). Modes are closely grouped and cannot be used to subdivide the quartz monzonite; therefore the plots in figure 23 are grouped on the basis of grain size and mutual intrusive relations.

The field characteristics that differentiate these siliceous granitic intrusive rocks from the granitic gneisses of the metamorphic rocks are (1) lack of felsic-mafic mineral compositional banding, (2) extreme homogeneity in composition and texture of rock types over a large area, (3) sharp and regular contacts of individual rock types with one another, and (4) consistent determination of the relative age of rocks in contact. The intrusive rocks have a narrow range of chemical composition (see Page and Nokleberg, 1972).

Coarse-grained quartz monzonite.—Major minerals in this coarse-grained porphyritic to inequigranular rock are plagioclase, potassium feldspar, quartz, and biotite (fig. 24*A*). Minor minerals are apatite, zircon, and oxide and sulfide minerals; sericite, chlorite, and epidote are secondary minerals. Each of the primary felsic minerals occurs both as phenocrysts and in the groundmass. Plagioclase forms euhedral to subhedral phenocrysts that are 0.5 cm to about 2 cm long, are locally zoned, and in places occur in clots or groups; in the groundmass, it occurs as euhedral to subhedral albite-twinned 0.075-0.3-mm-long crystals loosely packed in a potassium feldspar and quartz matrix. Potassium feldspar, microcline-perthite (mainly string type) rarely with tartan twinning, forms phenocrysts, 0.3-1.5 cm long. The phenocrysts are Carlsbad twinned and enclose irregular grains of quartz and plagioclase. The phenocrysts have a fairly regular shape but have highly irregular boundaries with the groundmass and locally have biotite inclusions in the margins of the crystal. In the groundmass of the rock, tartan-twinned microcline that is locally perthitic occurs as very irregular anhedral 1-2-mm grains. Quartz occurs in 0.4-1-cm clots of individual anhedral locally undulant grains 2-4 mm in diameter. Locally the margins of the clots are finer grained and appear to be recrystallized. Quartz also occurs as irregular anhedral grains in the groundmass. Biotite forms clotlike groups of flakes that are associated with oxides and sulfide minerals, zircon, and apatite.

Much biotite is altered totally or partially to chlorite. Myrmekitic intergrowths occur locally associated with the microcline. Page and Nokleberg (1972) recorded modes for three chemically analyzed samples; all the modes done on the coarse-grained quartz monzonite are plotted in figure 24. Electron microprobe analyses for microcline and plagioclase, calculated to the end-member molecules, albite (Ab), anorthite (An), and orthoclase (Or), are given in figure 25. The analytical technique used with the electron microprobe was discussed by Page and Nokleberg (1972).

Medium-grained quartz monzonite.—Major minerals in this medium-grained xenomorphic granular to inequigranular rock are plagioclase, potassium feldspar, quartz, and biotite (fig. 24*B*). Minor minerals are apatite, less abundant zircon, and oxide and sulfide minerals; sericite, locally muscovite, chlorite, and epidote are secondary alteration minerals. Plagioclase is zoned and forms subhedral to anhedral crystals 2–3 mm long. Potassium feldspar is mainly tartan-twinned microcline-perthite with vein and string perthite as the common type. Myrmekitic intergrowths are common. Biotite locally forms symplectic intergrowths with quartz and is in many places replaced partly by chlorite. Accessory minerals are associated with the biotite; apatite is more abundant than zircon. In some specimens two

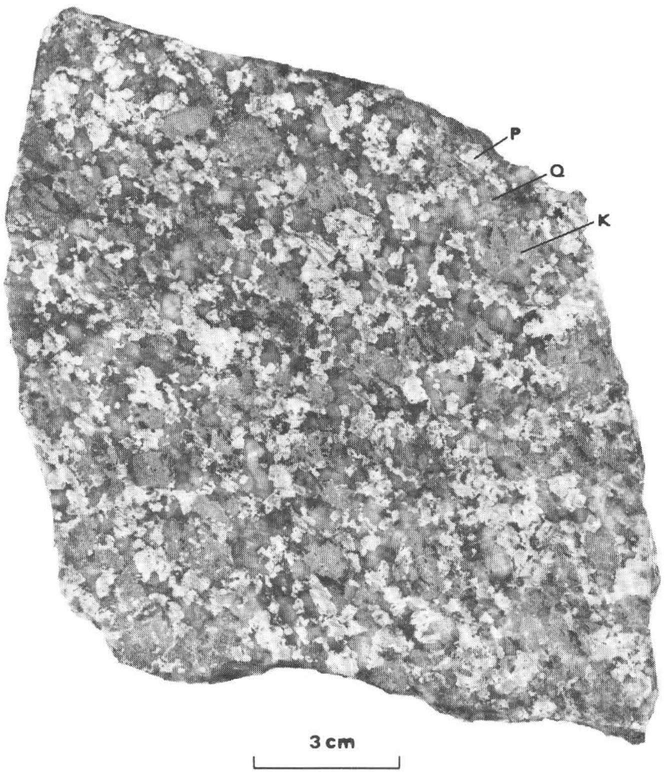

A

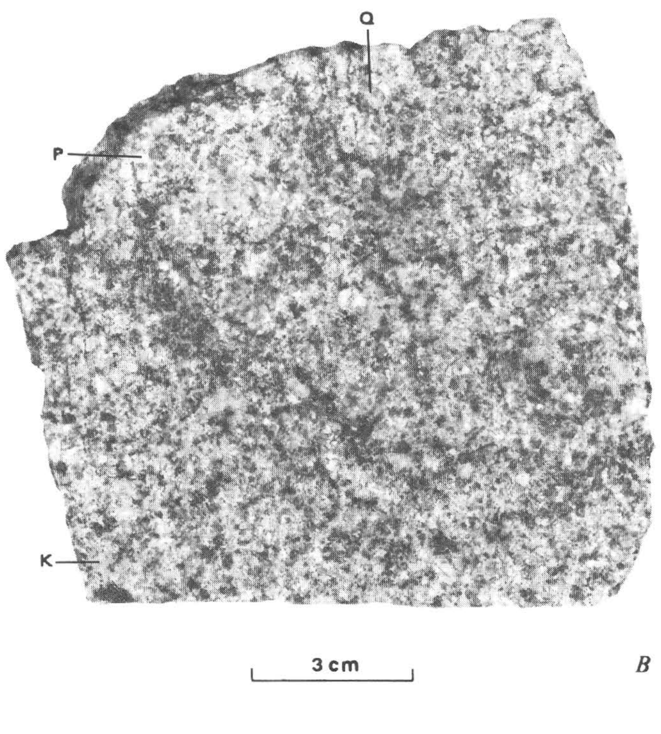

B

C

FIGURE 24.—Rock slabs showing different grain sizes of quartz monzonites. P, plagioclase; K, potassium feldspar; Q, quartz; black mineral, biotite. *A*, Etched and stained slab of coarse-grained quartz monzonite. *B*, Cut and etched slab of medium-grained monzonite. *C*, Cut and etched slab of fine-grained quartz monzonite.

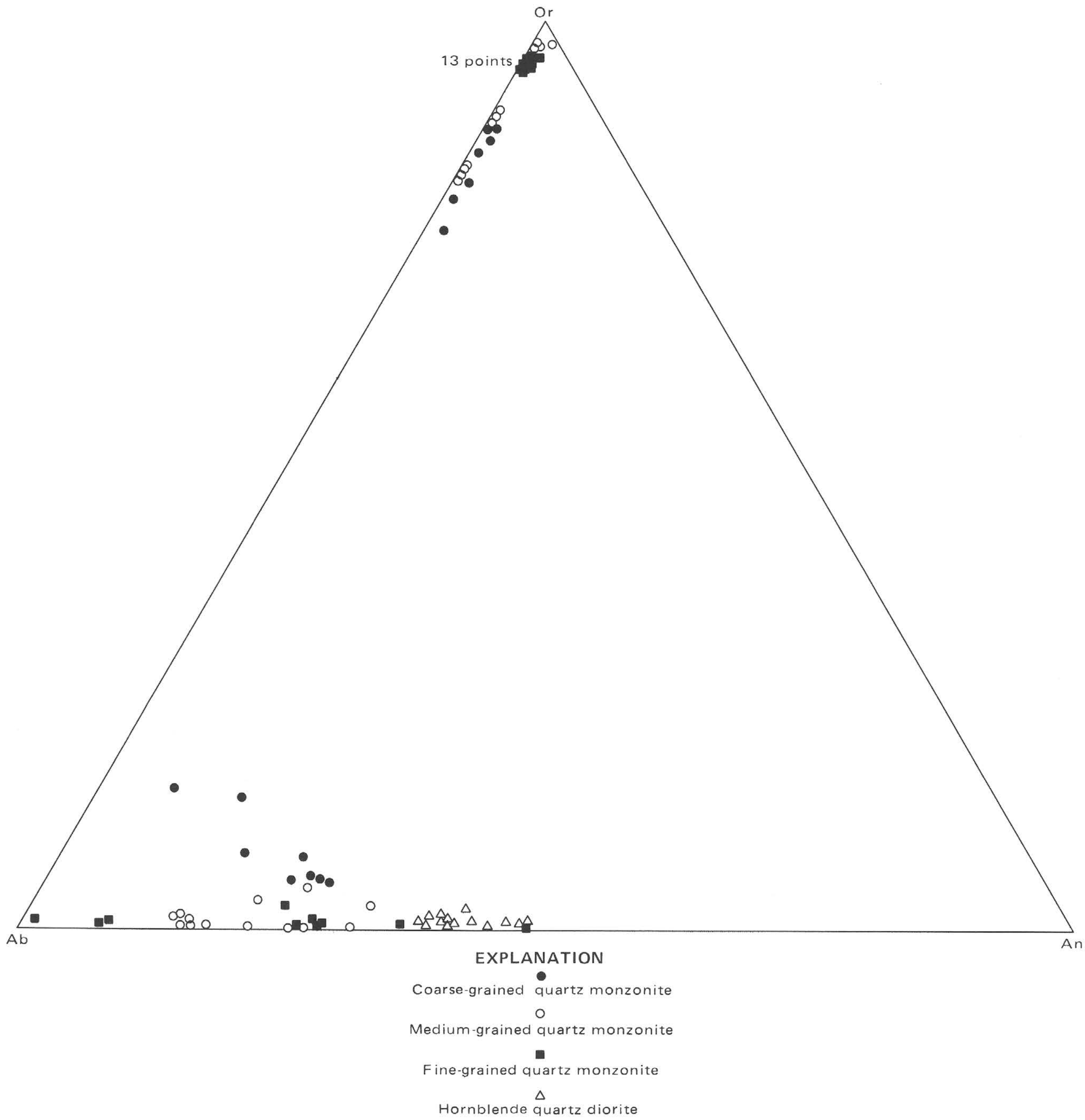

FIGURE 25.—Triangular diagram of feldspar compositions in intrusive granitic rocks.

generations of epidote occur; one generation forms euhedral to subhedral, zoned, yellow, strongly pleochroic crystals associated with biotite; the other forms anhedral, ragged, finer grained, weakly pleochroic crystals associated with sericite and muscovite that formed from the alteration of plagioclase. Page and Nokleberg (1972) recorded modes for five analyzed rocks; both those and new modes are plotted in figure 23. Electron microprobe analyses for microcline and plagioclase are given in figure 25.

Hornblende quartz diorite.—The hornblende quartz diorite is a medium-grained hypidiomorphic granular to inequigranular rock composed of the major minerals epidote, zircon, potassium feldspar, and opaque minerals. Chlorite and clay minerals are secondary. Page and Nokleberg (1972) gave a mode (fig. 23), chemical analysis, and plagioclase composition for this rock.

Fine-grained quartz monzonite.—The fine-grained quartz monzonite is a xenomorphic to hypidiomorphic inequigranular rock composed dominantly of plagioclase, microcline, quartz, biotite, and locally muscovite (fig. 24*C*). Minor minerals are chlorite after biotite, and epidote and sericite after plagioclase, apatite, zircon, and opaque minerals. Modes of two analyzed specimens were given by Page and Nokleberg (1972); other modes are shown in figure 23. Plagioclase and microcline analyses are given in figure 25.

Aplite.—Major minerals in this hypidiomorphic to xenomorphic fine- to medium-grained granular rock are quartz, plagioclase, and microcline. Minor minerals are biotite, muscovite, epidote, zircon, apatite, and opaque minerals. Rare orthopyroxene and cordierite are local contaminants. Modes of aplitic rocks are plotted in figure 23.

MAFIC INTRUSIVE ROCKS

AREAL EXTENT AND PREVIOUS WORK

Mafic dikes and sills of Precambrian age are widespread in the Beartooth Mountains (Prinz, 1964; Page and others 1973a, b; Butler, 1966). Within the area mapped in detail by Page and Nokleberg (1974) a large number of mafic dikes are found in fault zones, as noted by Jones, Peoples, and Howland (1960). Others occur with no obvious relations to fault zones within all the Precambrian units. The largest and best developed mafic dike is exposed discontinuously from Bluebird Peak to the headwaters of Bobcat Creek. The discontinuous nature of the dikes is most likely caused by postintrusion faulting and Quaternary covering units.

Prinz (1964) divided the mafic dikes into four groups on the basis of petrology and chemistry. Two of his groups occur in the Stillwater area: (1) Archean metadolerites and (2) late Precambrian dolerites. Field identification of these types of dikes is difficult, if not in most examples impossible, and Prinz (1964) based the distinction on a petrographic study. Mueller (1971) examined the geochemistry of 110 samples of mafic dikes and the geochronology of 52 of these samples from the southern Beartooth Mountains. He was able to divide the mafic dikes into four chemically distinguishable groups and into three and possibly four ages of mafic intrusion. His age group (1) 2,562±126 m.y. (concordant K-Ar and Rb-Sr ages) corresponds to Prinz' (1964) metadolerite group; his age group (2) 1,500-1,800 m.y. (discordant Rb-Sr and K-Ar ages) contains both Prinz' Archean Metadolerites and late Precambrian dolerites. Mueller (1971) could not resolve which age technique was correct for group (2), and unfortunately he does not present enough petrographic description to allow one to subdivide this group on the basis of mineralogic and textural criteria.

AGE RELATIONS

All the mafic dikes show intrusive relations that demonstrate they are younger than the other Precambrian rocks exposed in the Stillwater Complex and adjacent units. Although none of the dikes has been dated, comparison with Mueller's (1971) chemical and isotopic study suggests that the metamorphosed dikes were intruded about 2,562±126 m.y. ago and the unmetamorphosed ones at about 1,200-1,500 m.y. ago.

LITHOLOGY

Mafic dikes in the Stillwater Complex and adjacent rocks were not divided into groups in the field by Page and Nokleberg (1974), but some of them were divided by Page, Simons, and Dohrenwend (1973a, b) on the basis of petrographic criteria. The dikes from which samples were collected in the Stillwater area were divisible into two major petrographic types: (1) metamorphosed mafic dikes with clouded plagioclase and granoblastic aggregates of recrystallized pyroxene and (2) unmetamorphosed mafic dikes without these features. Group (1) was subdivided into metadolerite, metanorite, and porphyritic metadolerite; group (2) into quartz dolerite and olivine dolerite. Table 11 gives the location by coordinates of the dikes and the petrographic group and subgroup for the dikes examined.

METAMORPHOSED MAFIC DIKES

Metadolerite with hypidiomorphic to xenomorphic, subophitic to ophitic textures where least recrystallized, and with partly recrystallized plagio-

TABLE 11.—*Lithologic classification of mafic dikes in the Stillwater Complex and adjacent rocks*

Montana South coordinates		Group	Subgroup
North	East		
505,560	1,864,520	Metamorphosed	
504,040	1,866,390		Metadolerite
510,600	1,855,570		
499,180	1,880,820		
516,680	1,840,200		
506,770	1,856,180		Metanorite
494,840	1,907,310		Porphyritic metadolerite
502,790	1,903,080		
		Unmetamorphosed	
541,360	1,820,840		Quartz dolerite
497,570	1,919,170		
536,340	1,822,550		
490,910	1,915,630		
517,000	1,836,690		
508,950	1,900,740		Olivine dolerite

clase and granoblastic aggregates of pyroxene where most recrystallized is the common type of mafic dike rock. Major minerals are augitic pyroxene, orthopyroxene, plagioclase, and reddish-brown hornblende. Minor and accessory minerals are biotite, olivine, apatite, and oxide minerals. Secondary minerals produced by metamorphism, deuteric alteration, or weathering include blue-green amphibole, epidote, quartz, talc, actinolite, chlorite, serpentine, and clay minerals.

In a typical specimen, zoned plagioclase (An_{50}–A_{70}) forms 2–4-mm-long laths that are filled with inclusions or are clouded and intergrown with pyroxene. The clouding appears to consist of about 1 micrometer or less fluid inclusions, oxide, and silicate minerals that locally occur in definite zones and rarely cross crystal boundaries (see Armbrustmacher and Banks, 1974). Locally the plagioclase recrystallized to a granular mosaic of grains about 0.2–0.5 mm in diameter; these grains are not clouded. This recrystallization usually began at the margins of the grains. Orthopyroxene with exsolution lamellae forms 4–6-mm-diameter plates that make an ophitic texture with plagioclase. Clinopyroxene is the dominant pyroxene and locally replaces orthopyroxene forming a texture that is similar to clinopyroxene-orthopyroxene reaction textures described from the Stillwater Complex (Jackson, 1961). Clinopyroxene has recrystallized into granoblastic aggregates of grains a few tenths of a millimeter in diameter. When the clinopyroxene recrystallized, it seems to have freed iron that formed oxide mineral inclusions (probably magnetite or hematite) in the granoblastic pyroxene. Reddish-brown hornblende forms both euhedral crystals and anhedral masses that rim the oxide minerals and clinopyroxene. Biotite occurs as poikilitic flakes that rim the hornblende. Olivine is sparse, but where it occurs, it is in small subhedral grains enclosed in orthopyroxene. Apatite forms euhedral crystals that are poikilitically enclosed by biotite or brown hornblende. The oxide minerals form either vermicular intergrowths with clinopyroxene or inclusions in it. Blue-green amphibole locally replaced rims of the brown hornblende. Other secondary minerals generally destroyed most of the textures described in proportion to the amount of alteration.

Metanorite has a hypidiomorphic to idiomorphic texture and is composed of euhedral to subhedral orthopyroxene and minor clinopyroxene as phenocrysts in a lath-shaped plagioclase matrix. Other minerals present are biotite, brown-green hornblende, oxide minerals, talc, and serpentine. The pyroxene phenocrysts are 2–4 mm in diameter and have no apparent orientation. Clinopyroxene is twinned and locally appears to have replaced orthopyroxene. The plagioclase in the matrix is zoned and averages 1–2 mm in length; locally plagioclase is recrystallized into a granular mosaic that commonly consists of untwinned grains. The opaque minerals are associated with the biotite and hornblende. Round to subround areas of talc, serpentine, and magnetite may be pseudomorphs of olivine.

Porphyritic metadolerite has an ophitic to subophitic groundmass containing plagioclase phenocrysts up to 3 cm in maximum diameter. It has two different occurrences: (1) in individual dikes that may or may not have fine-grained margins and (2) as a local facies of the metadolerite dikes. Most examples, although extremely altered, contain abundant green-brown hornblende, tabular plagioclase, clinopyroxene, quartz, and oxide minerals as the groundmass and large plagioclase phenocrysts largely altered to sericite and epidote. Other abundant alteration products are talc, tremolite, chlorite, and serpentine.

UNMETAMORPHOSED MAFIC DIKES

Quartz dolerite is the most abundant of the unmetamorphosed dikes. It ranges from very fine grained to medium-grained ophitic to subophitic textured rocks. Major minerals in approximate order of abundance are plagioclase, clinopyroxene, green-brown hornblende, pigeonite, and orthopyroxene. Minor minerals are quartz, potassium feldspar(?), biotite, and oxide minerals. Secondary minerals include tremolite, talc, serpentine, chlorite, sericite, epidote, and clay minerals. Zoned plagioclase (An_{50-70}) forms euhedral to subhedral platelets that are intergrown with twinned anhedral masses of augitic clinopyroxene with subhedral grains of pigeonite and orthopyroxene in interstices. Hornblende forms anhedral crystals and rims (replaces?) clinopyroxene. Quartz and potassium feldspar form a micrographic intergrowth that fills some interstices.

Olivine dolerite forms a dike of subophitic to diabasic-textured rock with fine- to medium-grain size and consisting of (1) euhedral to subhedral zoned phenocrysts of clinopyroxene and orthopyroxene and (2) euhedral olivine in a lath-shaped locally poikilitic groundmass of zoned plagioclase. Biotite and iron oxides are the other minerals present. Only one dike of this type has been recognized; it is a composite with a quartz dolerite dike that occurs along the road in the Mountain View area (see table 10).

CHEMICAL CHARACTERISTICS

Because of the extensive chemical work (Mueller, 1971; Prinz, 1964) done on mafic dikes in the Beartooth Mountains and because the major objective of this study is not petrogenesis of mafic dikes, an extensive chemical study was not undertaken. Two samples of metadolerite, both from the same dike (one quartz dolerite and one olivine dolerite that contain less than 10 percent secondary minerals), were selected for analysis (table 12). Comparison with Mueller's (1971) criteria for distinguishing different groups of mafic dikes on the basis of TiO_2 content suggests that samples 19CM71 and 20CM71 fall into his group I. Amounts of K_2O, Fe as Fe_2O_3, and Al_2O_3 are also compatible with his group I. The samples also have low K-Rb ratios and moderately low Rb-Sr ratios similar to his group I.

TABLE 12.—*Chemical analyses of mafic dike rocks*

[Chemical analyses by S. D. Botts under supervision of Leonard Shapiro by rapid-rock methods; quantitative and semiquantitative spectrographic analyses by Chris Heropoulos]

	19CM71	20CM71
Chemical analysis (weight percent)		
SiO_2	49.1	48.9
Al_2O_3	15.1	15.0
Fe_2O_3	.90	1.8
FeO	10.9	10.4
MgO	7.9	6.4
CaO	10.9	10.5
Na_2O	2.2	2.4
K_2O	.27	.60
H_2O^+	1.0	1.4
H_2O^-	.02	.02
TiO_2	1.1	.99
P_2O_5	.13	.12
MnO	.16	.13
CO_2	.02	.08
Sum	100	99
F	.00	.00
Cl[1]	.013	.038
S[1]	.05	.07
Quantitive spectrographic and X-ray fluorescence analysis (parts per million)		
Co	40	49
Cr	300	52
Cu	140	200
Ni	100	130
Rb[1]	8	16
Sr[1]	145	179
Semiquantitative, six-step spectrographic analyses (parts per million)		
Mn	1,500	1,500
Ba	100	100
Co	50	50
Cr	300	50
Cu	150	200
Ni	150	200
Sc	50	30
Sr	150	150
V	200	150
Zn	30	15
Zr	50	50
Ga	15	20
Yb	3	3
Rb/Sr	.06	.09
K/Rb	280	311

[1]Elements analyzed by X-ray fluorescence by L. F. Espos and B. P. Fabbi.

19CM71—Coordinates: 516,690 N.; 1,840,220 E.
20CM71—Coordinates: 516,690 N.; 1,840,220 E.

PALEOZOIC AND MESOZOIC ROCKS

Paleozoic and Mesozoic rocks consist of about 2,440–3,050 m of alternating marine and continental sediments (pl. 1) deposited on the beveled edge of the gently inclined Stillwater Complex (Jones and others, 1960). The sedimentary rocks occur north of the complex in the Mt. Wood, Mt. Douglas, and Mt. Rae quadrangles (fig. 1). Downfaulted blocks of Middle and Upper Cambrian strata occur within the complex (Page and Nokleberg, 1974), and a downfaulted block of Paleozoic and Mesozoic sedimentary rocks occurs along the Mill Creek-Stillwater fault zone in the Mt. Douglas quadrangle (Page and others, 1973b). Because the Paleozoic and Mesozoic rocks were not studied in detail, the reader is referred to Vhay (1934), Richards (1958), and Jones, Peoples, and Howland (1960) for a discussion of these rocks.

TERTIARY ROCKS

A few dikes and sills of light-gray aphanitic felsic rocks with phenocrysts of biotite and potassium feldspar (such as at coordinates 513,520 N.; 1,862,550 E.) cut the Precambrian rocks (Page and others, 1973a, b). Vhay (1934) described several stocks that intrude sedimentary rocks of Paleozoic and Mesozoic age. The stocks, which are intermediate in composition, are of different ages. Rouse, Hess, Foote, Vhay, and Wilson (1937) described similar rocks along the northern flank of the Beartooth Mountains, and Vail (1955) found them along the Dry Fork thrust. Jones, Peoples, and Howland (1960) discussed the timing of this intrusive event and placed it as post-Cretaceous.

QUATERNARY DEPOSITS

During the Quaternary Period, the area was glaciated similar to that elsewhere in the Rocky Mountains. The history includes, from oldest to youngest, a pre-Bull Lake glaciation, the Bull Lake and Pinedale Glaciations, and two or three stades of Neoglaciation (Ten Brink, 1968, 1972). These resulted in deposits of moraine, glaciofluvial materials, till, and terrace gravels and silts. Large fans of reworked glacial debris occur at the mouths of most streams draining into the major rivers. The rivers have cut into the fans and deposited alluvial gravel- to silt-sized material on top of them. Large landslides, consisting of glacial debris, talus, and semicoherent large blocks of bedrock, occur on the steep canyon sides of the major drainages, especially the Stillwater River; parts of the landslides are so coherent that attempts were made to mine chromite zones in the large blocks (see Jackson and others, 1954, Mountain View map). Talus cones are quite extensively developed on all steeper surfaces (Page and Nokleberg, 1974).

METAMORPHISM

Within the Mt. Wood and Mt. Douglas quadrangles (Page and others, 1973a, b), two types of metamorphism are distinguished on the basis of their occurrence and mineral assemblages: (1) regional metamorphism characterized by widespread distribution of similar mineral assemblages throughout the metasedimentary and meta-igneous rocks that form gneisses and schists of the Beartooth Mountains and (2) contact metamorphism characterized by local distribution of mineral assemblages spatially related to the intrusions of the Stillwater Complex and the quartz monzonite sequence. As demonstrated by Butler (1966, 1969) and Eckelmann and Poldervaart (1957), the limited amounts of gneiss and schist within Page and Nokleberg's (1974) map area were formed during a widespread metamorphic event in the Beartooth Mountains that occurred about 2,750 m.y. ago (Gast and others, 1958). Physical conditions of the event correspond to those inferred for the amphibolite facies of Turner and Verhoogen (1960, p. 545). Butler (1966, p. 59–60) indicated that the metamorphic conditions for the gneiss and schist southof the Stillwater Complex were probably of slightly lower grade than those in the eastern Beartooth Mountains. The Stillwater Complex has a well-defined contact metamorphic aureole consisting of pyroxene-hornfels facies rocks in the immediately adjacent metasedimentary rocks and hornblende-hornfels facies rocks farther from the complex. Page and Nokleberg (1972) commented on the paucity of metamorphic effects associated with the quartz monzonite sequence. In the subsequent sections of this report the physical conditions of metamorphism are refined, and metamorphic problems for which solutions are unknown at the present time are discussed.

REGIONAL METAMORPHISM

At least three different questions arise in a discussion of regional metamorphism: (1) What were the physical conditions under which the schist, gneiss, and migmatitic rocks of the Beartooth Mountains formed? (2) Were the rocks that are now hornfels involved in this regional metamorphism before or after they were hornfelsed, or not at all? (3) Is there any evidence for a lower grade, perhaps retrogressive, regional metamorphism at about 1.6–1.8 b.y. (billion years) ago, as postulated by Giletti (1966), Brookins (1969), Nunes and Tilton (1971), and Rowan and Mueller (1971)? At the present time not all these questions can be completely answered.

PHYSICAL CONDITIONS OF REGIONAL METAMORPHISM

The conformable interlayering of biotite schist, granitic gneiss, and amphibolitic gneiss implies that they were all submitted to about the same physical conditions and that their mineral assemblages should be broadly compatible with those conditions. Two characteristics of the mineral assemblages produced by this regional metamorphism are the general lack of sillimanite, kyanite, or andalusite and the association of cordierite, staurolite, and anthophyllite in pelitic rocks with the requisite bulk compositions. This assemblage of minerals led Butler (1966) to suggest that the regional metamorphism was of a low-pressure intermediate type (Miyashiro, 1961) similar to Read's (1952) Buchan type. In order to refine the metamorphic conditions, the metamorphic mineral assemblages that occur are reviewed and compared with recent experimental and theoretical studies.

The association of anthophyllite, cordierite, garnet, and staurolite in the biotite schist, which also everywhere contains biotite, plagioclase, quartz, and oxide minerals, is probably the best available indicator of metamorphic conditions. All combinations of minor amounts of the first four minerals with the last four minerals are reported here, except that no rock containing all eight minerals has been found. Butler (1969, p. 84) reported the assemblage biotite-quartz-plagioclase-garnet-staurolite-cordierite anthophyllite from an unspecified location, which suggests that all combinations of assemblages are present. An analysis of the phases and components shows that all of the biotite schists formed under at least divariant conditions if not under higher variance. Assemblages of plagioclase-microcline-quartz-biotite-muscovite and plagioclase-quartz-biotite-muscovite are found in the granitic gneisses. The importance of these assemblages is the existence of muscovite+quartz and not the development of alumino-silicate polymorphs.

Experimental studies delineating the conditions of temperature and pressure necessary for the stability of most of the metamorphic minerals in the schists have been done. Those necessary to define a model of the metamorphic conditions are studies of cordierite, staurolite, muscovite, and anthophyllite. Figure 26 reproduces pressure and temperature plots of univariant reactions that limit the stability of these minerals.

Richardson (1968) examined the reactions that limit the stability of Fe-staurolite+quartz. Curves I–IV (fig. 26) outline the limits of stability of this

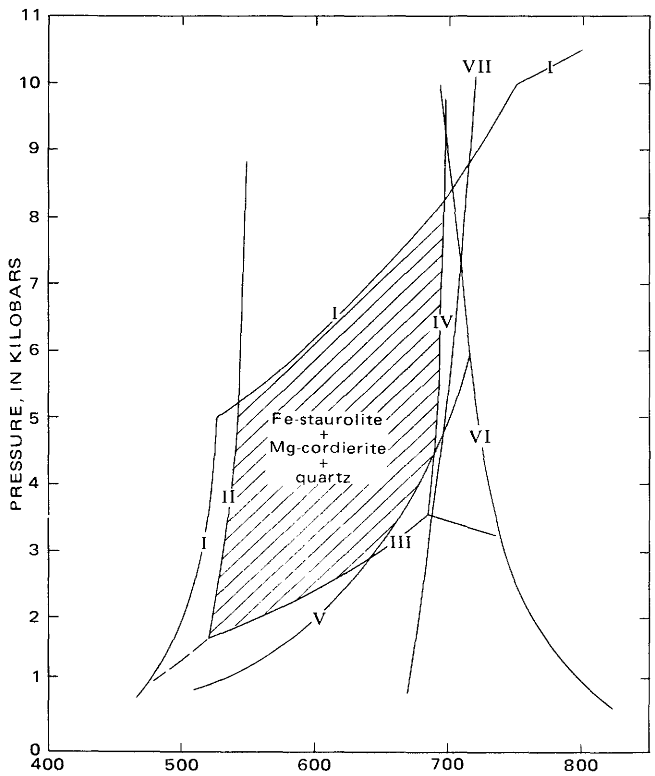

FIGURE 26.—Total pressure-temperature plot of various univariant metamorphic reactions that limit the stability of cordierite, staurolite, muscovite, and anthophyllite. Curve I, Mg-cordierite lower stability limit (Schreyer and Yoder, 1964; Schreyer and Schairer, 1961). Curve II, Fe-chloritoid+sillimanite=Fe-staurolite+quartz+water (Richardson, 1968). Curve III, Fe-cordierite+stillimanite+water=Fe-staurolite+quartz (Richardson, 1968). Curve IV, Fe-staurolite+quartz=almandine+sillimanite+water (Richardson, 1968). Curve V, muscovite+quartz=potassium feldspar+Al_2SiO_5 polymorph+water (Evans, 1965). Curve VI, beginning of melting for sanidine-quartz-water (Shaw, 1963). Curve VII, talc+forsterite=anthophyllite+water (Greenwood, 1963).

assemblage. In rocks, several differences from this experimental model can be expected. The addition of MgO to the system will probably make the field of staurolite+quartz slightly wider in temperature and raise the lower pressure limits of staurolite+quartz (Richardson, 1968, p. 486). The experimental work was done under quartz-fayalite-magnetite buffered oxygen fugacity, and the oxygen fugacity in the gneisses and schists is unknown. In addition the pressure of the fluids in the experimental study must be assumed to be equal to total pressure in the natural system.

Curve I for Mg-cordierite (Schreyer and Yoder, 1964; and Schreyer and Schairer, 1961) limits the stability of Mg-cordierite to the area below the curve. Fe-cordierite (Schreyer, 1965) breaks down at slightly lower pressures. Curves I-IV define the limits of the stability of the assemblage Mg-cordierite, Fe-staurolite, and quartz and form a model for limits of temperature and pressure under which the biotite schist with these assemblages crystallized. Biotite, plagioclase, and garnet are also stable within the same field.

Greenwood's (1963) work on the lower stability of anthophyllite (curve VII) implied that anthophyllite should not coexist in equilibrium with cordierite, staurolite, and quartz. Although the experimental work was done on the magnesium end member anthophyllite, calculations by Trommsdroff and Evans (1972) show that the addition of about a tenth of a mole fraction iron to anthophyllite will lower the equilibrium temperatures about 10°C. Therefore the addition of iron alone will not lower the stability of anthophyllite enough to put it in the Fe-staurolite+Mg-cordierite+quartz field. Possibly a combination of increasing the mole fraction of iron in anthophyllite and magnesium mole fraction in staurolite would make the stability fields overlap.

The assemblage muscovite+quartz is stable only above curve V (Evans, 1965), and where this cuts through the Fe-staurolite+Mg-cordierite+quartz field, it also probably limits the lower pressure conditions of biotite schist formation since gneisses containing this assemblage are interlayered with the schist. The association of migmatites and pegmatites with the schists and gneisses suggests conditions near the minimum melting of quartz-sanidine-water (curve VI). Butler (1969) reviewed the evidence and evaluated the different models for development of granitic gneiss and migmatite in the Beartooth Mountains. Magmatic, anatectic, or metasomatic models or combinations thereof would require temperatures near the minimum melting curve of quartz-sanidine and water.

Other experimental and theoretical studies on the paragenesis of cordierite in pelitic rocks are not applicable because they require the presence of either potassium feldspar (Reinhardt, 1968; Hess, 1969) or an Al_2SiO_5 polymorph (Hensen and Green, 1971).

Mineral assemblages, rock compositions, and experimental data suggest that the regional metamorphic rocks in the Stillwater Complex area were under conditions shown by the patterned area in figure 26. Limited occurrences of the assemblage cordierite-sillimanite in biotite schists from other parts of the Beartooth Mountains (T. J. Armbrustmacher, oral commun., 1972) suggest the higher pressure part of the patterned area.

REGIONAL METAMORPHISM OF THE HORNFELS

The question of regional metamorphism of the hornfels is complicated by confusion over the extent of the thermal aureole of the Stillwater Complex and by the relative similarity in ages of the aureole and the main phase of the metamorphism. Previous confusion over the extent of the metamorphic aureole of the Stillwater Complex was caused by the nearby existence of two biotite-bearing schistose rocks with closely comparable isotopic ages. One is the pelitic biotite schist, which contains minor amounts of cordierite and is interlayered with the gneiss and migmatite; the other is the magnesium and iron-enriched schistose rock, which is part of the metasedimentary rocks in the Stillwater aureole and contains major amounts of cordierite. In the Mt. Douglas quadrangle, both rocks are adjacent to one another but are separated by the projected extension of the Mill Creek–Stillwater fault zone in the glacial-debris-filled valley of the West Fork of the Stillwater River (see fig. 2).

Butler (1966, p. 52) considered the Stillwater aureole to consist of an inner part made up of cordierite-hypersthene hornfels that graded outward into a regional metamorphic biotite schist. The anthophyllite-cordierite rocks were not well known except along the Boulder River and were thought to be part of the regional metamorphic sequence (Butler, 1966, p. 59). This belief was based on their similarity to the schists and granofels containing minor amounts of cordierite and anthophyllite that had been found previously in the gneiss. Mapping and compilation by Page, Simmons, and Dohrenwend (1973a, b) showed that the two biotite schists are separate units; all the cordierite-rich rocks north of the Mill Creek-Stillwater fault zone are part of Stillwater aureole.

The 390 m.y. between the maximum and minimum ages for the development of the hornfels aureole and the 2,750±150-m.y. date of amphibolite facies metamorphism of the gneiss offer many possibilities of overlap of events in time and interpretation of the metamorphic history of the hornfels. There is little direct geologic evidence for the relative age of the gneiss and the Stillwater Complex because they are nowhere in contact. The hornfels aureole of the complex has not been observed in other than fault contact with the gneiss (Page and Nokleberg, 1974; Page and others, 1973a, b). All that can be stated is that all three groups of rocks are older than 2,750±60 m.y., the age of the intrusive quartz monzonites. Butler (1966) interpreted the data by suggesting that regionally metamorphosed rocks were thermally metamorphosed by the Stillwater Complex. Evidence from the styles of folds, rock compositions, and metamorphic mineralogy suggests that the hornfels was not involved with Butler's 2,750-m.y. amphibolite facies metamorphism. Table 13 summarizes what is known of the characteristics and ages of metamorphic events in various parts of the Beartooth Mountains and shows this interpretation.

Unless the development of a schistose fabric in the biotite- and cordierite-rich rocks north of the Mill Creek–Stillwater fault zone in the Mt. Douglas quadrangle is taken as evidence of a regional low-grade amphibolitic facies metamorphism older than the development of the thermal aureole, there is no evidence that the Stillwater block was affected by the 2,750-m.y. event. The eastern third of the Stillwater block was intruded at 2,750±60 m.y. by quartz monzonites that apparently reset most of the isotopic clocks; I interpret ages at about 2,750 m.y. as the quartz monzonite contact metamorphic event in the Stillwater River area. The fold styles within the hornfels appear to be very different from the tectonic fabric developed in the regionally metamorphosed rocks. Therefore, no strong correlation of structural style can be used to infer that the hornfels structures were developed at the same time as the gneiss structures. The compositional differences between the hornfels and schist of the regional metamorphic rocks are extreme and afford little opportunity for relating the metamorphic histories of the two terranes. Also, there are no metamorphic minerals or assemblages in the hornfels north of the Mill Creek-Stillwater fault zone that require an origin other

TABLE 13.—*Correlation of metamorphic events in the various parts of the Beartooth Mountains*

			Stillwater Complex area	
	Eastern Beartooth Mountains (Rowan and Mueller, 1971)	North Snowy block (McMannis and others, 1971a,b,c)	Gneiss terrane (Butler, 1966; this report)	Hornfels terrane (this report)
Characteristics		Hornblende-granulite facies.		Stillwater Complex thermal aureole-pyroxene to hornblende-hornfels facies
Age		?		3.14–2.75 b.y.
Characteristics	Amphibolite facies associated with F_2 open-isoclinal folding.	Amphibolite facies, Buchan type, associated with isoclinal F_2 folds.	Amphibolite facies, Buchan type, associated with open isoclinal folding.	Quartz monzonite intrusion, local low-grade contact metamorphism
Age	2,750±150 m.y.	2.7 b.y. ?	2.75 b.y.	2.75±0.06 b.y.
Characteristics	F_3 open folds, no metamorphism reported.	Greenschist or epidote-amphibole facies associated with F_3 isoclinal flow folds.		Low-grade greenschist facies metamorphism associated with penetrative foliation development
Age	1.6–1.8 b.y.	1.7 b.y.		1.6 b.y.

than by thermal metamorphism caused by the Stillwater Complex. These arguments do not deny the possibility that the hornfels was regionally metamorphosed before emplacement of the Stillwater Complex. But neither do they indicate with certainty that it was.

LOW-GRADE REGIONAL METAMORPHISM

Three types of evidence suggest that the Stillwater Complex hornfels, quartz monzonite, and mafic dikes were involved in a weak low-grade metamorphic event at about 1,600-1,800 m.y. ago. The evidence includes (1) the development of a penetrative foliation with (2) the growth of low-grade mineral assemblages (Page and Nokleberg, 1970a, 1972) and (3) lead loss or uranium gain in apatite (Nunes and Tilton, 1971). The rest of the rocks that now form the Beartooth Mountains were involved in a greenschist-facies metamorphic event between 1,600 and 1,800 m.y. ago (table 13) that had its strongest effects in the North Snowy block and is barely recognizable in the southeastern Beartooth Mountains. Since there is no evidence to suggest that the Stillwater Complex and adjacent rocks have not been part of the Beartooth Mountains since about 2,750 m.y. ago, some evidence of the 1,600–1,800-m.y. event should exist within the rocks of the Stillwater block.

A metamorphic mineral foliation that strikes east-west and dips northward was observed and described in the quartz monzonite sequence, in biotite gneiss pendants in the quartz monzonites, in the hornfels pendants, the Ultramafic zone of the Stillwater Complex, and locally in the granitic gneisses. In all the above rock groups, except the Ultramafic zone, the penetrative mineral foliation is defined by epidote and parallel chlorite and mica flakes. In the Ultramafic zone it is defined by serpentine-magnetite veins and by flattened, parallel orthopyroxene oikocrysts. The widespread extent of a similar foliation in rocks of diverse origins and ages is evidence for a penetrative deformation that occurred (1) after the emplacement of quartz monzonite sequence, (2) after emplacement of the Stillwater Complex, (3) after the generation of two sets of folds in the hornfelses, and (4) after the development of F_2 folds in the metamorphic rocks. Although many of the younger mafic dikes are altered to chlorite and epidote, their position in fault zones makes it difficult to separate effects of a regional metamorphic event from other hydrothermal alteration. Therefore, without more detailed study of dikes within the Stillwater block, they cannot be definitively used to date the low-grade metamorphic event.

Epidote, locally after plagioclase, and chlorite are widely developed in the mafic dikes, the quartz monzonites, the anorthosites and gabbros of the Banded and Upper zones, and locally in the hornfels. Gabbroic and anorthositic rocks in the western part of the complex appear to contain more chlorite and epidote than those in the eastern part. The development of the assemblage chlorite and epidote and its wide distribution are evidence for a low-grade regional metamorphism. In the Ultramafic zone, the development of serpentine-magnetite assemblages in veins and fractures parallel to a penetrative foliation also indicates a low-grade metamorphic change. Both groups of low-grade minerals are ascribed to the 1,600–1,800-m.y. event.

Nunes and Tilton (1971) reported U–Pb age determinations for four apatites from a biotite schist in the Stillwater aureole, a quartz monzonite, and a granitic gneiss. Although the apatite analyses alone could not be uniquely interpreted, when combined with other isotopic data, they suggest a regional episodic gain or loss of lead in the apatite at about 1,600 m.y. ago. Nunes and Tilton (1971) also investigated U-Pb ages of plagioclase from an anorthosite from the Stillwater Complex and obtained a model lead age of 1,700±300 m.y. I interpret these ages as indicating that the Stillwater block was affected by a low-grade regional metamorphic event between 1,600 and 1,700 m.y. ago.

CONTACT METAMORPHISM

Thermal aureoles produced by the Stillwater Complex and by the intrusive quartz monzonites have been recognized. The Stillwater aureole is the older and more extensive of the two, but both intrusive events developed mineral assemblages belonging to the same metamorphic facies. No metamorphic effects of the mafic dikes have been found.

THERMAL AUREOLE OF THE STILLWATER COMPLEX

Rocks belonging to the thermal aureole occur extensively in the Mt. Douglas quadrangle (Page and others, 1973b) and to a limited extent adjacent to the Basal zone of the Stillwater Complex in the Mt. Wood quadrangle (Page and others, 1973a). Exposures of the aureole are limited to the area north of the Mill Creek–Stillwater fault zone and by the southern limit of the complex in the Mt. Wood quadrangle (see fig. 1). The exposures attain a maximum map width of about 9.7 km perpendicular to traces of the metamorphic facies boundaries. In the Mt. Wood quadrangle, exposures of the aureole rocks occur between the Basal zone and the intrusive quartz monzonite as inclusions in the lower part of the Stillwater Complex and as pendants in the quartz monzonite. Assemblages of the pyroxene hornfels facies are found in the exposures in the Mt. Wood quadrangle and in the band of exposures nearest the complex in the Mt. Douglas quadrangle. South of the Chrome Mountain area the band attains a maximum width of about 2.4 km. The change to hornblende hornfels-facies rocks is marked by the disappearance of orthopyroxene and the appearance of anthophyllite or cummingtonite, or both. The band of exposures with hornblende hornfels assemblages has an irregular map width but attains a maximum thickness of about 3.2 km on the cliffs east of the Boulder River. The disappearance of anthophyllite marks the next change of facies to the albite-epidote hornfels facies, which attains a maximum map thickness of about 5.6 km on the cliffs east of the Boulder River. Traces of the facies boundaries are fairly straight and indicate that the planes separating the facies are fairly steep or vertical.

Lithologies involved in the aureole include massive and layered metasedimentary rocks, metaquartzites, and iron-formation. Rock compositions of the massive and layered metasedimentary rocks plotted on A-C-F and A-K-F diagrams in figures 27 and 28 illustrate their calcium- and potassium-poor nature as well as the limited variation in rock compositions found in the layered rocks. Minerals and tie-lines joining mineral assemblages in rocks of the pyroxene and hornblende hornfels facies are shown also (figs. 27 and 28), and the observed mineral assemblages (table 4) are consistent with those predicted by bulk composition.

Pressure and temperature conditions of metamorphism may be estimated for that part of the aureole immediately adjacent to the Basal zone. Irvine (1970), in a discussion of crystallization sequences in layered intrusions based on the sequence found in the Ultramafic zone and the estimated initial magma composition and experimental phase diagrams, suggested a total pressure of 4.5 kb during crystallization of the Stillwater Complex. Such a value seems too large because the complex is 4,880–6,100 m thick and no roof rocks are known, but it is compatible with the mineral assemblages found in the aureole and probably represents a maximum value. The initial magma of the Basal zone probably had temperatures between 1,200° and 1,300°C, and so the immediate contact hornfels could have had temperatures approaching these. Calculations of heat supply to surrounding country rock plotted as temperature versus distance from the contact (Jaeger, 1959; Winkler, 1965) accord with the widths of the metamorphic zones in the aureole of the Stillwater Complex.

THERMAL AUREOLE OF INTRUSIVE QUARTZ MONZONITE

Page and Nokleberg (1972) commented on the paucity of thermal effects associated with intrusive quartz monzonite, especially along the contact be-

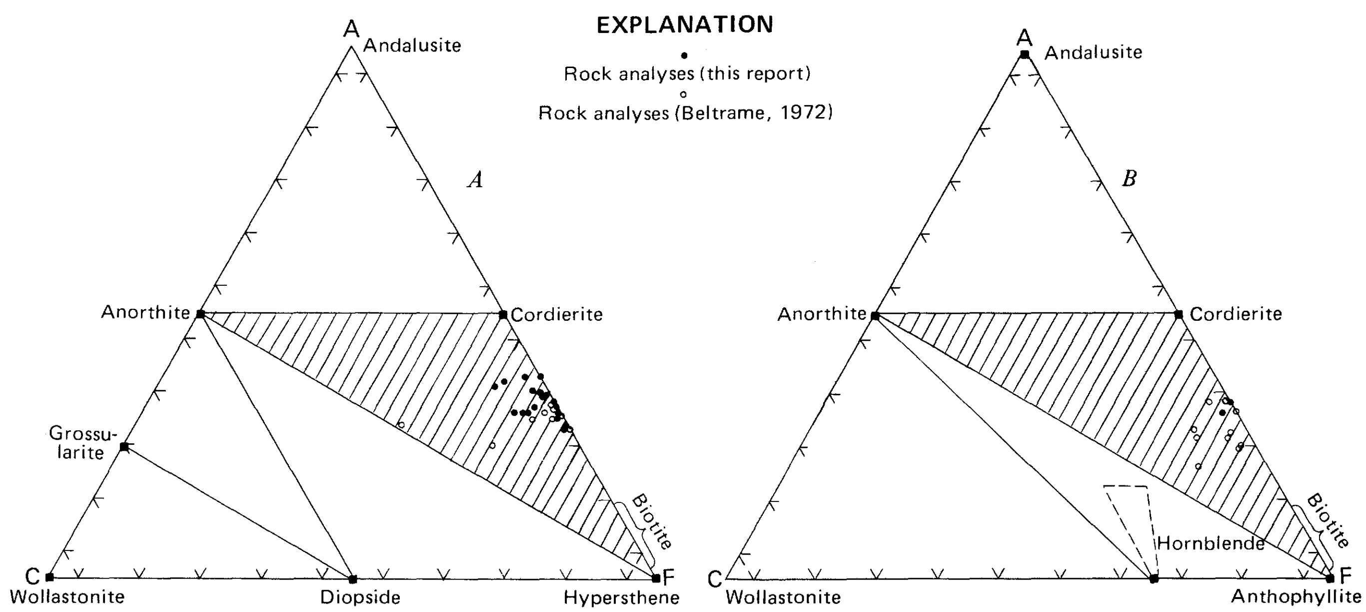

FIGURE 27.—A-C-F diagrams showing rock compositions and observed mineral assemblages in the Stillwater thermal aureole. Quartz may be an additional mineral present. A=Al_2O_3+Fe_2O_3+(Na_2O+K_2O), C=CaO–($3P_2O_5CO_2$), F=MgO+FeO+MnO in molecular percents and normalized to 100 percent. Lined area represents mineral assemblages present. *A*, Pyroxene hornfels mineral assemblages. *B*, Hornblende hornfels mineral assemblages.

tween the Basal zone and coarse-grained quartz monzonite from the Benbow area to the Stillwater River. They ascribed the following thermal and metamorphic effects to the quartz monzonite: (1) local development of hornfels-textured rocks composed of interlocking antigorite laths with minor magnetite and relict olivine, orthopyroxene, and clinopyroxene in the Ultramafic zone and Basal bronzitite cumulate member, (2) coarsening in grain size of the hornfels in the Granite Ridge area toward the contact with the coarse-grained quartz monzonite, and (3) increased growth of biotite in the hornfels pendants along the ridge north of Flume Creek. The lack of observable thermal effects from Benbow to the Stillwater River is probably caused by later faulting and shearing along the contact, which acted as a channelway for solutions to chloritize and alter the original rock. In Nye Basin, the assemblage of cordierite-spinel in clots at the margins of one dike of quartz monzonite suggests that an aureole was developed.

Since Page and Nokleberg's study (1972), hornfels near its contact with quartz monzonite has been found to contain metamorphic effects. These effects near aplite and quartz monzonite-hornfels contacts include (1) the development of assemblages containing microcline, spinel, and garnet (table 6), (2) inclusions in aplite dikes of hornfels that are now cordierite-spinel clots, cordierite-garnet, xenocrysts of cordierite and garnet, and cordierite-spinel- sillimanite clots, and (3) the development of potassium feldspar clots and lenses in the hornfels away from aplite dikes. As in the Nye Basin area, local metamorphic effects are associated with the quartz monzonite sequence, but the pyroxene hornfels facies rocks produced in the complex aureole are not retrograded by the quartz monzonite sequence.

The absence of retrogressive effects caused by the later quartz monzonite intrusion in the pyroxene hornfels facies rocks developed by the Stillwater Complex suggests fairly high temperatures of intrusion for the quartz monzonite sequence. The inclusions of cordierite-spinel-sillimanite possibly formed at fluid pressures greater than 1.5 kb between about 750° and 850°C or more as indicated by comparison with experimental work of Richardson (1968, fig. 6, p. 483). The presence of garnet-cordierite and spinel-cordierite assemblages in the inclusions and at the contacts of the aplites suggests temperatures nearer 800°C. Page and Nokleberg (1972) suggested two models for the intrusion of the quartz monzonite: (1) passive emplacement of quartz monzonite at conditions of the pyroxene hornfels facies before the country rock had cooled down from the intrusion of the Stillwater Complex and (2) emplacement of quartz monzonitic magmas and their crystallization at conditions of undersaturation with respect to water. Either model or a combination fits the temperatures, pressure, and field constraints suggested above.

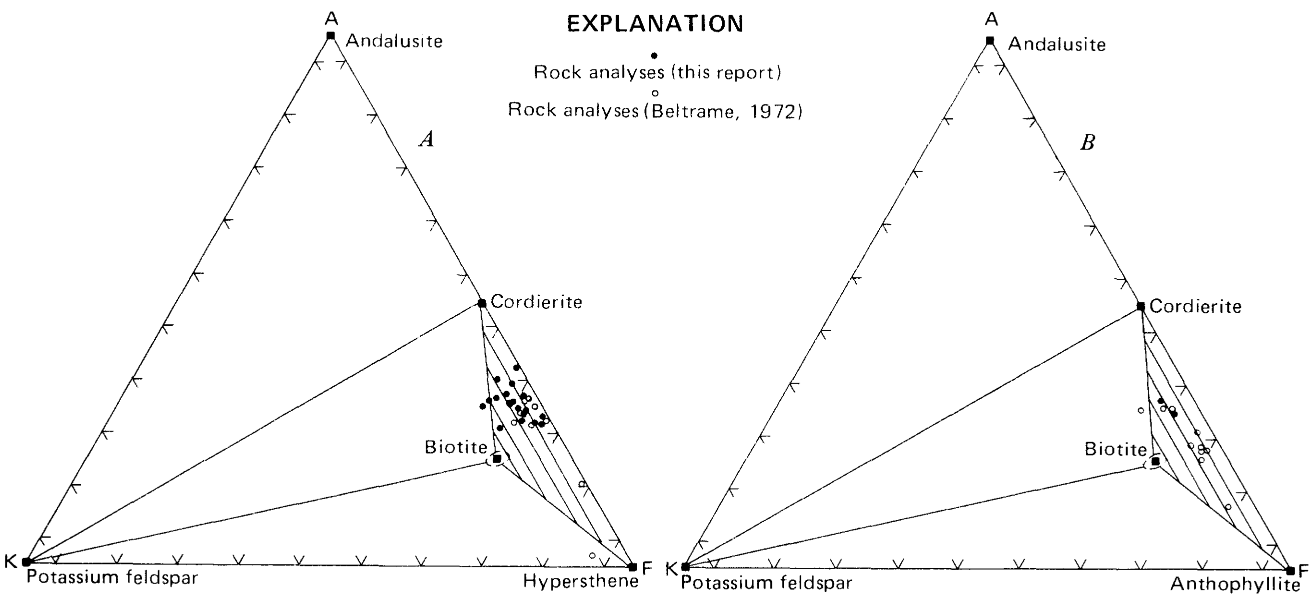

FIGURE 28.—A-K-F diagrams showing rock compositions and observed mineral assemblages in the Stillwater thermal aureole. Quartz may be an additional mineral present. A=Al_2O_3+Fe_2O_3–([CaO–($3P_2O_5$+CO_2)]+Na_2O+K_2O), K=K_2O, F=MgO+FeO+MnO in molecular percents and normalized to 100 percent. Lined area represents mineral assemblages present. *A*, Pyroxene hornfels mineral assemblages. *B*, Hornblende hornfels mineral assemblages.

STRUCTURE OF THE STILLWATER COMPLEX AND ADJACENT ROCKS

Northwest-trending bands of sedimentary, igneous, and metamorphic rocks that generally dip steeply to the north compose the overall structural pattern of the Stillwater Complex and adjacent rocks. However, this large-scale pattern is deceptively simple because each band contains several complex structural elements. Moreover, the boundaries between bands may also be complex structural features. In general, there are four groups of structures that may be distinguished in a relative time sequence. Three groups were developed during Precambrian time and include structures formed (1) before the Stillwater Complex was intruded, (2) during its intrusion, and (3) after its intrusion. The fourth group consists of structures developed during the Laramide orogeny. Except for the last group, the other groups of structures are generally limited to specific bands of rock. Therefore, the Stillwater Complex area was divided into 23 subareas (fig. 29) that reflect the relative age and limited distribution of penetrative and nonpenetrative structures to particular bands of rock. The subareas, numbered from 1 to 23, are arranged approximately in the order of formation with lower numbers assigned to the subareas containing the older structures.

The structural elements, described in the approximate order of formation during geologic time, are (1) those in the regionally metamorphosed rocks, (2) those in the hornfelses associated with the Stillwater Complex, (3) those in the Stillwater Complex, (4) those in the quartz monzonites, (5) those in Paleozoic and Mesozoic sedimentary rocks, and (6) faults and joints in all rock units. This order also represents the spatial distribution of structures in rock bands from south to north. Table 14 schematically outlines the development of penetrative structures to be discussed and lists the symbols used. The penetrative structural elements, which are those found throughout a group of rocks and which are repeated at distances that are small compared with the body of rock they pervade (Turner and Weiss, 1963, p. 11-32), consist of (1) planar features such as bedding, igneous layering, metamorphic foliations, cleavage, and axial planes of folds and (2) linear features such as fold axes, mineral lineations, and elongated bodies of rock. In addition to these elements, there are nonpenetrative planar structures, defined as discontinuities, that include faults, joints, igneous contacts, and unconformities large enough to be shown at map scale.

Structural terminology, symbology, and techniques follow those of Turner and Weiss (1963) except for the method of contouring fabric diagrams. Fabric or structure diagrams were prepared from structural observations plotted and contoured on equal-area lower hemisphere projections at 1E intervals where E is the expected number of points within the counting area for a uniform distribution across the stereogram using a method developed by Kamb (1959) and computerized by C. E. Corbató (written commun., 1970). The counting area varies and is a function of the total number of data points and of the number of times that the concentrations deviate significantly from a uniform distribution.

REGIONALLY METAMORPHOSED ROCKS

TECTONIC STYLE AND DESCRIPTION OF PENETRATIVE STRUCTURES

Compositional layering, planar mineral alinement, and axial planes of folds and fold axes are the penetrative elements found in the gneisses and schists (structural subareas 1 and 2) in metamorphic rocks of the Beartooth Mountains. Mineral lineations are rare, and none were measured. Compositional layering is defined by alternating bands of more felsic and mafic mineral layers in both the gneisses and schists. Parallel, elongate feldspar porphyroblasts and parallel mica and amphibole crystals form the mineral alinement that is called a metamorphic foliation. No structures or characteristics that could be assigned to a definite sedimentary origin were found in or associated with either planar structure, and since the two structures appear to be parallel and conformable, they are designated S_1 planes. Excellent examples of these are found in exposures along the trail nearest the Stillwater River (Page and others, 1973a), but exposures are generally poor.

A small number of mesoscopic folds were found in the gneisses and schists; some occur on the west side of the Stillwater River valley (coordinates: 501,110 N.; 1,893,050 E.) and some on the south side of the West Fork of the Stillwater River. At these localities, families of tight to moderately open isoclinal similar folds with wavelengths of 30 centimeters to a meter can be observed. In addition, at these localities the amphibolitic gneiss bodies form cores of somewhat larger folds in which the metamorphic foliations both within the amphibolitic gneiss and the granitic gneisses wrap around the nose of the fold. A few folds of a smaller scale, with wavelengths less than 30 cm but with the same style, were found in the biotite schists, especially along Bluebird Ridge (coordinates: 500,920 N.; 1,877,050 E.). The axial planes (S_2) of all the isoclinal folds observed are parallel to compo-

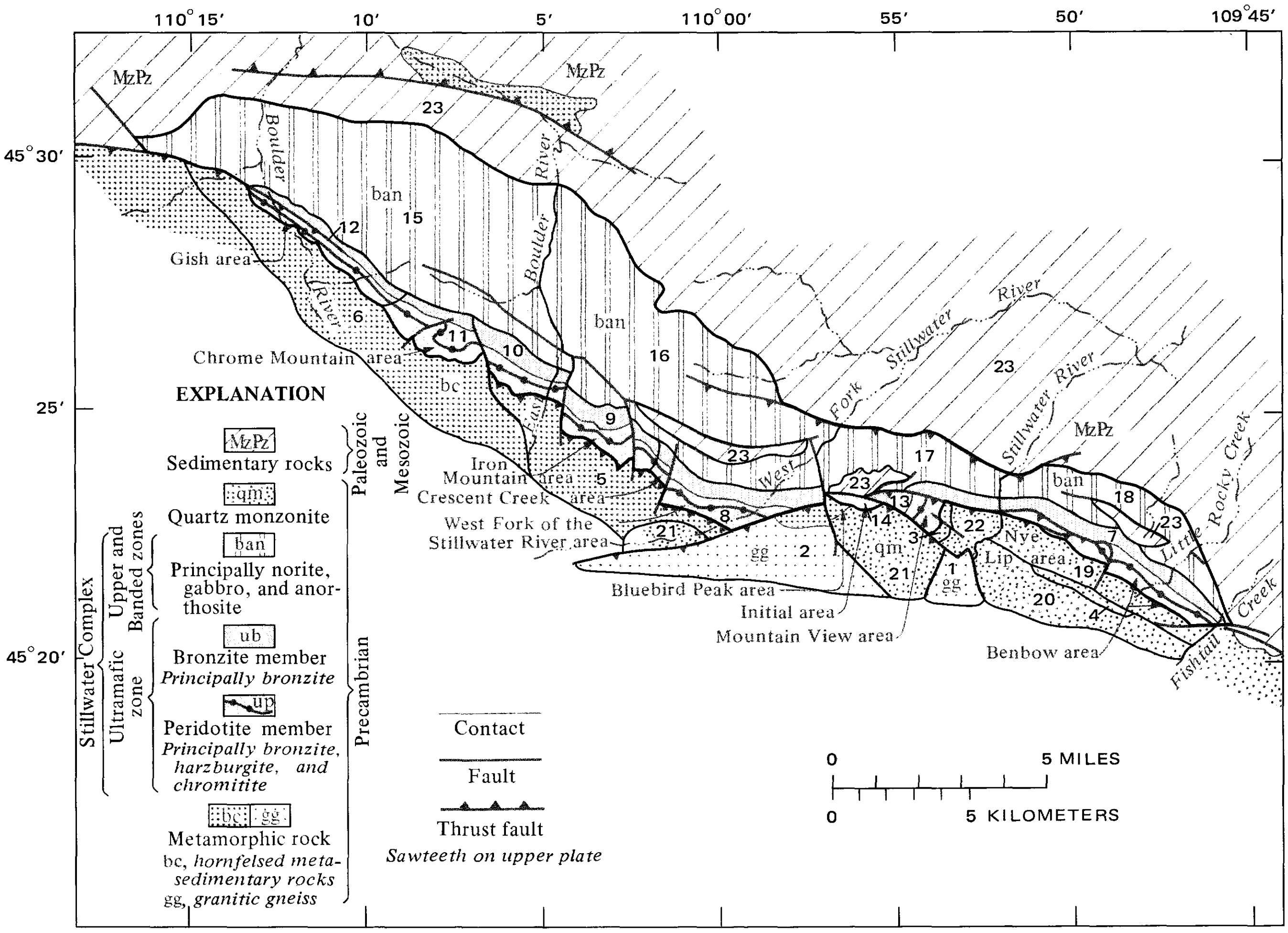

FIGURE 29.—Structural subareas (1-23) in the Stillwater Complex and adjacent rocks. Subareas, reflecting relative age and limited distribution of structures to particular bands of rock, are arranged in approximate order of formation with lower numbers assigned to subareas containing older structures.

sitional layering and foliation in the limbs of the individual folds. The measured fold axes are labelled L_1.

GEOMETRICAL ANALYSIS OF PENETRATIVE STRUCTURES

Poles to penetrative planar structural elements (S_1) measured in structural subareas 1 and 2 (fig. 29) are shown as contoured lower hemisphere equal-area plots in figure 30*A* and *B*. Both metamorphic foliation and compositional layering in granitic gneisses, biotite schists, and amphibolites are considered as one planar element because of the apparent correspondence between the two features. The poles to these planar features in structural subarea 2 suggest a girdle pattern and a β axis plunging N. 22° E. at 12° (figs. 30*B* and *C*). Isoclinally folded metamorphic foliation or compositional layering in the granitic gneisses is rare, but the seven observed fold axes (L_1) indicated in figure 30*C* have a scattered orientation between directions plunging northwest to northeast between 20° and 60° and by themselves offer no evidence that the β axis is indeed an axis of folding. The axial planes (S_2) of these folds were parallel with local S_1 in the limbs of the folds. The southward and northward spread of the maxima on the girdle of subarea 1 (fig. 30*A*) suggests a second fabric element that was not observed or separated in the field. A possible explanation of the divergence of the maxima in subareas could be the presence of northwest-plunging folds. The limited number (15) of observations in structural subarea 1 and the lack of a strong fabric orientation preclude an interpretation.

On the basis of reconnaissance mapping, Butler (1966) made a structural analysis of the granite gneisses in the Cathedral Peak area, which overlaps the subareas 1 and 2. He divided the Cathedral Peak area into subareas, two of which are separated by the Sioux Charley fault and correspond partly to sub-

TABLE 14.—*Relative ages and symbols used for penetrative structures in various rock groups*

Structure and development					
Regionally metamorphosed rocks	Hornfels associated with Stillwater Complex	Stillwater Complex	Intrusive quartz monzonite	Sedimentary rocks	Approximate age
Deposition of sediments S_0 bedding (hypothetical)	Deposition of sediments S_0 bedding				↑
Isoclinal folding to develop S_1 metamorphic foliation	Development of layering S_1 possibly by isoclinal folding intrafolial folds (F_2)				
	Asymmetric and concentric folding: Isoclinal folding of S_1 F_1 folds, S_2 axial planes, L_1 fold axes				
	Broad warping of S_1 and S_2 F_2 folds, S_3 axial planes, L_2 fold axes				Precambrian 3.14-2.75 b.y.
		Intrusion and development of layering, S_0			
Folding of foliation F_1 folds, S_2 axial planes Possible refolding of F_1 folds, F_2					
			Intrusion		2.7 b.y.
	Foliation in pendants	Metamorphic foliation, S_1	Metamorphic foliation, S_1		~1.6-1.8 b.y. ↓
				Deposition (S_0)	Cambrian
				Folding of S_0 F_1 folds, S_1 axial planes, L_1 fold axes	Late Cretaceous

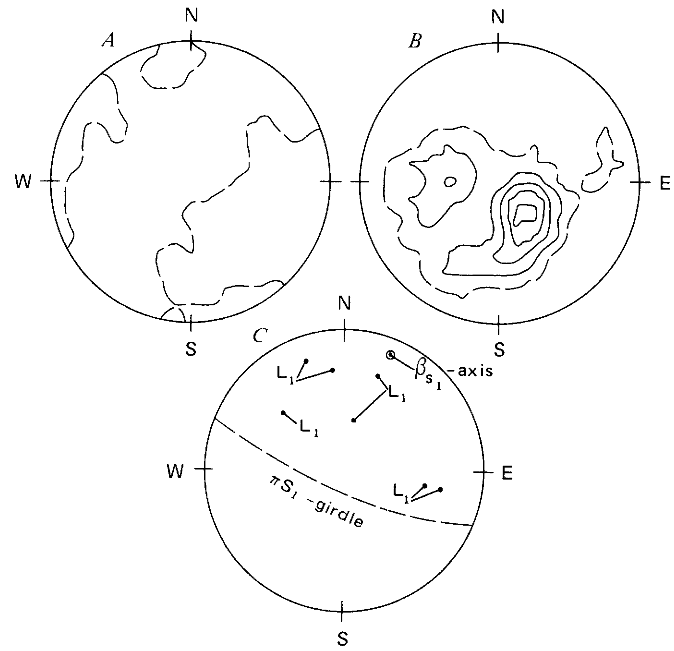

FIGURE 30.—Fabric diagrams of granitic gneisses and associated rocks in structural subareas 1 and 2. Contoured at 1E intervals where E is the expected number of points within the counting area for a random pattern using a method developed by Kamb (1959) and computerized by C. E. Corbató (written commun., 1970). Dashed contour is the 1E contour; solid contours are contours greater than 1E. *A*, Contoured poles to S_1 for subarea 1, 15 points, counting area=0.211, E=3.16. *B*, Contoured poles to S_1 for subarea 2, 115 points, counting area=0.034, E=3.87. *C*, L_1 fold axes and postulated πS_1-girdle and β_{S_1} axis for subareas 1 and 2.

areas 1 and 2 but which extend farther south. Butler interpreted the penetrative planar and linear features that he observed to be related to north-northwest shallowly plunging isoclinal folds and found a difference of 20°-40° in the plunge of these folds between the two subareas. He suggested that difference was due to rotation and movement on the Sioux Charley fault after the intrusion of the Stillwater Complex.

Our data combined with Butler's (1966) observations support the concept of large isoclinal folds in the granitic gneisses that plunge at low angles northward. Complete explanation of the complex structures in the granitic gneiss blocks must await detailed analyses of their fabrics that are beyond the scope of this study.

The gneissic subareas are unique in type of structure and the attitude of the planar and linear features and bear no similarity to the fabrics of the other groups of rocks. Because the gneiss terrane is older than the quartz monzonite sequence, these structures also probably are older than the quartz monzonites (older than 2,750 m.y.). Butler (1966, p. 61) believed that the fold axes formed before regional metamorphism and pegmatite formation; the pegmatites yielded ages of about 2,700 m.y. or slightly younger. The fabric elements of the northward-plunging isoclinal folds are therefore considered to be 2,750 m.y. old or older.

HORNFELS ASSOCIATED WITH THE STILLWATER COMPLEX

TECTONIC STYLE OF PENETRATIVE STRUCTURES

The metasedimentary rocks present a monotonous and enigmatic series of layered and massive structureless rocks. The distribution of iron-formation and blue metaquartzite outcrops within the extensive areas of hornfels from the West Fork of the Stillwater River to west of the Boulder River and the distribution and attitudes of foliation and layering indicate that the metasedimentary rocks are complexly folded and faulted. Mesoscopic folds within these units also indicate a complex structural history. Unfortunately, except in cliff faces, the metasedimentary rocks generally present relatively poor outcrops—a large part of their areal extent between Crescent Creek and Bobcat Creek having been inferred from float patterns and diamond-drill holes. The areas that were mapped on the basis of float are indicated on the 1:12,000-scale map (Page and Nokleberg, 1974) by the lack of structural symbols. In order to unravel the history of the metasedimentary rocks, this discussion first concentrates on an analysis of a well-exposed series in the Mountain View area and then interprets the other structures in the light of that analysis.

Penetrative planar elements in the hornfelsed rocks are of two types: (1) layering formed by variation in mineral proportions or grain size and (2) incipient cleavage, cleavages, and axial planes associated with mesoscopic folds. Three broad categories of layering in the hornfelses are distinguished: (1) relatively large scale layering associated with the interleaving of the different rock types such as iron-formation, blue metaquartzite, and cordierite-orthopyroxene hornfels, (2) small-scale layering caused by changes in mineralogy and texture that is relict sedimentary bedding, and (3) mineralogic and textural variations that cannot be shown or assumed to be bedding. All three types of layering are assigned to an S_1 family of planes although some S_1 layering may be transposed foliation and other S_1 may be bedding (S_0). The third category of layering is the most abundant and deserves some discussion here; both categories (1) and (2) are described in the stratigraphic section of this paper.

Most type 3 layers are 2.5–15.2 cm thick, but some are as much as 0.6 m thick. Layers are defined mainly by a variation in proportions of light-colored minerals (cordierite, quartz, and plagioclase) and dark-colored minerals (orthopyroxene and biotite). Some layers are isomodal, and others grade in mineral proportions; therefore some contacts are sharp, and others gradational. Layers may also be defined by textural criteria. For example, locally a layer contains orthopyroxene only as porphyroblasts, and the adjoining layer contains it as anhedral granular grains. Most layers seem to be continuous for meters to tens of meters along strike, but locally they are lenticular. The quartz-rich layers are generally lensoid. Figure 11 shows several examples of compositional layering in the hornfels. Some intrafolial isoclines make it questionable that this layering should be called bedding. It is possible that some, if not all, of this layering is transposed bedding and therefore a metamorphic layering.

All S_1 layering, regardless of origin, is folded (fig. 31). The folds of the first recognizable generation (F_1), not necessarily the oldest, are closed to open, similar to isoclinal, slightly asymmetric folds. They form families with wavelengths as small as a few centimeters, but most have a wavelength of 2–3 m with layering relatively thicker in the sharp to rounded hinge areas than on the limbs of the fold. Some limbs are sheared out and contain smaller minor folds with the same sense as the mesoscopic isoclinal folds. Figures 31 and 32 show the style of the F_1 folds. Axial planes (S_2) of these folds locally are paralleled by an incipient cleavage but generally are not accompanied by parallel cleavage or fracture planes, nor do any of the platy minerals seem to be alined parallel to the axial plane. Fold axes (L_1) are not accompanied by any observable mineral lineations. Most mesoscopic F_1 folds are similar in style and orientation to larger scale fold structures deciphered from outcrop patterns of the different lithologies in hornfels.

The S_1-layering and S_2-axial planes are refolded by broad warps (F_2). These warps have extremely open, rounded hinge areas that show no noticeable thickening compared with limb areas. A system of incipient cleavage or fracture planes, locally well developed, is parallel to the axial planes (S_3) of broad warps. A closely spaced joint system locally also parallels the axial planes. The fold axes (L_2) show no associated parallel mineral orientation.

Three other styles of folds were found in the hornfels, but owing to lack of exposures and the scarcity of these types of folds, their age relations could not be determined. About 20 intrafolial isoclinal folds (see Turner and Weiss, 1963, p. 116–117) were found in the S_1 layering (fig. 32*E*). They have extremely sharp hinges, and their limbs are parallel to adjoining layering. Axial planes of these folds are parallel to the limbs and S_1 layering. No examples were found in which these folds were refolded, but they probably represent remnants of pre-F_1 folding. They may also represent relict sedimentary slump structures.

Another style of fold occurs on the limbs of F_1 folds. These are moderately open to tight asymmetric isoclinal minor folds (fig. 32*B*) that fold S_1 but appear not to fold S_2. They have a reverse sense to any possible drag folds that might have developed as part of the F_1 folds. Their axial planes and fold axes also have a different orientation than possible drag folds would to the F_1 folds.

The third style of fold consists of bumps or open,

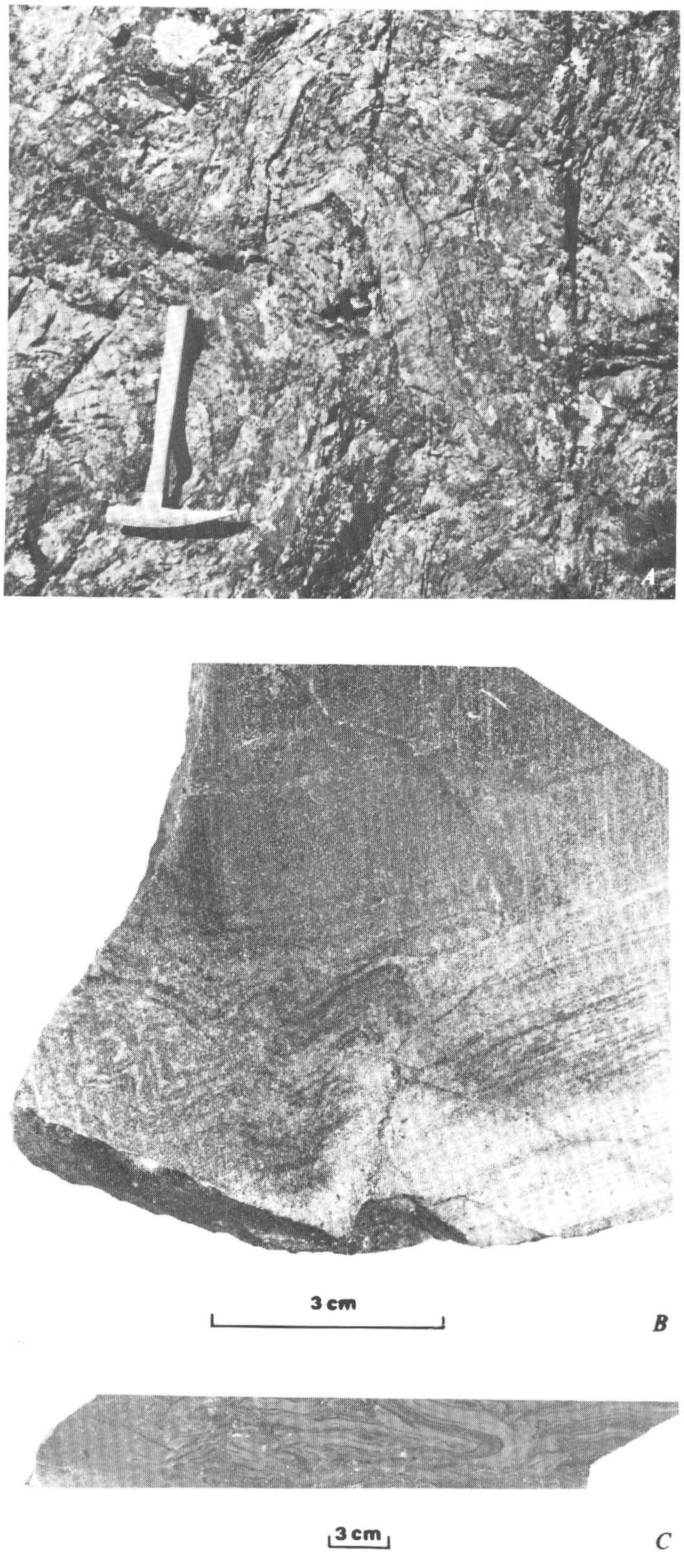

FIGURE 31.—Folded layering in the metasedimentary rocks. *A*, Open isoclinal fold in layered hornfels. *B*, Asymmetric folds in layered hornfels. *C*, Tight isoclinal folds and disrupted layers in layered hornfels. Length of specimen, about 30 cm.

apparently concentric folds that fold S_1 but not S_2 and are definitely discontinuous along their axial traces (fig. 32*E*). They have wavelengths of about 60 to 150 cm and fairly open, rounded hinge areas.

Mineral lineations are very rare and are formed by elongate orthopyroxene porphyroblasts. In no exposures could the orthopyroxene lineation be related to any of the fold structures.

GEOMETRICAL ANALYSIS OF PENETRATIVE STRUCTURES

MOUNTAIN VIEW AREA

An approximately 2½-square-kilometer area of glaciated outcrops centered on lower Verdigris Creek in the Mountain View area was studied in detail in order to unravel the deformation history of the metasedimentary rocks (structural subarea 3, fig. 29). These rocks lie between the Bluebird and Lake thrust faults and were rotated during Laramide deformation (Jones and others, 1960). Therefore, the present orientation of structures need not be consistent with similar structures in the metasedimentary rocks elsewhere. The hornfelses in the Mountain View area were intruded by the Stillwater Complex and by the quartz monzonites after the folding of the hornfelses, thus adding additional complications. The detailed area (pl. 2), an enlarged segment of the 1:12,000-scale map (Page and Nokleberg, 1974) with fabric diagrams, contains a large number of minor folds of various types and one large major fold that can be recognized on the basis of layering attitudes.

Inspection of the S_1 layering attitudes (pl. 2) shows a large fold, probably broken by the Verdigris fault. The attitudes indicate northwest and southeast limbs steeply dipping to the west-southwest and northwest, respectively. The layering in the nose area of the fold dips off toward the northeast, and the fold axis plunges about 60° to the northeast. The fold is an open isoclinal synform, the axial plane of which dips northwest.

Both limbs of the synform are not equally exposed; most of the outcrops occur on the southeast limb. Fabric diagrams for eight observation areas that were established in the field on the basis of amount of exposure and apparent homogeneity in their fabric are shown in plate 2. Areas 1 through 5 and 8 appear to have a fairly homogeneous fabric with respect to S_1. A summary diagram (fig. 33*A*) containing the maximum of each observation area plotted as a single pole supports this interpretation. The homogeneity of the fabric of these areas is a consequence of their location on the same southeast limb of the major fold. Observation areas 6 and 7 (pl. 2) have a different fabric with respect to S_1 as a consequence of

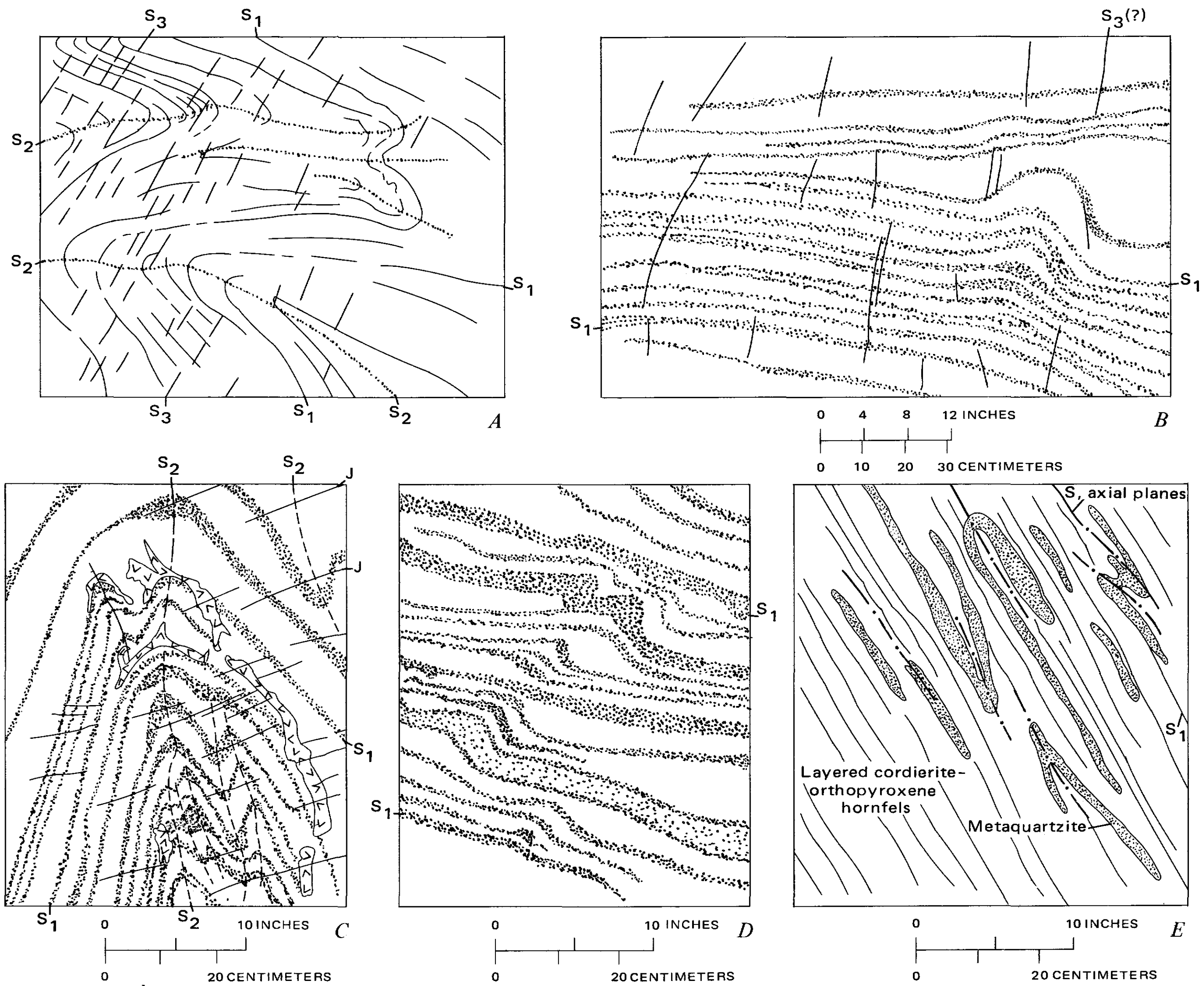

FIGURE 32.—Fold styles in hornfels. *A*, Open isoclinal folds (F_1) folding layering (S_1) and having axial plane traces (S_2) folded by broad warps (F_2) which produce axial plane cleavage (S_3). Width of *A* about 2.4 m. *B*, Asymmetric folds in S_1 (stippled pattern); possible S_3 fractures cutting S_1. *C*, S_1 (stippled pattern) folded by F, with axial plane traces (S_2). Joints (J) may be S_3. Checked pattern, aplite. *D*, Open concentric folds or bumps folding S_1 (stippled pattern). *E*, Tight isoclinal intrafolial folds of metaquartzite with axial planes parallel with S_1. View parallel to S_1. *A*, *B*, *C*, and *D* drawn from photographs.

their location on the northwest limb and the nose of the major fold. In the contoured composite S_1 pole diagram (fig. 33*B*), a determination of β_{S_1} is biased by the number of observations on the southeast limb and therefore is not a solution for the fold axis, $B_{S_1}^{S_2}$.

Minor open isoclinal folds with a similar style to the major synform yield fold axes (L_1) that are shown on contoured plots by observation area on plate 2. Fewer observations are available for the orientation of the L_1 fold axes because of the limited exposures; indeed in some areas there are not enough measurements to define the fabric orientation. Fabric maxima from the areas indicate minor fold axes trending between N. 48° E. and N. 17° W. and plunging between 47° and 72° in a northerly direction. The summary diagram of L_1 (fig. 34) from all observation areas shows a $B_{S_1}^{S_2}$ axis plunging N. 49° E. at 62° on the basis of the maxima, but the fabric tends to be dispersed along an L_1 maxima that lies along a great circle with an orientation of N. 47° W., 48° SW.

Contoured fabric patterns of axial planes (S_2) of mesoscopic folds in S_1 appear to be fairly homogeneous from one observation area to the next (pl. 2). Examination of the individual open isoclinal mesoscopic folds shows that their axial planes are folded and warped by broad open folds. Plots of pole

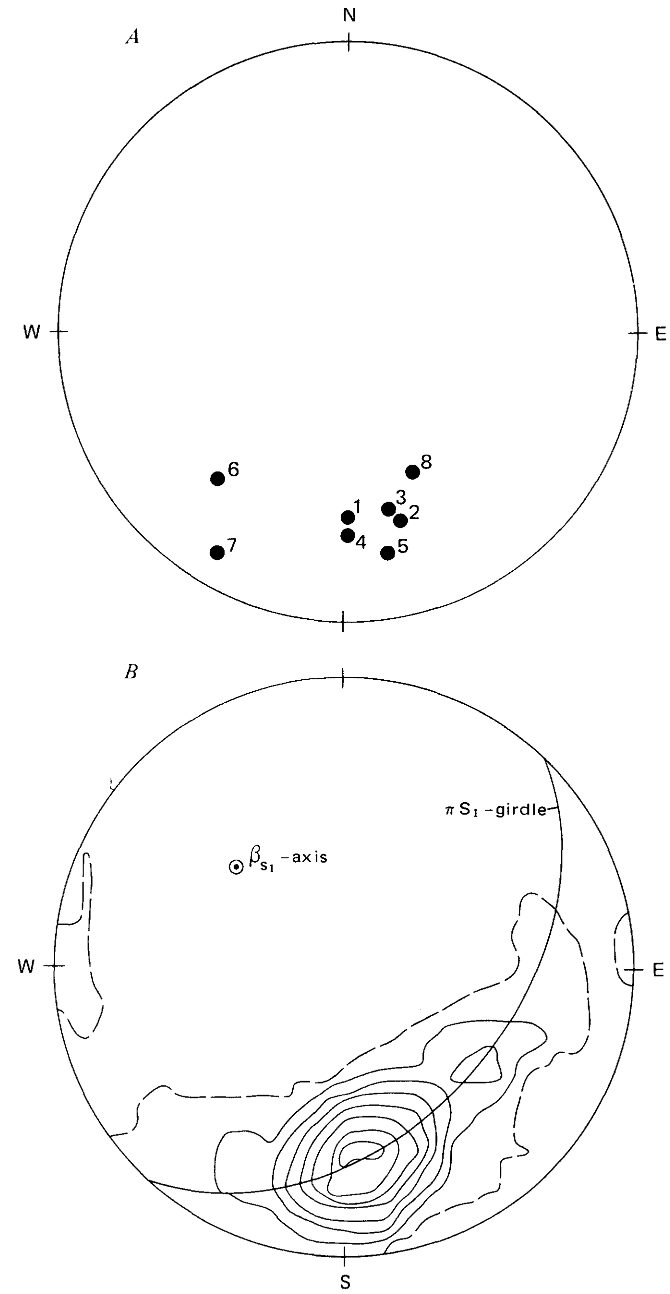

FIGURE 33.—Pole maxima and combined fabric diagrams of layering (S_1) for Mountain View observation areas 1-8 of plate 2. *A*, S_1 pole maxima. *B*, Contoured composite of S_1 poles, 297 points, counting area=0.013, E=3.95. See figure 30 for explanation.

maxima to axial planes (S_2) for all observation areas indicate that within individual areas the orientation of axial planes ranges in strike from N. 28° E. to N. 69° E. and in dip between 20° and 60° NW. (fig. 35). The orientation of the S_2 planes in the areas suggests the axial plane of the major fold is bent in an analogous way as the axial planes of the mesoscopic folds.

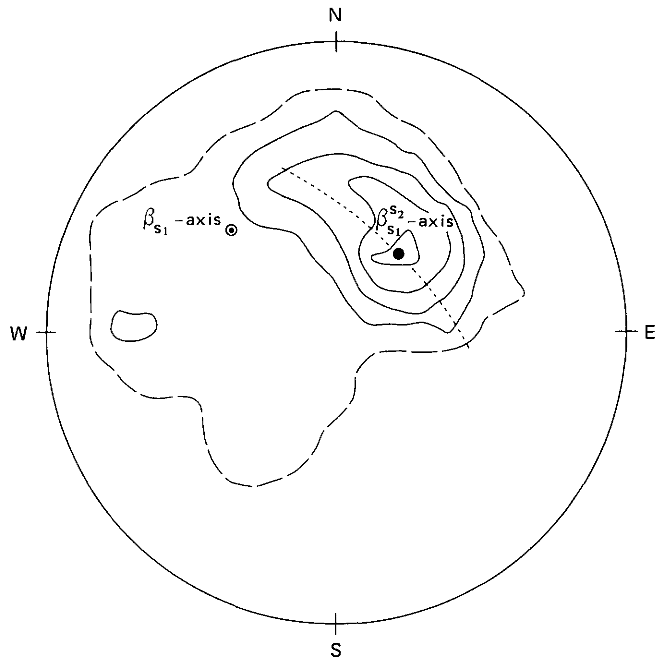

FIGURE 34.—Contoured fabric diagram of fold axes (L_1) for Mountain View observation areas 1-8 of plate 2. 79 points, counting area=0.048, E=3.81; dotted line shows dispersal of L_1. See figure 30 for explanation.

The second set of mesoscopic folds (F_2), broad warps, have fairly homogeneous fabrics with respect to their fold axes, L_2, and their axial planes, S_3, over structural subarea 3 on the basis of comparisons of area fabrics. Figure 36 shows contoured plots of L_2 and S_3 poles from all observation areas of plate 2. The second set of folds warp or fold both S_1 and S_2. The tendency for the S_2 fabric to be dispersed along a great circle trending N. 66° E. (fig. 35*B*) indicates a refolded fold. Comparison of B_{S_2} with the fold axes, L_2, measured in the field shows a close correspondence that indicates the β_{S_2} is representative of the fold axis B_{S_2} and that the outcrops examined offer a fairly valid sample of the second set of folds. The statistical axial plane, S_3, of the second folds trends N. 2° W. and dips 68° NE. (fig. 36*B*); the fold axis, $B^{S_1S_2}_{S_3}$, strikes N. 17° W. and plunges 48° NW. (fig. 36*A*). The slight dispersal of the L_1 poles along a great circle (fig. 35*A*) is probably due to rotation of the second set of broad warps.

Three other styles of folding were also observed within structural subarea 3, all of which fold the layering, S_1, but cannot be shown to fold or affect any other structures. Asymmetric folds and discontinuous broad folds are considered together in the fabric diagrams in figure 37. They have an average fold axis that trends N. 13° W. and plunges 53° NW. Examination of the geometry of the fold axes and

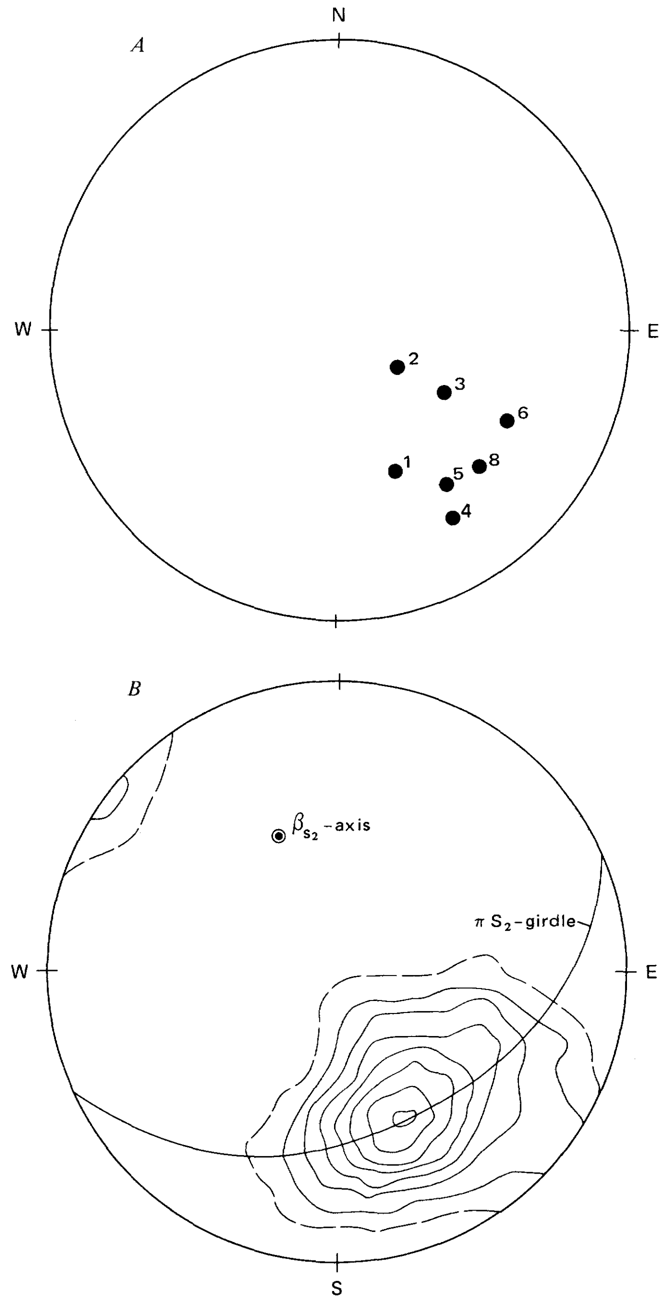

FIGURE 35.—Pole maxima and combined fabric diagrams of axial planes (S_2) for Mountain View observation areas (1–6, 8) of plate 2. *A*, S_2 pole maxima. *B*, Contoured composite of S_2 poles, 123 points, counting area=0.031, E=3.87. See figure 30 for explanation.

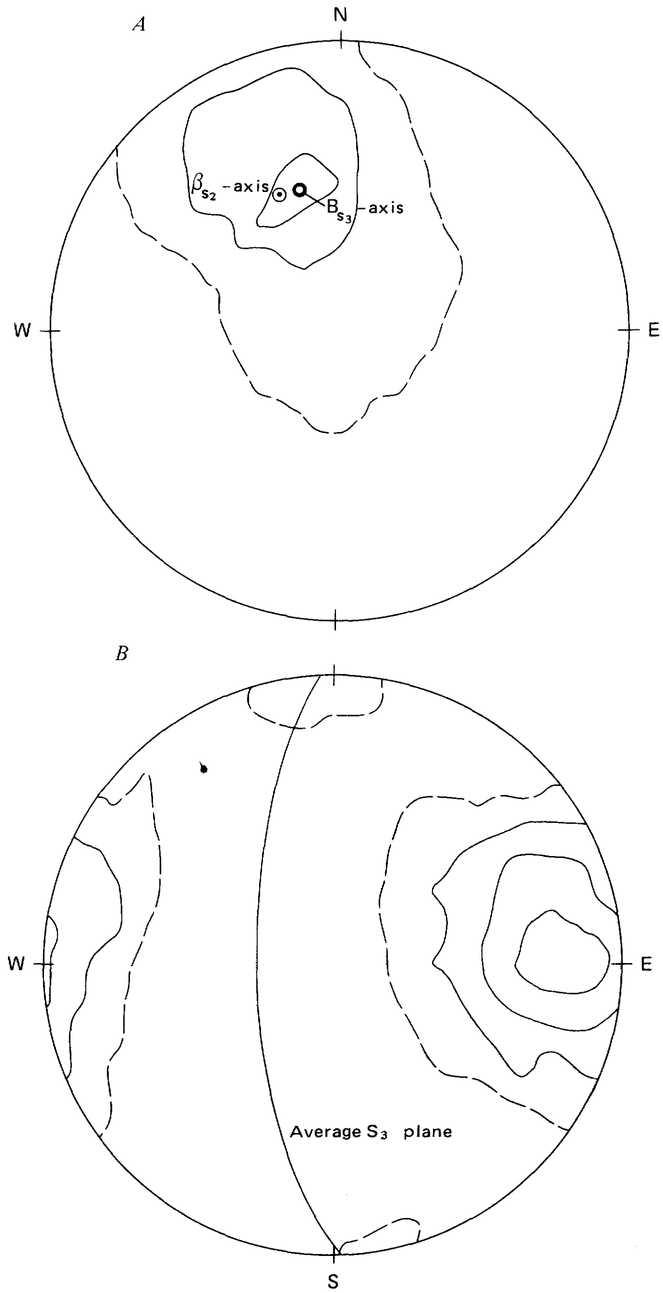

FIGURE 36.—Contoured fabric diagrams of fold axes (L_2) and axial planes (S_3) for all Mountain View observationa areas (1–8) of plate 2. *A*, L_2 poles, 24 points, counting area=0.43. *B*, Poles to S_3 and average S_3 of axial planes of mesoscopic folds (F_2), 48 points, counting area=0.077, E=3.69. See figure 30 for explanation.

axial planes suggests that they may have developed as part of the isoclinal open folding.

A few (14 measurable ones) tight intrafolial folds and isoclines, the third type of minor folds, were observed in the plane of layering, S_1. Their limbs and axial planes are parallel to S_1. Figure 38 summarizes the fabric of poles to axial planes and shows an average axial plane trending N. 75° E. and dipping 53° NW. Only threefold axes were measurable, and they plunge off to the northwest at angles of 30°–50°. This group of minor folds may represent folding that occurred before, and was almost completely obliterated by, the open isoclinal folding (F_1).

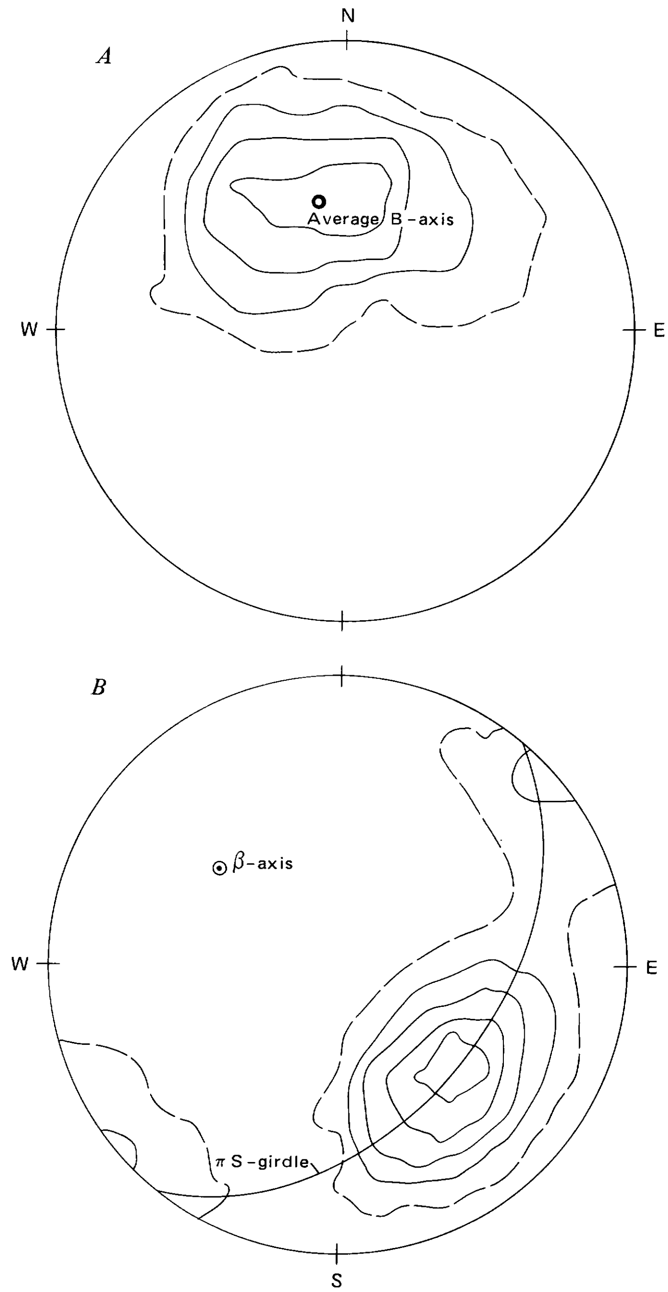

FIGURE 37.—Contoured fabric diagrams of fold axes ($L_?$) and axial planes ($S_?$) of discontinuous broad folds and asymmetric folds. *A*, $L_?$, 28 points, counting area=0.125, E=3.50. *B*, Poles to $S_?$, 55 points, counting area=0.068, E=3.73. See figure 30 for explanation.

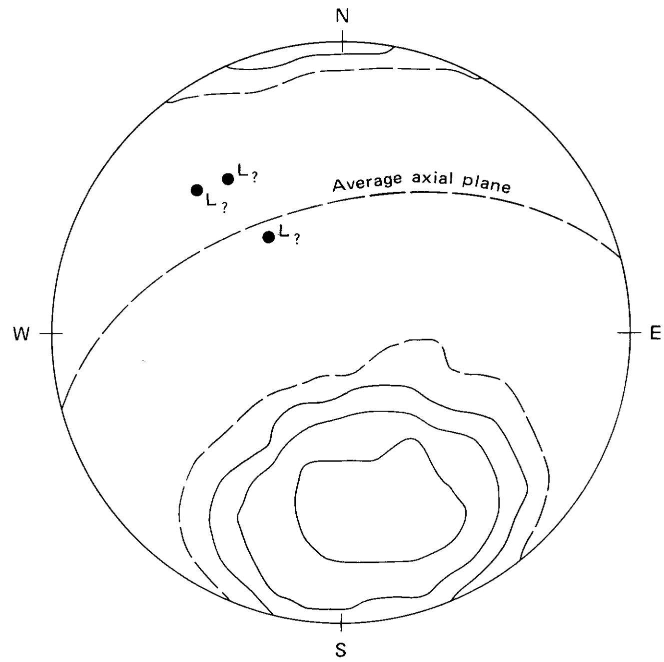

FIGURE 38.—Fabric diagram of contoured poles to axial planes showing average axial plane and threefold axes ($L_?$) of tight isoclinal folds in structural subarea 3 (fig. 29). 14 points, counting area=0.222, E=3.11. See figure 30 for explanation.

In summary, the layered metasedimentary rocks in the Mountain View area were folded into major and minor open isoclinal folds about axes that now have a northeast trend and about a 60° NE. plunge (F_1). These folds were warped or refolded into broad open folds about axes that now have moderately plunging northwest axes (F_2). Associated with the layering folded by F_1 are a few tight intrafolial folds that can be interpreted as a phase of folding earlier than F_1. If this interpretation is true, all or some of the layering in the metasedimentary rocks may be a transposed foliation. Two other styles of folds, asymmetric and broad discontinuous folds, are present, but their relation to F_1 and F_2 is unknown.

AREA FROM WEST FISHTAIL CREEK TO THE STILLWATER RIVER

Hornfelses have a limited distribution between West Fishtail Creek and the Stillwater River (structural subarea 4, fig. 29). They occur as inclusions in the Basal zone and as pendants and inclusions in the intrusive quartz monzonite sequence. Most exposures of inclusions in the Basal zone consist of float and rubble of massive, apparently structureless hornfels and therefore offer no possibility for structural interpretation. Although exposures in the pendants are extremely poor and the area that they underlie generally consists of float and rubble, both layering and a few minor folds were observed along the northern ridge above Flume Creek. Contoured poles to compositional layering (S_1)(fig. 39) indicate an average layering plane that strikes approximately east-west and dips north at about 60°. A few tight isoclinal folds (F_1) were observed with limbs and axial planes (S_2) apparently parallel with compositional layering. The axes (L_1) of the measurable

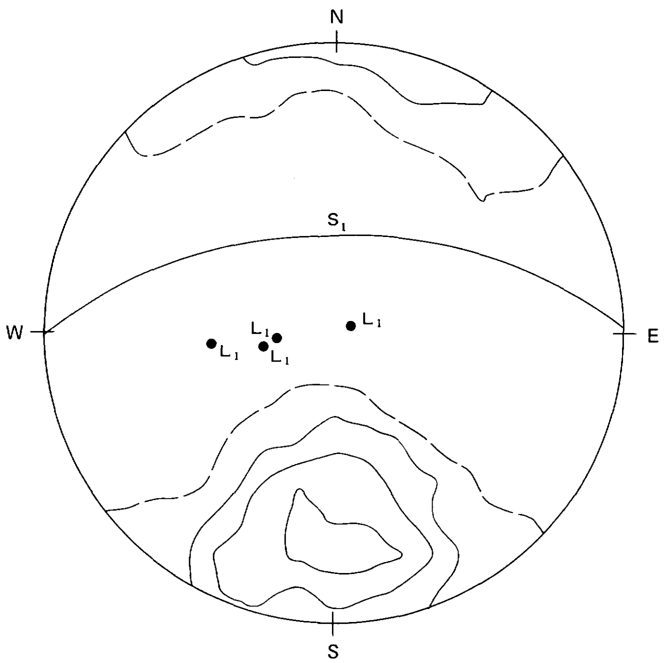

FIGURE 39.—Fabric diagram of layering (S_1), axial planes (S_2), and fold axes (L_1) in hornfels pendant in structural subarea 4 (fig. 29). Contours of poles of S_1 and S_2 based on 33 points, counting area=0.108, E=3.57. See figure 30 for explanation.

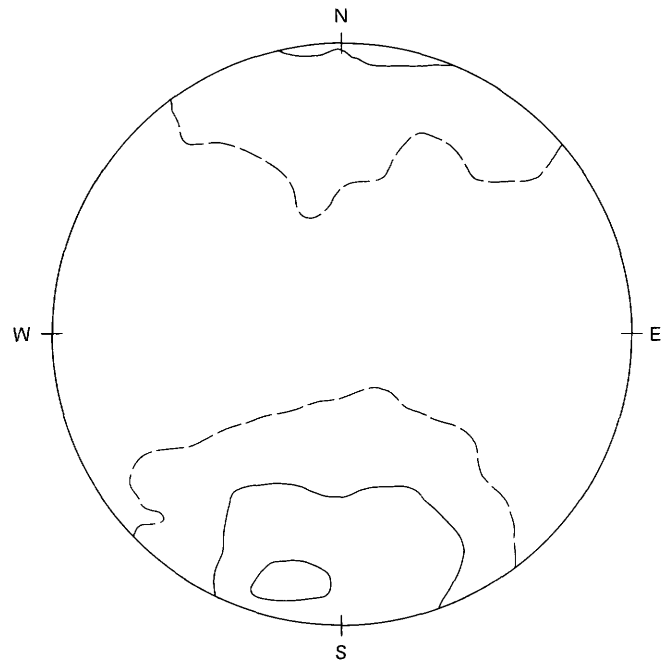

FIGURE 40.—Fabric diagram of contoured poles to layering S_1 for structural subarea 5 (fig. 29), 15 points, counting area=0.211, E=3.16. See figure 30 for explanation.

folds have an east-west trend and plunge east or west at angles greater than 45°. Both the axial planes and compositional layering are refolded by broader open folds (F_2). Unfortunately, these relations were observed only in larger pieces of rubble, and so the true orientations are unknown. The tight isoclinal folds probably correspond to the same style folds observed in the Mountain View area, and the broader, open folds may possibly correspond to the broad warps.

AREA FROM THE WEST FORK OF THE STILLWATER RIVER TO FORGE CREEK

Between the West Fork of the Stillwater River and the upper end of Forge Creek, structural subarea 5 (fig. 29), exposures of metasedimentary rocks are poor. The observed compositional layering (S_1) has an average trend of N. 78° W. and dips abut 75° N. (fig. 40). Minor tight open isoclinal folds were observed only in float of the iron-formation. The only other suggestion that the metasediments in this subarea are folded is the outcrop and float pattern of the blue metaquartzite near Iron Mountain (approximate coordinates: 512,300 N.; 1,855,000 E.). The lensoidal outcrop patterns resemble cores of isoclinal folds with axes trending about N. 70° W.

AREA FROM FORGE CREEK TO THE BOULDER RIVER

The distribution of the iron-formation and blue metaquartzite outcrops within structural subarea 6 (fig. 29) and the attitudes of compositional layering (S_1) in the metasediments suggest complex folding of this sequence of rocks; in addition, the observed minor folds support this concept. A contoured fabric diagram of all poles to compositional layering (fig. 41) in subarea 6 shows a very weak girdle with a weak maximum that may be a result of folding and complex faulting. In order to describe the structure, subarea 6 is broken up into smaller areas that are described from east to west.

Between upper Forge Creek and the headwaters of Bobcat Creek in the Forge Creek drainage, the map pattern of blue metaquartzite and the iron-formation trends approximately north-south (coordinates: 520,920 N.; 1,840,680 E.). The repetition of these rocks in this poorly exposed area suggests a major fold in the metasedimentary rocks that has an axial plane trending north-northeast.

Further west in the upper Bobcat Creek drainage, across a major fault zone, attitudes of compositional layering and minor folds suggest that a major fold axis plunges west at low angles; the axial plane trends northeast-southwest. Within this area poles to compositional layering (S_1) form a north-south πS_1 girdle (fig. 42) with an easterly plunging βS_1 axis. The shape of the major fold is unknown because of the lack of good marker horizons, but open isoclinal folds with a style nearly identical to the F_1 folds from

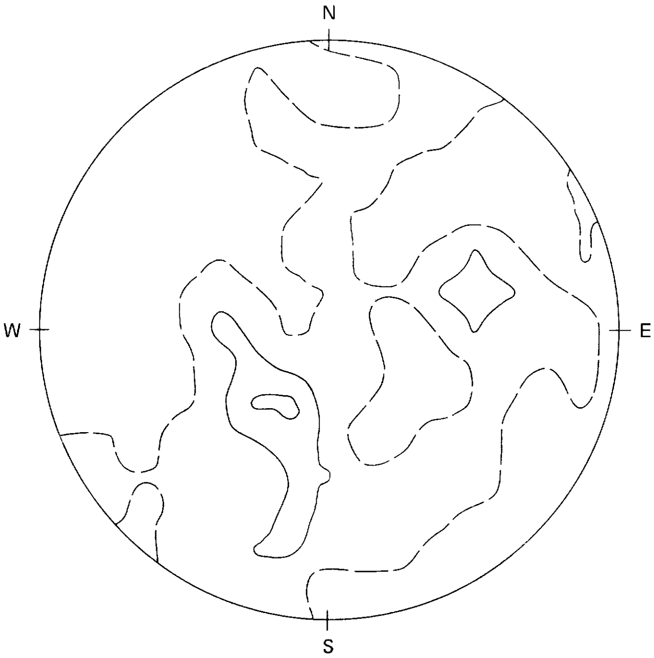

FIGURE 41.—Fabric diagram of contoured poles to compositional layering (S_1) for structural subarea 6 (fig. 29), 176 points, counting area=0.022, E=3.91. See figure 30 for explanation.

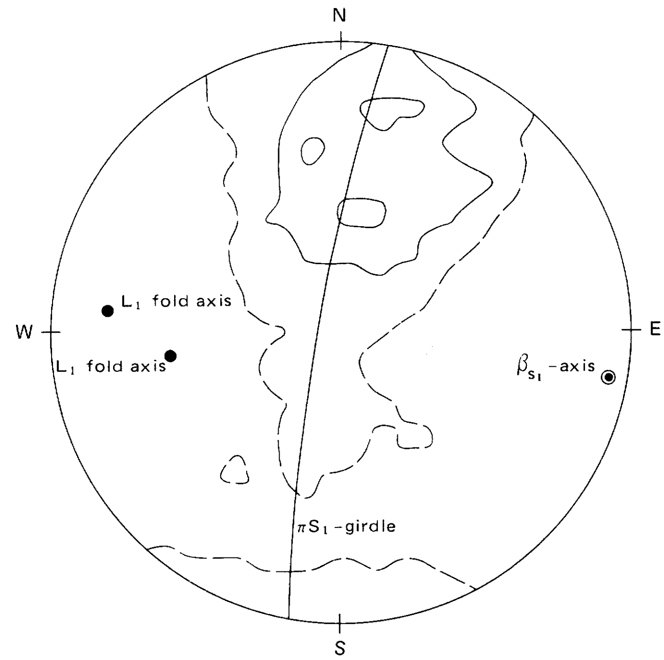

FIGURE 42.—Fabric diagram of contoured poles to layering (S_1) for the large fold in the headwaters of Bobcat Creek. 28 points, counting area=0.125, E=3.5. See figure 30 for explanation.

the Mountain View area have a similar orientation to the major fold. It is possible that the major fold has a similar shape.

From upper Bobcat Creek westward to the east side of the Boulder River, apparent major folds are present, and several minor ones are indicated by the outcrop patterns of the iron-formation and blue metaquartzite. Major folds probably are complexly faulted. The fold between Blakely Creek and the unnamed creek to the south appears to have an axial trace striking approximately N. 40° E., but the exposures are too poor for further analysis.

West of the Boulder River, in an area of slightly better exposure, the outcrops of iron-formation and blue metaquartzite can be interpreted as a series of broad to open folds below the base of the Stillwater Complex (fig. 43). Figure 43 (inset) shows a plot of S_1 poles that form a πS_1 girdle with a southwesterly plunging βS_1 axis. The few minor folds observed in this area are of two styles: (1) broad open warps and (2) open isoclinal folds.

In summary, the two dominant directions for axial planes of major folds between upper Forge Creek and the west side of the Boulder River are northeast and northwest (fig. 44). Those that trend northwest seem to be refolded about northeast axes (fig. 43). The few minor fold axes observed in the hornfels (fig. 44) are generally distributed along a north-south great circle.

ALL STRUCTURES EXCLUSIVE OF THE MOUNTAIN VIEW AREA

The overall structural pattern in the hornfels rocks is elusive mainly because well-exposed outcrops exist only in the Mountain View area. The interpretations of the contoured plots of poles to layering and fold axes for all of the areas combined except Mountain View should be considered tentative and speculative because of the lack of good marker beds. A contoured fabric diagram for layering (S_1) with two possible πS_1 girdles superimposed (fig. 45*A*) suggests that two sets of folds exist with fold axes that strike northeast for one set and northwest for the other set. Although the evidence is sketchy and sparse throughout the hornfels area, two fold styles were observed: (1) open isoclinal folds and (2) broad concentric folds. Only in few examples and usually in float blocks could the broad concentric style be observed to fold the open isoclinal type. Figure 45*B* is a contoured fabric diagram for all the observed mesoscopic fold axes. Observed fold axes (L) tend to lie on a weak girdle pattern that has a maximum plunging 35° to N. 22° W. In figure 45*C*, the βS_1 axes from each subarea, whether strongly or weakly developed, are plotted, and their distribution seems to form a small circle. The axis of the small circle shown in figure 45*C* is B_{S_2} fold axes from the Mountain View area (fig. 36*A*). The earlier fold axes (B_{S_1}) appear to have been rotated 30° by the next folds about the B_{S_2} axes.

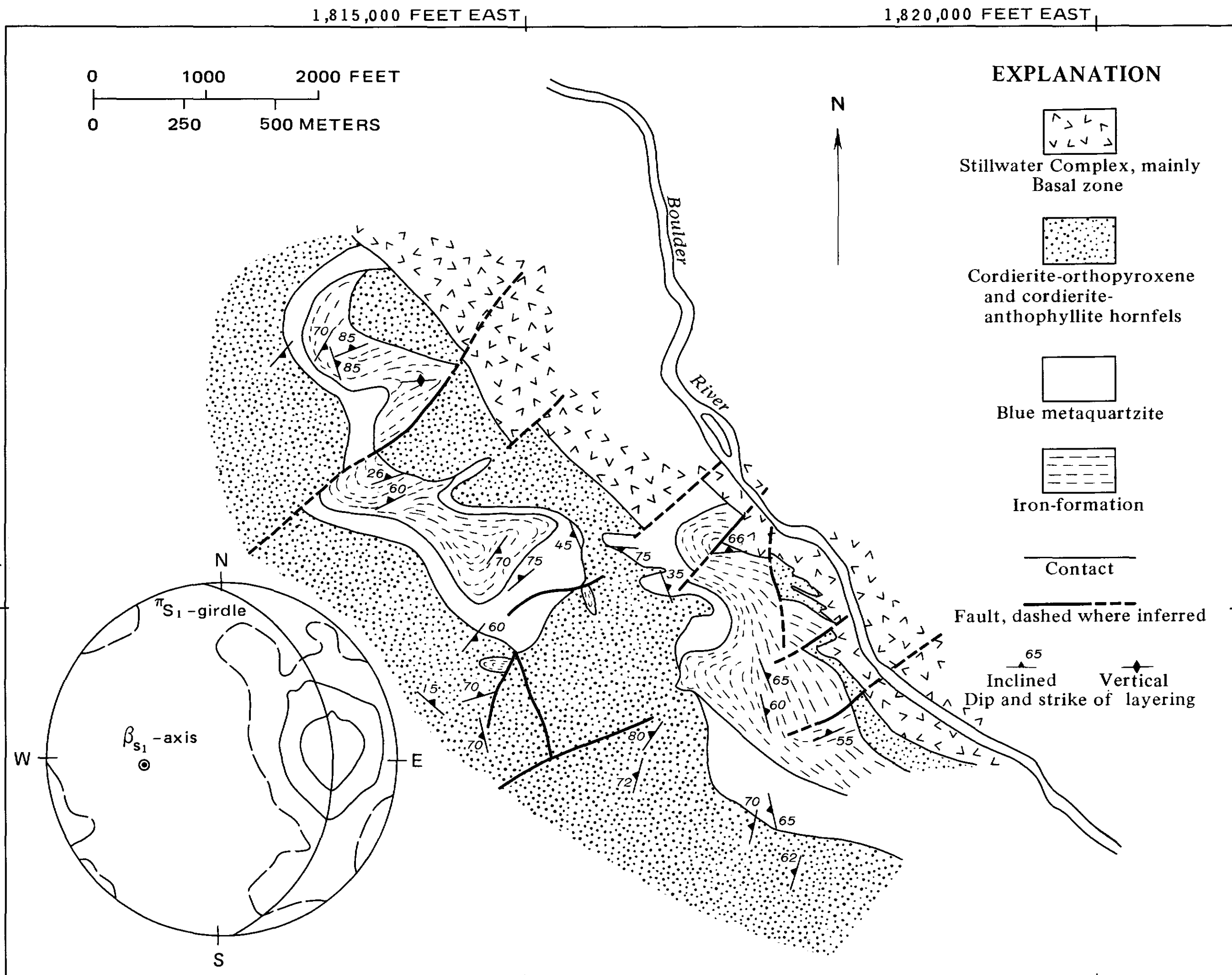

FIGURE 43.—Interpretative geologic sketch map of folds in metasedimentary rocks west of the Boulder River. Inset shows a contoured fabric diagram for poles to S_1 layering, 28 points (not all shown on sketch map), counting area=0.125, E=3.50; see figure 30 for explanation.

STILLWATER COMPLEX

DESCRIPTION OF IGNEOUS AND METAMORPHIC STRUCTURES

Since the early work of Peoples (1933, 1936), igneous layering in the Stillwater Complex has been the object of extensive studies. These include the descriptive work of Jones, Peoples, and Howland (1960), Hess (1960), and Jackson (1961, 1963, 1967, 1968, 1969, 1971). Igneous layering, defined as repetitions of continuous sheetlike cumulates having uniform or uniformly gradational properties, is of two types (Jackson, 1967, p. 22): (1) layering caused by variation in proportion of cumulus minerals and (2) layering caused by variation in physical properties or composition of cumulus minerals. Lamination is also present locally and is formed by planar parallelism of one or more cumulus minerals (Jackson, 1967, p. 22; Jones and others, 1960, p. 291-293). Petrofabric studies by Hambleton (1947) and Jackson (1961) on the orientation of tabular minerals showed that the planar lamination is generally parallel to the layering plane in the Stillwater Complex. Therefore, both layering and lamination in cumulate rocks were treated as primary igneous features and called S_0.

Another type of penetrative planar structure present in the Stillwater Complex consists of the development of fine fractures, which are found in the Ultramafic zone and are especially well developed in olivine and olivine-bronzite cumulates. They are accompanied by the formation of parallel veins of serpentine and magnetite. In the olivine cumulates the orthopyroxene oikocrysts are sheared and flattened parallel to the fine fractures. Figure 46 shows an example of this foliation that is probably a metamorphic foliation superimposed on the layered complex rocks.

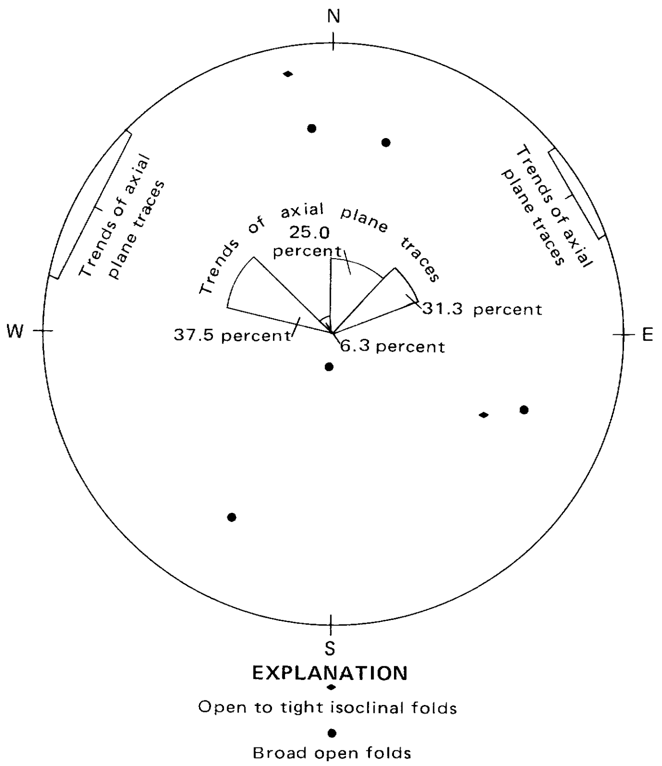

FIGURE 44.—Trends of axial plane traces and minor fold axes in metasedimentary rocks between Chrome Mountain and the west side of the Boulder River.

GEOMETRICAL ANALYSIS OF IGNEOUS STRUCTURES IN THE ULTRAMAFIC ZONE

Layering of structural subareas of the complex (fig. 29) is discussed from east to west. Mineralogical layering and laminations (S_1) and fine fractures (S_1) accompanied by serpentine and magnetite veins (S_1) were measured and analyzed. The measurements of fine fractures were combined for all subareas. Contoured plots of poles to cumulate layering (S_0) for each of the subareas in the Ultramafic zone are shown in figure 47*A-H*. These are summarized in figure 47*I*. Cumulate layering in general for subareas 7, 8, 10, 11, and 12 (fig. 47*A, C, E, F, G*) has a similar northwest strike and, except for layering in subarea 14 (fig. 47*H*) which dips steeply to the south, has a northward dip. In contrast, cumulate layering for subareas 13, 9, and 14 (fig. 47*B, D, H*) has a northeast strike and dips toward the north at moderate angles.

Layering in the Mountain View area, subarea 13 (fig. 47*B*), shows the greatest rotation with respect to the other cumulate layering in the Ultramafic zone. Contouring of poles to S_0 from the Mountain View area shows a girdle fabric oriented N. 43° E. and dipping 34° SE., whose βs_0 axis plunges 56° N.-47° W. A set of folds highly broken by faults was mapped in the Ultramafic zone of the Mountain View area by Jackson, Howland, Peoples, and Jones (1954) and Page and Nokleberg (1974). The major discernible folds have axial plane traces that trend about N. 60° W. The correspondence in trend within 15° between the traces of the axial planes and the statistical βs_0 axis suggests that the βs_0 represents the fold axis

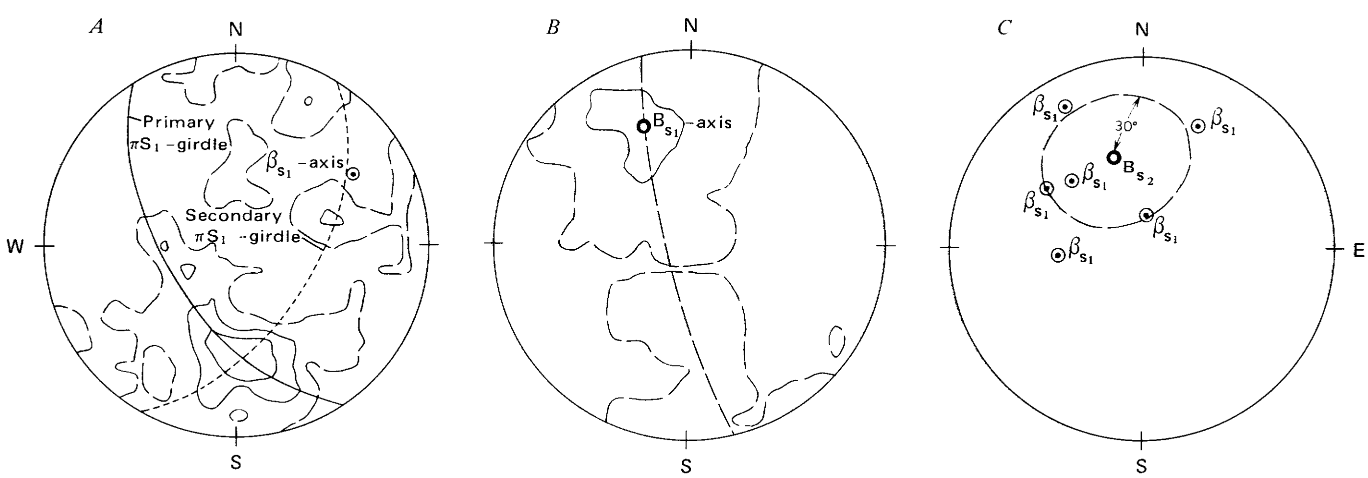

FIGURE 45.—Contoured fabric diagrams of all structures in structural subareas (1, 2, 4, 5, 6) exclusive of the Mountain View area (subarea 3). *A*, Poles to layering (S_1), 263 points, counting area=0.015, E=3.94; see figure 30 for explanation. *B*, L poles, 18 points, counting area=0.182, E=3.27. Long-dashed line, weak girdle formed by fold axes (L). *C*, Plot of β_{S_1} poles from all subareas (1-6) and parts of subareas. Dashed circle formed by β_{S_1} axes from each subarea. B_{S_2} fold axes from Mountain View area (fig. 36*A*).

FIGURE 46.—Olivine cumulate with flattened bronzite oikocrysts.

of the highly broken folds in the Ultramafic zone in the Mountain View area. These folds cannot be correlated with any folds found in the granitic gneisses or in the metasedimentary rocks but are thought to be a result of later folding related to compression between the Lake and Bluebird thrusts.

The present attitude of cumulate layering, striking toward the northeast, in subarea 14 (fig. 47*H*), is probably due partly to rotation and differential movement on this area between two thrust faults. A cross section (fig. 48) illustrates the structure in an adjoining area and shows the type of rotation of the Ultramafic zone between the Bluebird and an unnamed thrust to the south. The contoured plot of poles to cumulate layering for subarea 14 (fig. 47*H*) shows no evidence of a girdle pattern, and the layering shows no evidence of being folded. The N. 77° E. strike and nearly vertical dip of the average layering plane, a divergence from the northwest attitude, is most certainly a result of rotation between the two faults and is not considered to be the result of folding.

Mapping in structural subarea 9, near Iron Mountain, by Page and Nokleberg (1974) and Howland (1955) showed what appear to be folds in the Ultramafic zone. Jones, Peoples, and Howland (1960) suggested that the changes in attitude of the cumulate layering may be interpreted as a monoclinal bend, but the contoured plot of poles to the layering shows only a slight tendency, if any, to form a girdle pattern (fig. 47*D*). If the slight stretching out of the maxima pattern is interpreted as an incipient girdle, it would have a βS_0 axis plunging N. 50°-60° W. at about 55°. Possible axial plane traces in the Iron Mountain area have trends between N. 40° and 50° W. The lack of data precludes any more extended interpretation, but the questionable girdle pattern in figure 47*D* for the Iron Mountain subarea might be developed by a more detailed study of cumulate layering. The hypothesized fold patterns are similar to those in the Mountain View area, subarea 13, but the area containing them is not enclosed by identified thrust faults.

The curvilinear outcrop patterns of gently dipping layers in the Ultramafic zone between the East Boulder River and westward to the Boulder River generally reflect the mountainous topography. The outcrop patterns do not represent folds, and therefore the two western subareas (11 and 12, fig 29) have strong single maxima in contoured plots of poles to layering (figs. 47*F* and *G*) and represent fairly consistent attitudes in the Ultramafic zone.

Fine fractures accompanied by serpentine and magnetite veins and elongated orthopyroxene oikocrysts are superimposed on the igneous layering and lamination. Unfortunately, although this metamorphic foliation is common, it was not studied in detail during the field mapping, and few data were collected. Figure 50 summarizes the orientation data as poles to this plane (S_1) in the Ultramafic zone. This fabric has many similarities in orientation and style to the foliation in the intrusive quartz monzonite.

GEOMETRICAL ANALYSIS OF IGNEOUS STRUCTURES IN THE BANDED AND UPPER ZONES

Unlike the cumulus layering in the Ultramafic zone, the attitude of layering (S_0) in the Banded and Upper zones of the complex varies little in an east-west direction (figs. 50 *A–D*) and has an average attitude of N. 78° W. and 77° N. Subareas 15 and 16 (fig. 50*C*), the western areas, have far fewer structural data than do the other subareas and probably have less statistical validity. Within subareas, there are local departures from the average N. 78° W., 77° N. attitude, probably owing to differential movement on later faults. One example of differential movement is the slight difference in attitude between subarea 18 and subarea 17 (figs. 50*A* and *B*), Benbow to the Stillwater River and the Stillwater River to the West Fork, respectively. The difference is believed to be significant and may represent the amount of differential rotation along the postulated fault of Laramide age (Page and Nokleberg, 1974) in the Stillwater River valley. Similarly, the 17° difference in dip between subarea 17 and subareas 15 and 16

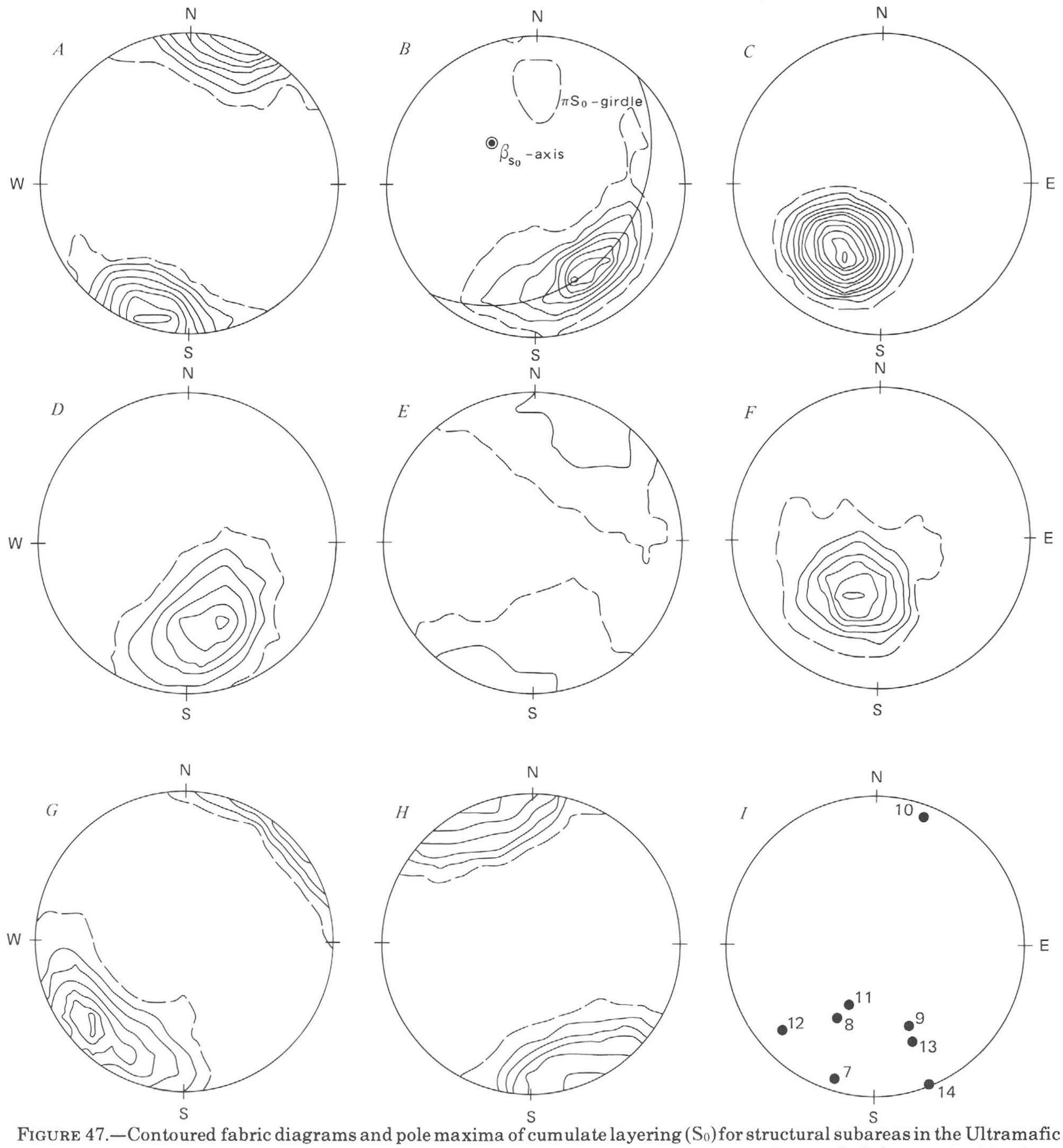

FIGURE 47.—Contoured fabric diagrams and pole maxima of cumulate layering (S_0) for structural subareas in the Ultramafic zone. See figure 30 for explanation. *A*, Subarea 7, 61 points, counting area=0.062, E=3.75. *B*, Subarea 13, 106 points, counting area=0.036, E=3.85. *C*, Subarea 8, 50 points, counting area=0.074, E=3.70. *D*, Subarea 9, 45 points, counting area=0.082, E=3.67. *E*, Subarea 10, 11 points, counting area=0.767, E=2.93. *F*, Subarea 11, 67 points, counting area=0.056, E=3.77. *G*, Subarea 12, 63 points, counting area=0.060, E=3.76. *H*, Subarea 14, 20 points, counting area=0.167, E=3.33. *I*, Summary of pole maxima; numbers refer to subareas.

probably represents the differential rotation on the Sioux Charley Lake fault zone of Butler (1966), the continuation of which separates subarea 17 from subareas 15 and 16.

A comparison of the attitudes of cumulate layering of the Upper zone with those of the Ultramafic zone is of value in unraveling the effects of tectonism on the Stillwater Complex after its emplacement. A

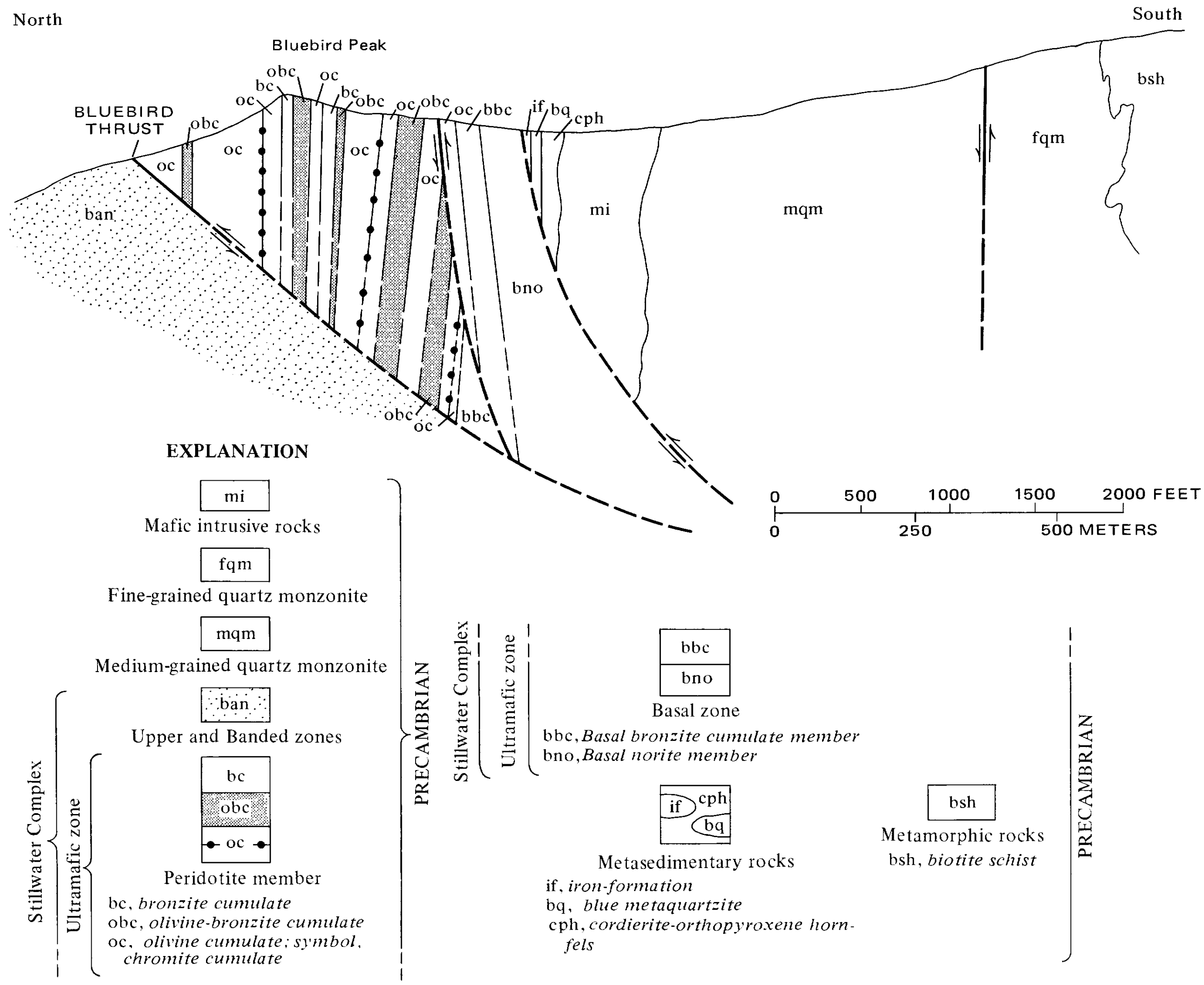

FIGURE 48.—Cross section (approximately north-south) along Bluebird Peak in structural subarea 14 (fig. 29).

comparison of mesoscopic fabrics shown on figures 47 and 50 shows that from West Fishtail Creek to the Stillwater River, subarea 7 (fig. 47*A*), the fabric of the Ultramafic zone is virtually the same as that of the Upper zone except that the Ultramafic zone has a slightly shallower dip. The close correspondence in attitude implies that after emplacement, the whole Stillwater Complex between West Fishtail Creek and the Stillwater River acted as a block under stress. In a general way, as noted by Jones, Howland, and Peoples (1960), the dip of the cumulate layering changes from overturned to the south near the mountain front at the north and gradually decreases in angle dipping toward the north in the southern exposures of the eastern part of the complex.

Other subareas in the Ultramafic zone, subareas 8, 11, and 10, also show a correspondence in attitude to the gabbroic rocks, except that in subareas 8 and 11, the dips are shallower and in subarea 10 the dip is steep and off to the south (compare figs. 47 and 50). These subareas were apparently more affected by fault rotation after the complex was emplaced than the area between West Fishtail Creek and the Stillwater River. The rotation of the strike of subarea 12 with respect to all the gabbroic rocks may have been caused by the Graham Creek fault in the Gish area.

The relation of subareas 13, 14, and 9 in the Ultramafic zone to the Banded and Upper zones is unique in that the cumulate layering of the Ultramafic rocks does not conform with the orientation of the layering in the Upper zone. In fact, all these subareas are rotated with respect to the Upper zone.

Overall, from east to west, there is a consistent decrease in dip of the cumulus layering in the gabbro

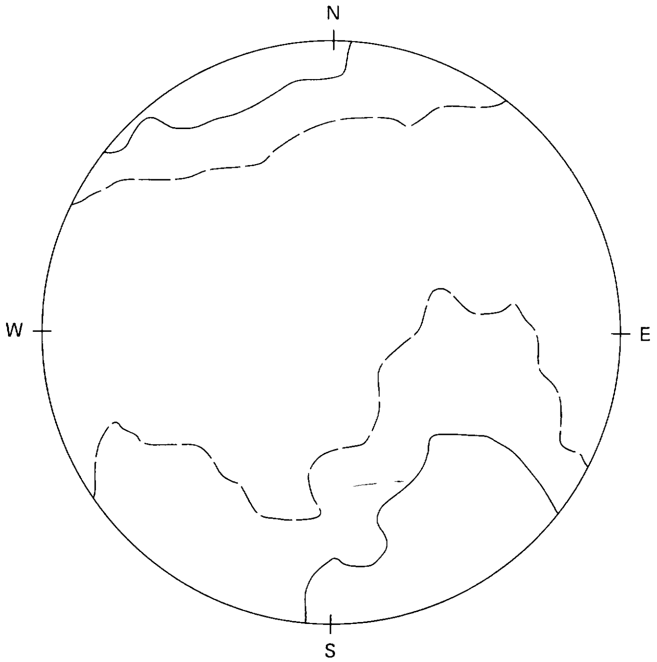

FIGURE 49.—Fabric diagram of contoured poles to metamorphic foliation (S_1) in the Ultramafic zone. 18 points, counting area=0.182, E=3.27. See figure 30 for explanation.

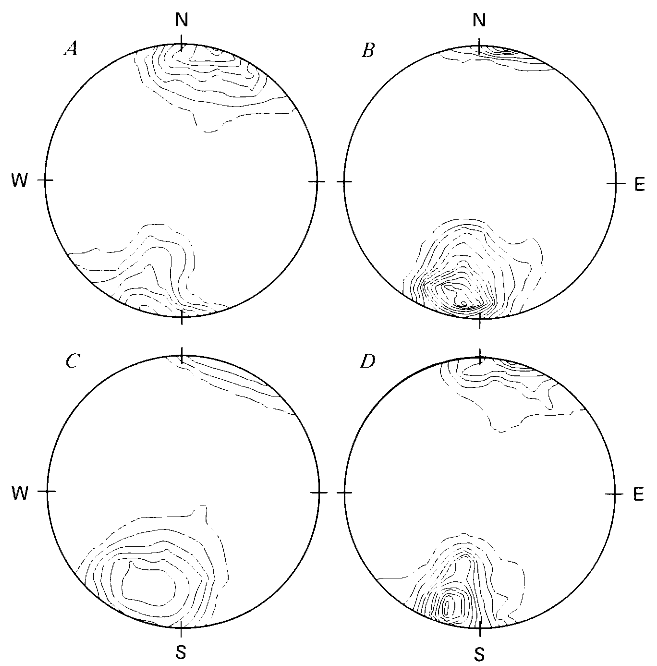

FIGURE 50.—Fabric diagrams of contoured poles to igneous layering (S_0) in the Banded and Upper zones of the Stillwater Complex. See figure 30 for explanation. *A*, Structural subarea 18, 118 points, counting area=0.033, E=3.87. *B*, Structural subarea 17, 98 points, counting area=0.039, E=3.84. *C*, Structural subareas 15 and 16, 27 points, counting area=0.129, E=3.48. *D*, All subareas combined, 243 points, counting area=0.016, E=3.94.

rocks from nearly vertical to overturned on the east end to near 60° N. on the west end of the complex. The elongation of the maximum in figure 50*D* reflects this change. This implies that to an observer looking west the cumulus layers were rotated clockwise about a horizontal axis, with the largest amount of rotation at the east end. The movement of a single layer is analogous to a twisted ribbon.

STYLE AND GEOMETRICAL ANALYSIS OF STRUCTURES OF THE INTRUSIVE QUARTZ MONZONITE SEQUENCE

No igneous planar or linear structures (Page and Nokleberg, 1972) have been observed in the intrusive quartz monzonite sequence of rocks. The planar feature formed by a late penetrative deformation (Page and Nokleberg, 1972) is a mineral foliation defined by elongated feldspar phenocrysts and parallel biotite and chlorite flakes (S_1). No folds or lineations have been observed associated with this mineral foliation.

Attitudes of foliation marked by alinement of platy and tabular minerals in the quartz monzonite intrusive sequence are divided into four structural subareas (fig. 29). Subareas 19 and 20 lie between West Fishtail Creek and the Stillwater River; subarea 19 is totally in the coarse-grained quartz monzonite, and subarea 20 consists dominantly of medium-grained quartz monzonite. Subarea 22 contains all the rocks of the quartz monzonite sequence, west of the Stillwater River, that are between the Bluebird and Lake thrusts. All of the rest of the quartz monzonite sequence to the west of the Mountain View area is contained in subarea 21. Contoured plots of the poles to the foliation for each subarea are given in figure 51. The foliation is a penetrative structure, but no linear structures associated with the foliation were observed; that is, there are no known folds or mineral lineations within the quartz monzonite sequence.

Subareas 19 and 20 were divided in order to compare fabrics between the coarse- and medium-grained quartz monzonites. The fabrics from subareas 19 (fig. 51*B*) and 20 (fig. 51*A*) show very little difference. The average attitudes between the two subareas differ by 13° in strike and 14° in dip. The change in dip is similar to the change from north to south observed within the Stillwater Complex and shows a general decrease toward the south. The overall fabric patterns are so similar that they imply that the medium- and coarse-grained quartz monzonite reacted homogeneously to the process that caused the foliation. Quartz monzonite in the Mountain View area, subarea 22 (fig. 51*C*), has a fabric very similar to subareas 19 and 20.

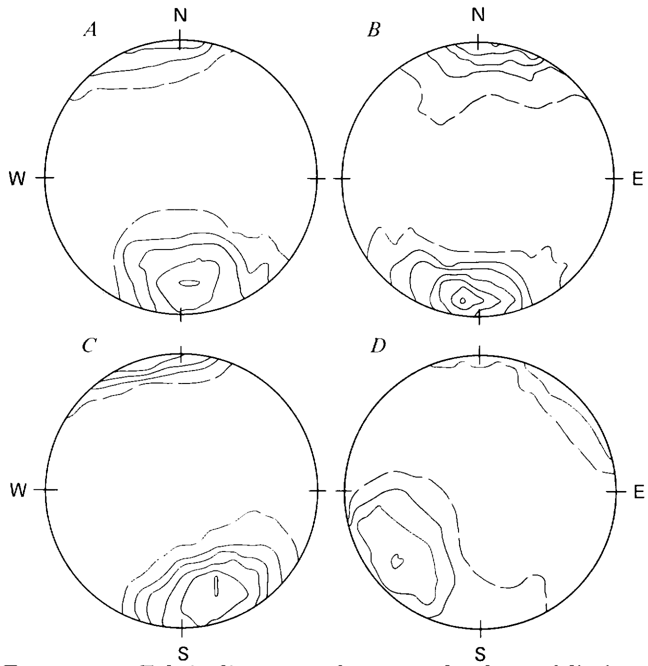

FIGURE 51.—Fabric diagrams of contoured poles to foliation for structural subareas of quartz monzonite. *A*, Medium-grained quartz monzonite, subarea 20, 22 points, counting area=0.154, E=3.38. *B*, Coarse-grained quartz monzonite, subarea 19, 67 points, counting area=0.056, E=3.77. *C*, Subarea 22, Granite Ridge area, 27 points, counting area=0.129, E=3.48. *D*, Subarea 21, 22 points, counting area=0.154, E=3.38. See figure 30 for explanation.

The foliation in subarea 21 (fig. 51*D*) forms a fabric with difference in strike of 40°-45° from the other three subareas. This suggests the possibility that the quartz monzonites in the Bluebird-Initial area were rotated with respect to the other subareas after the foliation was formed. Probably this rotation was due to differential movement on later faulting—possibly on the Sioux Charley Lake fault zone.

Comparison of fabrics of the granitic gneisses to the south (fig. 30) and the quartz monzonite sequence (fig. 51) shows an extreme contrast: (1) folds are lacking in the quartz monzonite sequence and (2) the strike of the foliation is approximately east-west in the quartz monzonite sequence in contrast to the northward strike in the granitic gneisses. This structural contrast between the terranes cannot be reconciled by rotation and displacement by later faults. The quartz monzonite sequence and the granitic gneisses must have had different structural histories.

STRUCTURES IN THE PALEOZOIC AND MESOZOIC SEDIMENTARY ROCKS

Attitudes of bedding of sedimentary rocks that occur as downfaulted blocks within the Stillwater Complex and along the northern margin of the complex (structural subarea 23, fig. 29) were collected and their poles contoured in figure 52. The resulting pattern is a girdle with a βS_0 axis that plunges gently southeast. Asymmetrical folds, inclined toward the north, have been mapped (Jones and others, 1960; Page and Nokleberg, 1974) in the infaulted segments of the strata and on the margin of the complex. The axes of these folds generally plunge gently southeast, and the axial plane traces trend northwest. Therefore the βS_0 axis in figure 52 is assumed to represent the BS_0- fold axis for the sedimentary rocks. The attitude of these folds bears no correspondence of similarity to folds, foliations, or lineations described in the Precambrian crystalline rocks. Jones, Peoples, and Howland (1960) explained the development of these folds as part of the faulting and adjustment necessary for the Laramide deformation of what is now the Beartooth Mountains.

Bedding in the Paleozoic and Mesozoic rocks on the north edge of the complex (fig. 52) and cumulus-layering in the Banded and Upper zones (fig. 50) have similar orientations along the mountain front. This implies that the present attitude of both rock types developed concomitantly in post-Cretaceous time.

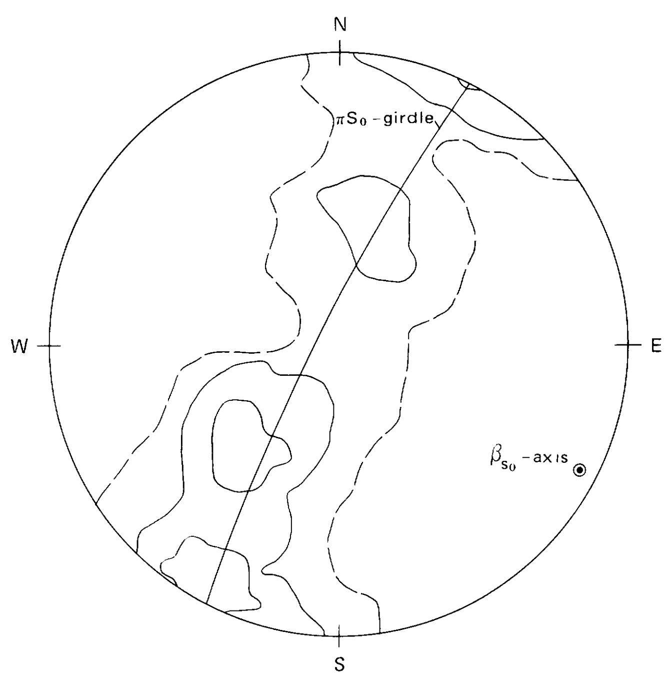

FIGURE 52.—Fabric diagram of contoured poles to bedding (S_0) for Paleozoic and Mesozoic rocks in structural subarea 23, showing constructed πS_0 girdle and βS_0 axis. 75 points, counting area=0.051, E=3.80. See figure 30 for explanation.

Another noticeable feature concerning the sedimentary and gabbroic rocks (Page and Nokleberg, 1974) is the general parallelism of the bedding of the sedimentary rocks and the cumulus layering in the gabbroic rocks. Except between West Fishtail Creek and Grassy Knob, the West Fork of the Stillwater and the East Boulder River, and near Mount Ray and the extreme west end of the complex (Jones and others, 1960), the strike of the layering in gabbroic subareas is within 10° or 15° of the average strike of the contact of the complex and the Paleozoic rocks. In the excepted areas the divergence in strike reaches a maximum of 55° and must represent the apparent discordance, locally between the Stillwater Complex and the lowest of the Middle Cambrian strata.

ROTATION OF STRUCTURES TO A PRE-MIDDLE CAMBRIAN POSITION

In order to compare geometries of folds and other structures in the Stillwater Complex, we must know their attitudes with the effects of Laramide deformation removed. Also, in order to compare the folds in the metasedimentary rocks along the base of the complex with those in the Mountain View area where they are best analyzed, it is necessary to eliminate the Laramide deformation. However, it is impossible at the present time to compare structures in the hornfels throughout the study area because the appropriate geometrical conditions do not exist to enable a rotation model to be developed.

In any attempt to remove effects of Laramide deformation, there are several assumptions. The assumptions used here are: (1) All the tilt of Paleozoic and Mesozoic sedimentary rocks is due to Laramide deformation, (2) most of the rotation and differential displacement along faults is a result of the Laramide deformation, (3) the Middle Cambrian and later sedimentation was on a virtually horizontal surface, and (4) the cumulus layering in the Stillwater Complex formed after intrusion on virtually horizontal surfaces.

Assumption (1) is probably reasonable, but no Cenozoic rocks are exposed along the mountain front immediately adjacent to the complex, so it is difficult to assess the effects of later deformation. Assumption (2) is most certainly a poor assumption because the association of mafic dikes of late Precambrian age with faults suggests that some of the faults were active before Laramide time. Assumption (3) has its weakness because the discordance of the Middle Cambrian strata and the Upper zone is known locally to reach a maximum of 55°. Also, as the Lower Cambrian section is missing above the Stillwater Complex, Jones, Peoples, and Howland (1960) postulated that the complex formed an ancestral Precambrian-Lower Cambrian mountainous terrain. However, assumption (3) is supported by the general close parallelism of the Stillwater Complex and sediments along the upper contact. Assumption (4) is probably generally true; however, the contact at the base of the Stillwater Complex is known to be irregular locally, and there is a large-scale irregularity consisting of a sequence of what may be termed basins and topographic highs. Page (unpub. data) documented the irregularities in the Basal zone, and Jackson (1963) showed that these irregularities continue up through the Peridotite member of the Ultramafic zone. W. J. Nokleberg (oral commun., 1969) documented local discordances of a few degrees between cumulus layers in the Banded zone. In addition, Jones, Peoples, and Howland (1960) referred to lensoid shapes of individual units within the complex. In general, the cumulus layers must have been nearly horizontal.

Accepting these assumptions and using bedding and cumulus-layering attitudes in local domains between West Fishtail Creek and the Stillwater River, each domain was rotated to the attitude that it had pre-Middle Cambrian time. In each of the 14 subareas the present strike of the bedding was taken as the rotation axis, and the amount of rotation was the amount necessary to rotate the bedding from its present attitude to horizontal. The cumulus layering in each domain was then rotated by the same amount which then gives the apparent (nominal) attitude of the Stillwater Complex in pre-Middle Cambrian time. An example of the nominal attitude of cumulus layering in pre-Middle Cambrian time in the Benbow-Nye Basin area is shown in figure 53. Because of the geometry used in the rotation process, not all cumulus layering is inclined at 25°-35° NE. as suggested by Jones, Peoples, and Howland (1960, p. 325). Some of the differences in attitude may be evidence of differential rotation or displacement on the various fault systems that is not accounted for by the rotation.

Analysis of possible rotation axes, their amounts, and directions of rotation in the 14 separate areas suggests that the more likely rotation axis, applicable to the gabbroic and ultramafic rocks, is one striking N. 298.5° E. with a rotation to the south of 69.1°. This is the arithmetic average rotation axis for the 14 areas. When applied to maxima from the contoured plot of poles to cumulus layering (fig. 54) in the Benbow to the Stillwater River area, it results in rotation of the present attitudes to nearly east-west-

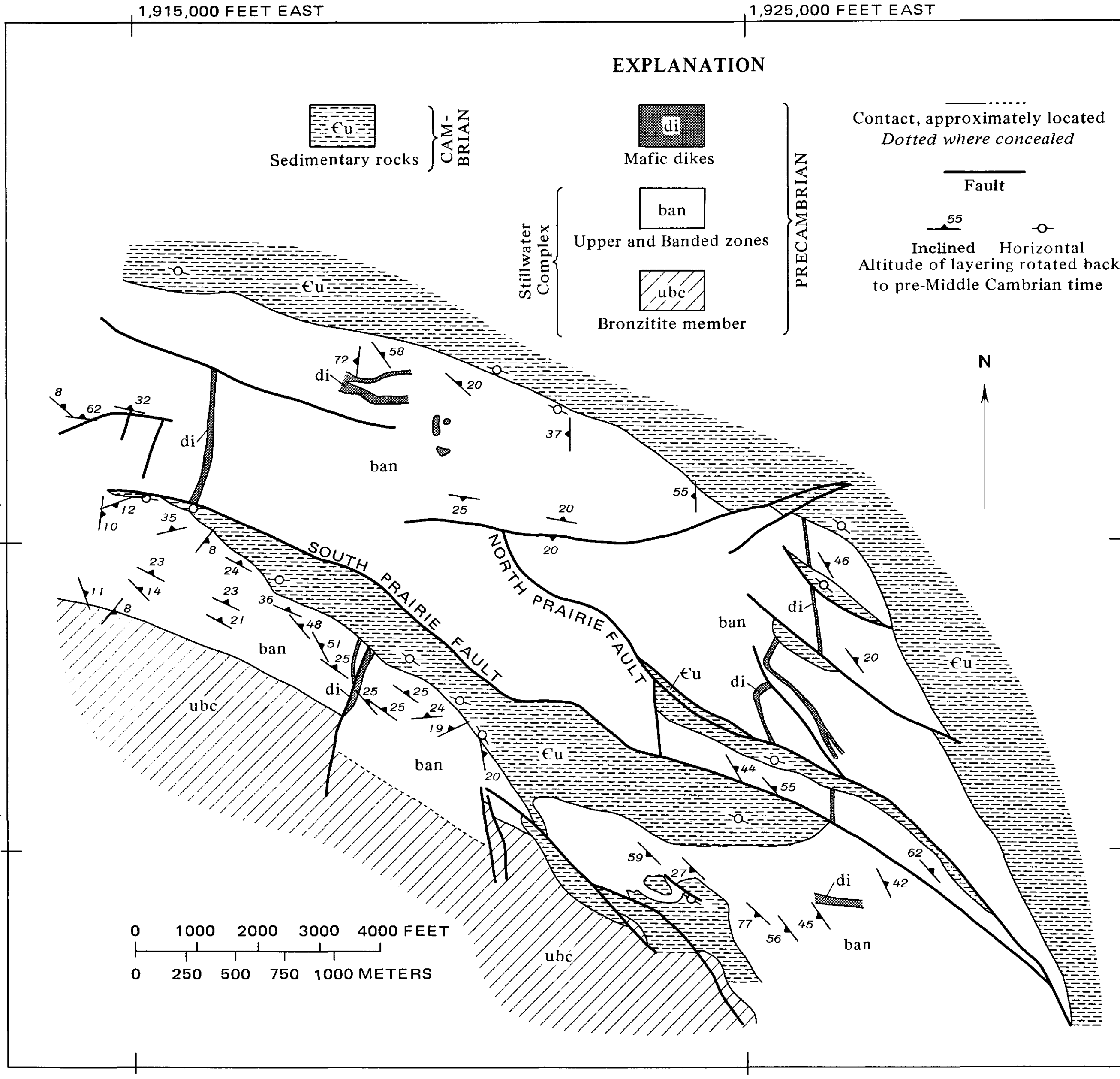

FIGURE 53.—Geologic sketch map of Benbow-Nye Basin areas showing nominal attitudes of cumulus layering rotated back to pre-Middle Cambrian time.

trending, gently north-dipping maxima for cumulus layers in the Ultramafic, Banded, and Upper zones at the onset of Middle Cambrian sedimentation.

In the area between the Stillwater River and the West Fork of the Stillwater River, it is much more difficult to establish a rotation axis by the above method. Most of the contact of the complex with overlying sedimentary rocks is a thrust fault and cannot be used for rotation. In addition, the downfaulted inliers of Cambrian sedimentary rocks on the Banded and Upper zones are highly folded and not easily unfolded and rotated back to a horizontal plane. There are two ways of estimating a rotation axis for this block of ground. One is to assume that the cumulus layering in the Banded and Upper zones was parallel to the cumulus layering in the Benbow to the Stillwater River area. This results in a rotation axis of N. 286° E. and a rotation of 56°–63° (average 59.5°) counterclockwise to the south. The other method is to use one of the rotation axes necessary to make contact with the Cambrian horizontal at the beginning of sedimentation. Most such axes would

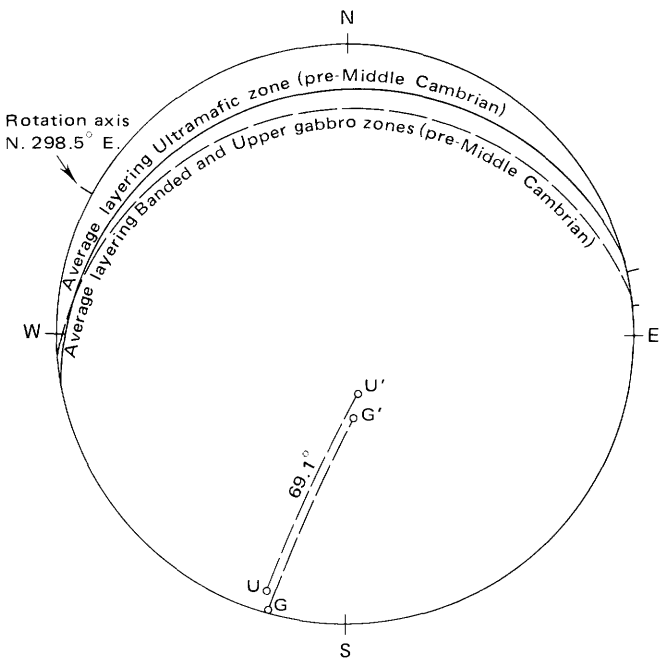

FIGURE 54.—Rotation of poles to cumulate layering for the Ultrasonic, Banded, and Upper zones in the Benbow to Stillwater River area to pre-Middle Cambrian positions. U, Ultramafic zone maxima, present orientation; G, Banded and Upper zone maxima, present orientation; U′, Ultramafic zone position, pre-Middle Cambrian; G′, Banded and Upper zone position, pre-Middle Cambrian.

trend between east-west and north-northwest, but the sense of rotation and amount would be variable and offers no unique solution with which to obtain the upper Precambrian-pre-Middle Cambrian nominal attitude of the cumulus layering. Therefore, the first method was used for rotation of the cumulus layering in the Stillwater River to West Fork of the Stillwater River area. Figure 55 shows the results of this rotation for the contoured maxima of poles to cumulus layering (fig. 55*A*) for the Ultramafic, Banded, and Upper zones.

The cumulus layering in the Ultramafic zone and that in the Banded and Upper zones are not parallel from this rotation. The Ultramafic zone in the Mountain View area, subarea 3, lies between the Bluebird and Lake thrusts and was probably rotated during thrusting either during Laramide time or before. In order for the cumulus layering in subarea 3 to parallel the cumulus layering in the Banded and Upper zones, the layering in subarea 3 must be rotated about a N. 327° E. axis through 34° to the north (the poles of layering to the south). Figure 55*B* shows the results of the rotation.

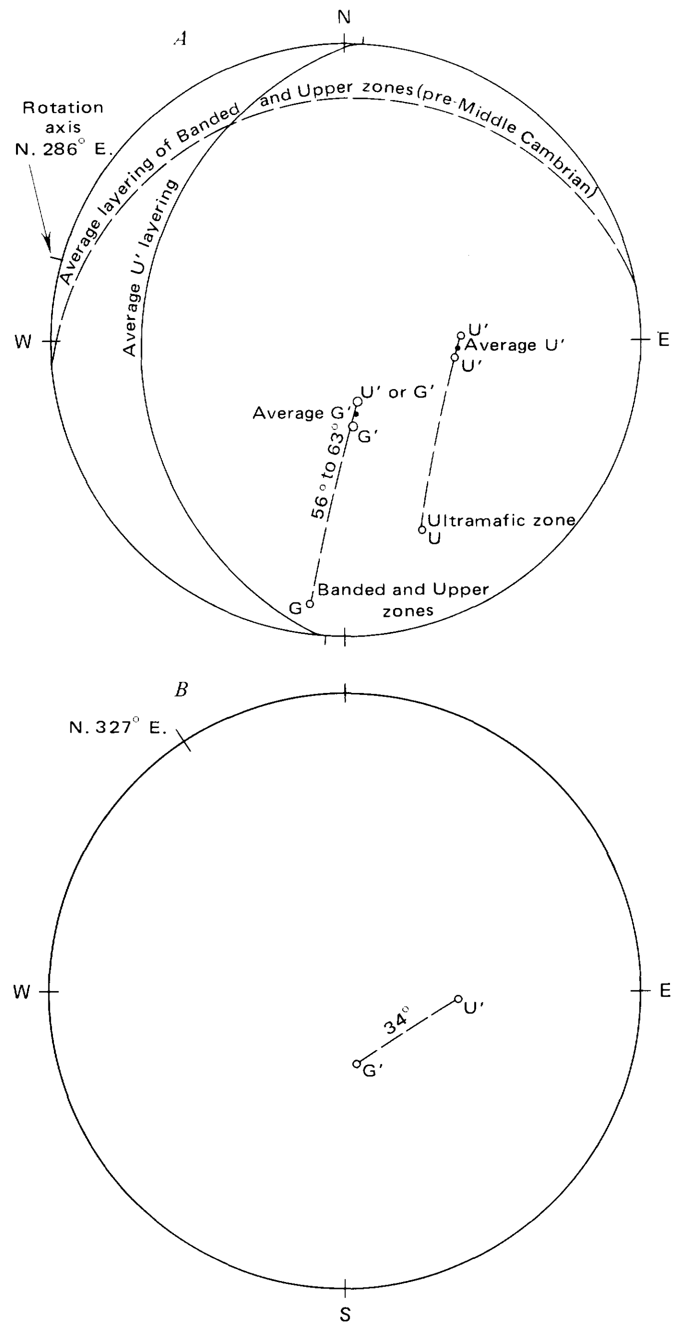

FIGURE 55.— Rotation of poles to cumulus layering for the Ultramafic, Banded, and Upper zones in the Stillwater River to West Fork of the Stillwater River area to pre-Middle Cambrian positions. U, Ultramafic zone, present orientation; G, Banded and Upper zones, present orientation; U′, Ultramafic zone position pre-Middle Cambrian; G′, Banded and Upper zones position pre-Middle Cambrian. *A*, Rotation to pre-Middle Cambrian. *B*, Rotation of axis necessary to make layering in the Ultramafic zone and the Banded and Upper zones parallel.

After establishing a technique of reasonable rotations to obtain parallelism of cumulus layering from the Benbow area to the West Fork of the Stillwater River area, including the Mountain View area, the rotations were applied to the structures in the hornfels in the Mountain View area. Table 15 compares the attitudes of the structures in the metasedimentary rocks at the present time, pre-Middle Cambrian time, and the time of intrusion of the Stillwater Complex. In order to obtain the attitudes of the structures in the metasedimentary rocks at the time of intrusion of the Stillwater Complex, the attitude of the pre-Middle Cambrian cumulus layering in the complex must be rotated to horizontal. The rotation axis necessary to do this is N. 80° E. and 20° toward the south for the layering (fig. 56). Figure 56 shows the results of rotating some of the hornfels.

From the West Fork of the Stillwater River to the Boulder River and western end of the Stillwater Complex, there is very little information available to establish rotation axes. Further detailed mapping in

TABLE 15.—*Rotated attitudes of structures of hornfels in the Mountain View area*

Structure	Present orientation		Cambrian orientation		Orientation before intrusion	
	Strike	Dip	Strike	Dip	Strike	Dip
πS_1 circle (layering)	N. 43° E.	42° SE.	N. 65° E.	79° NW.	N. 85° W.	8° SW.
B_2 (fold axis)	N. 38° E.	62° NE.	N. 19° E.	32° NE.	N. 15° E.	14° NE.
B_3 (fold axis)	N. 17° W.	48° NW.	N. 78° E.	25° NE.	N. 69° E.	23° NE.

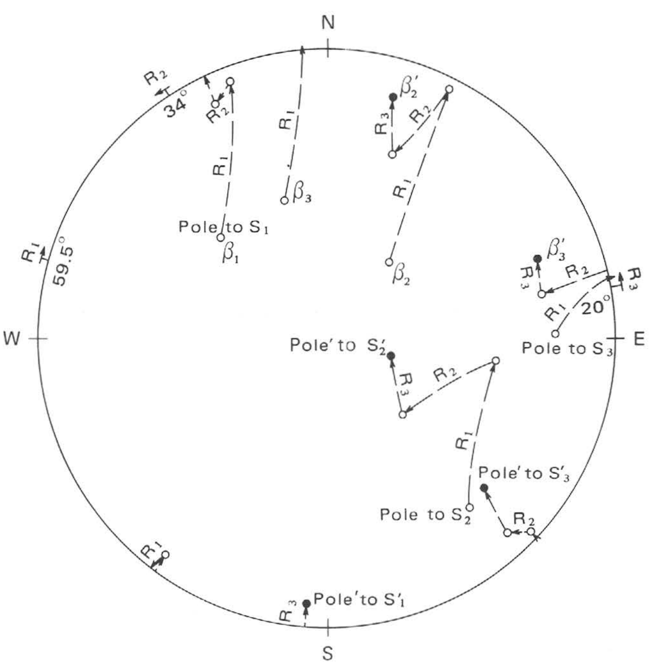

FIGURE 56.—Rotation of attitudes of cumulus layering (S_1), axial pland cleavage (S_2), cleavage (S_3), and fold axes (β_{S_1}) and β_{S_2}) in hornfels in the Mountain View area to their position at the time of intrusion of the Stillwater Complex. Rotation axes: R_1 N. 298.5° E., 59.5° counterclockwise to south; R_2, N. 327° E., 34° clockwise to north; R_3, N. 80° E., 20° clockwise to south.

the Banded and Upper zones of the complex and of the contact with Paleozoic and Mesozoic sedimentary rocks would change this situation. Examination of cumulus layering in the complex implies that the amount of rotation would be less. Jones, Peoples, and Howland (1960) also suggested that there would be less twist west of the West Fork of the Stillwater River.

DESCRIPTION AND ANALYSIS OF FAULTS

AGE AND PREVIOUS WORK

Most of the faults within the Stillwater Complex are believed to have developed during the Laramide orogeny; some were probably active in Precambrian time since they contain Precambrian mafic dikes. However, the region seems to have been active on through the Cenozoic Era and into the Holocene epoch (Pardee, 1947), when movement along some faults was probably renewed. Movement on most of the faults can be dated no more closely than post-Cretaceous because the youngest rocks cut by the faults are Late Cretaceous in the Mt. Wood and Mt. Douglas areas (Page and others, 1973a, b). Some of the faults may have developed more recently than the Laramide orogeny; north of Chrome Mountain (coordinates: 528,730 N.; 1,835,130 E.) a fault appears to have a scarplet less than a meter high developed in glacial deposits (fig. 57). The scarplet also lines up

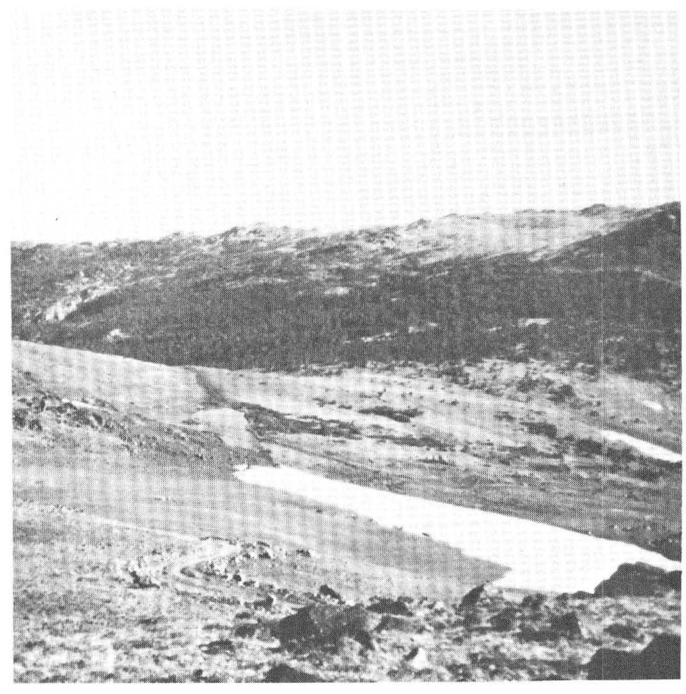

FIGURE 57.—Fault scarplet (center) 2–3-ft-high in glacial deposits northeast of West Serpentine (Montana South coordinates: 528,730 N.; 1,835,130 E.) Photograph by R. A. Koski.

with a small sag pond to the south. This fault most certainly has been active in Holocene time.

Jones, Peoples, and Howland (1960, p. 312-321) described some of the major faults found in the Stillwater area and recognized four types: (1) longitudinal ramp and thrust faults that strike N. 40°-80° W. and dip northeast, (2) westerly striking, south-dipping, longitudinal steep reverse or flat thrusts, (3) vertical faults that trend east-west, and (4) steeply dipping, transverse faults striking between N. 30° E. and N. 30° W. Table 16 shows the categories of faults, the names assigned, and the characteristics of those structures.

At the time of Jones, Peoples, and Howland's work (1960), the northeast-dipping thrust faults and vertical east-west-trending faults were thought to be earlier structures than the others, but no differences in age between the south-dipping thrust and transverse faults were recognized. Since then, mapping by Page and Nokleberg (1974) has shown that many of the northeast-dipping ramp faults and south-dipping reverse or thrust faults are offset by the steeply dipping transverse faults. In other examples, offset between the two fault sets cannot be proved because of lack of exposures, but it is suspected to occur. The south-dipping thrust between Crescent Creek and Upper Forge Creek at the Stillwater Complex-hornfels contact is an excellent example of this relation (Page and Nokleberg, 1974). Jones, Peoples, and Howland's (1960) fault categories (1) and (2) are probably older relative to their category (4).

TABLE 16.—*Faults and their characteristics described by Jones, Peoples, and Howland (1960)*

Name of fault	Type	Attitude		Remarks
		Strike	Dip	
Iron Creek	Ramp and thrust.	N. 65° W.	50° NE.	Flattens(?) with depth; believed by Jones, Peoples, and Howland (1960) to be connected with Brownlee Creek fault.
Brownlee Creek	do	N. 80° W.	50° NE.	
South Prairie	do	N. 40°-60° W.	50°-80° NE.	Related casually to parallel folds in Paleozoic strata; offset at depth by Horseman thrust(?).
North Prairie	do	N. 60°-70° W.	55°-80° NE.	
Castle Creek	do	N. 60°-70° W.	Northeast	
Dry Fork	Thrust	N. 60°-70° W.		North of northern margin of complex. See Vail (1955).
Suce Creek	Ramp and thrust.	West north-west	North	See Richards (1952, p. 56).
Horseman thrust.	Thrust	N. 75°-80° W.	30°-35° S.	Some drag effects on sediments; 457 m stratigraphic throw maximum.
Lake fault	do	N. 75°-80° W.	55°-60° S.	Follows mafic dike.
Nye Creek	do	East-west	45°-55° S.	Assumed to be eastern continuation of Lake fault; used to account for about 900 missing meters of ultramafic zone.
Bluebird thrust.	do	N. 65°-90° W.	40°-60° SW.	Hanging-wall block thrust in a northerly direction for about 900 meters.
East of Fishtail Creek.	do	N. 90°-80° E.	South	
Graham Creek	do	N. 60° N.	60°-70° S.	Dip slip equals about 91 m.
Mill Creek-Stillwater fault zone.	Wrench	About east-west	About vertical	Pivotal motion; south block moved east relative to north block, see Wilson (1936).
Lost Creek fault	do	About N. 80° W.		See Richards (1952).
Big 7	Transverse	N. 5°-15° E.	85°-90° W.	Associated with mafic dikes apparent offset of about 305 m
Central Benbow shift zone.	do	N. 5°-15° E.	Steeply east or west.	Apparent offset of about 610 m.
Other minor faults Benbow area.	do	N. 15° E. - N. 15° W.		Aggregated apparent offset of about 305 m; many follow mafic dikes.

GENERAL ATTITUDE AND OFFSET

Although the distribution of faults and their strike directions can be assessed from the 1:12,000-scale maps (Page and Nokleberg, 1974), a more concise summary of fault strikes is shown in the rose diagram of figure 58. From the 1:12,000-scale maps the characteristics of 501 faults were cataloged. The properties included strike or trend, dip, offset, and strike separation. The measured strikes are the basis for figure 58 from which the three most frequently occurring groups of strikes can be distinguished. One group lies between N. 80° E. and N. 80° W., another group between due north and N. 30° E., and a third group between due north and N. 30° W. The most frequently occurring strike directions are those between N. 30° E. and N. 30° W. and account for about half the faults cataloged. The N. 80° E.-N. 80° W. group consists dominantly of ramp faults; the other, two groups of transverse faults.

Dip directions on faults are much more difficult to obtain because of the lack of good exposures in the critical areas, but 206 dip directions were observed and measured. They were recorded either during the 1:12,000-scale mapping or in earlier planetable mapping at various scales of small areas—maps of which have been either open filed or published (Howland and others, 1949; Howland, 1955; Jackson and others, 1954; Peoples and Howland, 1940; Peoples and others, 1954). Poles to the 201 fault planes were computer plotted and contoured on a lower hemisphere net (fig. 59). The contoured pattern has several maxima lying in an east-west girdle, indicating the general north-south trend of measured faults and the spread in amount and direction of dip. The maxima represent the following approximate planes: N. 88° W., 31° S.; due north, 78° E.; N. 8° E., 52° E.; N. 19° E., 76° E.; and N. 31° E., 70° E. (fig. 59). The N. 88° W., 31° S. average fault plane represents a generalized attitude for thrust faults, whereas the other maxima are typical of the transverse faults. Most measured transverse faults strike between north and northeast and dip between 52° and 78° E.; the dip values are slightly lower than those inferred by Jones, Peoples, and Howland (1960) for transverse faults.

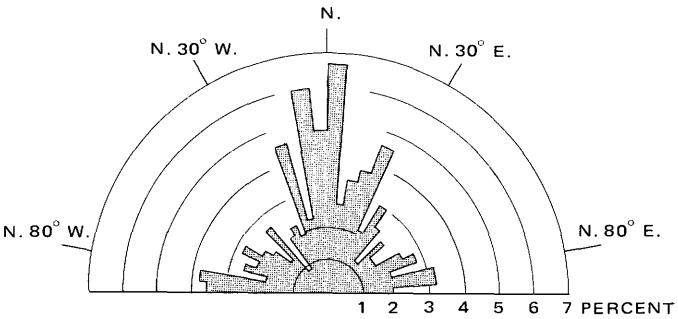

FIGURE 58.—Strikes of 501 faults, measured from the 1:12,000-scale maps of the Stillwater Complex area (Page and Nokleberg, 1974).

The amounts and nature of movement along the faults can only be determined in a limited number of examples, but measurements of strike separation and offset[2] were possible for 142 faults, a large proportion of which are transverse faults that cut the Ultramafic zone. Figure 60 shows the frequency of occurrence of strike separation and offset at 15-m intervals. Over half of the measured offsets and separations lie between 0 and 30 m and most between 0 and 90 m, although one measurement is over 750 m.

THE MILL CREEK-STILLWATER FAULT ZONE

The Mill Creek-Stillwater fault zone was traced across the northwestern part of the Beartooth Mountains by Wilson (1936) from Mill Creek, a tributary of the Yellowstone River, to the West Fork of the Stillwater River (fig. 1). Authors since then, including Roberts (1972), and Jones, Peoples, and Howland (1960), have placed the eastern continuation of this fault somewhere south of the Stillwater Complex running from the West Fork of the Stillwater River to West Fishtail Creek. Jones, Peoples, and Howland (1960), following Wilson (1936), dashed its continuation up Flume Creek eastward through the saddle between Flume and Rocky Creeks and through Chrome Lake on the basis of the alinement of stream drainages. Although there is shearing and quartz veining in the saddle, first described by Wilson (1936) (coordinates: 493,160 N.; 1,917,220 E.), there is no evidence of faulting or shearing either east or west of the saddle where the Mill Creek-Stillwater fault is postulated to go. Neither Butler (1966), Page, Simons, and Dohrenwend (1973a, b), nor the present study could find evidence for a vertical fault of the type described by Wilson (1936) continuing farther east than where the Sioux Charley fault zone intersects the West Fork of the Stillwater River. Even

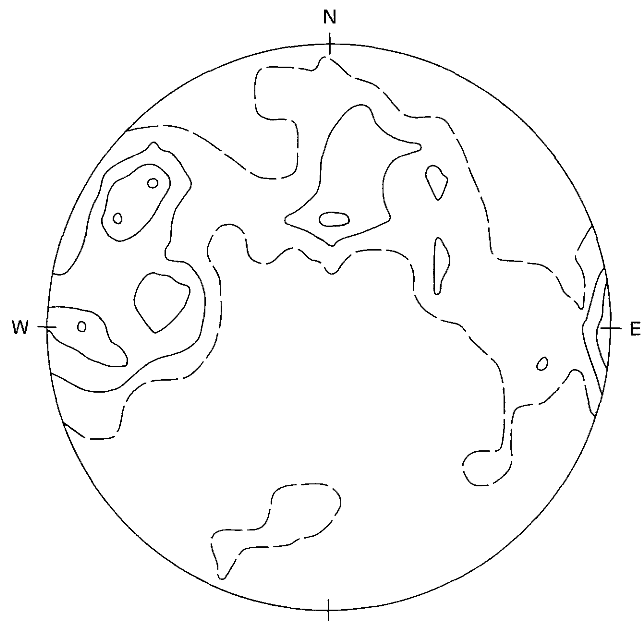

FIGURE 59.—Contoured poles to 201 measured fault planes. 201 points, counting area=0.019, E=3.92. See figure 30 for explanation.

Wilson (1936, p. 85) was not able to trace the fault across Saderbalm Creek (coordinates: 503,440 N.; 1,874,660 N.) and based the eastward continuation on the alinement of Flume Creek and an unnamed creek adjoining the Stillwater River at the Beartooth Ranch.

West from the Sioux Charley Lake fault zone on the west edge of the Mt. Wood quadrangle and in the Mt. Douglas quadrangle, the Mill Creek-Stillwater fault zone follows the valley of the West Fork of the Stillwater River and westward over the East Boulder Plateau where it juxtaposes regional metamorphic rocks and the magnesium- and iron-enriched metasedimentary rocks of the Stillwater thermal aureole. The fault also puts a syncline of Paleozoic and Mesozoic sediments in contact with the regional metamorphic rocks, suggesting that the upthrown side is on the south. Wilson (1936) estimated that on the East Boulder Plateau there was at least 366 m of stratigraphic throw on the fault zone. The Paleozoic and Mesozoic rocks in the fault zone suggest that there probably was movement on the fault in the Laramide orogeny. West from the Boulder River, the fault zone was traced by Wilson (1936) up Four Mile Creek, along the East Fork of Mill Creek, through Arrow Peak into the Yellowstone Valley where it either terminates or is offset by the Emigrant fault. Along the western extension the north side is upthrown, which led Wilson (1936) to describe the fault

[2]Strike separation and offset are used in the sense defined by Billings (1954, p. 136).

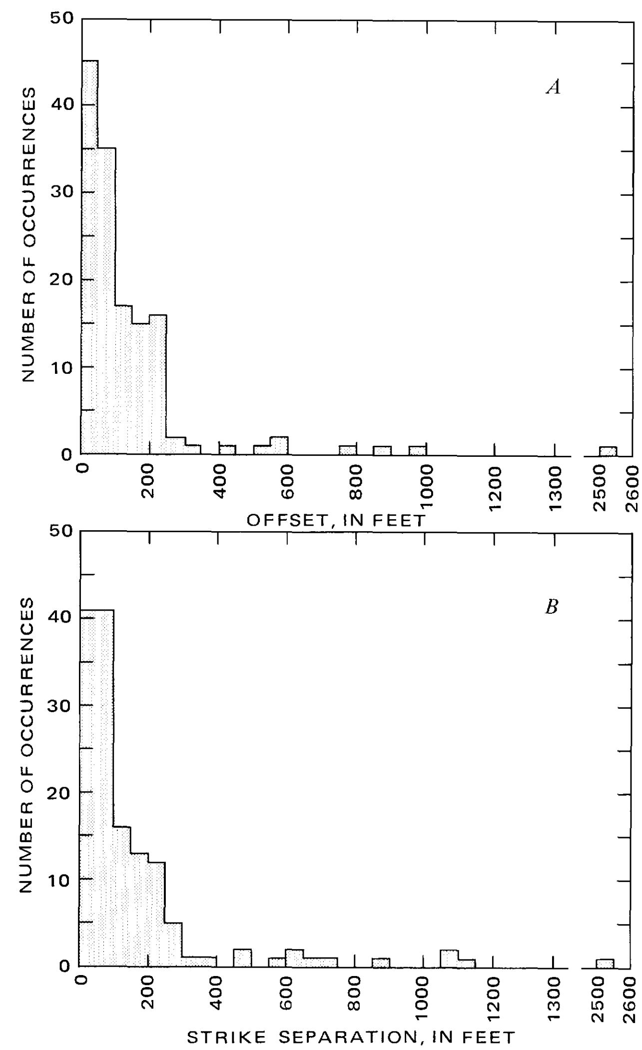

FIGURE 60.—Frequency of occurrence of measurable offset and strike separation for 142 faults on the 1:12,000-scale map of Page and Nokleberg (1974).

zone as having pivotal motion with the south block moving east relative to the north block.

We can speculate on where the Mill Creek-Stillwater fault zone may have continued east of Saderbalm Creek and how Laramide movement on it may have been distributed to the east. The fault zone, as a vertical one, ends on the Sioux Charley fault zone, but eastward there are a series of thrusts, including the Bluebird and Lake faults, that may have dissipated the movement on the Mill Creek-Stillwater fault zone. Both Jones, Peoples, and Howland (1960) and Butler (1966) suggested this interpretation in showing a split of the Mill Creek-Stillwater fault zone continuing as the Bluebird thrust. The alinement of hornfels pendants at the contact of the medium- and coarse-grained quartz monzonites on the northern ridge of Flume Creek suggests the possibility of an east-west preintrusion fault. The Mill Creek-Stillwater fault zone and the postulated preintrusion fault have comparable attitudes, which suggests to the author that the Mill Creek-Stillwater fault zone may have had an eastern extension and may be an extremely old (at least 2,750 m.y.) structure or structural zone. Such a structure would allow the juxtaposition of orogenic Beartooth regional metamorphic rocks with a fairly stable cratonal Stillwater block in the Precambrian and would act as a zone of crustal weakness in which to introduce the 2,750-m.y.-old quartz monzonite sequence between the two terrains. Laramide movement on the eastern extension would be limited by a fairly cohesive stable block that might then cause the movement to be taken up in-thrusting such as observed in the Mountain View area.

THE BLUEBIRD THRUST

Although used by Jones, Peoples, and Howland (1960) as the name of the thrust that runs fron Bluebird Ridge to the Stillwater River valley, the term Bluebird thrust is used here for the family of thrust faults that are found near the base of the Stillwater Complex both east and west of Bluebird Ridge. Mapping (Page and Nokleberg, 1974) has shown that the Bluebird thrust (in the strict sense) and an accompanying thrust south of it place a block of the Ultramafic zone northward up and over the Banded and Upper zones of the complex and emplace quartz monzonites up and over the Ultramafic zone (see cross section, fig. 48). The Bluebird fault appears to have its eastern ends in the Stillwater River valley. Westward from Bluebird Ridge, regional metamorphic rocks are thrust over the Ultramafic zone; only outcrops of the Bronzitite member could be found in the poorly exposed area east of the West Fork of the Stillwater River (coordinates: 504,870 N.; 1,876,560 E.). On the north side of the West Fork of the Stillwater River westward to the Crescent Creek area, the projection of the thrust is assumed to emplace hornfels northward up and over the lower part of the Stillwater Complex. From Crescent Creek westward to upper Forge Creek area, the thrust emplaces hornfels northward up and over the Basal zone of the complex. One member of the thrust emplaces quartz monzonite northward and over the hornfels (coordinates: 503,530 N.; 1,862,420 E.). In upper Forge Creek (coordinates: 522,060 N.; 1,842,810 E.), this system of thrusts seems to end on a fairly steep fault trending about N. 30° W.

Evidence for the westward continuation of the Bluebird thrust comes from (1) the low dip of the contact between the complex and the hornfels especially in the Crescent Creek area (coordinates: 505,000 N.; 1,866,980 E.), (2) the existence of windows through the upper plate in the Iron Mountain area (coordinates: 504,540 N.; 1,858,900 E.), (3) the existence of klippe in the Iron Mountain area (coordinates: 511,340 N.; 1,856,540 E.), (4) the lack of exposures of the Basal zone of the complex, and (5) drilling data in the Iron Mountain and Crescent Creek areas. Earlier workers probably mistook the float of a fine-grained diabase dike in the Iron Mountain area for the Basal zone, did not recognize the absence of the Basal zone in this area, and therefore did not interpret the contact as a fault. In drill core, the fault zone is marked by extensive shearing and alteration over at least a 50-m interval, and from the outcrop pattern and drill data the fault zone dips shallowly to the south. Both surface and subsurface information were used in constructing an interpretive cross section across the thrust in the Iron Mountain area (fig. 61).

Westward from the Stillwater-West Fork of the Stillwater River divide, the trace of this thrust system is not continuous but is offset on many transverse faults. These transverse faults occur in Cathedral Creek (coordinates: 507,350 N.; 1,882,630 E.), at the northward continuation of the Sioux Charley fault zone (coordinates: 504,480 N.; 1,877,860 E.), in the Crescent Creek area (coordinates: 506,880 N.; 1,864,080 E.), near Iron Mountain, on the east side of the East Boulder River (coordinates: 515,000 N.; 1,851,080 E.), and in Upper Forge Creek. The thrusting preceded the approximate north-south steep normal faulting.

INFERRED STILLWATER RIVER VALLEY FAULT

The mismatch of geologic contacts and faults between the west and east sides of the Stillwater River valley suggests the existence of a transverse fault (here named the Stillwater River valley fault) in the valley, which is now covered by extensive alluvial and glacial deposits. Figure 62 shows an interpretative geologic sketch map of the structural relations in the Stillwater River valley. The mismatch between projected structures and contacts, such as the Horseman thrust, the Lake-Nye Creek fault, and the thrust separating medium-grained quartz monzonite and granitic gneisses are clearly shown. All the separations between structures across the valley have the same sense in that the east side moved north relative to the west side. Yet all the structures show different amounts of separation by the inferred fault. The pattern of the thrust faults being offset by a trans-

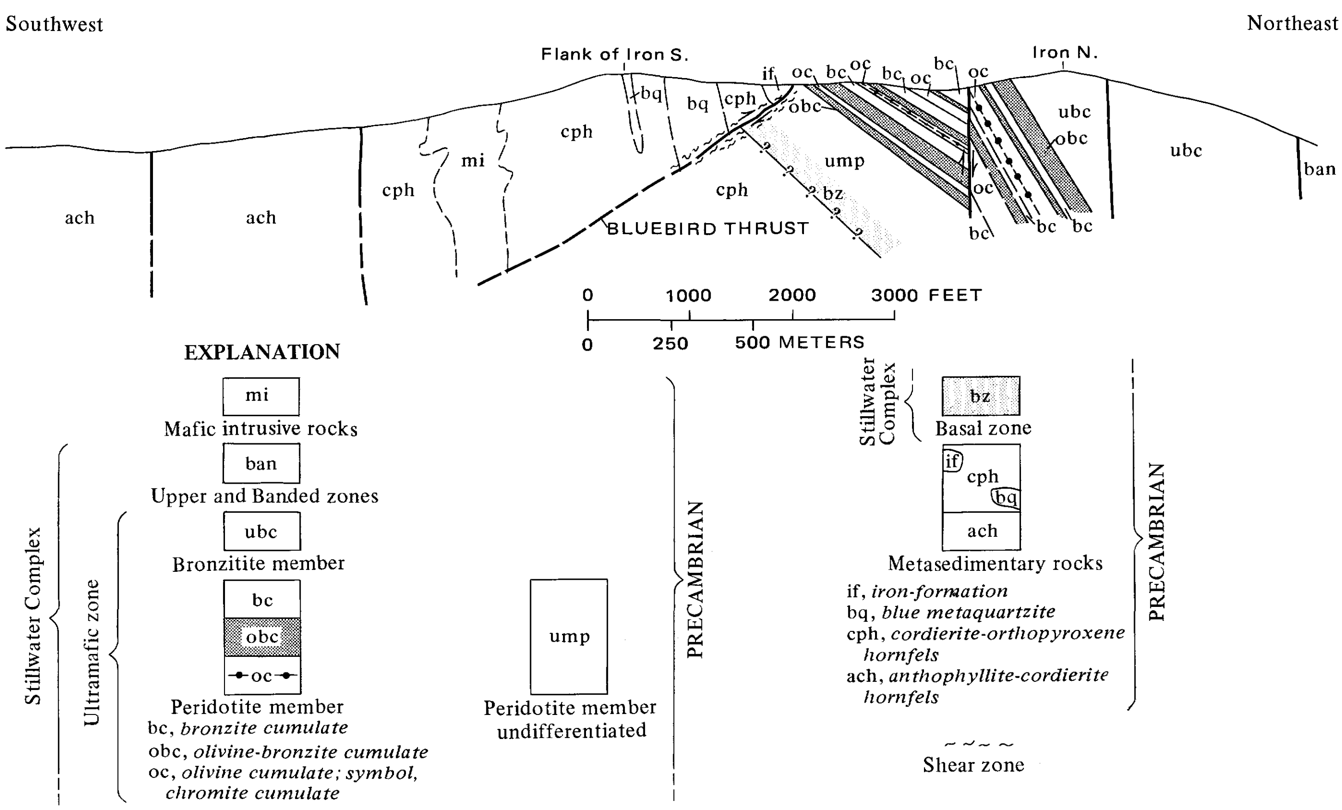

FIGURE 61.—Cross section of Bluebird thrust in the Iron Mountain area.

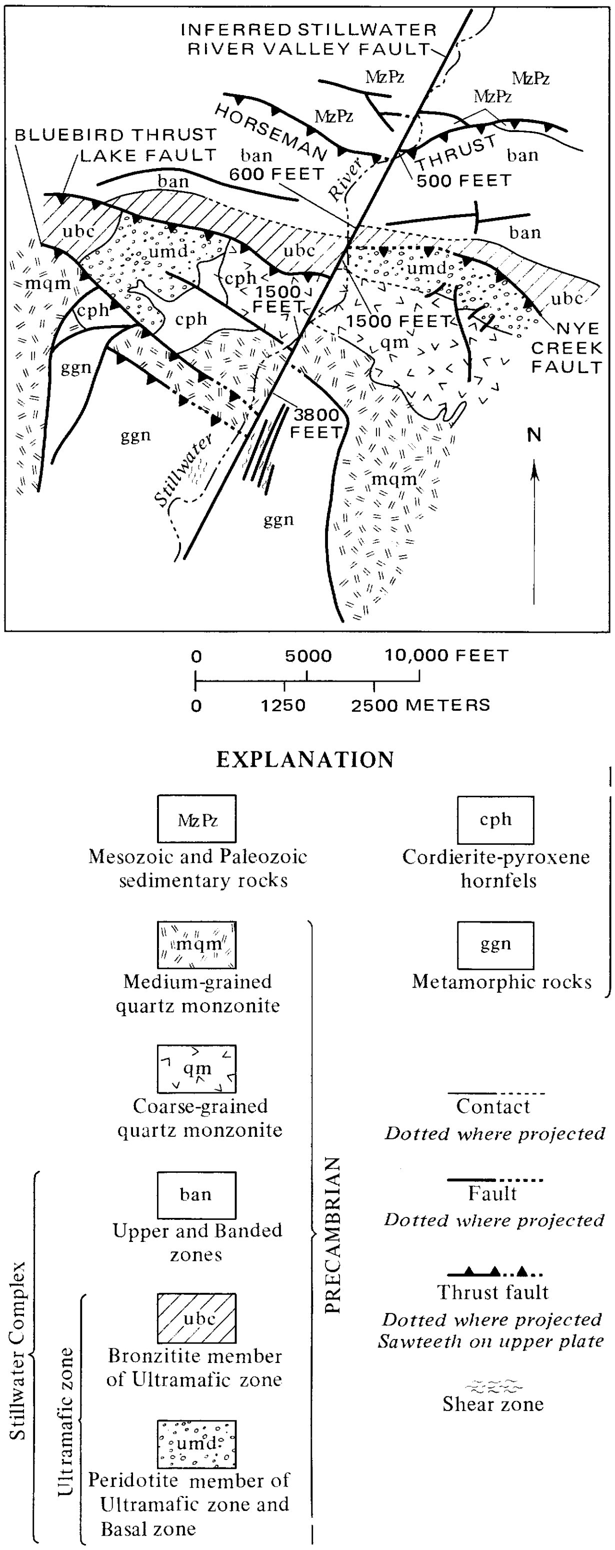

FIGURE 62.—Interpretative geologic sketch map of part of the Stillwater River valley showing structural relations and separation, in feet, along the inferred Stillwater River valley fault. Geology modified from Page, Simons, and Dohrenwend (1973a).

verse fault is consistent with other observations to the west of the area. In addition the projected Ultramafic-Banded zone contact shows a similar sense and magnitude of separation. As can be seen from figure 62, the amount of apparent separation along the fault is greatest in the southern part of the area and appears to die or decrease toward the north. The data suggest that the west side of the inferred fault is structurally higher relative to the east side. This is consistent with ideas that the coarse-grained quartz monzonite on Granite Ridge represents part of the quartz monzonite intrusion near its top and that the exposures along Flume Creek-Nye Basin ridge represent a slightly deeper level in the intrusion.

Other evidence for the fault in the Stillwater River valley includes extensive shearing and parallel minor faults east of the Beartooth Ranch (coordinates: 495,000 N.; 1,900,680 E.). Shear zones and joints parallel to the inferred valley fault are found (1) on Granite Ridge in the coarse-grained quartz monzonite (coordinates: 502,610 N.; 1,902,030 E.), (2) in granitic gneiss south of the Beartooth Ranch near the bridge crossing the Stillwater River (coordinates: 494,250 N.; 1,898,100 E.), and (3) in the plagioclase gneiss east of the Beartooth Ranch. The parallel faults, east of the Beartooth Ranch, trend northeast and dip between vertical and 50° both east and west. They are interpreted as steeply dipping normal faults. The inferred Stillwater River valley fault is probably a steep normal fault, the west side up relative to the east side, with a rotational component that resulted in greater separation along its southern part.

SIOUX CHARLEY LAKE FAULT ZONE

Several parallel, nearly vertical, northwest-striking faults form a fault zone that extends from Sioux Charley Lake (see the Mount Wood quadrangle) on the Stillwater River to the West Fork of the Stillwater River northeast of Saderbalm Creek and continues into the Banded and Upper zones of the complex; it is called the Sioux Charley Lake fault zone. This zone seems to terminate the Mill Creek-Stillwater fault zone. These faults are best shown on the map by Page, Simons, and Dohrenwend (1973a), and parts of them were first described by Butler (1966) who stated that these faults are associated with mylonites and altered rocks within the regional metamorphic rocks. Within the Stillwater Complex, however, they are marked by shear zones and serpentinite. One of the faults that juxtaposes the Bronzitite member against the Banded zone and shows at least 450 m of offset is fairly well exposed in the cliffs south of the West Fork (coordinates: 506,140 N.; 1,877,490 E.). Another parallel fault in Cathedral Creek, which offsets the Bluebird thrust (coordinates: 507,350 N.; 1,882,630 E.), probably continues northward across the West Fork of the Stillwater River, and although it could terminate against the Iron Creek fault, the fault probably offsets the Iron Creek fault. Offset on a transverse fault could explain the difficulty in identification of the Iron Creek fault east of the West Fork of the Stillwater River, as discussed by Jones, Peoples, and Howland (1960, p. 314).

FAULTS IN CRESCENT CREEK

Several northward-trending steeply dipping faults are found in the Crescent Creek area with an aggregate offset of the complex of more than 610 m. The result of this faulting was to move the Stillwater Complex northward on the west side of Crescent Creek. Some of the northward-trending structures offset the Bluebird thrust, but of more interest are the structures (for example, coordinates: 508,400 N.; 1,863,540 E.) that apparently do not offset the thrust. They offer some suggestion that rocks beneath the thrust have been affected by a set of prethrust transverse faults.

FAULT ON THE EAST SIDE OF THE EAST BOULDER RIVER

A major transverse fault occurs on the east side of the East Boulder River (coordinates: 515,000 N.; 1,851,080 E.) that has about 600–1,200 m of offset along it. The northward extension of this fault probably continues parallel to or in the East Boulder Valley. If it does continue northward, the projections of the Iron Creek and Brownlee Creek faults would not connect, as suggested by Jones, Peoples, and Howland (1960), and may represent offset segments of the same northeast-dipping fault.

JOINTS

Although joints are common throughout the area of the Stillwater Complex, they were not systematically studied except in the Verdigris Creek part of the Mountain View area. Within this area attitudes of 62 joints were measured. The results of contouring poles to these joints are shown in figure 63. The average joint plane strikes about N. 8° W. and dips about 87° NE. Comparison of this pattern with the S_3 axial plane fabric (fig. 36) or with the fault pattern (fig. 59) shows many similarities, and it is difficult to decide which feature more closely correlates with the joint pattern.

SUMMARY OF STRUCTURAL HISTORY

Structural development and history in the Stillwater Complex area falls naturally into two distinct time periods, Precambrian and Laramide. The present attitude and position of most rock units were finalized in the Laramide orogeny, but a large part of the intricate folding developed in Precambrian time. The intrusive quartz monzonites (≈2,750 m.y.) are important to the history of the Precambrian because they separate the development of folding of the hornfelsed metasedimentary rocks and intrusion of the Stillwater Complex from a penetrative deformation in the younger Precambrian. These siliceous intrusive rocks also separate the terrane north of the Mill Creek-Stillwater fault zone, here called the Stillwater block, from the terrane south of the fault zone, here called the Beartooth block (see fig. 1).

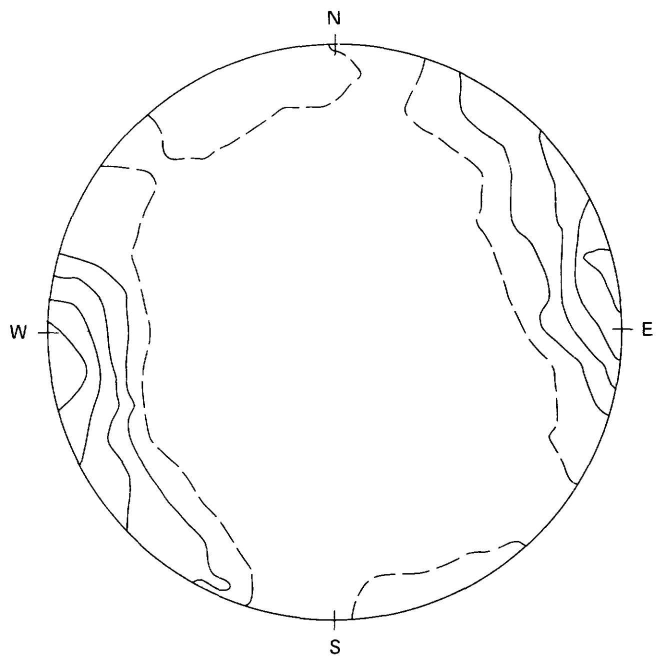

FIGURE 63.—Contoured poles to joint planes from the Verdigris Creek part of the Mountain View area. 62 points, counting area=0.061, E=3.76. See figure 30 for explanation.

A diagrammatic summary of the structural events in the major lithologic units is given in figure 64. At least two and possibly three sets of folds were developed in the metasedimentary rocks prior to the intrusion of the Stillwater Complex. The latest folds, broad warps (F_2), have northwest-plunging fold axes and north-striking, eastward-dipping axial planes. The original orientation of the fold axes and axial planes of F_1, open isoclinal folds, cannot be defined because they were rotated about the F_2 folds. Most open isoclinal folds that were observed have axes plunging northeast and axial planes striking northeast. A deformation event before the open isoclinal folding probably formed the few intrafolial folds, but

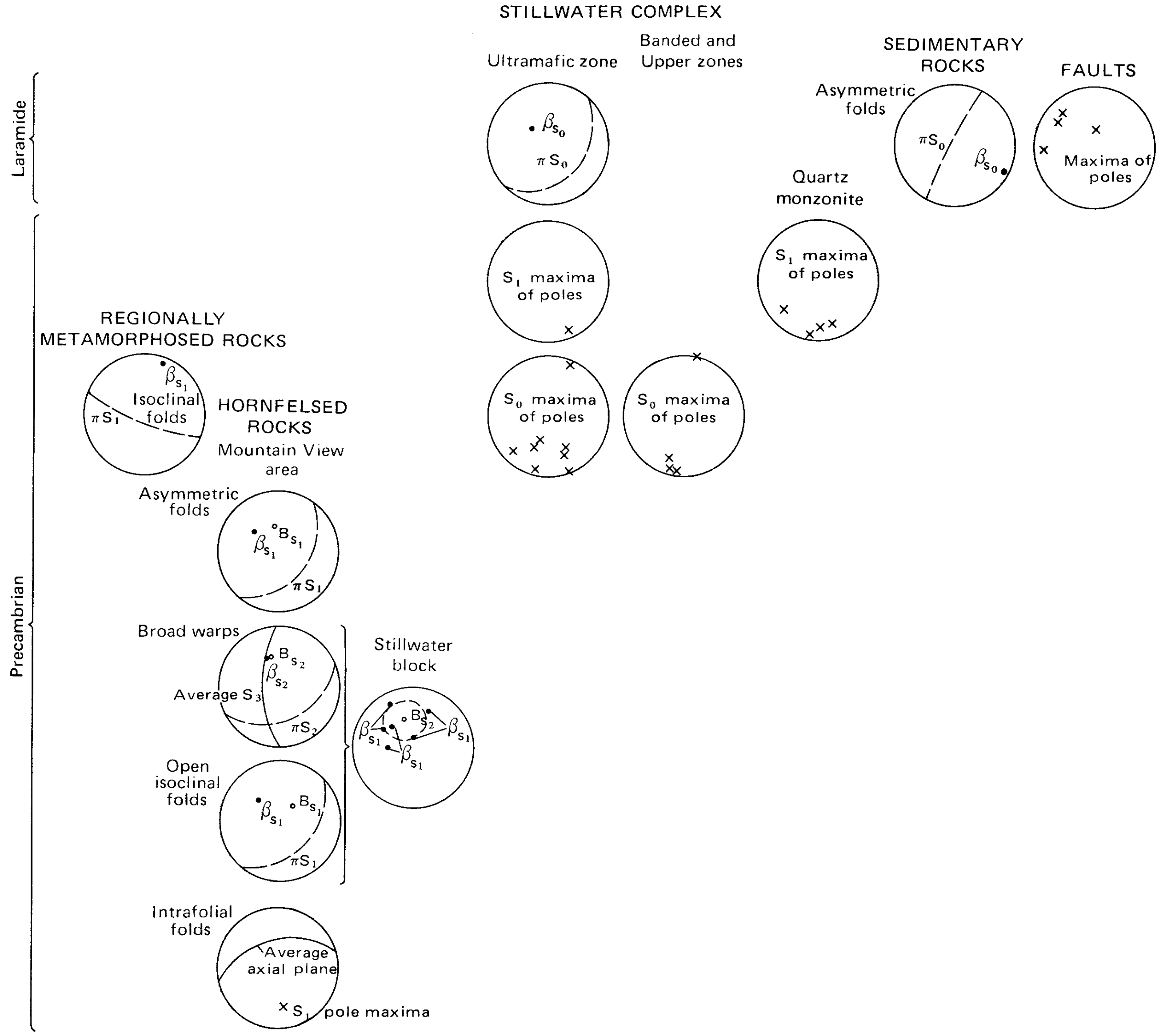

FIGURE 64.—Summary of structural events in the Stillwater block. Structures plotted on lower hemisphere nets summarize previously presented data. See text for explanation.

because of the limited data on these structures, they have not been assigned to a fold generation. The asymmetric folds in the hornfels seem to have similar attitudes to the open isoclinal folds and are probably related to the event.

The Stillwater Complex intruded the folded metasedimentary rocks and formed virtually horizontal layers of cumulates. The present northward tilt of cumulate layering and lamination was caused by late Precambrian and Laramide orogenies. In the late Precambrian, a penetrative presently steeply dipping east-west-trending foliation was developed in the Stillwater Complex. This metamorphic foliation has the same attitude as the foliation observed in the intrusive quartz monzonites.

During Laramide time folding, faulting, and tilting were dominant processes. Asymmetric folds with shallowing, southeast-plunging axes were developed in the Paleozoic and Mesozoic sedimentary rocks. These folds probably developed in response to southward and northward thrusting along northwest-striking faults. Folds were formed at the Mountain View area in the Ultramafic zone as a result of compression between two thrusts. Most if not all the thrust and transverse faults were either formed during the Laramide orogeny or were Precambrian structures reactivated during the Laramide orogeny in order to tilt and place the Stillwater block into its present attitude.

SUMMARY OF GEOLOGIC HISTORY OF THE STILLWATER AREA

Any discussion of geologic history that concentrates on the older Precambrian should be considered highly interpretative because the evidence upon which it is based is extremely fragmentary. Most of the events within the Stillwater block, before the intrusion of the quartz monzonites 2,750 m.y. ago, may have occurred in an area many miles removed from the other structural blocks. After the intrusion of the quartz monzonite all the events that have affected the Beartooth block should also have affected the Stillwater block.

Sometime before 3,140 m.y. ago, a source area existed for the sediments that are now hornfels, and a basin or basins in which they were deposited formed. The source area probably contained abundant exposures of mafic and ultramafic rocks that, when weathered, could produce the high contents of magnesium, iron, nickel, and chromium observed as compositional components of the hornfels. Siliceous rocks must have also been present in the area as a source for the relict clastic quartz, feldspar, and rock fragments found in the hornfels. The probability of a mixed clastic and chemical precipitate origin of these rocks and the presence of iron-formation and metaquartzite (possibly chert?) suggest that the basin of deposition may have at times been of a very local nature. Sedimentary structures in the hornfels imply deposition under water, and the fine scale of the sedimentary features may imply a high-energy environment such as a surf zone or turbidite environment for part of the sedimentation. The fairly extensive, although thinly interbedded diamictite may indicate some local glaciation.

Probably soon after deposition, these rocks were isoclinally folded and then refolded by broad warps along northwest-plunging axes. Previous to or at this time they may have been subjected to low-grade metamorphism. After folding, the rocks were intruded by the Stillwater magma, which cooled and crystallized in a nonorogenic environment, as evidenced by the continuously traceable thin cumulate layers. The complex may have been intruded either in a fault zone or along an unconformity because its eastern part cuts out some of the stratigraphy recognized in the western exposures of hornfels. Heat from the cooling and crystallizing complex produced a metamorphic aureole in the folded sediments. In the early stages of cooling, that is during the time represented by the Basal zone, there probably was minor tectonism that caused some of the irregularities in the basement contact. Before or immediately after intrusion of the complex, some mafic dikes and sills were intruded into the metasedimentary rocks.

No evidence for either structural features or metamorphic features formed during the 2,750-m.y. event in the North Snowy block or in the Beartooth block is found within the Stillwater block (see fig. 1). The contact zone between the Stillwater block and the Beartooth block is occupied by intrusive quartz monzonites about 2,750 m.y. old, which suggests that the Stillwater block moved into its present position before the intrusion of quartz monzonite and after the peak of deformation and metamorphism in the Beartooth block. The Stillwater block probably moved along wrench faults similar to those now marked by the Mill Creek–Stillwater fault zone and the West Boulder fault. After the positioning of the Stillwater block, the complex and the hornfels were intruded by a sequence of quartz monzonites with the accompanied metamorphic effects.

Between 1,600 and 1,800 m.y. ago the Stillwater and surrounding blocks were involved in a weak low-grade regional metamorphic event, and a penetrative foliation developed. This event is documented in the southern Beartooth Mountains by Rowan and Mueller (1971) and by McMannis, Palmquist, and Reid (1971a, b, c) in the North Snowy block. At about the same time or possibly after the event, more mafic dikes and sills were emplaced throughout the region.

By Middle Cambrian time, faulting had elevated, and erosion exposed the upper part of the complex. The complex was also slightly deformed and tilted northward. Elsewhere in the Beartooth Mountains, the Flathead Sandstone lies unconformably on the Precambrian basement, but it is absent over the Stillwater Complex. This implies that the complex formed a topographic high at the beginning of Cambrian sedimentation (Jones and others, 1960).

REFERENCES CITED

Armbrustmacher, T. J., and Banks, N. G., 1974, Clouded plagioclase in metadolerite dikes, southeastern Bighorn Mountains, Wyoming: Am. Mineralogist, v. 59, nos. 7-8, p. 656-665.

Bateman, P. C., Clark, L. D., Huber, N. K., Moore, J. G., and Rinehart, C. D., 1963, The Sierra Nevada batholith, a synthesis of recent work across the central part: U.S. Geol. Survey Prof. Paper 414-D, 46 p.

Beltrame, R. J., 1972, Petrography and chemistry of metasedimentary rocks at the base of the Stillwater Complex, Montana: Cincinnati Univ., Cincinnati, Ohio, M.S. thesis, 106 p.

Bentley, R. D., 1966, Regional distribution of amphibolites in the southeastern Beartooth Mountains, Montana and Wyoming [abs.]: Geol. Soc. America, Ann. Mtg., San Francisco, Calif., 1966, Program, p. 14-15.

Billings, M. P., 1954, Structural geology [2nd ed.]: Englewood Cliffs, N.J., Prentice-Hall, Inc., 514 p.

Brookins, D. G., 1969, Rb-Sr and K-Ar age determinations from the Precambrian rocks of the Jardine-Crevice Mountains area, southwestern Montana: Earth Sci. Bull., v. 1, no. 2, 5-9.

Butler, J. R., 1966, Geologic evolution of the Beartooth Mountains, Montana and Wyoming—Pt. 6, Cathedral Peak area, Montana: Geol. Soc. America Bull., v. 77, no. 1, p. 45-64.

——1969, Origin of Precambrian granitic gneiss in the Beartooth Mountains, Montana and Wyoming, *in* Igneous and metamorphic geology: Geol. Soc. America Mem. 115, p. 73-101.

Calvert, W. R., 1916, Geology of the Upper Stillwater Basin, Stillwater and Carbon Counties, Montana, with special reference to coal and oil: U.S. Geol. Survey Bull. 641-G, p. 199-214.

Casella, C. J., 1964, Geologic evolution of the Beartooth Mountains, Montana and Wyoming—Pt. 4, Relationship between Precambrian and Laramide structures in the Line Creek area: Geol. Soc. America Bull., v. 75, p. 969-986.

——1969, A review of the Precambrian geology of the eastern Beartooth Mountains, Montana and Wyoming, *in* Igneous and metamorphic geology: Geol. Soc. America Mem. 115, p. 53-71.

Catanzaro, E. J., and Kulp, J. L., 1964, Discordant zircons from the Little Belt (Montana), Beartooth (Montana), and Santa Catalina (Arizona) Mountains: Geochim. et Cosmochim. Acta, v. 28, p. 87-124.

Clarke, F. W., and Washington, H. S., 1924, The composition of the earth's crust: U.S. Geol. Survey Prof. Paper 127, 117 p.

Condie, K. C., 1967, Geochemistry of early Precambrian graywackes from Wyoming: Geochim. et Cosmochim. Acta, v. 31, no. 11, p. 2135-2150.

Condie, K. C., Macke, J. E., and Reimer, T. O., 1970, Petrology and geochemistry of early Precambrian graywackes from the Fig Tree Group, South Africa: Geol. Soc. America Bull., v. 81, p. 2759-2776.

Cornwall, H. R., 1966, Nickel deposits of North America: U.S. Geol. Survey Bull. 1223, 62 p.

Danchin, R. V., 1967, Chromium and nickel in the Fig Tree Shale from South Africa: Science, v. 158, p. 261-262.

Dayton, Stan, 1971, Hot air over Stillwater, profile of a hearing on mineral entry: Eng. and Mining Jour., v. 172, no. 10, p. 75-84.

Deer, W. A., Howie, R. A., and Zussman, J., 1962, Rock-forming minerals—Vol. 1, Ortho- and ring silicates: New York, John Wiley and Sons, 333 p.

Eckelmann, F. D., and Poldervaart, Arie, 1957, Geologic evolution of the Beartooth Mountains, Montana and Wyoming—Pt. 1, Archean history of the Quad Creek area: Geol. Soc. America Bull., v. 68, p. 1225-1261.

Evans, B. W., 1965, Application of a reaction-rate method to the breakdown equilibria of muscovite and muscovite plus quartz: Am. Jour. Sci., v. 263, p. 647-667.

Evans, H. T., Jr., Appleman, D. E., and Handwerker, D. S., 1963, The least squares refinement of crystal unit cells with powder diffraction data by an automatic computer indexing method [abs.]: Am. Cryst. Assoc., Ann. Mtg., Cambridge, Mass., Program, p. 42-43.

Fenton, M. D., and Faure, G., 1969, The age of the igneous rocks of the Stillwater Complex of Montana: Geol. Soc. America Bull., v. 80, p. 1599-1604.

Foose, R. M., Wise, D. V., and Garbarini, G. S., 1961, Structural geology of the Beartooth Mountains, Montana and Wyoming: Geol. Soc. America Bull., v. 72, p. 1143-1172.

Gast, P. W., Kulp, J. L., and Long, L. E., 1958, Absolute age of early Precambrian rocks in the Bighorn Basin of Wyoming and Montana, and southeastern Manitoba: Am. Geophys. Union Trans., v. 39, p. 322-334.

Giletti, B. P., 1966, Isotopic ages from southwestern Montana: Jour. Geophys. Research, v. 71, no. 16, p. 4029-4036.

Greenwood, H. J., 1963, The synthesis and stability of anthophyllite: Jour. Petrology, v. 4, p. 317-351.

Hambleton, W. W., 1947, A petrofabric study of layering in the Stillwater Complex, Montana: Evanston and Chicago, Ill., Northwestern Univ., M.S. thesis, 62 p.

Harris, R. L., Jr., 1959, Geologic evolution of the Beartooth Mountains, Montana and Wyoming—Pt. 3, Gardner Lake area, Wyoming: Geol. Soc. America Bull., v. 70, p. 1185-1216.

Harwood, D. S., and Larson, R. R., 1969, Variation in the delta index of cordierite around the Cupsuptic pluton, west-central Maine: Am. Mineralogist, v. 54, p. 896-908.

Hensen, B. J., and Green, D. H., 1971, Experimental study of the stability of cordierite and garnet in pelitic compositions at high pressures and temperatures—I. Compositions with excess aluminosilicate: Contr. Mineralogy and Petrology, v. 33, p. 309-330.

Hess, H. H., 1938a, A primary peridotite magma: Am. Jour. Sci., 5th ser., v. 35, no. 209, p. 231-344.

——1938b, Primary banding in norite and gabbro: Am. Geophys. Union Trans., 19th Ann. Mtg., Pt. 1, p. 264-268.

——1939, Extreme fractional crystallization of a basaltic magma—The Stillwater igneous complex [abs.]: Am. Geophys. Union Trans., 20th Ann. Mtg., Pt. 3, p. 430-432.

——1940, An assay review—The petrology of the Skaergaard intrusion Kangerdlugsuag, East Greenland: Am. Jour. Sci., v. 238, p. 372-378.

——1941, Pyroxenes of common mafic magmas: Am. Mineralogist, v. 26, pt. 1, no. 9, p. 515-535; pt. 2, no. 10, p. 573-594.

——1949, Chemical composition and optical properties of common clinopyroxenes, pt. 1: Am. Mineralogist, v. 34, p. 621-666.

——1960, Stillwater igneous complex, Montana—a quantitative mineralogical study: Geol. Soc. America Mem. 80, 230 p.

Hess, H. H., and Phillips, A. H., 1938, Orthopyroxenes of the Bushveld type: Am. Mineralogist, v. 23, p. 450-456.

——1940, Optical properties and chemical composition of magnesian orthopyroxenes: Am. Mineralogist, v. 25, p. 271-285.

Hess, P. C., 1969, The metamorphic paragenesis of cordierite in pelitic rocks: Contr. Mineralogy and Petrology, v. 24, p. 191-207

Himmelberg, G. R., and Jackson, E. D., 1967, X-ray determinative curve for some orthopyroxenes of composition Mg_{48-85} from the Stillwater Complex, Montana, *in* Geological Survey research, 1967: U.S. Geol. Survey Prof. Paper 575-B, p. B101-B102.

Howland, A. L., 1933, Sulphides and metamorphic rocks at the base of the Stillwater Complex, Montana: Princeton Univ., Princeton, N. J., Ph.D. thesis, 76 p.

——1954, Relations of regional and thermal metamorphism near the base of the Stillwater complex, Montana [abs.]: Geol. Soc. America Bull., v. 65, p. 1264-1265.

——1955, Chromite deposits in the central part of the Stillwater complex, Montana: U.S. Geol. Survey Bull. 1015-D, p. 99-121.

Howland, A. L., Garrels, E. M., and Jones, W. R., 1949, Chromite deposits of Boulder River area, Sweetgrass County, Montana: U.S. Geol. Survey Bull. 948-C, p. 63-82.

Howland, A. L., Peoples, J. W., and Sampson, Edward, 1936, The Stillwater igneous complex and associated occurrences of nickel and platinum metals: Montana Bur. Mines and Geology Misc. Contr., v. 7, 15 p.

Iiyama, Toshimichi, 1956, Optical properties and unit cell dimensions of cordierite and indialite: Mineral. Jour. (Sapporo, Japan), v. 1, p. 372-394.

Irvine, T. N., 1970, Crystallization sequences in the Muskox intrusion and other layered intrusions—I. Olivine-pyroxene-plagioclase relations: Geol. Soc. South Africa, Spec. Pub. 1, p. 441-476.

Jackson, E. D., 1960, X-ray determinative curve for natural olivine of composition Fo_{80-90}, *in* Geological Survey research, 1960: U.S. Geol. Survey Prof. Paper 400-B, p. B432-B434.

———1961, Primary textures and mineral associations in the ultramafic zone of the Stillwater Complex, Montana: U.S. Geol. Survey Prof. Paper 358, 106 p.

———1963, Stratigraphic and lateral variation of chromite composition in the Stillwater Complex: Mineral. Soc. America Spec. Paper 1, p. 46-54.

———1967, Ultramafic cumulates in the Stillwater, Great Dyke, and Bushveld intrusions, *in* Wyllie, P. J., ed., Ultramafic and related rocks: New York, John Wiley and Sons, p. 20-38.

———1968, The chromite deposits of the Stillwater Complex, Montana, *in* Ore deposits of the United States, 1933-1967 (Graton-Sales Volume), V. 2: New York, Am Inst. Mining, Metall., and Petroleum Engineers, p. 1495-1510.

———1969, Chemical variation in coexisting chromite and olivine in chromite zones of the Stillwater Complex, *in* Magmatic ore deposits, a symposium: Econ. Geology Mon. 4, p. 41-71.

———1970, The cyclic unit in layered intrusions———A comparison of repetitive stratigraphy in the ultramafic parts of the Stillwater, Muskox, Great Dyke, and Bushveld Complexes: Geol. Soc. South Africa, Spec. Pub. 1, p. 391-424.

———1971, The origin of ultramafic rocks by cumulus processes: Fortschr. Mineralogie, v. 48, p. 128-174.

Jackson, E. D., Howland, A. L., Peoples, J. W., and Jones, W. R., 1954, Geologic maps and sections of the eastern part of the Stillwater Complex in Stillwater County, Montana: U.S. Geol. Survey open-file report.

Jackson, E. D., Stevens, R. E., and Bowen, R. W., 1967, A computer-based procedure for deriving mineral formulas from mineral analyses, *in* Geological Survey research, 1967: U.S. Geol. Survey Prof. Paper 575-C, p. C23-C31.

Jaeger, J. C., 1959, The temperature in the neighborhood of a cooling intrusive sheet: Am. Jour. Sci., v. 255, p. 306-318.

James, H. L., 1946, Chromite deposits near Red Lodge, Carbon County, Montana: U.S. Geol. Survey Bull. 945-F, p. 151-189.

———1966, Chemistry of the iron-rich sedimentary rocks, Chap. W, *in* Data of geochemistry [6th ed.]: U.S. Geol. Survey Prof. Paper 440-W, 60 p.

James, H. L., Dutton, C. E., Pettijohn, F. J., and Wier, K. L., 1968, Geology and ore deposits of the Iron River-Crystal Falls district, Iron County, Michigan: U.S. Geol. Survey Paper 570, 134 p.

Jones, W. R., Peoples, J. W., and Howland, A. L., 1960, Igneous and tectonic structures of the Stillwater Complex, Montana: U.S. Geol. Survey Bull. 1071-H, p. 281-340.

Kamb, W. B., 1959, Ice petrofabric observations from Blue Glacier, Washington, in relation to theory and experiment: Jour. Geophys. Research, v. 64, no. 11, p. 1891-1909.

Kistler, R. W., Obradovich, J. D., and Jackson, E. D., 1969, Isotopic ages of rocks and minerals from the Stillwater Complex, Montana: Jour. Geophys. Research, v. 74, p. 3226-3237.

LaFountain, L. J., 1971, The origin of amphibolites by discriminant function analysis [abs.]: Geol. Soc. America, Abstracts with Programs, v. 3, no. 6, p. 391.

Larsen, L. H., Poldervaart, Arie, Kirchmayer, Martin, 1966, Geologic evolution of the Beartooth Mountains, Montana and Wyoming—Pt. 7, Structural homogeneity of gneisses in the Lonesome Mountain area: Geol. Soc. America Bull., v. 77, p. 1277-1291.

Leonard, B. F., Desborough, G. A., and Page, N. J , 1969, Ore microscopy and chemical composition of some laurites: Am. Mineralogist, v. 54, p. 1330-1346.

McMannis, W. J., Palmquist, J. C., and Reid, R. R., 1971a, Origin of gneisses in North Snowy block, Beartooth Mountains, Montana [abs.]: Geol. Soc. America, Abs. with Programs, v. 3, no. 6, p. 395.

———1971b, Precambrian geologic history, North Snowy block, northwestern Beartooth Mountains, Montana [abs.]: Geol. Soc. America, Abs. with Programs, v. 3, no. 6, p. 394.

———1971c, Structural evolution of the North Snowy block, Beartooth Mountains, Montana [abs.]: Geol. Soc. America, Abs. with Programs, v. 3, no. 6, p. 395-396.

Mason, B. H., 1958, Principles of geochemistry [2nd ed.]: New York, John Wiley and Sons, 310 p.

Miyashiro, Akiho, 1957, Cordierite-indialite relations: Am. Jour. Sci., v. 255, p. 43-62.

———1961, Evolution of metamorphic belts: Jour. Petrology, v. 2, p. 277-311.

Miyashiro, Akiho, Iiyama, Toshimichi, Yamasaki, Masao, and Miyashiro, Tami, 1955, The polymorphism of cordierite and indialite: Am. Jour. Sci., v. 253, p. 185-208.

Mueller, P. A., 1971, Geochemistry and geochronology of the mafic rocks of the Southern Beartooth Mountains, Montana and Wyoming: Rice Univ., Houston, Tex., Ph.D. thesis, 58 p.

Nanz, R. H., 1953, Chemical compositions of pre-Cambrian slates with notes on the geochemical evolution of lutites: Jour. Geology, v. 61, p. 51-64.

Naqvi, S. M., and Hussain, S. M., 1972, Petrochemistry of early Precambrian metasediments from the central part of the Chitaldrug schist belt, Mysore, India: Chem. Geology, v. 10, no. 2, p. 109-135.

Nunes, P. D., and Tilton, G. R., 1971, Uranium-lead ages of minerals from the Stillwater Igneous Complex and associated rocks, Montana: Geol. Soc. America Bull., v. 82, no. 8, p. 2231-2250.

Page, N. J, 1971a, Comments on the role of oxygen fugacity in the formation of immiscible sulfide liquids in the H chromitite zone of the Stillwater Complex, Montana: Econ. Geology, v. 66, no. 4, p. 607-610.

———1971b, Sulfide minerals in the G and H chromitite zones of the Stillwater Complex, Montana: U.S. Geol. Survey Prof. Paper 694, 20 p.

———1972, Pentlandite and pyrrhotite from the Stillwater Complex, Montana—iron-nickel ratios as a function of associated minerals: Econ. Geology, v. 67, p. 814-820.

Page, N. J, Clark, A. L., Desborough, G. A., and Parker, R. L., 1973, Platinum-group metals, *in* Brobst, D. A., and Pratt, W. P., eds., United States mineral resources: U.S. Geol. Survey Prof. Paper 820, p. 537-545.

Page, N. J, and Dohrenwend, J. C., 1973, Mineral resources potential of the Stillwater Complex and adjacent rocks in the northern part of the Mount Wood and Mount Douglas quadrangles, southwestern Montana: U.S. Geol. Survey Circ. 684, 9 p.

Page, N. J, and Jackson, E. D., 1967, Preliminary report on sulfide and platinum-group minerals in the chromitites of the Stillwater Complex, Montana, *in* Geological Survey research, 1967: U.S. Geol. Survey Prof. Paper 575-D, p. D123-D126.

Page, N. J, and Koski, R. A., 1973, Precambrian diamictite below the base of the Stillwater Complex, southwestern Montana: U.S. Geol. Survey Jour. Research, v. 1, no. 4, p. 403-414.

Page, N. J, and Nokleberg, W. J., 1970a, A suite of granitic intrusive rocks below the base of the Stillwater Complex, Mount Wood quadrangle, Montana [abs.]: Geol. Soc. America, Abs. with Programs, v. 2, no. 5, p. 342.

——1970b, Preliminary geologic map of the Stillwater Complex, Montana: U.S. Geol. Survey open-file report.

——1972, Genesis of mesozonal granitic rocks below the base of the Stillwater Complex, in the Beartooth Mountains, Montana, *in* Geological Survey research, 1972: U.S. Geol. Survey Prof. Paper 800-D, p. D127-D141.

——1974, Geologic map of the Stillwater Complex, Montana: U.S. Geol. Survey Misc. Inv. Map I-797, 5 sheets, scale 1:12,000.

Page, N. J, Riley, L. B., and Haffty, Joseph, 1969, Platinum, palladium, and rhodium analyses of ultramafic and mafic rocks from the Stillwater Complex, Montana: U.S. Geol. Survey Circ. 624, 12 p.

——1971, Lateral and vertical variation of platinum, palladium, and rhodium in the Stillwater Complex, Montana: Geol. Soc. America, Abs. with Programs, v. 3, no. 6, p. 401.

——1972, Vertical and lateral variation of platinum, palladium, and rhodium in the Stillwater Complex, Montana: Econ. Geology, v. 67, no. 7, p. 915-924.

Page, N. J, Shimek, Richard, and Huffman, Claude, Jr., 1972, Grain-size variations within an olivine cumulate, Stillwater Complex, Montana, *in* Geological Survey research, 1972: U.S. Geol. Survey Prof. Paper 800-C, p. C29-C37.

Page, N. J, Simons, F. S., and Dohrenwend, J. C., 1973a, Reconnaissance geologic map of the Mount Douglas quadrangle, Montana: U.S. Geol. Survey Misc. Field Studies Map MF-488.

——1973b, Reconnaissance geologic map of the Mount Wood quadrangle, Montana: U.S. Geol. Survey Misc. Field Studies Map MF-491.

Pardee, J. T., 1947, Late Cenozoic faulting in Montana [abs.]: Geol. Soc. America Bull., v. 58, p. 1215.

Peoples, J. W., 1932, The geology of the Stillwater igneous complex: Princeton Univ., Princeton, N. J., Ph. D. thesis, 180 p.

——1933, The Stillwater igneous complex, Montana: Am. Mineralogist, v. 18, p. 117.

——1936, Gravity stratification as a criterion in the interpretation of the structure of the Stillwater complex, Montana: Internat. Geol. Cong., 16th, 1933, Rept., v. 1, p. 353-360.

Peoples, J. W., and Howland, A. L., 1940, Chromite deposits of the eastern part of the Stillwater complex, Stillwater County, Montana: U.S. Geol. Survey Bull. 922-N, p. 371-416.

Peoples, J. W., Howland, A. L., Jones, W. R., and Flint, Delos, 1954, Geologic map, sections, and map of underground workings of the Mountain View Lake area, Stillwater County, Montana: U.S. Geol. Survey open-file report.

Pettijohn, F. J., 1957, Sedimentary rocks [2nd ed.]: New York, Harper and Bros., 718 p.

——1963, Chemical composition of sandstones—excluding carbonate and volcanic sands, Chap. S, *in* Data of geochemistry [6th ed.]: U.S. Geol. Survey Prof. Paper 440-S, 21 p.

Poldervaart, Arie, and Bentley, R. D., 1958, Precambrian and later evolution of the Beartooth Mountains, Montana and Wyoming, *in* Billings Geol. Soc., Guidebook, 9th Ann. Field Conference: p. 7-15.

Powell, J. L., Skinner, W. R., and Walker, David, 1969, Whole-rock Rb-Sr age of metasedimentary rocks below the Stillwater Complex, Montana: Geol. Soc. America Bull., v. 80, p. 1605-1612.

Prinz, Martin, 1964, Geologic evolution of the Beartooth Mountains, Montana and Wyoming—Pt. 5, Mafic dike swarms of the southern Beartooth Mountains: Geol. Soc. America Bull., v. 75, p. 1217-1245.

Read, H. H., 1952, Metamorphism and migmatisation in Ythan Valley, Aberdenshire: Edinburgh Geol. Soc. Trans., v. 15, p. 265-279.

Reinhardt, E. W., 1968, Phase relations in cordierite-bearing gneisses from the Gananoque area, Ontario: Canadian Jour. Earth Sci., v. 5, p. 455-482.

Richards, P. W., 1952, Structural geology of the Crazy Mountain Syncline-Beartooth Mountains border east of Livingston, Montana: Cornell Univ., New York, N. Y., Ph. D thesis.

——1958, Geology of the area east and southeast of Livingston, Park County, Montana: U.S. Geol. Survey Bull. 1021-L, p. 385-438.

Richardson, S. W., 1968, Staurolite stability in a part of the system Fe-Al-Si-O-H: Jour. Petrology, v. 9, no. 3, p. 467-488.

Roberts, A. E., 1972, Cretaceous and early Tertiary depositional and tectonic history of the Livingston area, southwestern Montana: U.S. Geol. Survey Prof. Paper 526-C, 102 p.

Rouse, J. T., Hess, H. H., Foote, Freeman, Vhay, J. S., and Wilson, K. P., 1937, Petrology, structure, and relation to tectonics of porphyry intrusions in the Beartooth Mountains, Montana: Jour. Geology, v. 45, p. 717-740.

Rowan, L. C., 1969, Structural geology of the Quad-Wyoming-Line Creeks area, Beartooth Mountains, Montana, *in* Igneous and metamorphic geology: Geol. Soc. America Mem. 115, p. 1-18.

Rowan, L. C., and Larsen, L. H., 1970, Precambrian history of the Beartooth Mountains-Hellroaring Lakes area, Montana [abs.]: Geol. Soc. America, Abs. with Programs, v. 2, no. 5, p. 347.

Rowan, L. C., and Mueller, P. A., 1971, Relations of folded dikes and Precambrian polyphase deformation, Gardner Lake area, Beartooth Mountains, Wyoming: Geol. Soc. America Bull., v. 82, p. 2177-2186.

Schreyer, W., 1965, Zur Stabilität des Ferrocordierits: Beitr. Mineralogie u. Petrographie, v. 11, p. 297-322.

——1967, A reconnaissance study of the system MgO-Al_2O_3-SiO_2H_2O at pressures between 10 and 25 kb: Carnegie Inst. Washington Yearbook, v. 66, p. 380-392.

Schreyer, W., and Schairer, J. F., 1961, Compositions and structural states of anhydrous Mg-cordierites—A re-investigation of the central part of the system MgO-Al_2O_3—SiO_2: Jour. Petrology, v. 2, no. 3, p. 324-406.

Schreyer, W., and Yoder, H. S., Jr., 1964, The system Mg-cordierite-H_2O and related rocks: Neues Jahrb. Mineralogie Abh., v. 101, no. 3, p. 271-342.

Schwartzman, D. W., 1970, Possible primordial Ar-36 in Stillwater pyroxenes [abs.]: Am. Geophys. Union Trans., v. 51, p. 449.

Schwartzman, D. W., and Giletti, B. J., 1968, Excess argon in minerals from the Stillwater Complex, Montana [abs.]: Am. Geophys. Union Trans., v. 49, p. 359.

Shaw, H. R., 1963, The four-phase curve sanidine-quartz-liquid-gas between 500 and 4,000 bars: Am. Mineralogist, v. 48, p. 883-896.

Skinner, W. R., 1969, Geologic evolution of the Beartooth Mountains, Montana and Wyoming—Pt. 8, Ultramafic rocks in the Highland Trail Lakes area, Wyoming, *in* Igneous and metamorphic geology: Geol. Soc. America Mem. 115, p. 19-52.

Skinner, W. R., Bowes, D. R., Khoury, S. G., 1969, Polyphase deformation in the Archean basement complex, Beartooth Mountains, Montana and Wyoming: Geol. Soc. America Bull., v. 80, p. 1053-1060.

Taylor, S. R., 1969, Trace element chemistry of andesites and associated calc-alkaline rocks, *in* Andesite Conf., Eugene and Bend, Oreg., 1968, Proc. (Internat. Upper Mantle Project. Sci. Rept. 16): Oregon Dept. Geology and Mineral Industries Bull. 65, p. 43-63.

Ten Brink, N. W., 1968, Pleistocene geology of the Stillwater drainage and Beartooth Mountains near Nye, Montana: Franklin and Marshall College, Lancaster, Pa., M.S. thesis, 172 p.

——1972, Glacial geology of the Stillwater drainage and Beartooth Mountains near Nye, Montana [abs.]: Geol. Soc. America, Abs. with Programs, v. 4, no. 6, p. 415.

Trommsdorff, Volkmar, and Evans, B. W., 1972, Progressive metamorphism of antigorite schist in the Bergell tonalite aureole (Italy): Am. Jour. Sci., v. 272, no. 5, p. 423-437.

Turner, F. J., and Verhoogen, John, 1960, Igneous and metamorphic petrology [2nd ed.]: New York, McGraw-Hill, 694 p.

Turner, F. J., and Weiss, L. E., 1963, Structural analysis of metamorphic tectonites: New York, McGraw-Hill, 545 p.

U.S. Geological Survey, 1971, Aeromagnetic map of the Stillwater Complex and vicinity, south-central Montana: U.S. Geol. Survey open-file report.

Vail, P. R., 1955, The igneous and metamorphic complex of East Boulder River area, Montana: Northwestern Univ., Evanston and Chicago, Ill., Ph. D. thesis.

vandeKamp, P. C., 1969, Origin of amphibolites in the Beartooth Mountains, Wyoming and Montana—New data and interpretation: Geol. Soc. America Bull., v. 80, no. 6, p. 1127-1135.

Veizer, Jan, 1973, Sedimentation in geologic history—Recycling vs. evolution or recycling with evolution: Contr. Mineralogy and Petrology, v. 38, p. 261-278.

Vhay, J. S., 1934, Geology of part of the Beartooth Mountain front near Nye, Montana: Princeton Univ., Princeton, N. J., Ph. D. thesis.

Vinogradov, A. P., 1962, Average contents of chemical elements in the principal types of igneous rocks of the earth's crust: Geokhimiya, no. 7, p. 555-571. [In Russian, translation in Geochemistry, 1962, no. 7, p. 641-664.]

Wager, L. R., and Brown, G. M., 1967, Layered igneous rocks: San Francisco, Calif., W. H. Freeman, 588 p.

Wager, L. R., Brown, G. M., and Wadsworth, W. J., 1960, Type of igneous cumulates: Jour. Petrology, v. 1, p. 73-85.

Westgate, L. G., 1921, Deposits of chromite in Stillwater and Sweet Grass Counties, Montana: U.S. Geol. Survey Bull. 725, p. 67-84.

Wilson, J. T., 1936, Geology of the Mill Creek-Stillwater area, Montana: Princeton Univ., Princeton, N. J., Ph. D. thesis.

Wimmler, N. L., 1948, Investigation of chromite deposits of the Stillwater and Sweetgrass Counties, Montana: U.S. Bur. Mines Rept. Inv. 4368, 41 p.

Winkler, H. G. F., 1965, Petrogenesis of metamorphic rocks: New York, Springer-Verlag, 220 p.

☆U.S. GOVERNMENT PRINTING OFFICE:1983-381-614/198